Aerosolisation and in-vitro deposition of an artificial lung surfactant

Aydin, Murat

Award date:
1999

Awarding institution:
University of Bath

AEROSOLISATION AND *IN-VITRO* DEPOSITION OF AN ARTIFICIAL LUNG SURFACTANT

Submitted by
Murat Aydin B.Sc.(Hons)
for the degree of Doctor of Philosophy
of the University of Bath
1999

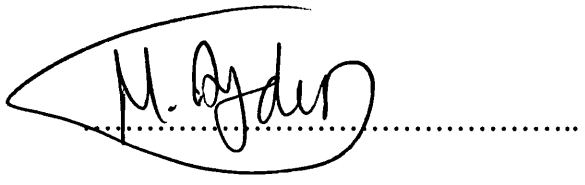

ProQuest LLC
789 East Eisenhower Parkway
P.O. Box 1346
Ann Arbor, MI 48106-1346

Acknowledgements

I would like to thank my research supervisors, Professor John Staniforth and Mr Brian Meakin, for their advice, guidance and innovative ideas over the course of this study. I am delighted to have had the opportunity to work within an established centre of research excellence, with its unique facilities.

A very special thank you to Dr. Paul Young who took me under his wing and encouraged me to think radically on the outset of my research career. He was by far the most versatile and competent scientist I have ever met.

I would like to thank Martyn Clarke for his friendship and company during the more enduring times of this research programme. The many nights we spent in the same laboratory experimenting, keeping each other going and talking makes everything worthwhile.

I am also very grateful to all the help given to me by Dr Mike Tobyn, even though I was not his student.

Thank you also to Fraser Steele and Jason McConville for their technical expertise, assistance and advice.

I was lucky to be at Bath when there were so many characters and personalities around. Therefore, a big thank you to Graham Kay, Gareth Adlam and James Chapman for all their practical jokes, banter and philosophical discussions in the local drinking establishments.

I would also like to thank the technical staff, namely, Kevin Smith, Don Perry, Chris Coy, Peter Dimond, Rod Murray and Steve Phillips for their help and assistance.

A special thank you to Richard Sadler, Susan Johnson and Laura Batterbee for all their ordering and secretarial support.

This research would not have been possible without the funding and support from Britannia Pharmaceuticals Ltd. I would like to Mr Derek Woodcock for his endless patience and understanding.

Finally, I very big thank you to my mother for her love, understanding and for being there when I needed her.

Abstract

Pumactant (also called ALEC^{TM}) is a synthetic lung surfactant currently licensed in the UK for use in the treatment of neonatal respiratory distress syndrome (RDS). It contains two naturally occurring surface-active phospholipids (SAPL): dipalmitoylphosphatidylcholine (DPPC) 70% and unsaturated phosphatidylglycerol (PG) 30%. Both of these phospholipids are present in the human lung, abdominal cavity and the middle ear. Recent theories have suggested that surfactant therapy may be viable in asthma, intraperitoneal post-surgical adhesions and otitis media with effusion (glue-ear). Thus, a comprehensive characterisation of SAPL as a powder for use in such medicinal therapies was undertaken in the present study. The physicochemical properties of SAPL were characterised and are described. The use of imaging and particle size measurement techniques enabled the characterisation of SAPL. Fluid-energy milling was used to micronise coarse SAPL and *in-vitro* aerosol performance of various formulations were assessed using traditional pharmaceutical testing apparatus and procedures. Conventional dry powder inhaler formulation strategy, using coarse-carrier and aggregated powder systems, as well as novel delivery devices and methods were also investigated. The novel delivery devices for asthma and intraperitoneal post-surgical adhesions were developed with the view to their use in the clinic.

It is hoped that the present study provides new and useful information concerning the testing of the novel delivery devices, and the results obtained provide the basis for further study and development of SAPL for the benefit patients.

List of Common Abbreviations

ASP	Agglomerated SAPL Particle
ADS	Adhesions Delivery System
ARDS	Adult Respiratory Distress Syndrome
CONC.	Concentration
CORR.	Corrected
CPL	Coarse Particle Lactose
DPAG	Dry Powder Aerosol Generator
DPI	Dry Powder Inhaler
DPPC	Dipalmitoylphosphatidylcholine
DUSA	Dose Unit Sampling Apparatus
D(0.1 or 10%)	Particle Diameter at the 10% point on the percentage cumulative undersize graph, i.e. 10% of the particles are below the stated value.
D(0.5 or 50%)	Particle Diameter at the 50% point on the percentage cumulative undersize graph, i.e. average particle size.
D(0.9 or 90%)	Particle Diameter at the 90% point on the percentage cumulative undersize graph, i.e. 90% of the particles are below the stated value.
$ECD_{50\%}$	Effective Cut-Off Diameter
ED	Emitted Dose
FDS	Freeze-Dried SAPL
FEV_1	Forced Expiratory Volume in 1 Second
FPL	Fine Particle Lactose
FR	Flow Rate ($Lmin^{-1}$)
FVC	Forced Vital Capacity
GEDD	Glue Ear Delivery Device
HFA	Hydro Fluoro Alkane
HPLC	High Performance Liquid Chromatography
ID	Identification or Internal Diameter
INT.	Intensity
KF	Karl Fischer
LALLS	Low Angle Laser Light Scattering

LFDS	Labelled Freeze-Dried SAPL
LFDMS	Labelled Freeze-Dried Micronised SAPL
LFDUS	Labelled Freeze-Dried Unmicronised SAPL
MS	Micronised SAPL (Non -Freeze-Dried)
MSLI	Multi-Stage Liquid Impinger
NMR	Nuclear Magnetic Resonance
nRDS	Neonatal Respiratory Distress Syndrome
OD	Outside Diameter
PG	Phosphatidylglycerol
pMDI	Pressurised Metered Dose Inhaler
RBB	Rotary Bladed Blender
RH	Relative Humidity
RSD	Relative Standard Deviation
SAPL	Surface Active Phospholipid
SD	Standard Deviation
SEM	Scanning Electron Microscopy
ST	Surface Tension
TSI	Twin Stage Impinger
UMS	Unmicronised SAPL (Non -Freeze-Dried)
VMD	Volume Median Diameter
Wt.	Weight
XRPD	X-Ray Powder Diffraction

Contents

Chapter 1

General Introduction

1 Background

The technological development of inhaled drug delivery systems is currently of great interest. An attraction of the inhalation route for drug delivery is that unlike other routes of administration, adverse systemic side effects can be minimised. Other reasons for inhalation being a preferred drug delivery route includes:

a) Locally acting compound is delivered directly to the site of action, leading to a rapid onset of action (Timsina *et al* 1994).

b) The very large pulmonary surface area (70-80m^2, Weibel 1962), coupled with a good blood supply, provide excellent conditions for efficient drug absorption.

c) Hepatic first-pass metabolism and / or degradation within the gastrointestinal tract are not an issue for drugs delivered via inhalation (Lalor and Hickey 1998).

d) Potent drugs can be administered at generally reduced doses, decreasing the likelihood of unwanted side effects.

Patients with respiratory diseases such as asthma, adult respiratory distress syndrome (ARDS), neonatal respiratory distress syndrome (RDS), and chronic obstructive pulmonary disease (COPD) are likely to require continued maintenance using inhaled medication. Thus, improvements to inhaled drug delivery systems are very desirable.

The fundamental properties of aerosols have been studied using different techniques, for more than a hundred years (Colbeck 1998). Today, new applications for aerosols are being developed, involving not only the treatment of pulmonary diseases, but also the delivery of drugs for treatment of non-pulmonary conditions, such as A.I.D.S, cystic fibrosis, and diabetes (Wood and Knowles 1994). The increasing use of aerosol therapy is due to better understanding of the pathophysiology of diseases, allowing physicians to envisage a broader range of therapeutic options. In particular, systemic delivery of peptides and proteins (via the inhalation route), has generated great interest in recent years and this trend is set to continue (Grossman 1994, Edwards *et al* 1998a). Advances in recombinant DNA technology and aerosol generation and delivery can only serve to increase the number and the different types of drugs delivered as aerosols.

1.1 Structure and Function of the Respiratory Tract

The primary function of the respiratory tract (RT) is gas exchange: facilitating the movement of oxygen into the blood and removing carbon dioxide from the circulation through a very thin blood-gas barrier in the exchange areas (Gonda 1990). A secondary function appears to be the cleaning and humidifying of the incoming air to prevent damage to this vital organ. Although the nose is an integral part of the RT, aerosol delivery of drugs to it or through it for systemic activity, is a topic with its own distinct issues. Therefore, only delivery by breathing via the mouth is considered in this report.

The RT is broadly divided into three regions: 1) The upper RT, also called oropharyngeal region, consists of the mouth, pharynx and larynx. 2) The conducting airways, which include the trachea, bronchi and bronchioles. 3) The lower RT, also called the alveolar or pulmonary region, which extends from the respiratory bronchioles to the distal alveolar sacs (Kumar and Clark 1990, Byron 1994).

The function of the upper RT is to heat and moisten, as well as remove particulate matter from the inspired air. The inspired air passes down the trachea and through the bronchioles, respiratory bronchioles, and alveolar ducts to the alveoli. Between the trachea and the alveolar sacs the airways divide as many as 23 times to form an asymmetric, continuous, dichotomously branching structure (Weibel model A) (Weibel 1963). The first 16 divisions are in the upper conducting airways that transport air to and from the outside environment. The last seven divisions are in the lower pulmonary region where gas exchange occurs by diffusion (Ganong 1989). The walls of the conducting airways consist of cartilage, which gradually decrease in thickness from the trachea to the bronchi, and are absent from the bronchioles and the bronchi. Smooth muscle is also found in the trachea and its function is to link the cartilage. The presence of smooth muscle increases from the bronchi to the bronchioles. The alveoli are lined by two types of epithelial cells: primary lining cells and granular pneumocytes. The physiological function of these cells is to secrete surfactant into the lungs. The surfactant is a mixture of lipids, which reduces surface tension in the lungs, and prevents lung collapse. The multiple divisions in the airways greatly increase the cross-sectional area of the airways, consequently, the air flow velocity in the upper airways (approx.

$60Lmin^{-1}$) decreases to $5Lmin^{-1}$ in the lower airways. The diameter of the upper airways starts at approximately 2cm and decreases to 0.35 mm in the alveoli. In adults, the diameter and total depth of the average alveolus is in the region 250-300μm, and the total surface area of the alveoli is approximately 70-80m^2 (Weibel 1962). The diameter of the alveolar ducts and sacs varies between 150-400μm in children and 200-600μm in adults. The average length of the alveolar ducts and sacs is approximately 0.7-1mm (Weibel 1963).

1.1.1 Pulmonary Clearance

The respiratory airways that lead from the exterior to the alveoli do more than serve as gas conduits; they play a role in the lung's defence mechanisms and clearance (Ganong 1989). An average adult who has a daily intake of ~10m^3 of air (light activity), may inhale as much as 10mg of particulate matter which translates to an annual payload of more than 3g. To prevent large accumulation of particulate matter in the airways over a lifetime of exposure, the RT has a clearance mechanism. The respiratory airways are ciliated and covered by a viscoelastic gel or mucus (Gonda 1990). The composition of mucus is complex and varies between individuals, regions, modes of breathing, and in disease. Pulmonary surfactant is an important constituent of mucus as it lowers the surface tension at the gas-liquid interface and therefore reduces the workload on the lung preventing it from collapsing and helping it to re-inflate (Bangham 1987). When particles in the range of 2 to 10μm are captured in the upper and conducting airways, they are transported upwards from the site of deposition on a mucus blanket, by the beating action of the cilia. This moving blanket of mucus is called the mucociliary escalator (Brain *et al* 1985). Final removal of particulate matter transported to the throat is commonly by swallowing or expectoration.

If particulate matter (<2μm) deposits on alveolar surfaces, it is usually ingested by pulmonary alveolar macrophages (also called dust cells). These cells come from the bone marrow and are actively phagocytic, ingesting inhaled bacteria and small particles. They also help process inhaled antigens for immunologic attack, and secrete substances that attract leukocytes to the lung (Ganong 1989). In addition to phagocytosis, an excess of particles may be removed (drained) by the network of lymphatic channels that line the lung. The drained particles may

enter the blood stream or become bound to the lung tissue. If the load deposited in the lungs is too large, or if the clearance mechanisms are impaired, a sequestering tissue reaction (pneumoconiosis) occurs which may be followed by other pathological events.
For aerosols that deposit in the airways and elicit a physiological response, the relative amount of initial trapping along the upper and conducting airways may not be so important. Rather, it is the amount of subsequent clearance rather than the initial response that predominates whether or not a harmful reaction is felt over long periods of exposure.

1.2 Respiratory Diseases

Diseases of the respiratory system are a major cause of morbidity and mortality throughout the world (Kumar and Clark 1990). In the UK, respiratory diseases account for approximately 20% of all deaths (Byron 1994). In the USA, cases of asthma have risen by 46% between 1982 and 1993 (Edwards *et al* 1998a). Respiratory disorders are the single biggest cause of days lost from work, and asthma is a major cause of hospitalisation (Frew and Holgate 1993).

1.2.1 Asthma

Asthma is defined as a partial obstruction of air flow in the thoracic airways that varies in severity over short periods of time, relief being achieved either spontaneously or as a result of treatment (Kumar and Clark 1990). Asthma is also described as a respiratory disease marked by recurrent paroxysms of difficult breathing following spasmodic contraction of the bronchi (Wade 1988).

1.2.1.1 Symptoms

Although there are many different definitions of asthma, what is certain is that some or all of the following symptoms are observed: breathlessness, coughing, wheezing or tightness in the chest, exhaustion, speech problems, reduced levels of consciousness, and other such symptoms. Asthma attacks tend to be more severe at night and during the early morning hours. This is because there is a circadian rhythm in bronchial tone, with maximal constriction about 6am and maximal dilation about 6pm (Ganong 1989). Compared with non-asthmatics, the airways of patients with the disease tend to be hyperresponsive to constrictor effects of a large number of different stimuli, such as exercise, cold air, hyperventilation and chemical agents.

1.2.1.2 The Inflammatory Process and Bronchial Epithelium

Asthma is a disorder of the conducting airways that contract too much and too easily, producing variable airflow obstruction. Asthma is also recognised as an inflammatory disorder, with oedema and airway leakage of plasma proteins (Kurashima *et al* 1997). The role of inflammatory cells, mediators and the mechanisms by which the inflammatory reaction develops is complex. Chung (1986), Kay (1991), Sheth and Lemanske (1995), Adkins and Brogden (1998) give comprehensive accounts of the inflammatory process. Briefly, inflammation involving mast cells, eosinophils and T-cells is a hallmark of asthma. Mast cells are wandering cells found in large numbers in tissues that are rich in connective tissue. Mast cells have IgE receptors on their surfaces that discharge the contents of their granules (release of histamine from basophils) when IgE-coated antigens bind to the receptors. Mast cells also bring about the secretion of leukotrines, which are inflammatory mediators. Leukotriene release produces bronchoconstriction (bronchial hyperactivity), constricts arterioles, increases vascular permeability, promotes increased mucus production, and attracts neutrophils and eosinophils to the inflammatory site. Hence, leukotrines play an important role in the pathogenesis of asthma. A study carried out by Woltmann *et al* (1997) has shown that

induced sputum measurements can be used to non-invasively assess airway inflammation in asthmatic patients. The levels of eosinophils were measured in healthy and asthmatic patients, with the results showing marked differences between the two sets studied.

Although the inflammatory process described above causes bronchial hyperactivity, Holgate (1998) postulated that bronchial epithelium acts as a key regulator of airway inflammation and remodelling in asthma. This theory appears to be supported by Reddington *et al* (1998), who states that restructuring of the airway wall is a cardinal feature of the disease, which may be directly related with chronicity and altered airway mechanics. Although airway remodelling has previously been considered to occur late in the pathogenesis of asthma, biopsies from children as young as two years of age, who later develop asthma, indicated that thickening of the bronchial epithelial membrane is already apparent (Phunek *et al* 1997). Since bronchial epithelium in asthma is exposed to a variety of allergens capable of causing tissue injury, damage alteration to the regulation of the bronchial epithelium may lead to chronic mucosal inflammation.

1.2.1.3 Classification, Diagnosis and Prevalence

Asthma can be classified into different categories depending on the type of stimuli that gives rise to the hyper-responsiveness and hyper-activity of the lung muscles. The three categories are:-

a) Atopic (Extrinsic) Asthma:- Atopy is the tendency to develop specific IgE antibodies to commonly encountered allergies by natural sensitisation (Barnes and Rodger 1989). The peak period of sensitisation is in the third decade of life. These allergens include pollen, fungal spores, animal danders and household dust or mites (Dolovich *et al* 1983). Other allergens, less frequently encountered, include various plant parts (tobacco leaf, coca bean etc.), insect dusts, and bacterial enzymes.

b) Non-Atopic (Intrinsic) Asthma: This type of asthma tends to develop in adulthood and is caused by such factors as exercise, viral infections and irritants.

c) Occupational Asthma: This type of asthma is due to agents or factors encountered at work. Once sensitisation to the specific agent has occurred, nearly all workers with occupational

asthma develop asthma related to non-specific stimuli such as exercise, infection, cold air and fog. In this way, they are similar to patients with non-occupational asthma (Barnes and Rodger 1989). The list of sensitisation agents can be long and varied but may include the following: Arthropods, crustaceans, fungi, bacteria, wood, metals, chemicals, flour, drugs, dyes and enzymes.

The difficulty in diagnosing asthma is influenced by which category the disease falls in. For example, with allergic asthma, diagnosis may often be made through review of the medical history of the patient and relations. Once the possible trigger factors have been identified, then the diagnosis may be fairly accurate.

Asthma affects about 10 million people in the USA (Lalor and Hickey 1998) and about 5% of the population worldwide (Crompton 1993). It can range in severity from mild and intermittent to severe and chronic, in extreme cases, may be disabling or even life threatening. In children, where asthma onset occurs, the majority develops symptoms before the age of five. In addition, approximately twice as many boys experience symptoms in childhood, although this difference disappears towards adolescence. There is no satisfactory explanation for this observed pattern. Between 25-75% of children make full-recoveries and are free of their symptoms by adulthood. This may be due to enlargement of their airways during normal growth that reduces the significance of the obstruction. In adults, there are no appreciable differences between the number of men and women that suffer from the disease. Approximately 2000 people a year die from asthma-related illness in the UK (Grossman 1994).

Geographical variations occur in asthma distribution: It is more common in Western and developed countries, than in Far-Eastern or less-developed countries (Kumar and Clark 1990). In developing countries, the cases of asthma may rise as individuals' life-styles become more 'Westernised.' Studies of occupational asthma suggest that up to 20% of the work force may become asthmatic if exposed to potent sensitisers.

1.2.1.4 Treatment

Inhalation therapy is the preferred technique (by patients and physicians) for the treatment asthma. The majority of devices are pressurised metered-dose inhalers (pMDIs) and a smaller, but increasing, number of dry powder inhalers (DPIs). Since asthma is characterised by inflammation and obstruction of the airways, the treatment is aimed at eliminating or controlling both these factors. Preventative medicine and a reduction in exposure to sensitising agents and trigger factors should also be considered when dealing with the disease.

A pharmacologically active group of compounds used in asthma therapy, adrenoceptor stimulants (β_2-stimulants, β_2-agonists) may be sub-divided into selective and non-selective categories. The selective category includes: salbutamol, terbutaline, rimeterol, fenoterol, salmeterol, formoterol and reproterol, of which terbutaline and salbutamol have been considered amongst the safest and most effective beta-stimulants (BNF, No 35, 1998). Salbutamol and terbutaline are available in the widest range of formulations. Salmeterol and formoterol are longer acting and are not suitable for the relief of an acute attack, but instead should be used in long term treatment of nocturnal and exercised-induced asthma (Wallin *et al* 1993).

β_2-agonists cause activation of adenylate cyclase which in turn catalyses the conversion of adenosine triphosphate (ATP) to cyclic adenosine monophosphate (cAMP), activating specific protein kinases which reduce phosphorylation of myosin, causing a reduction in calcium-dependant coupling of actin and myosin and thus leading to smooth muscle relaxation in the bronchioles. Stimulation of the β_2-adrenoceptors (found in the airways) also inhibits mediator release by mast cells, basophils and eosinophils. In addition, levels of mucosal oedema are reduced and mucociliary clearance is increased (Barnes and Rodger 1989).

Non-selective β_2-agonists include ephedrine and orciprenaline. These are less safe for use than other selective agents, because they are more likely to cause arrhythmias and other side effects.

Anticholinergic drugs act as competitive antagonists of acetylcholine at muscarinic / cholinergic receptors (Partridge and Sanders 1981). The precise term for these types of compounds are antimuscarinic drugs, but they are commonly referred to as anticholinergic

drugs because of their action against acetylcholine. Examples include ipratropium and oxitropium. These drugs are regarded as been more effective in relieving bronchoconstriction associated with chronic bronchitis in patients who fail to respond to selective bronchodilators. In large doses, they can have a weak local anaesthetic effect and in very large doses, they may block nicotinic receptors at the ganglia (Bowman and Rand 1980). Anticholinergic drugs are not recommended as first-line agents in the treatment of asthma because they have a relatively weaker bronchodilatory effect than β_2-agonists (Gross 1988).

Bronchodilation occurs as a result of stimulation of muscarinic receptors which cause reduced vagal tone. This effect occurs in both healthy subjects as well as patients with asthma (Partridge and Sanders 1981).

Xanthines, also known as methylxanthines, have been used in the management of asthma since the mid-19th century. Although theophylline preparations fall into this class, the narrow range and extrapulmonary side effects are a limiting factor in their clinical use. The proposed mechanism of action of theophylline and other anti-asthmatics in this class is based on the inhibition of phosphodiesterase, leading to increased production of cAMP, thus causing bronchodilation.

Drugs such as sodium cromoglycate (SCG) and nedocromil sodium are anti-allergic. These drugs are called anti-allergic because they interfere with the pathway that gives rise to mast cell activation and cause mediator release, which in turn interacts with primary and secondary effector cells in the airways, thus preventing bronchoconstriction. SCG is a synthetic derivative of bis-cromone which comes from a herb called Khellin. SCG is a mast-cell stabilising agent and inhibits IgE-mediated release of histamine. Nedocromil sodium possesses similar properties to SCG but is more potent. These drugs are active prophylactically rather than therapeutically and are used primarily in the long-term management of asthma because of their ability to reduce airway inflammation (Bernstein and Bernstein 1993). Neither SCG nor nedocromil are effective in treating patients with acute asthma and should not be used if immediate effects are desired.

Corticosteroids have been used in asthma therapy as early as 1950 (Keeder and MacKey). Steroids used in the treatment of asthma include drugs such as beclemethasone and budesonide. These drugs are used for prophylactic treatment when patients are using β_2-stimulants more than once a day. When inhaled, corticosteroids produce many fewer side

effects than those associated with systemic administration. However, in severe asthma and some other respiratory disorders, oral or intravenous corticosteroids are more beneficial than inhaled corticosteroids (Smith and Bernstein 1996). The ability to deliver these drugs in larger doses, either orally or parenterally, with greater systemic availability is the reason for this discrepancy. Corticosteroids reduce bronchial mucosal inflammation and thus reduce oedema and secretion of mucus into the airways. Inhaled corticosteroids have been shown to suppress airway hyper-responsiveness and are effective at controlling symptoms in a broad spectrum of patients (Kaliner 1990).

Other / alternative therapies include the use of antihistamines, mucolytics and α-adrenoceptor antagonists. Histamine is known to cause bronchoconstriction by direct stimulation of smooth muscle via stimulation of the vagus nerve, therefore, treatment is aimed at preventing this event from occurring. Anti-histamines can have a sedative effect and may cause drowsiness. Mucolytics are prescribed to aid the ejection and reduction of sputum viscosity in chronic asthma patients. Heparin, usually used as an anticoagulant, has anti-inflammatory properties which may be effective in asthma, efficacy studies in animals have shown encouraging results.

1.2.2 Adult Respiratory Distress Syndrome (ARDS) and Neonatal RDS

ARDS was first described by Asbaugh and co-workers in 1967, but the aetiology and clinical management strategies of the disease is still wide and varied. Statistically, the incidence of ARDS varies from 1,000 to 15,000 cases a year in the UK and up to 150,000 cases a year in the USA (Lee *et al* 1994). ARDS results from either direct or indirect injury to the pulmonary epithelium and endothelium (Luce 1998) and refers to the acute onset of hypoxaemia and decreased lung compliance following certain risk factors such as: aspiration (or other forms of pneumonitis); sepsis; acute pancreatitis; multiple blood transfusions; burns; massive trauma; inhalation of smoke or other toxic gases and near-drowning (Jones 1990, Zachariades *et al* 1993, Raymondos *et al* 1999). However, since these conditions are non-specific and can result from a number of other conditions, there is no precise test for ARDS and the diagnosis can only be descriptive (Lachmann and van Daal 1992). Nevertheless, diagnosis criteria for ARDS includes: acute onset; chest radiography; monitoring of pulmonary arterial pressure;

impaired oxygenation. In a consensus conference in 1994, it was agreed that ARDS is the most severe end of the spectrum of Acute Lung Injury (ALI) and that the term for the disease should be changed to "acute" rather than "adult." The overall mortality was about 60% (Pepe *et al* 1990) but has improved to <50% due to new approaches in mechanical ventilation, patient positioning, and other new therapy strategies (Luce 1998).

1.2.2.1 Pathogenesis of ARDS

As mentioned earlier, ARDS results from direct or indirect injury to pulmonary epithelium and endothelium. The decrease in lung compliance is associated with acute lung injury which itself is associated with damage to the alveolar membrane by increased capillary permeability to water and proteins (Watling and Yanos 1995). The damage to the alveolar membrane results in pulmonary oedema, containing serum proteins of all classes and an increased number of inflammatory cells (Lachmann and van Daal 1992). This, in turn, causes damage to the pulmonary surfactant in patients with ARDS. As yet, the precise mechanisms, regulatory agents and mediators involved in the inflammatory process are unclear.

1.2.2.2 The Clinical Course of ARDS

The course of ARDS can be divided into four phases. The first phase is characterised by breathing difficulties and the rate of breathing may also increase, a chest radiograph is taken at this stage. The second stage is usually a silent phase, during which the patient appears to be doing well. However, measurement of lung compliance or of the alveolar to arterial oxygen tension gradient indicate deterioration of pulmonary function and the chest radiograph may show minor abnormalities. The third phase is characterised by pulmonary insufficiency and represents the fully developed syndrome. The last phase is characterised by dense fibrosis of the lung and is terminal (Katzenstein 1982).

1.2.2.3 Pulmonary Surfactant Function and Dysfunction in ARDS

Surfactant dysfunction has been demonstrated in the initial phases of ARDS and is linked to alveolar instability and collapse (Kennedy *et al* 1997). Several abnormalities in surfactant composition have been described, these include: a decrease in phosphatidylcholine content, an increase in minor phospholipid subtypes, an increase in the surfactant total protein to total phospholipid and decreases in surfactant apoprotein content (Kennedy *et al* 1997). It is important to understand the normal composition and function of the pulmonary surfactant before the disease state is discussed.

1.2.2.3.1 Pulmonary Surfactant Composition and Production

Lipids (see section 1.2.2.3.4, page 23, for general background information) constitute the major part of the pulmonary surfactant, approximately ~90%. Analysis of the composition of lipids in surface-active material has shown that 80-90% is phospholipids (Sanders 1982). Phosphatidylcholine (PC) constitutes about 70-80% of the phospholipids, of which about 60% contains two saturated fatty-acyl moieties. This di-saturated PC (DSPC) is largely dipalmitoyl PC (DPPC). The second major phospholipid is phosphatidylgycerol (PG), which makes up about 10% of the lung surfactant. Structures of PG and DDPC are shown in Figure 1, page 13.

DPPC: 1,2-Dipalmitoyl-sn-glycerol-3-Phosphorylcholine

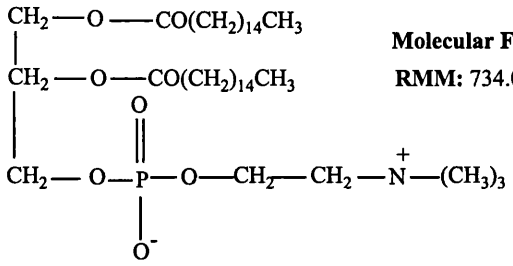

Molecular Formulae: $C_{40}H_{80}NO_8P$

RMM: 734.05

PG: 1,2-diacyl-sn-glycerol-3-phosphorylglycerol

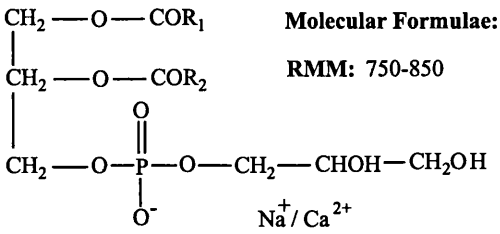

Molecular Formulae: $C_xH_yO_{10}P$

RMM: 750-850

Figure 1: Structures of DPPC and PG (Ratio 7:3, % w/w), the two components that make up SAPL.

Where: R_1 and R_2 are fatty acids (see Appendix 14: Additional Information on SAPL, page 275).

Other phospholipids include phosphatidylinositol (PI), and the presence of PI and the ratio of PG to PI give an indication of lung maturity. A low PG/PI ratio is a sign of immaturity. In addition to the lipids, the surfactant also contains several specific proteins (also called apoproteins or surfactant proteins (SP)-A, SP-B, SP-C and SP-D (Hawgood and Clements 1990). Detailed biosysnthesis pathways of the various components of lung surfactant can be found elsewhere (Batenburg 1995).

The pulmonary surfactant is produced by type II alveolar epithelial cells. The proteins are also produced by these cells, but with the exception of SP-C, which are formed in bronchiolar epithelial cells (Norton 1990). Once produced, the surfactant is packaged and stored in lipid bi-layers in lamellar bodies in the alveolar lumen. The lamellar bodies are secreted into the alveolar space where the surfactant is converted to lattice-like structures called tubular myelin (See Figure 2, page 14). The tubular myelin serves as the precursor for the phospholipid monolayer formed at the air-water interface. Small aggregate material are formed from the

monolayer, these are called vesicles. These vesicles are taken up by type II cells and / or alveolar macrophages for recycling and degradation.

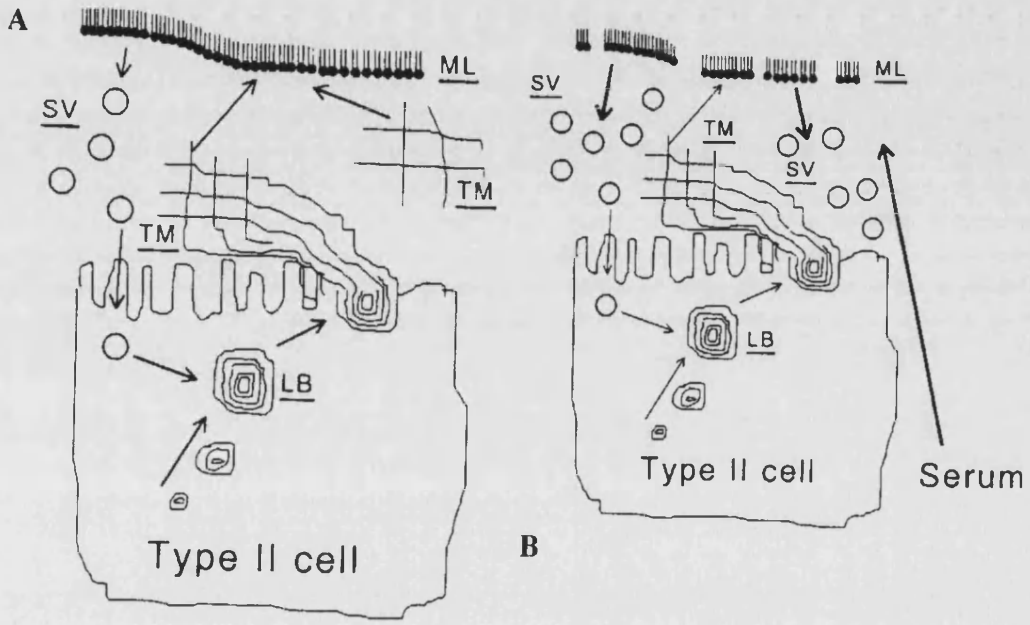

Figure 2: Schematic representation of the life cycle of the pulmonary surfactant in normal (A) and injured (B) lungs.

Key: LB: Lamellar Body, TM: Tubular Myelin, ML: Monolayer, SV: Small Vesicles

1.2.2.3.2 Physiological Mechanisms for the Action of Pulmonary Surfactant

The main function of the surfactant is to help maintain proper lung function, to act as a surface tension lowering agent at the air liquid interface of a continuous liquid layer, or aqueous hypophase, assumed to line the alveoli and adjacent terminal airways at all times. This action of the surfactant allows collapsed alveoli to open at lower inspiratory pressures and to protect the alveoli against collapse during expiration. The continuous layer of surfactant also helps to lubricate the mucosal environment (Hills 1988). A full, detailed, review of pulmonary surfactant functions, associated mechanisms of action of the various models, surface tension measurement techniques, and other possible roles are given elsewhere (Robertson *et al* 1984, Hills 1988, Hills 1991). Briefly, when surfactants act at air-liquid interfaces, the orientation of

the molecules are such that polar head groups are in the aqueous phase and the non-polar groups point towards the air. This orientation of the monolayer reduces surface energy and, thus, the surface tension which can be measured by a number of techniques (e.g. The Langmuir trough, Wilhelmy plate method, du Nuoy tensiometer, Pulsating-bubble surfactometer and capillary rise method). The surfactant model described above (called the 'bubble' model) for the alveoli was first introduced by von Neegaard in 1929 and refined by Clements (1962). However, today, other conflicting models describe the action of the surfactant on the alveoli. These models include:

1. The 'Totally Dry'- model- proposed by Colacicco (1985).
2. The 'Shell'or 'Geodesic-Dome' Model- Proposed by Morley, Bangham and co-workers (1987).
3. The New (Discontinuous) Model- Proposed by Hills (1997, 1998, 1999).

The totally dry and the shell / geodesic-dome models are outside the scope of this report. But briefly, the totally dry model proposed by Colacicco (1985) states that, under normal physiological conditions, the alveoli are dry with no fluid even in the septal corners (see Figure 5d, page 19 and Figure 6a, page 20). It further states that both the liquid and surfactant linings seen in SEM images are artefact and that type II cells only release surfactant in response to flooding. Thus, surfactant is present in the airways of the neonate. Colacicco (1985) also proposes that, by reducing the surface viscosity of fluid that has acquired protein in distal airways, surfactant can facilitate the removal of fluid. The validity of the totally dry model hinges upon whether so much of the reported morphology is artefact. Hills' (1997) discontinuous model challenges these artefact issues with apparent proof that alveolar surfactant is adsorbed on to the alveolar epithelium.

At the opposite end of the spectrum of models are those with continuous liquid linings such as the traditional bubble model. A variation of this model that allows for a higher melting point of a supernatant surfactant layer arises if the concept of a monolayer is dispensed with. The geodesic-dome or shell model proposes that the liquid-air interface is masked by a solid phase of DPPC. Galdston and Shah (1967) and Bangham *et al* (1978) compared this solid surfactant layer to "icebergs" or "rafts", depicting multiple layers as shown in Figure 3.

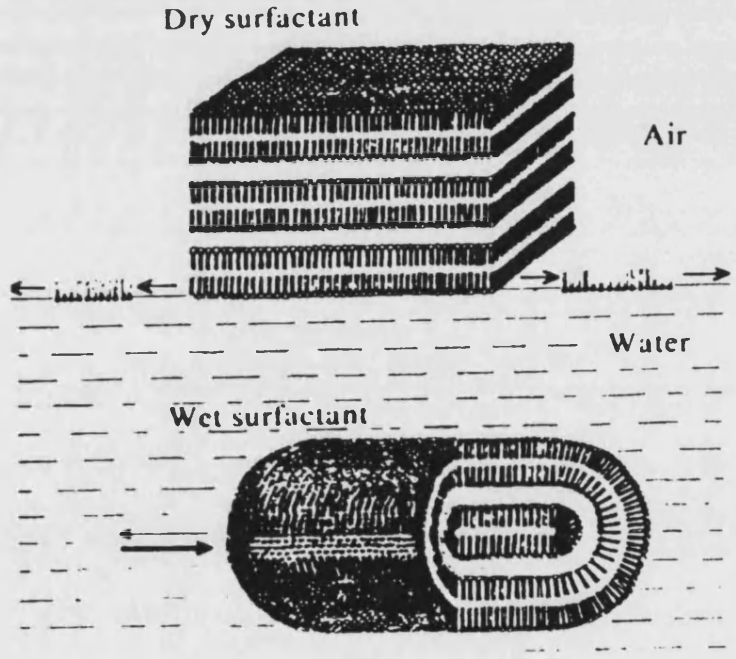

Figure 3: Molecular configuration of a wet and dry surfactant.

With the wet surfactant, aggregates in water form a smectic mesophase with few molecules free to reach the interface. The rafts of dry surfactant have an open-ended structure from which molecules can spread freely at the interface to form a monolayer. Refer to Figure 4, page 17 for a graphical representation. Reproduced from Bangham *et al* (1978) with permission.

The solid surfactant opens on expansion / inspiration, to expose a true liquid surface to which more surfactant can be recruited from the hypophase. On subsequent compression, this recruited surfactant can be condensed to a solid and compacted to form uniform oligolamellar rafts. Bangham (1998) proposes that, at end expiration, these floating solids come together to form a rigid structure resembling a geodesic dome, thus resisting further collapse and establishing alveolar stability. Upon expansion, the solids require an appreciable pressure

difference before they are prized apart to explain the inspiratory delay in volume increase, otherwise attributed to 'alveolar recruitment / opening' following closure at end expiration (Greaves *et al* 1986).

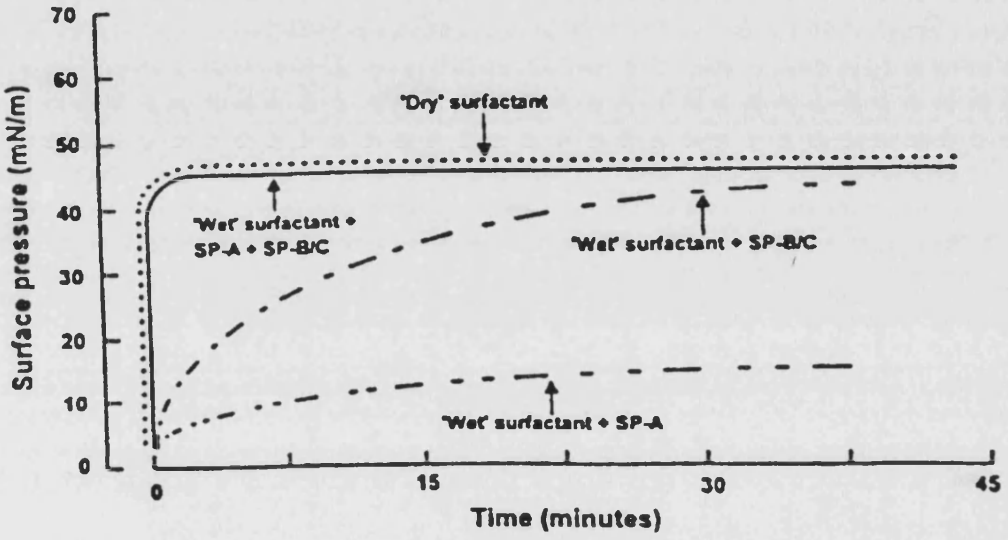

Figure 4: Graph showing the relative performances of wet and dry surfactants with various combinations of surfactant proteins.

From the graph it can be seen that dry surfactant spreads fastest at the air-water interface followed by wet surfactant with combinations of surfactant proteins A and B.

Hills' (1997)discontinuous model suggest that in the normal air-filled lung, water repellency is imparted by an adsorbed pseudo-cationic surfactant in the form of surface active phospholipid (SAPL), is responsible for alveolar fluid being confined to 'pools' observed (e.g. by Weibel 1982) in the septal corners, and 'pits' (see Figure 5(d) and Figure 6(a), page 19) elsewhere along what is otherwise an apparently fluid free surface (Hills and Masters 1998, Hills 1999). Hills argues that in the 'bubble' model, the continuous fluid lining (see Figure 5(c), page 19 and Figure 6 (b), page 20) can be regarded as a one-sided bubble whose collapsing pressure (ΔP) would be far too large to be physiologically compatible unless surfactant greatly reduced the surface tension (γ) from the very high value for water, as related by the Laplace equation:

$$\Delta P = 2\gamma / r \qquad \textbf{Equation 1}$$

where r is the radius of curvature. The other major requirement of the 'bubble' model is that surface tension of the liquid-air interface is 'near-zero' (Guyton *et al* 1984, Hawgood and Clements 1990), otherwise the force (ΔP) of the concave fluid surface sucking fluid into the air space at the septal corners (r decreases in the Laplace equation) would be impossible to balance by normal homeostatic mechanisms. Bangham (1987), has claimed that surface tension (γ) can reach 'near-zero' transiently during the respiratory cycle, but this have been disputed by others (Barrow 1979, Hills 1988).

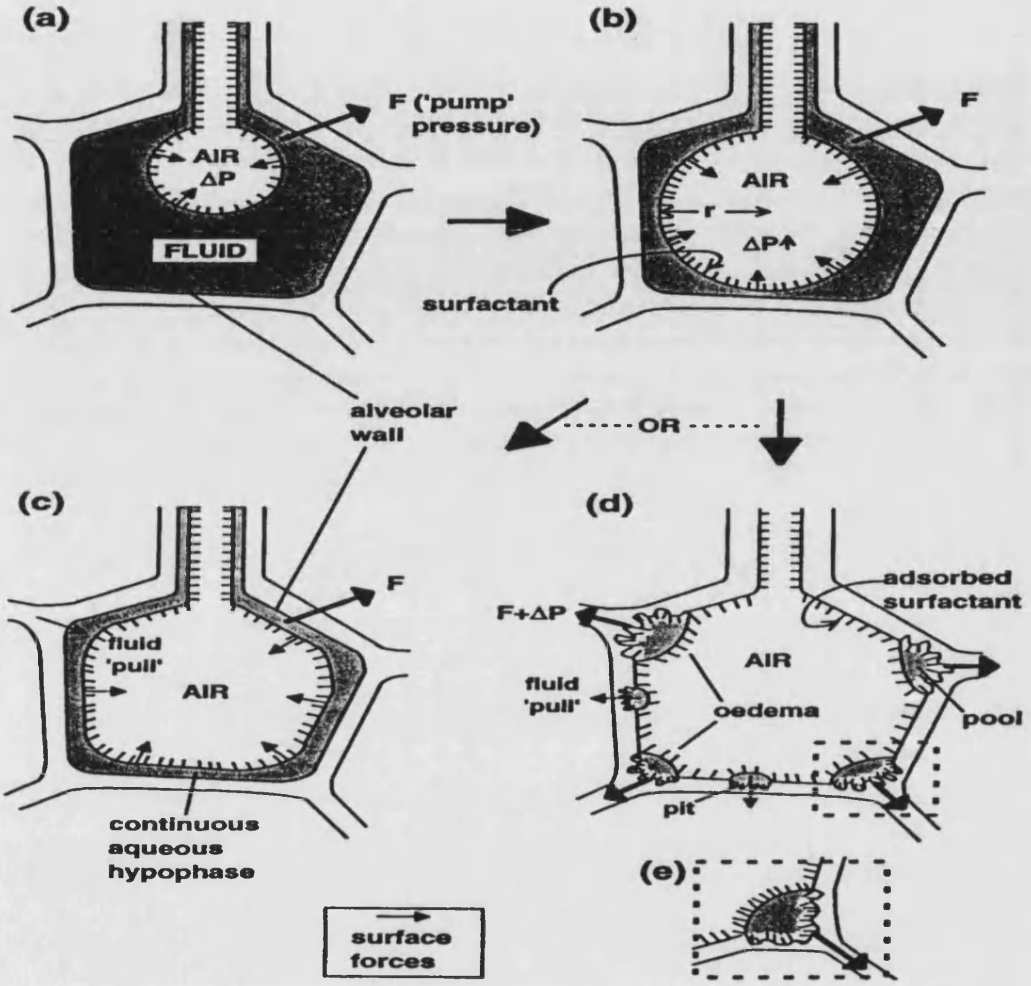

Figure 5: Visual representation of the various events used to describe the role of the pulmonary surfactant.

a) The alveoli at birth- Air replaces the fluid in the lungs to form central cores. b) Emptying of the lung fluid and establishment of the bubble. c) Formation of the continuous aqueous hypophase and surfactant lining. d) Discontinuous model proposed by Hills (1988, 1997), see Figure 6, page 20 for more detail.

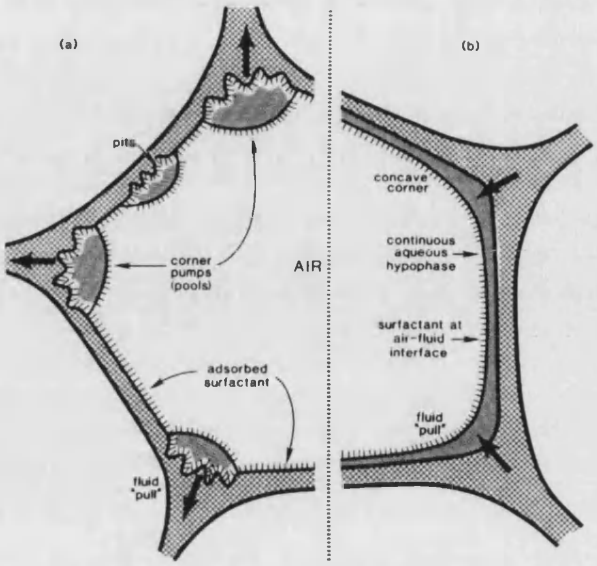

Figure 6: The discontinuous model of the alveolus

a) With fluid confined to 'pools' and 'pits' from which it can tension the dry patches of the wall by pulling in excess epithelial membrane as 'pleats'. The gas-transfer surface is kept essentially dry by water repellency induced by a layer of surfactant directly adsorbed onto the epithelial surface. The 'pools' can assume a convex profile to act as 'corner pumps' (Hills 1982) for returning fluid to the interstitium. If flooding continues, the 'pools' will link up to form the 'bubble' model (b), but as the pathological and not the normal physiological state.

Morphological evidence for the adsorption of surfactant to the alveolar epithelium tissue has been given via electron microscopy, by Ueda *et al* (1985) for the adult lung, and separately by Hills and Masters (1998). Hills and Chen (1998) carried out *ex-vivo* experiments using bronchial epithelium (derived from porcine lungs) to prove the hypotheses that: exogenous surfactant can directly bind to various tissue surfaces where the adsorption of indigenous surfactant had been demonstrated; and how (phosphatidylgycerol) (PG) has a physiological role in promoting DPPC adsorption. Hills argues that, if his hypothesis is correct, then SAPL would already be in place, adsorbed at the alveolar epithelium in a normal mature foetus before delivery, then it should also be in place in a still-born human baby. To test his hypothesis, necropsy (autopsy) was carried out in a human foetus of 41 weeks gestational age, which had died from non-respiratory causes. Peripheral lung tissues were studied using epifluorescence microscopy.

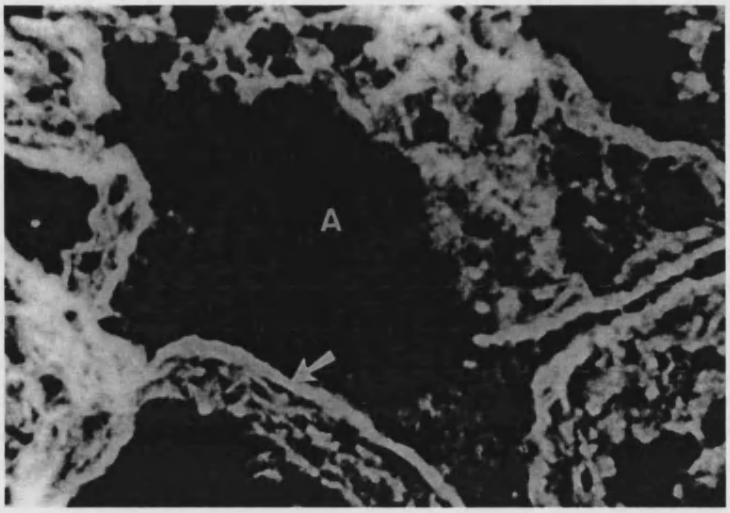

Figure 7: Electron photomicrograph of alveolar tissue excised from a still human foetus at 41 weeks gestation, taken by epifluorescence microscopy using Phospholipin E as the hydrophobic probe.

Note the SAPL lining layer bordering the potential air space as indicated by the arrow, magnification x300.

The results clearly show that the outermost layer lining foetal alveolar epithelium at term is SAPL (Hills and Masters 1998). Spectral analysis, using a scanning spectrophotometer, of the fluorescent light emitted from the arrow shown in Figure 7 produced a spectrum (see Figure 8, page 22) that was identical to the spectrum of synthetic DPPC shown by Bangham and Horne (1964) to produce oligolamellar SAPL (liposomes) when ultrasonicated in water. This spectral analysis (Figure 8, page 22) is also consistent with the lamellated alveolar lining shown in the adult lungs and in the upper airways by Ueda *et al* (1985).

In order to substantiate his discontinuous model further, and to prove that alveolar surfactant is adsorbed on to the alveolar epithelium, Hills and Masters (1998) and Hills (1999) state that, if the exogenous surfactant used in the treatment of neonatal RDS spreads instantaneously at the air-liquid interface (as predicted by the bubble theory), why is it that improvements in gas exchange are noticed some 48 hours after administration? This time lapse was first reported by Milner (1993) and is consistent with the much slower rates for surfactant binding to solids than spreading over liquid surfaces (Hills 1988).

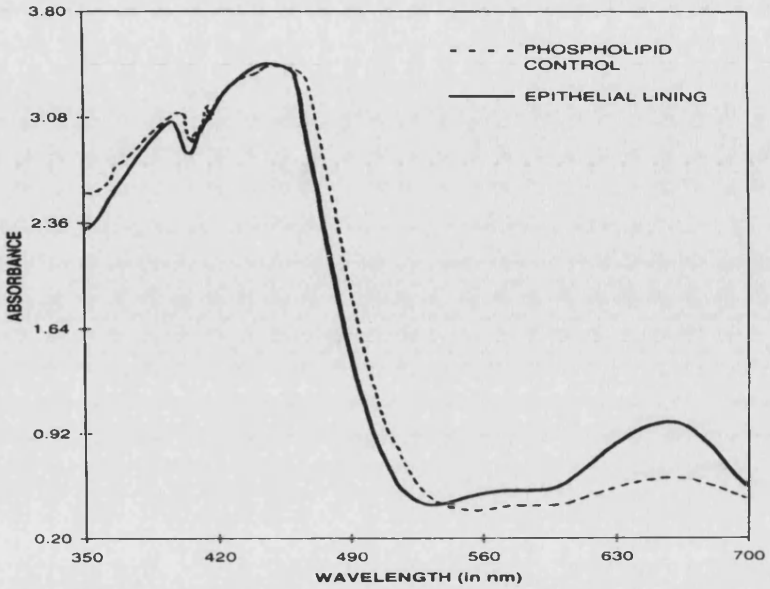

Figure 8: Spectral analysis of the fluorescent light (from arrow in Figure 7). The spectrum is identical to that of synthetic DPPC transformed into its oligolamellar state as liposomes by ultrasonication in water.

Other functions for the pulmonary surfactant have been suggested, they include: Contribution to the host defence mechanism (McFadden *et al* (1994); Enhancement of ciliary beat frequency (Kakuta *et al* 1991); Role in maintaining the patency of the conducting airways (Enhorning *et al* 1996). In addition to these functions, the potential use of exogenous surfactant in other lung diseases such as pneumonia and bronchial asthma may be a possibility (Lewis and Veldhuizen 1995). The potential use of pulmonary surfactant as a physical barrier against asthma will be discussed later.

1.2.2.3.3 Surfactant Dysfunction

As mentioned earlier, surfactant alterations during ARDS are somewhat more complex than the primary surfactant deficiency noted in neonatal RDS. Typical alterations to the surfactant include altered phospholipid composition, where levels of PC, PG and PI are all decreased. There is also a decrease in the levels of SP-A, SP-B, and SPC. SP-A is known to bind lipids

(Hawgood 1992), to aid vesicle formation, play a role in tubular myelin formation, also thought to be involved in defence mechanisms (Wang *et al* 1998). SP-B is thought to play a role in monolayer formation, and SP-C is believed to promote the adsorption of the phospholipids to the air-liquid interface (Batenburg 1995). SP-D plays a role in defence mechanisms (Wang *et al* 1998) where it activates alveolar macrophages and binds to lipopolysaccharides. The combined result of the alterations to the phospholipid and protein levels leads to a loss in the ability of the surfactant to reduce surface tension. Furthermore, surface activity of the surfactant is further impaired by the increased influx of serum proteins into the alveolar space due to the increased epithelial permeability associated with ARDS (Lewis and Veldhuizen 1995). Disturbance in the levels of surfactant will result in pulmonary airway swelling and will hence affect lung compliance and gas exchange.

1.2.2.3.4 Other Phospholipids and Liposomes

Molecules with combinations of hydrophilic and lipophilic moieties are termed amphipathic. Some amphipathic molecules are better at reducing interfacial free energy than others and these are termed surfactants (Hills 1988). Hydrophilic moieties of surfactant fall into four basic categories depending upon whether they carry no net charge (non-ionic), a negative charge (anionic), a positive charge (cationic) or both, in which case they are termed zwitterions. Thus, the ends of a surfactant molecule are often referred to as 'polar' or 'non-polar' and all except the non-ionic variety are electrolytes. Phosphatidylcholines become cationic below a pH of 3 because this is the pK value of the phosphate group in the zwitterions, leaving a net positive charge on the terminal quaternary ammonium ion (Phillips and Chapman 1968). Lipids are naturally occurring compounds that are esters of long chain fatty acids, which are insoluble in water but soluble in organic solvents such as acetone, alcohol, chloroform or ether. Alkaline hydrolysis (known as saponification) gives rise to the alcohol and the sodium or potassium salt of the constituent fatty acids (Plummer 1987). There are four basic types of lipids- acylglycerols, phosphoglycerides (also referred to as phospholipids or phosphatides), sphingolipids, and waxes. These differ in the backbone structure to which the fatty acids are covalently bound. Neither the waxes nor the

acylgylcerols are amphiphatic, leaving two groups that are highly surface active (Kondoh *et al* 1987). The backbone of phospholipids are produced by the esterification (using phosphoric acid) of one of the hydroxyl groups of glycerol and both D and L forms are produced (Lehninger 1976), refer to Appendix 15: Structures of Lipids, page 276. The polar heads on the phospholipids are varied and can include choline, ethanolamine, inositol, serine, and glycerol. Bangham and Dawson (1959) concluded that phosphatidylcholines have a slight net positive charge and thus migrate to the cathode under electrophoresis, whilst, most other phosphoglycerides have a net negative charge.

Sphingolipids contain sphingosine (refer to appendix 15 for structures,) as the backbone and are important membrane components in animals. The most abundant sphingolipids are sphingomyelins, produced by esterification of the primary alcohol group with phosphatidyl ethanolamine and the fatty acid residue is present as the acyl derivative of the amino group. Sphingomyelin is present in the myelin sheet, which acts as an insulator for nerve fibres.

Esters of glycerol and fatty acids are called acylglycerides or glycerides. The trihydric alcohol can be esterified to give mono-, di- and triglycerides. The fatty acids may be the same or different and, on saponification, free glycerol and fatty acid can be obtained (Plummer 1987). Triglycerides are the predominant form in nature, although mono- and diglycerides are known. The acylglycerols are uncharged molecules and for this reason are known as neutral lipids. They are called fats or oils depending upon whether they are solid or liquid at room temperature. If the fatty acids (see Table 1, page 25 for examples) substituted in positions 1 and 3 are different the C-2 becomes a chiral centre and two streoisomers are possible, although most triglycerides in nature are the L form.

PG portion of SAPL contains some of the fatty acids listed in Table 1, (page 25), (see also Appendix 14: Additional Information on SAPL, page275). The unsaturated fatty acids in Table 1 contain double bonds, and introduction of these double bonds into the fatty acid part of an acylglycerol lowers the melting point of the compound. Thus, animal fats, which contain high amounts of triglycerides with fully saturated fatty acids are solid at room temperature, while vegetable and fish oils which have a high proportion of unsaturated fatty acids, are liquid at the same temperature.

Name	Type	Formula	Symbol
Lauric	Saturated	$CH_3(CH_2)_{10}COOH$	12:0
Mystric	Saturated	$CH_3(CH_2)_{12}COOH$	14:0
Palmitic	Saturated	$CH_3(CH_2)_{14}COOH$	16:0
Stearic	Saturated	$CH_3(CH_2)_{16}COOH$	18:0
Oleic	Unsaturated	$CH_3(CH_2)_7CH{=}CH(CH_2)_7COOH$	$18:1^{\circ 9}$
Linoleic	Unsaturated	$CH_3(CH_2)_4CH{=}CHCH_2CH{=}CH(CH_2)_7COOH$	$18:2^{\circ 9,12}$
Linoleni	Unsaturated	$CH_3(CH_2)CH{=}CHCH_2CH{=}CHCH_2\,CH{=}CH(CH_2)_7COOH$	$18:3^{\circ 9,12,15}$
Arachiod	Unsaturated	$CH_3(CH_2)_4(CH{=}CHCH_2)_3CH{=}CH(CH_2)_3COOH$	$20:4^{\circ 5,8,11,14}$

Table 1: Some Common Fatty Acids Found in Living Organisms.

In Table 1, the first number denotes how many carbon atoms are in the chain, and the second number indicates the number of double bonds. The symbol and a number indicate the location of the double bond. Autoxidation and photo-oxygenation are two aspects of the non-enzymic reaction between oxygen and unsaturated fatty acids (Gunstone *et al* 1994). Lipids are liable to undergo oxidation during storage and handling, involving complex substrates and ill-defined reaction conditions. The primary oxidation products are often converted to secondary products of several kinds. Autoxidation is a radical chain process involving initiation, propagation and termination reactions. Photo-oxidation involves interaction between a double bond and singlet oxygen produced from ordinary triplet oxygen by light in the presence of a sensitiser such as chlorophyll. Photo-oxidation is a quicker reaction than autoxidation. A detailed account of the oxidation of lipids is given elsewhere (Chan 1987).

Liposomes, or lipid vesicles, are spherical, self-closed structures composed of curved lipid bilayers, which entrap part of the solvent, in which they freely float, into their interior (Lasic 1993). Liposomes vary in size from 20nm to several dozen μm, while the thickness of the membrane is around 4nm. Liposomes are made predominantly from amphiphatic molecules, such as lecithin, and are not water soluble, instead they form colloidal dispersions. Hydrophilic portions of liposomes tend to be in contact with water whilst the hydrophobic parts prefer to be hidden in the interior of the structures. Liposomes can be large or small and may be composed of several hundred concentric bilayers. A detailed account of all aspects of liposomes can be found elsewhere (Lasic 1993).

1.2.2.4 Neonatal RDS (nRDS)

In the late 1950s, it was shown that premature babies were deficient in pulmonary surfactant and that this was closely associated with RDS and hyaline membranes in the lungs of those babies who died (Avery and Mead 1959).

The foetus in the uterus makes respiratory movements, but its lungs remain collapsed at birth. After birth, the infant makes several strong inspiratory efforts, the lungs expand, and the surfactant prevents them from collapsing again. Surfactant deficiency is the cause of hyaline membrane disease, known as RDS, which is a serious pulmonary disease that develops in the newborn and premature babies born before their surfactant system is fully functional. Surface tension in the lungs of babies is high and there are many areas in which the alveoli are collapsed (atelectasis). RDS seems to be more common in neonates with low plasma levels of thyroid hormones than in those with normal plasma levels. As many as 40,000 infants develop RDS in the US, annually (Ishisaka 1996). The incidence of the disease is inversely proportional to the gestational age of the neonate, and more than 70% of babies born with between 25-30 weeks are affected. The symptoms, which include grunting, tachypnea, nasal flaring and increased oxygen requirements usually develop within six hours of birth (Ishisaka 1996).

The standard treatment consists of nebulised surfactant being linked to the ventilation system in intensive care units. The different types of treatment for RDS will be discussed later.

1.2.2.5 Treatment

At present, therapy of patients with ARDS is supportive (Spragg *et al* 1992) and the pulmonary permeability cannot be reversed directly (Watling and Yanos 1995, Bersten *et al* 1998). Gas exchange in patients is maintained with supplemental oxygen and mechanical ventilation. However, as yet, a definitive role and frequency of ventilation in the treatments of ARDS has not been established because large multi centre trials researching this avenue has not been initiated (Herridge *et al* 1998).

Attempts have been made to treat ARDS with the delivery of exogenous surfactant (Lachmann 1989, Norton 1990, Nosaka *et al* 1990, Anzueto *et al* 1994, Gregory *et al* 1994, Spragg *et al* 1994, Lewis Veldhuizen 1995, Balaraman *et al* 1998). Delivery has either been via tracheal instillation or by aerosolisation. Animal studies have shown that several factors influence the degree of efficacy, these include: the delivery method; the timing of surfactant treatment over the course of the injury; the specific surfactant preparation used; and the dose administered. Each of these factors alone or in combination may affect the patient's alveolar environment, and thus the effect of the treatment. Results have shown that in the early stages of injury, aerosolised surfactant does benefit the patient. At later stages, large quantities of instilled surfactant are necessary to achieve any benefit. Whether tracheal instillation or aerosolisation of the surfactant is the preferred treatment is still being established. Instillation delivers more surfactant to the injured lung over a relatively short period of time compared to aerosolisation. However, delivering large boluses of material into an acutely injured lung may not be optimal. Therefore, although surfactant therapy is possible in adults, only modest improvements in gas exchange are observed, which may vary from patient to patient (Nosaka *et al* 1990, Wiedemann *et al* 1992). One pattern which has appeared from the various forms of treatment is that, ARDS due to sepsis and pneumonia is associated with a high mortality rate, whereas ARDS secondary to trauma has better prognosis (Nolan *et al* 1997, Vanderzwan *et al* 1998, Raymondos *et al* 1999).

As mentioned earlier, unlike neonatal RDS which is caused by surfactant deficiency, the lung injury associated with ARDS is much more complex and therefore harder to treat. Other treatments, apart from surfactant therapy, have included the non-steroidal anti-inflammatory

drugs (NSAIDs) in animal models (Messent and Griffiths 1992) and corticosteroids (Bernard *et al* 1994) in humans. NSAIDs were chosen in animals because they are able to decrease the inflammatory process in the lung, no human trials have been carried out. Corticosteroids also have anti-inflammatory properties but have shown no significant effect against the disease. In summary, mortality from ARDS is usually due to multiple-organ failure, rather than causes directly related to lung injury (Montgomery *et al* 1985). Studies on survivors of ARDS have shown that lung mechanics return to normal within one year (Elliot *et al* 1981, McHugh *et al* 1994).

Surfactant therapy for the treatment of RDS in neonates is now an established and essential element in the care of the preterm infant (Griese and Westerburg 1998, Lemons *et al* 1999). The therapy is divided into two categories: Surfactants derived from natural sources: artificial or synthetic surfactants made in the laboratory (Morley 1988). Surfactant therapy is aimed at premature babies <30 weeks of gestation. An improvement in lung compliance and general condition of the infant is apparent within 48 hours of surfactant administration. Mechanical ventilation strategy during RDS is characterised by positive end-expiratory pressure, increase in the respiratory time, and high inspiratory oxygen concentration (Fraisse *et al* 1998).

1.2.2.5.1 Naturally Derived Surfactants

Some examples of surfactants used in clinical trials, which are derived from natural sources include: Surfactant TA (Surfacten®, Tokyo Tanabe, Tokyo, Japan). Calf-Lung Surfactant Extract (CLSE, NY, USA), Porcine surfactant (Curosurf®, Serono Laboratories (UK) Ltd.), Human Amniotic Fluid Surfactant (HAFS) (currently, not in use), Beractant (Survanta®, Abbott Laboratories Ltd., UK), Infasurf (Forest Labs, St.Louis, USA) and Alveofact (Thomae GmbH, Biberach, Germany). These drugs are all administered via an endotracheal tube installation and are intended to replenish the reduced levels of indigenous surfactant within premature babies.

Surfactant TA was developed by Fujiwara *et al* (1980) and is derived from homogenised bovine lungs and was the first efficacious surfactant used in humans. The medicine contains 84% phospholipids, 8% palmitic acid, 7% tripalmitin and 1% SP-B and SP-C. It is a freeze-dried preparation and between 100-120mg is sonicated for 5 minutes in physiological saline (3-4ml) and administered.

CLSE is also naturally produced and is made by washing the surfactant out of bovine lungs with physiological saline. It was developed in collaboration of groups from USA, UK, and Canada. The preparation contains 63% saturated PC, 32% other phospholipids, 4% cholesterol and cholesterol esters, and 1% hydrophobic protein (SP-B and SPC). Controlled trials of prophylactic use of CLSE have been done in infants of 24-28 weeks' and 25-29 weeks' gestation (Kwong *et al* 1985). Mortality and morbidity was decreased significantly.

Curosurf® is obtained from minced porcine lungs by chloroform-methanol extraction and liquid gel chromatography. It contains 41-48% saturated PC, 51-58% other phospholipids, and about 1% SP-B and SP-C, without triglycerides, cholesterol or fatty acids. It is used as a suspension of 80mg/ml and at 200mg/kg (Noack *et al* 1987). Prophylaxis therapy in multi-centre trials has shown a decrease in the incidence and severity of RDS (Egberts *et al* 1993).

HAFS a modified natural surfactant produced by collecting amniotic fluid from caesarean sections of some foetal deliveries. Amniotic fluid provides the foetus with favourable conditions for absorbing mechanical pressures and yet allowing freedom of movement. While the foetus skin is still permeable, the fluid forms an extension to the foetal extracellular fluid. When the skin becomes impermeable, the balance of amniotic fluid is that added by foetal urine and that taken away by foetal swallowing. Changes in fluid levels can give an indication of lung maturity in premature babies (Hallman *et al* 1985). HAFS was used as 60mg suspended in 3-5ml of 0.6% saline. This product was only used for efficacy trials and is not available commercially.

Survanta® is a natural bovine lung extract containing phospholipids, neutral lipids, fatty acids, and surfactant-associated proteins. Additional DPPC, palimitic acid, and tripalmitin are added

to improve its surface tension lowering properties. Each dose of Survanta® is 4ml/kg. Several randomised trials have shown the drug to be effective either prophylactically or as rescue therapy, with immediate improvements in gas exchange (Sehgal *et al* 1994).

Infasurf® is a chloroform-methanol extract of neonatal calf lung lavage without supplements. It contains 35mg/ml of phospholipids, 55-70% of which is saturated PC and the dose is 3ml/kg. Infasurf contains SP-B and SP-C, but not SP-A. Since it is prepared from lung lavage rather than lung mince, it may contain less unwanted ingredients. Trials have shown the drug to increase the survival chances of infants with birth weights <1000g (Repka *et al* 1992).

Alveofact is obtained from bovine lung lavage and contains up to 1% SP-B and SP-C, 88% Phospholipids, 4% Cholesterol, and 8% other lipids. The dosing is 1.2ml/kg and delivers about 50mg/kg of phospholipids. Trials in Germany have shown increased survival rate against a control group (Gortner *et al* 1992).

1.2.2.5.2 Artificially Derived Surfactants

Artificially derived surfactants for use in RDS treatment have included: Exosurf® (Wellcome UK), and Artificial Lung Expanding Compound (ALEC), (Britannia Pharmaceuticals). Like naturally derived surfactants, these too are administered via an endotracheal tube instillation.

Exosurf® (Colfosceril Palmitate) is a synthetic, protein free surfactant consisting of 85% DPPC, 6% tyloxapol (non-ionic surfactant) and 9% hexadecanol (cetyl alcohol) by weight. It comes as lyophilised powder and is administered as a suspension and contains 67.5mg/5ml of drug substance, which is re-constituted (108mg) with 8ml of water for injections. The tyloxapol and cetyl alchol facilitate the adsorption and spreading of the DPPC. In multi-centre trials a single dose, used prophylactically, has been shown to reduce infant mortality (Durand *et al* 1985, Stevenson *et al* 1992).

ALEC (also called Pumactant) was synthesised in 1977 at Cambridge, UK, by Morley. It is composed of DPPC and unsaturated phosphatidylglycerol in the ratio of 7:3 (see Figure 1, page 13 for structures). It contains no protein and has been used in trials both as a powder and as a suspension (50-100mg in 1ml cold saline). The compound is a white, sterile, freeze-dried powder contained in vials and is ready for reconstitution. When reconstituted, the product is a white, creamy suspension and contains about 10.8mg of sodium. ALEC contains no antimicrobial preservatives and should therefore be reconstituted and used within 8 hours. It has been shown to reduce the severity of RDS in neonates and has few or no undesirable side-effects (Morley 1987). In a multi-centre trial on 328 premature babies, between 25-29 weeks gestation, neonatal mortality was reduced from 27% to 14%, the need for respiratory support was also significantly reduced (Ten Centre Study Group 1987). A follow-up study carried out by Morley (1990) on the same babies, three years later, showed no difference between treated and control groups in the incidence of mental impairment, respiratory infections, allergies, or hospital admissions. Precisely 57% of the treated group were still alive compared with 41% of the control group.

To date, over 10 000 infants have been treated in randomised clinical trials using surfactant therapy (Hellmann 1995). Currently, there is no conclusive data to support the routine use of one surfactant over another (Ishisaka 1996, Griese and Westerburg 1998). However, specific preparations under a specific clinical situation may be preferable (e.g. natural surfactants may be preferred in cases where the biological system is poorly functional). New surfactants are being developed and evaluated, new techniques of administration such as aerosols, are being tried and improved, and new applications for pulmonary surfactant may become established in the near future.

1.3 Surfactant Therapy

Publications over the years have indicated that a dysfunction of pulmonary surfactant system might partially explain the pathophysiology of asthma, and COPD (Chen *et al* 1998, Enhorning *et al* 1996, Hills *et al* 1996a, 1996b, Holgate 1998, Kurashima *et al* 1991, Liu *et al* 1995, 1996, 1997, Postle 1995, Vanderzwan *et al* 1998, Wang *et al* 1998). Some authors (Holgate 1998, Reddington *et al* 1998) have also outlined that surfactant dysfunction is indirectly responsible for airway inflammation and subsequent alteration of airway mechanics (see 1.2.1.2 The Inflammatory Process and Bronchial Epithelium, page 5). From the relatively few studies carried out, it has also been suggested that pulmonary surfactant may have a protective role against the pathogenesis of asthma by acting as a potential prophylactic agent, by forming a physical barrier against potential irritants that may initiate inflammation of the airways. A hypothesis for this barrier model will be proposed, and results of clinical trial of surfactant administration to date will be reviewed.

1.3.1 Potential Uses in Asthma

The concept of a partial barrier function of surfactant separating bronchial air from the receptors that elicit bronchoconstriction was outlined by Hills *et al* (1996a, 1996b) and further endorsed by Hohlfeld *et al* (1997). Hills has used his argument of surfactant binding to epithelium tissue (see 1.2.2.3.2 Physiological Mechanisms for the Action of Pulmonary Surfactant, page 14) to prove the existence of surfactant in the upper airways (Ueda *et al* 1985, Hills 1990, Hills *et al* 1996). This proof is in the form of electron photomicrographs of the epithelial cells in the airways, which are lined with multilamellar (oligolamellar) layers of SAPL (see Figure 9, page 33).

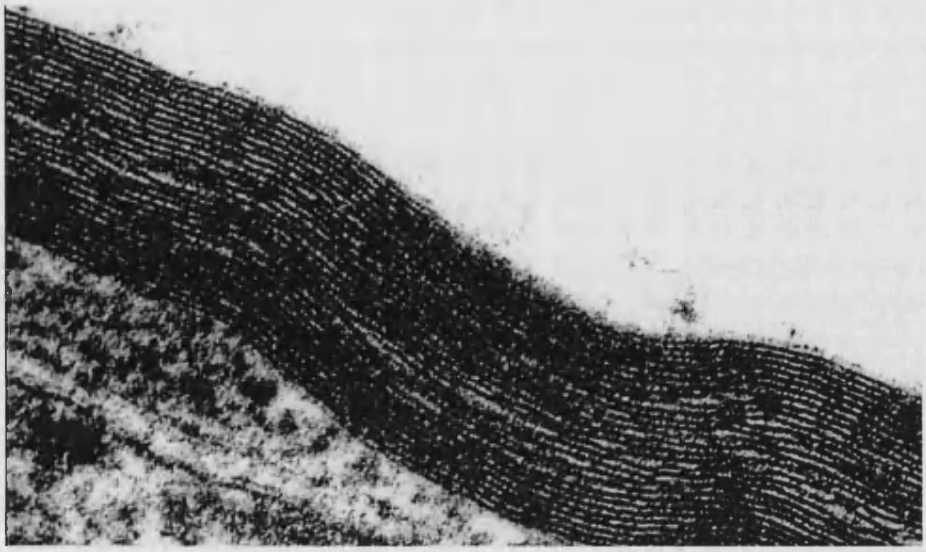

Figure 9: An electron photomicrograph of bronchial epithelium, rinsed free of mucus. Note the oligolamellar layers of surface-active phospholipid (SAPL).

These same oligolamellar layers have also been described adjacent to the taste receptors of the tongue (Sbabarti *et al* 1991) which led to Hills' (1996a) hypothesis of the physical barrier concept for the surfactant. The theory states that the function of SAPL layers in the airways is to 'mask' smooth muscle and nerve terminal receptors and, thus, moderate the bronchoconstrictive reflex to any noxious stimuli or other airborne triggers, which may lead to airway hyperresponsiveness and inflammation (Hills *et al* 1996b). This theory is an extension of the concept derived by Pride (1989), that asthma represents a loss of normal mechanisms restricting the effects of smooth muscle contraction. The source of the surfactant found in the upper airways are lamellar bodies (Haller 1994), which have also been observed on epithelial surface (Hills 1995) and in the Golgi complex associated with the cells secretory system. These cells are directly exposed to any noxious agents in the inspired air and they appear to be secreting SAPL to mask their own receptors, thus, moderating the sensitivity of the constrictive reflex.

The 'unmasking' or 'uncovering' of receptors as a mechanism for explaining sensitisation of a particular reflex is commonly used in neurophysiology. Typically, only 1-5% of the receptors are unmasked at any one time, and 95-99% remain masked. Knowing that phospholipids and phosphatidylcholines (PC) in particular are present in every cell in the body, and in their

disaturated form (DSPC) constitute the lung surfactant. It can be argued that, surfactant molecules can pack together very tightly as depicted in Figure 10. Surfactant is also present in the stomach where DSPC has been demonstrated to be a corrosion inhibitor, proving Davenport's original concept of a gastric mucosal barrier (Hills *et al* 1983).

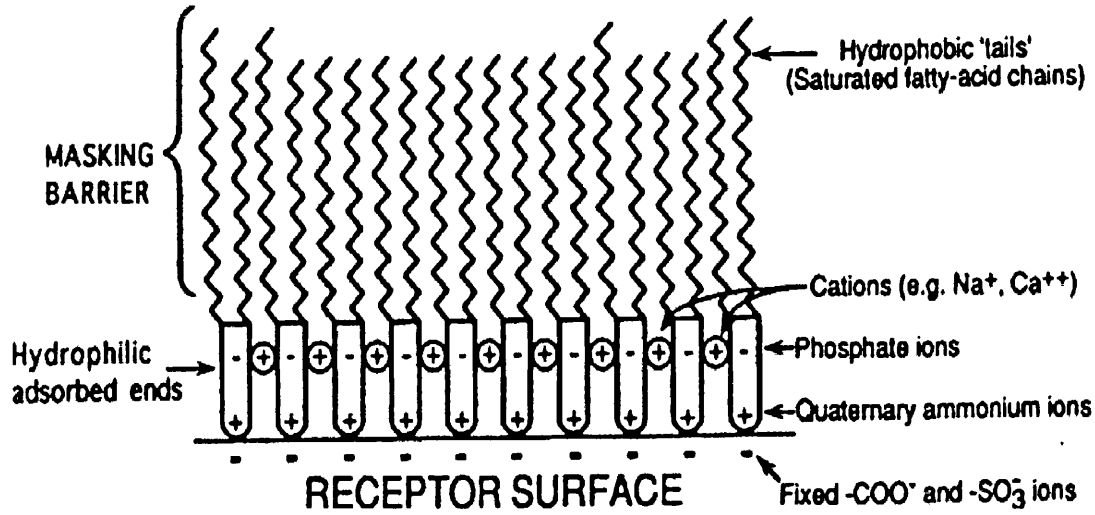

Figure 10: A diagram showing the adsorption of DSPC molecules to a receptor surface.

The above is achieved by reversible binding of the positive charge at the polar end to negative charges that are present on all tissue surfaces. The non-polar ends are orientated outwards and, as straight (saturated) fatty-acid chains, pack together to form a barrier and render the surface hydrophobic. Reproduced from Hills *et al* (1996b), with the author's permission.

Agents which may promote or compromise the non-specific barrier of SAPL and cause adsorption or desorption of surfactant include the following:-

a) Physical Agents: Any layer of SAPL renders the surface hydrophobic, therefore, impermeable to water and resistant to fluid shifts across the epithelial surface. However, strong osmotic gradients could cause the barrier to be ruptured, explaining bronchial hyperresponsiveness to non-isotonic aerosols (Smith and Anderson 1990). With hypertonic aerosols (e.g. seawater spray) the outward shift of fluid from the tissue would lift the coating off the receptors. However, hypertonic aerosols do not strip the airways of epithelial cells, so a coating of adsorbed surfactant could provide a semi-permeable membrane. Fluid shifts across into the airways occur during increased ventilation (e.g. exercise), explaining why

some asthmatics become more sensitised during this period (Woodcock 1992). Some airborne particles such as α-quartz have a strong affinity for surfactant and would, hence, compete with the receptors for adsorbed SAPL. This competitive adsorption could explain dust-induced asthma or similar forms of occupational asthma.

b) Dietary Aspects: One important aspect of the adsorbed SAPL layer is its need to be comprised of DSPC, so that it can form the close mosaic packing depicted in Figure 10. Therefore, a dietary change from a predominantly saturated to unsaturated fats could lower the proportion of SAPL being DSPC. This would result in a less-effective masking agent, which may explain the link in switch from butter to margarine over the last decade, which has coincided with a ten-fold increase in childhood asthma over this period (Hodge *et al* 1994). Claims have also been made that consumption of fish oil, rich in saturated lipids, leads to lower incidences of asthma (Hodge *et al* 1995).

c) Chemical Agents: If the gastric mucosal barrier theory is correct, then agents which compromise the barrier and lead to ulcers should also provoke asthma. One such agent is bile, known to induce heartburn if present in gastro-oesophageal reflux. There are suggestions that bile in its aspirated form may travel up the airways and potentiate asthma (Urschel and Paulson 1967). Some enzymes which can potentially break down the surfactant barrier are contained in the faeces of house dust mite, known to cause asthma (Voorhorst *et al* 1967). Leakage of plasma proteins into the airways during the inflammation process (as described in 1.2.1.2 The Inflammatory Process and Bronchial Epithelium, page 5) have been shown to be reduced by surfactant secretion, thus, preserving the adsorbed SAPL layer (Robertson and Taeusch 1980).

d) Other Agents: Steroids have been shown to promote the secretion of SAPL in the lung (Torday *et al* 1975), thus replenishing the SAPL barrier resulting from inflammation. Mucus may have an important role in stabilising the hydrophobic layer of the SAPL barrier by reducing its interfacial energy with bronchial fluid, thus, SAPL deficiency could be linked to viscid mucus plug found in the airways of asthmatic patients (Barnes and Thompson 1992). Prostaglandin (PGE_2) has been shown to have an inhibitory effect in the airway nerves, reducing the bronchoconstrictor response. PGE_2 is also known to be involved in surfactant synthesis (Lichtenberger *et al* 1985). β_2-agonists are known to invoke an immediate and

dramatic release of airway surfactant when administered, so they help in the replenishment of the barrier (Enhorning 1989).

e) Asthma Challenge Agents: Histamine or Methacholine are used in diagnostic challenge tests in asthma. These substances test the integrity of the SAPL barrier by competing with SAPL for adsorption sites on the epithelium receptor surfaces. Methacholine and its isomer, acetylcholine, both posses a quaternary ion, which as a positively charged group, enables SAPL to bind to negatively charged epithelium. Hohlfeld *et al* (1997) has suggested that surfactant aerosol may prevent acetylcholine from reaching the airway smooth muscle.

Use of exogenous surfactant to treat asthma was first carried out in a pilot study undertaken by Kurashima *et al* (1991). Exosurf® was administered via nebulisation (10mg/ml dose) to eleven volunteers with allergic asthma. Results showed marked improvements in respiratory functions including improvements in: Forced Vital Capacity (FVC), Forced Expiratory Volume in 1 second (FEV_1), Maximal Mid-expiatory Flow (MMF), and improvements in gas exchange. Since Kurashima's pilot study, published papers indicate that surfactant aerosolisation has either led to improvements in or has an important role in the following:-

a) Maintaining the patency and stability of the small airways- as shown by (Enhorning *et al* 1995, 1996, Hohlfeld *et al* 1997, Liu *et al* 1991, 1996, and Vanderzwan *et al* 1998).

b) Improvements in Bronchial Clearance- as shown by Schurch *et al* 1990.

c) Modulation of the function and repair mechanisms of respiratory inflammatory cells- (Van Iwaarden 1992, Holgate 1998, Hoymann *et al* 1998).

d) Increase in airway hyperresponsiveness, a decrease in surfactant production and activity in asthmatics due to plasma protein leakage into the airways or other factors- (Hoymann *et al* 1998, Kurashima *et al* 1997, Lemarchand *et al* 1992, Liu *et al* 1995 and 1997).

e) Improvements in Pulmonary Function- (Anzueto *et al* 1997, Kurashima *et al* 1991)

Future investigations are likely to concentrate on:-

a) Attaining a better understanding of the role of the surfactant in the inflammatory process, both *in-vitro* and *in-vivo*.

b) Attaining more human data on the effect of aerosolised exogenous surfactant on asthma.

c) Definitive elucidation of the pathogenesis of asthma with respect to the pulmonary surfactant.

d) Mechanisms and pathways leading to increased secretion of indigenous surfactant.

1.3.2 Potential Uses in Non-Respiratory Disorders

The potential use of surfactant therapy in areas other than respiratory disorders have been outlined by a number of authors (Hills 1984, Fornadley and Burns 1994, Nemechek *et al* 1997, Yamanaka 1991). Interest in this area has arisen because of the discovery of the existence of surfactant producing (lamellar body) secreting cells in extrapulmonary sites (Dobbie and Anderson 1996). These sites include the serosal mesothelium (peritoneum, pluera, and pericardium), and joints (type A and type B synovocytes). Thus, research into non-respiratory, systemic conditions has intensified, where for the first time an organelle and associated proteins (i.e. SP-A and SP-A like proteins) provide a link between diverse tissues affected by a common substance (i.e. surfactant).

1.3.2.1 Intraperitoneal Postsurgical Adhesions

The presence of surface active phospholipids (SAPL) has been demonstrated to be present in the pleural surfaces of dogs as far back as 1982 (Hills *et al* 1982). Hills postulated that SAPL might have effects such as lubrication and conferring of water repellency to surfaces. Furthermore, he went on to say that phospholipids adhered to both parietal and visceral pleural surfaces, held in place by the attraction of the positive charge of the choline head group to the negative charge of the pleural surface. Grahame *et al* (1985) made the implications of these findings to patients with adhesions. Since then, some authors have reported that phosphatidylcholine (PC) reduces post-surgical adhesions in animal models (Rozga *et al* 1990, Rajab *et al* 1991, 1995, Hills 1992a, 1992b, Hills *et al* 1996c, 1998, Kappas *et al* 1992, Snoj *et al* 1992). More recently, lamellar bodies have been shown to be present in the human peritoneum in a detailed study carried out by Dobbie and Anderson (1996). Hills *et al* (1996c)

further proved the existence of SAPL as oligolamellar layers adsorbed to pleural mesothelium. He postulated that SAPL probably lubricates pleural sliding, and this concept has been transposed to the peritoneum where SAPL has been detected in the dialysate fluid following continuos ambulatory peritoneal dialysis. Heu *et al* (1997) confirmed the presence of PC in the peritoneum along with surfactant proteins SP-A, SP-B and SPD. It is proposed that the SAPL is very similar in composition to surfactant on the alveolar surface of the lung.

Postoperative adhesions (after laparotomy) are a common and serious surgical problem resulting in considerable morbidity and economic loss (Beck 1997). In a British study carried out in 1990 and 1993, adhesions were found in ~24,000 patients, 93% of patients who had undergone abdominal procedures (Menzies and Ellis 1990, Scott-Coombes *et al* 1993). Whilst in the USA over 400, 000 surgeries were performed for adhesiolysis in 1993 (Beck 1997). The average hospital stay for adhesion patients is ~15 days, with the cost of hospitalisation and subsequent care running into millions of pounds and dollars.

Figure 11: An example of a real adhesion operation in the clinic

Adhesions are the main cause of mechanical small bowel obstruction and female infertility (Ellis *et al* 1999, Rajab *et al* 1991). Furthermore, the presence of these adhesions makes re-operation difficult. Treatment and prevention of adhesions have included the use of mechanical barriers, topical agents, anti-inflammatory drugs, physical agents, anticoagulants, fibrinolytic agents and enzymes (Rajab *et al* 1991). Osada *et al* (1999) have reported the use of a haemostatic and anti-adhesion preparation to prevent post-surgical adhesions.

TachoComb, an experimental product, consisting of equine collagen in a sponge-like form coated on one side with human fibrinogen and bovine thrombin was used as a haemostatic and a physical barrier to inhibit post surgical adhesions. However, as yet, there is no established treatment. The use of SAPL in the treatment of adhesions is a real possibility.

1.3.2.2 Otitis Media with Effusion (Glue Ear)

Persistent otitis media with effusion (OME), or glue ear, is the most common cause of hearing loss during childhood, and the most frequent cause for elective surgery in children (Maw *et al* 1999). If left untreated, glue ear can lead to impairments in language and speech development. In the short term, the hearing deficit due to effusion in the middle ear is correctable by insertion of a ventilation tube (grommet). In the long term, hearing gain after ventilation tube is not maintained. Whilst effective, ventilation tubes do carry the risk of allowing water (and thereby infection) into the ear and therefore the patient must keep their ears dry for the duration that the tube is in place (8-12 months). Ventilation tubes also carry the additional risks of causing: 1) infection by acting as a nidus and 2) residual perforation of the eardrum after the tube has been extruded.

Under normal physiological conditions, the middle ear (an air filled cavity) opens via the auditory (Eustachian) tube into the nasopharynx and through to the exterior. The tube is usually closed, but during swallowing, chewing, and yawning it opens, keeping the air pressure on both sides of the eardrum equalised. However, glue ear in children may develop as a result of viral, bacterial, or allergic agents that cause fluid accumulation. As a result the mucous membranes at the aural end of the Eustachian tube have been described as been 'glued together', which in turn prevents the normal flow of gases (Pearlman 1967).

It has been hypothesised that SAPL plays a role in normal Eustachian tube function, and *in-vivo* animal studies have shown that surfactant treatment by direct, topical application of drug to the middle ear may be a viable alternative to surgery (Hills 1984, 1992a, Fornadley and Burns 1994, Nemechek *et al* 1997). SAPL found in the Eustachian tube has essentially the same physical and chemical properties as surfactant present in the lung (Birken and Silen

1973). Middle ear exudate contains an appreciable amount of proteins (Juhn and Huff 1976). Proteins are very effective adhesives and serous otitis media is a condition in which the luminal surfaces of the Eustachian tube become very adhesive due to serous effusion resulting in poor middle ear ventilation and fluid accumulation leading to hearing difficulties. The SAPL identified in the Eustachian tube are absorbed to the epithelial cells lining the walls of the tube where they form a protective barrier and oppose the strongly adhesive nature of these proteins (Hills 1984). It has been shown that indigenous SAPL recovered from irrigation of the Eustachian tube with saline is an excellent release agent, reducing the force of adhesion between two surfaces glued by albumin by 94% (Hills 1984). This implies that applying exogenous surfactant (i.e. SAPL) to the Eustachian tube would facilitate tubal opening and, thus, reduce the risk of serious otitis media.

1.4 Aerosol Characteristics

The use of inhaled therapeutic aerosols is a common and established method for the treatment of lung diseases such as asthma and irreversible chronic obstructive lung disease.

An aerosol is defined as a relatively stable colloidal suspension of solid or liquid particles in a gas, usually air (Byron 1990). The aerosols may either be in the form of a pressurised metered dose inhaler (pMDI), a dry powder inhaler (DPI), or a nebuliser (See 1.5 Inhalation Devices, page 53).

1.4.1 Ideal Aerosols

The efficacy of the inhaled aerosol depends upon some factors regarding the particles that comprise the aerosol. The aerosol must be able to reach the desired site of action in the respiratory tract (i.e. pulmonary region). Effective, therapeutic concentrations of the aerosol must be delivered within a small number of breaths for a device or formulation to be practical. The aerosol particles must be capable of releasing the drug particle at the site of action, before clearance mechanisms carry the compound away from the deposition site.

1.4.2 Dry Powder Formulations for Inhalation

Dry powder formulations can consist of: drug particles with no other components, drug with a coarse carrier particle (a binary blend), drug and carrier particle plus other excipient(s) (ternary blend), or even more complex systems involving carrier particles of different sizes and excipients as well as the active compound. A variety of terms (e.g. ED, FPF, FPD) are used to describe the aerosol performance, in-vitro. These terms are defined in Table 5, page 70.

In order for a drug particle to reach the lung, it must have an aerodynamic size range of 1-5μm (density ~1 ±0.5 g/cm^3), termed the respirable fraction. However, recent publications by Edwards *et al* (1997, 1998a, 1998b) have argued that large porous particles of insulin with mass density <0.4g/cm^3 and aerodynamic diameters of >5μm are also respirable. Edwards has shown that these particles escape the clearance mechanisms of the lung by virtue of their size, and that delivery of insulin to the systemic system resulted in elevated levels of the drug for up to 96 hours. *In-vitro* studies showed a fine particle fraction (FPF) of 50 ±10%. *In-vivo* studies in rats showed that tracheal deposition of the porous particles were 46% compared with 79% for non-porous particles. The percentage porous particles reaching the rat lung were an order of magnitude higher than the non-porous material.

To get the desired size range, techniques such as milling and spray-drying may be employed. To aid dispersion of the small drug particles and increase the emitted dose from a delivery

device, coarse and / or fine carrier particles (usually lactose) may be used in the formulation. In addition, the various physical forces that govern particle aggregation and adhesion must be well understood.

1.4.2.1 Particle Size

Particle size is the most important parameter for characterising the physical behaviour of aerosols (Colbeck 1998). Aerosols can have a wide variety of shapes and size (termed polydisperse). The particles in question may be spherical, fibrous, or aggregates of small particles of similar or different shapes. Consequently, it is difficult to describe an aerosol using a single number. The term aerodynamic diameter (D_A) is one way of describing size of a particle and is related to the settling velocity of that particle in air. D_A is the diameter of a perfect sphere of unit density (1 g/cm^3, equivalent to 10^3 kgm^{-3} in S.I. units) that has the same terminal settling velocity in air as the particle in question (Byron 1990).

To describe an aerosol, precisely, one needs to describe the size of the particles in terms of some measure of the shape of the distribution. The most popular size distribution of physical phenomena is the normal (Gaussian) distribution (Colbeck 1998). This distribution can be described by the mean value and the standard deviation. However, this type of distribution is not seen in aerosol science except in cases where particles are monodisperse. Aerosols exhibit a skewed distribution due to their polydispersity, with a long tail in the distribution curve that extends out to relatively large particles. These types of distributions are often described as being log-normal. Therefore, geometric mean (GM) value and geometric standard deviation (GSD) are used to describe the distribution. GM and GSD are obtained from count or mass distributions. The median diameter (which for a log-normal distribution equals the geometric mean) is termed the count median diameter (CMD) or mass median diameter (MMD). Therefore, CMD is equivalent to the particle diameter at which 50% of all particles in a polydisperse, log-normally distributed, systems have a larger diameter than this value.

MMD is the particle diameter above which 50% of the aerosol mass is contained. Area median diameter (AMD) is the particle diameter above which 50% of the aerosol surface area is contained. The GSD and GMD can be used to calculate the MMD and AMD in a log-

normal aerosol distribution using the equations first derived by Hatch and Choate in the 1920s. Mass median aerodynamic diameter (MMAD) can be calculated by first calculating the MMD and then manipulating the figure to take account of the particle density. MMAD is the particle diameter at which 50% of the aerosol mass is contained in particles above that diameter and 50% is contained in particles below that diameter (Brain and Blanchard 1993).

1.4.2.1.1 Methods for Altering and Controlling Particle Size

Coarse powders can be made respirable by milling, types of which include ball milling, colloid milling, hammer milling, and air-jet (also called fluid energy or attrition) milling. The majority of inhalation powders are prepared by jet milling employing a process known as micronisation. This and the other types of milling are destructive in the sense that solid particles are shattered, and reduced in size due to collision or grinding (Johnson 1997). Constructive methods of particle reduction also exist, they are spray-drying, freeze-drying (lyophilisation), and supercritical fluid particle generation (Sacchetti and Van Oort 1996).

The type of milling employed generally depends on the required products. Hammer and ball milling generally reduce particle size to ~50μm, although smaller particles can be obtained depending upon how brittle the sample is. Ball milling has been around for about 100 years, and utilises the motion of tumbling bodies (usually spherical stainless steel balls) within a closed container which rotates (Prior *et al* 1990). When the sample is introduced, direct pressure is applied by impaction or shear to pulverise and grind the material.

Colloid mills are wet mills that consist of high-speed, profiled, disc-shaped rotors, which force the suspension, under high pressure, through narrow gaps into a housing. The particle size reduction is dependent on the size of the gap and the rate at which the material is forced through it.

Hammer mills reduce particle size by applying impact stress on the solid surface, from implements that swing from a rotor. The velocity of the rotor and the grinding action of the implements allow for continuous milling, limited only by the feed rate of the sample. There may also be a grate or a screen, and the perforations on them determine the final particle size.

In air-jet milling, size reduction is obtained by particle-particle collision and attrition (Carstensen 1993). Particles are carried on a high-velocity air jet in a direction opposed by an equally large opposing jet. The resulting turbulence causes particles to collide at high speed and to fracture into smaller ones. The gas stream moves in a spherical path and smaller particles exist near the mill's centre (cyclone) and are directed into a collection vessel. Large particles are forced to the periphery by centrifugal forces and stay in the cyclone to undergo more inter-particle collisions, until they are small enough to be directed into the collection vessel. Crystalline or friable material can be micronised to <5μm, ductile materials are unsuitable for micronisation and may require chilling or immersion into liquid nitrogen in order to make them more brittle. The rate of micronisation depends upon the dimensions of the feed hopper and the nature of the sample.

These destructive methods of milling although good at reducing particle size, have some disadvantages, they include: sample charging, production of cohesive products, being unsuitable for some products (e.g. micro-crystalline cellulose), loss in crystallinity and scale-up problems (York and Hanna 1997).

The constructive methods for altering and controlling particle size include freeze-drying, spray-drying, and supercritical fluid technology. Freeze-drying or lyophilisation is used extensively in the preparation of protein and peptide formulations. However, one cannot control the size or morphology of the particles, and powders produced are often coarse / amorphous and require milling or spray drying for reduction in size (Johnson 1997). Spray drying is a one-step process that converts a liquid feed to a dried particulate form (Sacchetti and Van Oort 1996). The feed can be a suspension / slurry, colloidal dispersion (e.g. emulsions, liposomes etc.), or paste. The fluid is atomised to a spray form which is incontact with a hot gaseous medium. The large surface area of contact results in rapid evaporation of the droplets to form dried solid, often spherical, particles. Application of spray-drying to powder formulations for inhalation is increasing. In particular, pulmonary delivery of peptides and proteins (by spray drying) and subsequent powder formulation has been demonstrated, amongst others, by Lucas *et al* (1997). The main advantage of spray-drying with respect to pulmonary drug delivery are the ability to manipulate and control particle size, size distribution, particle shape, and density in addition to macroscopic powder properties such as bulk density, flowability, and dispersibility.

Supercritical fluids (SCFs) have been in use in analytical chemistry for many years. However, it has recently been applied to powder technology for its potential to produce uniform particles where the size distribution and morphology can be controlled (York and Hanna 1997). Above a fluid's critical point, a solute's solubility can be altered considerably by small changes in pressure. A rapid de-pressurisation of a SCF containing a solute causes supersaturation, which leads to high nucleation and crystal formation. Carbon dioxide is used as a solvent in SCF applications where it is dissolved in organic solvents. The dissolved gas expands the liquid phase, which decreases its cohesive energy density and causes a solute to precipitate (Johnson 1997).

Once the desired particle size is obtained by using one or more of the methods described, it may be fractionated using sieving methods. The two most commonly used techniques are mechanical sieve analysis and air-jet sieve analysis.

1.4.2.2 Agglomerated and Carrier-Based Systems

Drug-only formulations for inhalation which consist of the active compound, and no other excipient, may be processed using the techniques described previously to achieve the particle range (1-5μm) necessary for deep and peripheral lung penetration. However, powder formulations usually utilise carrier particles (lactose, occasionally dextrose) as bulking agents. The carrier particles are introduced to the drug by various mixing techniques. These small particles associated with the carrier are inherently cohesive, thermodynamically unstable due to excessive levels of surface free energy, and have poor flow properties. Cohesion and adhesion of the particles to form agglomerates, and to adhere to surfaces of carriers serves to lower the surface-free energy and to produce more stable, ordered units that should be more free flowing (Lord and Staniforth 1996). These agglomerates are intended to break-up on delivery and inspiration to produce discrete particles for inhalation.

1.4.2.2.1 Mixing Theory

Various types of mixing include random mixing, non-random mixing, ordered mixing, and total mixing. Staniforth (1982) and Travers (1988), amongst others, have extensively reviewed the theory and the mechanisms involved in each case. Briefly, random mixing was described by Yeung (1979) as a statistical process by which the bed of particles is repeatedly split and recombined until there is an equal chance of any individual particle being at any given point in the mix at any one time. The mechanisms of random theory, which include shear mixing, diffusive mixing, and convective mixing were outlined by Lacey (1954).

In practice, pharmaceutical powders are never random, and the theory of non-random mixing states that the probability of finding any constituent particle in a mix is not equal (Williams 1969).

In order to produce a solid-solid mix, which may typically contain coarse and fine particles as described above, work must be done overcome the influence of gravity on the particles (Staniforth 1982). The system produced by mixing coarse and fine powders has been described as interactive or ordered. Such a system was first described by Hersey (1975). Ordered mixing depends upon the adhesion or cohesion of fine particles onto a host or carrier particle. Travers and White (1971) were the first to note that adsorption of fine particles onto the carrier crystal prevented the segregation normally associated with differences in particle size predicted by the theory of random mixing. Travers (1975) later stated that some sites in an ordered mix were more strongly binding than others. This was confirmed and enhanced by the findings of Lai and Hersey (1979), who proposed that competition for binding sites existed when a third component was added to the mix. Kassem and Ganderton (1990) found that low surface rugosity appeared to allow redispersion of the drug particles more effectively than carriers with high surface rugosity. More recently, Staniforth (1997) used atomic force microscopy (surface topography studies) to prove that there were high and low energy binding sites on the surface of carrier lactose particles. Furthermore, it was suggested that these high-energy sites adversely affected the fine particle fraction (FPF) in formulations, because the force of deaggregation does not exceed the force of adhesion of the drug particles to the carrier surface. Staniforth (1997) proposed that these high energy sites on coarse lactose

particles may be rendered inactive by pre-blending with fine lactose particles (FPLs), leaving the more passive sites available for drug adhesion. As a consequence, the FPF of subsequent formulations treated in this way were higher than the untreated lactose carriers. In addition to this, Lucas *et al* (1997) showed that addition of FPLs to a coarse carrier not only inactivated high-energy sites, but that FPLs also existed as individual particles or fine particle multiplets (FPMs). When the drug component was added to the mix, it was shown that the drug was associated with the FPMs as well as adhering to sites on the coarse carrier. It was proposed that the liberation of the drug particles from the FPMs occurred more readily than from the coarse carrier. In conclusion, it was proposed that distribution of the FPL and the ternary drug compound on the surface of the carrier was not uniform, and combinations of FPL-FPL-Drug, FPL-Drug-Carrier, and Drug-carrier aggregations were present in the formulations. Staniforth (1997) also proposed the action of FPL on agglomerated powder systems. It was suggested that the presence of FPLs served to disturb interactions between cohesive drug particles so facilitating deaggregation.

Total mixing theory has been described by Staniforth (1981), amongst others. It encompasses both random and ordered events to produce a homogeneous final mix. Hence, it is considered that mixes produced for dry powder drug delivery contain particles mixed in a random, non-random, ordered, or partial ordered random configuration, or by any combination of these mechanisms (Staniforth 1982).

Segregation of particles in a mix occurs due to significant differences in particle size, shape, and density (Travers 1988). Segregation is most likely to occur in free flowing powders with large particle size distributions (Johanson 1996). Mechanisms of segregation include trajectory segregation, percolation segregation, and densification segregation and are reviewed in detail elsewhere (Staniforth 1982, Carson 1988, Chowhan 1995).

1.4.2.2.2 Interparticulate Forces

Interparticulate forces can be broadly divided into two groups depending upon whether they arise principally due to electrostatic or molecular interactions. In 1982 Staniforth and Rees showed that during mixing, powder components could become charged due to electrostatic interactions, and postulated that the mixing vessel itself could influence the charging. Triboelectric charging (or triboelectrification) is a phenomenon, which occurs due to erratic movement of powder particles in mixes and other such environments, causing frequent collisions of particles with each other and with the surfaces of the vessel in question (Balachandran 1987, Vissier 1989). This leads to contact charging which occurs when there is an imbalance in the work functions between contacting solids (Stewart 1986). The work function is the difference in energy between the outermost conduction band of electrons (i.e. Fermi level), and some outer reference level (i.e. vacuum energy level). Therefore, an interfacial charge transfer of electrons takes place between two dissimilar materials, and the direction of the transfer depends upon which of the two materials (or material Vs surface) has a higher affinity for the electrons in that contact area (Fuhrer 1996). Once an electrostatic charge has developed, two types of interaction may contribute to the adhesion process in ordered mixes, namely the formation of electric double layers (formed at interface upon contact between two particles), and Coulombic interactions which arise due to interactions between charged particles and uncharged surfaces. Unlike chemical linkages, electrostatic interactions cannot be saturated and they play a vital role in particle cohesiveness and adhesion. Measurement of electrostatic forces and investigations into triboelectrification, charging mechanisms of lactose with different surfaces and measurement of adhesive forces has been extensively studies by Peart (1996)

Molecular interactions also have the nature of electrostatic interactions but with small charges or polarisations on the molecule or only on some atoms of the molecule that are responsible for the valencies of secondary bonds (Fuhrer 1996). These secondary bonds or van der Waals' forces of attraction are classified into dipole-dipole or van der Waals'-London interactions. These forces are effective at short distance (0.2-1nm), when two molecules are close to each other and decrease rapidly with distance. The effect of these forces are only noticeable when

they are greater than the gravitational forces or hydrodynamic interactions influencing the powder particles.

Interparticulate forces and interactions are influenced by a number of factors, such as: particle size, shape, texture, drug to carrier ratio and humidity (Bailey 1984). If the primary particles are irregular in shape, or deviate significantly from sphericity, their aerodynamic behaviour is affected, hence, shape is a component in the expression of particle diameter (Hickey and Concessio 1997). A variety of methods are used to define particle shape including microscopy, Fourier analysis and fractal analysis. These methods result in dimensionless numbers that reflect the magnitude of particle shape irregularity. In terms of adhesion of particles, as sphericity decreases, contact area between particle and carrier increases, leading to increases in adhesion force. However, Wong and Pilpel (1988) reported that irregular shaped particles formed more stable ordered mixes than spherical particles. This reason for this was that there were fewer contact points between irregular shaped particles and carriers compared with spherical particles. As the contact area increases, so do the influence of molecular interactions and the effects of van der Waals forces. The techniques used for altering particle size should be considered carefully when formulating powders, since it may effect particle shape. Generally, micronisation leads to irregular shaped particles, whereas spray-drying and SCF lead to more spherical particles. In addition, as particle size increases, so does surface roughness, as a result, greater energy is required to remove drug particles from clefts on the carrier surface (Staniforth 1987, Kassem and Ganderton 1990). Therefore, a compromise needs to be made between the size of the carrier particles, their surface roughness, and shape / size of the drug particles to compile a dry powder formulation with adequate deep-lung deposition profile.

The effect of humidity on adhesive forces has been studied by a number of authors (Karra Fuerstenau 1977, Stephenson and Thiel 1980, Thiel and Stephenson 1982, Kulvanich and Stewart 1988). The basic conclusion is that, adhesive forces are humidity dependent and adversely affect the fine particle deposition from formulations (Jashani *et al* 1995, Braun *et al* 1996). At low relative humidities (RH) (<30%), electrostatic forces of interaction are dominant, but as %RH increases van der Waals' forces become more prominent. At high RH values (>60%), water may be adsorbed on to the surfaces, causing particle growth and liquid bridges at contact points between carrier and drug particles. The rate of growth and the

formation of the liquid bridges are dependent on how hygroscopic the drug particles are. Drying of formulation and / or drug particles may cause the liquid (forming the bridges) to be evaporated off, but this may lead to the formation of solid bridges between two particles. Solid bridges will also influence the deposition behaviour of the formulation. Therefore, hygroscopic materials may need to be stored under special conditions, such as in a desiccator with a saturated salt solution of low RH.

1.4.3 Aerosol Deposition Mechanisms

The three, main, mechanisms by which aerosols are deposited in the respiratory tract are inertial impaction, sedimentation, and diffusion (Hinds 1982,1999, Byron 1990). Other mechanisms such as electrostatic deposition and thermophoresis (thermodiffusion) have been proposed (Brain and Blanchard 1993), however. These mechanisms are considered to make only a minor contribution to aerosol deposition. The theories underlined in this report will therefore concentrate on the primary mechanisms.

1.4.3.1 Inertial impaction

A particle moving in an airstream from the nasopharynx to the tracheobronchial tree has to negotiate the bifurcations of the upper airways. Whether or not a given aerosolised particle can do this depends upon its inertia (momentum), size, mass and the velocity of the particle in question. When a spray leaves a pMDI (see section 1.5.1 Pressurised Metered Dose Inhalers (pMDIs), page 54) actuator, it does so at high velocity (~100km/h) (Current Perspectives in Inhaled Drug Therapy 1994). The average adult inspires at a velocity of approximately 45 km/h. Because of this linear velocity miss-match, most of the aerosol never reaches the lungs. Rather, inertial impaction of high velocity, high momentum particles occurs in the oropharynx, tongue and soft palate, accounting for some 80-90% of the aerosol that does not reach the lungs. This is a typical scenario for most particles greater than 5μm (Hinds 1982, 1999), although for particles less than 5μm other deposition mechanisms can prevent deep

lung penetration. The probability of impaction in the upper airways can be calculated as follows:

$$Stk = \frac{\rho d^2 V}{18\eta R}$$ **Equation 2**

Where Stk= Stokes number (a dimensionless function), ρ= Particle density
d= Particle diameter, V= Velocity of air, η= Air viscosity, and R= Airway radius

The higher the Stokes number, the higher the probability that larger particles will diverge from airflow streamlines, particularly in the carinal bridges of bifurcations.

1.4.3.2 Sedimentation

Sedimentation due to gravity affects particles in the size range of 1-5μm and is a time dependant process. Those particles that are <0.5μm are influenced by diffusion. Deposition via sedimentation is the main mechanism by which the aerosol particles are deposited in the pulmonary region (small airways and alveolar spaces), during either breath-holding or slow tidal breathing. However, whether or not the particle reaches this region depends upon the following factors:

a) Viscous forces (drag due to the airstream) acting on the vertical direction of the particle.
b) The location of the particle within the airstream and its position with respect to the bifurcating airways.
c) Velocity of the particle.
d) The angle of inclination of the airway with respect to the horizontal (called the zenith angle).

Therefore, if the particle is located close to the walls of the lower airways and / or does not have sufficient velocity, or the angle of inclination is too great to be successfully negotiated, then the particle will sediment due to gravity. Landahl first calculated the probability of

sedimentation in the lower airways in the 1950s. The rate of sedimentation in air can be calculated using Stokes settling equation as follows:

$$u = \frac{gd^2(\rho_1 - \rho_2)}{18\eta}$$ **Equation 3**

Where u= Terminal rate of sedimentation, ρ_1= Density of particle, ρ_2= Density of air
d= Particle Diameter, η= Viscosity of air.

This equation shows that the rate of sedimentation is dependent on particle size and density, it is only applicable for spherical particles settling in air.

1.4.3.3 Diffusion (Brownian Motion)

Diffusion is defined as the process whereby gasses and liquids of different concentrations intermingle when brought into contact, so that their concentration becomes equalised throughout the system (Roper 1987). Brownian motion refers to the bombardment and transfer of energy from air molecules to other larger particles causing these particles to undergo random motion (Hinds 1982, 1999, Byron 1990). The theory of Brownian motion (diffusion) was originally deduced by Einstein and republished in the 1950s.
Aerosol particles, like gas molecules, will tend to diffuse from regions of high particle concentration to regions of low particle concentration. Only particles <0.5μm are affected by diffusion and diffusion is the main mechanism of deposition of these particles in the lower airways. Compared with the previous two mechanisms, diffusion probably has the least influence on deposition patterns of aerosols, since most therapeutic aerosols have a low percentage, by volume, of particles <0.5μm diameter.

1.4.3.4 Other Mechanisms

Particles in the airstream may be subjected to other mechanisms such as interception or electrostatic forces. Interception affects fibrous particles and occurs when the edges of the particle make contact with the walls of the airways due to its relative position and trajectory in the airstream. Electrostatic forces may also be responsible for depositing particles in the airways (Balachandran *et al* 1991). Particles produced by high velocity dispersions of solid or liquid material may be highly charged and if inhalation occurs without neutralisation in the atmosphere, then this mechanism may influence particle deposition.

1.5 Inhalation Devices

Despite the numerous methods that can be employed to generate aerosols, only three basic systems have found commercial success, these are: pressurised metered dose inhalers (pMDIs), dry powder inhalers (DPIs), and nebulisers, (Newman 1991, Dalby and Tiano 1996). There is great interest in the development of new inhalation devices and delivery systems to make inhalation therapy easier and more reliable for patients, to develop inhalers using alternative propellants, and to deliver a range of novel compounds to the lungs (Newman 1994). In order for an inhalation system to be acceptable for clinical use, it must meet certain criteria:

a) It must generate an aerosol with most of the drug carrying particles less than 10μm, and ideally in the range of 0.5-5μm, the exact size depending on the intended application.

b) It must produce reproducible drug dosing during the period of its use.

c) It must protect the physical and chemical stability of the drug from the external environment.

d) It must be relatively portable and inconspicuous during use.

e) It must be readily used by the patient with minimal training.

Apart from these minimal requirements, the device should ideally provide multiple dosing with minimal excipient inhalation. Ergonomic design, patient convenience, dose counters, an indication of appropriate inhalation flow rates, power-assistance, an alarm to indicate next dose, and other useful features are also desirable.

1.5.1 Pressurised Metered Dose Inhalers (pMDIs)

The introduction of the pMDI in 1956 allowed effective portable aerosol administration for the first time. The development of progressively more specific and effective anti-asthma therapy from the pMDI has improved the quality of life for the typical asthma patient (Clark 1995a, Jackson 1995). This has made the pMDI the most popular form of respiratory drug delivery system.

A pMDI is made up of five main components: a canister, a metering valve, the liquified propellant with excipients, the active compound (either in a suspension or solution), and an actuator housing complete with the mouthpiece for inhalation (Lalor and Hickey 1998).

Chlorofluorocarbons (CFCs) 11, 12 and 114 are used as propellants: a suspension of micronised drug substance, rather than solution, is preferred since most drugs are not soluble in CFCs (Pauwels *et al* 1997). Formulations also incorporate co-solvents such as ethanol to improve the solubility of the drug and / or help control the particle size of the aerosolised cloud. Flavours (such as dissolved mint extract) and suspended sweeteners (e.g. saccharine) may be used to mask the taste of the drug deposited in the throat. To enhance the stability, antioxidants (e.g. ascorbic acid) may be used in formulations where the drug is dissolved. In addition, surfactants (soya-derived lecithin and sorbitan trioleate) are added to the formulation to improve the dispersion of suspended particles or dissolution of a partially soluble drug. Surfactants also maximise aerosolisation (and increase fine particle fraction) of the drug and on release lubricate the valve mechanism of the canister. The canister design has changed very little since the first pMDI. However, great advances have been made in the metering technology, which has led to increased control of particle size of the aerosol as well as the fine particle fraction (Meakin 1998).

Although pMDIs are small, portable and unaffected by the external environment, they nevertheless have a number of disadvantages, which include:-

a) Co-ordination problems: co-ordination between actuation and inhalation by the patient is essential for effective lung deposition (Crompton 1982). However, many patients cannot achieve this requirement, even with training; the importance of patient training has been underestimated (Amirav *et al* 1994). Breath-actuated pMDIs were developed to overcome co-ordination problems. The canister in such devices is spring-loaded and is balanced on top of a flap valve. When the patient breathes through the mouthpiece, the valve opens and the canister is automatically depressed, delivering drug at the ideal time, just at the start of the inspiratory effort. Studies have shown that patients handled breath-actuated pMDIs better than conventional pMDIs and required less training. The use of spacing devices another way of improving co-ordination in pMDIs (Chapman 1994). Spacers force patients to breathe at a distance from the canister orifice, where the spray front is moving much more slowly

b) Incorrect inhalation: Some patients stop inhaling when they feel the aerosol cloud in their mouth, thus failing to inhale it into the lungs.

c) Adverse effects: The propellant / surfactant mixture may cause initial bronchoconstriction. This effect has been reported, using both active and placebo inhalers (Yarborough 1985, Jackson 1995).

d) Humidity problems: High humidity may pose problems in the use of pMDIs (Miller 1990), and they cannot be used effectively in temperatures <5°C (41°F).

e) Residual drug content: There is insufficient information about the quantity of drug remaining in a pMDI. The device may become suddenly and unexpectedly exhausted, thus failing to dispense the required dose (Williams *et al* 1993).

f) Propellant effect: CFC gases (Freon) are harmful to the ozone layer and are the subject of an international treaty (Montreal protocol, 1987) of limitation. Under the latest upgrading of the Montreal protocol, CFC production was banned as of 1st January 1996 and in the European Union the ban took effect on 1st January 1995. At present, developing countries are excluded from the ban for a further 10 years. Current research is in progress on pMDIs that can be operated by hydrofluoroalkanes (HFAs): 134a (Dymel®) and 227 (Solkane®). Please refer to Appendix 1: Summary of the Physical Properties of Hydro Fluoro Alkane (HFA) 134a and *227*

3M HealthCare was the first company to market a non-CFC MDI (Airomir™) in 1995, and studies have shown the efficacy of this product to be better than the original CFC formulation (Purewal 1998). A recent presentation (Meakin 1998) showed that a solution-based pMDI for the delivery of Beclemethasone (using HFA 134a) produced uniform dose delivery in *in-vitro* studies. Furthermore, the study showed that drug stability was not an issue, and a greater control in particle size of the aerosol was attainable using advanced valve systems.
Complete transition from CFC based formulations to HFAs, in America & EU, is expected in the first half of the next decade.

1.5.2 Dry Powder Inhalers (DPIs)

The first, modern DPI marketed was the Spinhaler™, designed and used exclusively for the inhalation of disodium cromoglycate (DSCG) (Crompton 1991). Today there are over 20 existing devices and at least 30 currently known to be under development (Anderson 1998). Examples of these devices are given in Table 2, page 58. Early DPIs showed an equivalence to MDIs, more recently, advances in device and formulation changes have shown an enhancement over MDIs (Nichols 1997).
In 1976, it was reported that patients who could not use conventional pMDIs were able to use the Spinhaler™ (Patterson and Crompton 1976). With most inhalers, like the Rotahaler™, the active compound is mixed with a carrier-powder (usually lactose). The drug particles adhere to the carrier as a result of surface electrical interactions mediated by an electrostatic mechanism, and become separated from the carrier at the time of actuation (Dunbar *et al* 1998). With single-dose inhalers, a capsule is loaded into the inhaler, and subsequently, mechanically punctured or opened in the device using a blade or pin and the dose emitted is inhaled by the patient's inspiratory effort. All currently marketed DPIs are both inspiratory flow-driven and inspiratory flow-actuated (Clark 1995a, Nichols 1997,).
Multi-dose DPIs were developed for the inhalation of bronchodilators and steroid drugs, and to be able to deliver large numbers of metered-doses from reservoirs (e.g. Turbuhaler™) or a set number of deliveries from pre-packaged foil blisters (e.g. Diskhaler™). DPIs were intended to deliver the drug both accurately and precisely, but this point is subject to debate

since the Turbuhaler™ varies considerably in its performance. However, multi-dose DPIs are easier to use than the original, single-dose inhalers (e.g. Rotahaler™), which is another reason for their development.

As a result of the decline in the popularity of the pMDI on the part of manufacturers, as well as the realisation that systemic delivery of drugs (e.g. peptides and proteins, Johnson 1997) could be achieved via the lung has led to increased research into DPIs. By delivering systemic drugs to the lung 'first-pass' hepatic metabolism as well as enzymatic and chemical degradation in the GI tract can be avoided, and the lung can be used as a portal of entry to the body (Newman 1996a). Thus, lower doses would be needed to achieve a therapeutic effect due to advances in DPI drug-deaggregation technology, which has led to increases in the fine particle dose delivered to the patient.

Table 2, page 58, shows some of the DPIs currently available or in development. The active compound delivered by each DPI has been omitted, because in most cases the devices are universal (i.e. capable of delivering more than one type of drug). The metering and dispersion mechanisms have been simplified, and multiple numbers of doses is denoted in cases where the number of doses is not certain.

Device	Type	Dispersion Principle	Metering Mechanism	No. of Doses
Accuhaler	P	Cyclone System	Blister Roll	60
Airboost	A	Compressed Air	Reservoir	M
Biohaler	A	Compressed Air	Blister Cartridge	7
Bulkhaer	P	Cyclone System	Reservoir	200
Clickhaler	P	Spiral System	Reservoir	200
Cyclohaler	P	Deaggregating Mesh	Capsule	Single
Diskhaler	P	Cyclone System	Blister Cartridge	M
E-Haler (Eclipse)	P	Cyclone System	Capsule	4
Flow Caps	P	Cyclone System	Capsule	8
Omnihaler (Kohlerhaler)	A	Vacuum	Reservoir	M
Miat-Haler I	P	Spiral System	Reservoir	M
Mikro-Haler	P	Cyclone System	Reservoir	200
Prohaler	A	Compressed Air	Reservoir	100
Pulvinal	P	Swirl Chamber	Reservoir	M
Rotahaler	P	Deaggregating Mesh	Capsule	Single
Serpracor	P	Venturi Principle	Blister Cartridge	M
Spinhaler	P	Spiral System	Capsule	Single
Spiros	A	Fan assistance	Blister Cartridge	30
Taifun	P	Cyclone System	Reservoir	200
Tape Device	A	Hammer Assistance	Disposable Cassette	M
Technohaler	A	Vacuum	Disposable Cassette	M
Turbospin	P	Cyclone System	Capsule	M
Turbuhaler	P	Spiral System	Reservoir	60-200
Ultrahaler	P	Cyclone System	Reservoir	100+

Table 2 Examples of DPIs currently available or in development.

Key: A (Active), P (Passive), and M (Multiple).

1.5.2.1 Device Design

All DPIs have four basic features: A dose metering mechanism, an aerosolisation mechanism, a deaggregation (dispersion) mechanism, and an adaptor to direct the aerosol into the patient's mouth (Clark 1995a, Prime *et al* 1997). All these features vary from inhaler to inhaler.

Design and engineering of DPIs is an evolving process (Bell and Treneman 1994). The most difficult problems to overcome are reproducible dose metering and acceptable dispersion of the powder. For this reason, the DPIs on the market or in development have either employed pre-filled capsules (e.g. Spinhaler™), multiple depression aluminium blister packages (e.g. Diskhaler™), or metering of a specified mass of powder from a reservoir (e.g. Turbuhaler™).

Metering of powders is a mechanical process and varies from inhaler to inhaler, and is affected by particle size and associated factors discussed previously (section 1.4.2 Dry Powder Formulations for Inhalation, page 41).

The advantages of a pre-metered dose are: firstly, precision in which the dose can be metered in the factory is superior to that which can be achieved by the device alone, and secondly, sealed / protected pre-metered doses can be better protected against the environment. The second point is less of an issue than the first since most modern DPIs offer adequate protection from the environment (Prime *et al* 1997). The advantage of a reservoir metering system is the relative ease and cost of manufacture, since these devices can be bulk-filled with high throughput.

As Table 2, page 58 shows, the dispersion principles used by the various inhalers vary considerably. The Bernoulli, or Venturi effect has received some attention (Cheng *et al* 1989), as well as gas propulsion (Jager-Waldau *et al* 1994), negative vacuum aerosolisation (Nichols 1997), and external mechanical assistance in the form of a battery driven motor. In addition, cyclone and spiral systems utilise the flow path of the incoming air to spin the capsule or subject the drug to a deaggregating mesh / grill to aid dispersion. Devices that use a mechanism of dispersion additional to the patient's inspiratory breath are termed 'active devices' (e.g. Spiros^{TM}). These devices are activated during the inspiratory cycle and provide 'power-assisted' inhalation to the patient. Devices that do not have an additional dispersion feature, rely solely on the turbulence created by the patient's breath to deaggregate drug particles and are termed 'passive'. Currently, the majority of the devices are passive, but development trends point in favour of active devices. Flow path of the incoming air and the design of the mouthpiece (e.g. Turbuhaler^{TM}) can be utilised to create maximum turbulence within a device and further aid dispersion. The Accuhaler^{TM} (Diskus device) has an extremely short flow path (Prime *et al* 1997) and as a results drug losses within the device are minimised. The flow path of the Turbuhaler^{TM} on the other hand is long, specifically designed to maximise turbulence through the spiral channels in order to generate shear forces that would disperse the drug aggregates, and produce good fine particle mass (Wetterlin 1988). A disadvantage with a long flow path is increased device resistance. Higher the resistance, the greater the effort needed by the patient in order to achieve a given flow rate, which may hinder

device performance (Clark and Hollingworth 1993). An in-depth review of device resistance and implications for testing is given elsewhere (Peart 1996).

1.5.2.2 General Advantages and Disadvantages of DPIs

a) Ease of use: a comparison of the ease of use of the Turbuhaler™ compared with a pMDI, showed that a majority of patients (84%) who had never seen any form of inhalation device could use the DPI after reading the instruction pamphlet, and all could be taught to use the device by verbal instruction (Duncan *et al* 1990).
b) Absence of additives and propellants: the original, single-dose, DPIs (e.g. Rotahaler™) used lactose as a carrier for micronised drug. However, new multi-dose DPIs, may only contain micronised drug, leading to less complicated formulations and cheaper DPIs in the future. DPIs do not contain harmful propellants like CFCs, therefore, they are more environmentally friendly.
c) Dosage Control: by giving them a device that has a limited number of actuations, physicians can control the number of doses a patient receives over a period of time. This may be an advantage in patients with low compliance.

The potential disadvantages of DPIs are:
a) Device loading: loading the single-dose inhalers may be too difficult for some patients, therefore, they may need training.
b) Loss of delivery sensation: if the device delivers a small dose (e.g. Turbuhaler™, 0.5mg) the patient may not get the sensation of having inhaled anything, which is not the case with pMDIs. Therefore, the patient may stop inhaling causing a reduction in efficacy of the device.
c) Peak inspiratory flow (PIF) / Device resistance: the PIF required to obtain a therapeutic dose from a DPI may not be attainable by patients suffering from acute severe asthma.
In summary, DPIs are unlikely to completely replace MDIs, but increased research and development of DPIs can only serve to increase their use.

1.5.3 Nebulisers

Nebulisers are devices designed to convert a drug solution or suspension into a therapeutic mist or cloud consisting of aerosolised droplets (Horsley 1988). There are two methods of producing a fine mist from a nebuliser, one is jet nebulisation and the other is ultrasonic nebulisation.

Jet nebulisers are by far the most commonly used and work on the Venturi effect produced by a Bernoulli nozzle. When air is forced through a fine nozzle it forms an area of negative pressure when the high-speed jet of gas emerges. If a tube is placed in this area with the other end in a pool of liquid, the liquid is drawn up, mixed with the high-speed jet and blown out as a cloud of particles. The baffle traps any large particles and they coalesce to fall back into the solution reservoir. The particle size distribution and the density of the aerosol produced depends upon the type of baffle used (Steventon and Wilson 1986).

Ultrasonic nebulisers use a piezo-electric crystal to generate the aerosol. By varying the voltage or current applied across the crystal, one can influence and change the shape of it. The high frequency source is matched to the resonant frequency of the transducer, causing a wave pattern that breaks up the solution above into fine aerosol particles. The particle size produced depends upon the resonant frequency of the transducer, and variations in its amplitude determine the rate of aerosol production (Taylor and McCallion1997).

The aerosol produced may be inhaled either by a facemask or a mouthpiece. Generally, a facemask is considered to be less satisfactory in delivering the aerosol than a mouthpiece, as less drug is deposited in the lung and some is deposited on the mask itself (Dalby and Tiano 1996)

There are three main reasons why nebuliser therapy is effective:

a) The patient requires minimal co-ordination or even co-operation, drugs may be inhaled during normal tidal breathing (McCallion *et al* 1996).

b) The vehicle used (normal, physiological saline) tends to soothe the airways.

c) The dose of the drug administered is large, often 10 to 20 times that received from a pMDI or DPI. Therefore, drugs that do not formulate well in MDIs and DPIs can be delivered.

A variety of nebulisers, operated by electric compressors or by air cylinders are used in hospitals and homes (Flament *et al* 1995). Although nebulisation therapy can be effective in

dealing with asthma, it is nevertheless not without problems and hazards. In hospitals, and at home, problems may arise because of a lack of understanding of administration parameters that affect the performance of the nebuliser and, thus, affect the dose received by the patient. The flow rate of the gas which drives the nebuliser and the fill-volume are of utmost importance in the performance of the device. The fill-volume is important because all nebulisers have a 'dead-volume' (i.e. a residual volume of solution which remains in the device). Therefore, the greater the fill-volume, the greater the fraction of drug released, and the greater the dose received. To avoid problems such as this, training, especially for home use, is essential. Another problem, associated with nebuliser use in hospitals, is that the solution used for nebulisation should be as near isotonic as possible. If a solution for nebulisation needs to be diluted, water should never be used, since this would cause hypotonicity and when nebulised, it could provoke bronchospasms and hence an asthma attack.

The amount of aerosol reaching the lungs from a jet or ultrasonic nebuliser is ~10-20% of the dose placed in the reservoir of the device (Hardy *et al* 1993). However, Knoch and Wunderlich (1994) reported fine particle fractions of 30-35% *in-vitro*, which is about twice the conventional delivery.

Studies have shown great variability in the amount deposited from various nebulisers (Newman 1993a), there are several factors which influence deposition:

a) The type of nebuliser: ultrasonic nebulisers tend to have higher droplet size values (MMDs) than jet nebulisers, but this is not an invariable rule, since the size also depends on flow rate of the compressed gas in the case of the jet nebuliser and the frequency of the signal fed to an ultrasonic nebuliser (Clay and Clarke 1987).

b) Inhalation rate affects particle size and, thus, deposition of the aerosol. If people do not breathe normally, rapid inhalation rates can lead to the formation of larger particles which would normally fall back into the nebuliser reservoir by gravitational forces, but may be drawn up into the inspired aerosol, increasing the MMD values. Humidity of the air, drawn into a nebuliser to provide the auxiliary air necessary for inspiration, may also affect particle size, and hence, deposition. The MMD values increase with increasing % relative humidity values. This is because, when the inspirate is unsaturated, evaporation readily takes place leading to a rapid decrease in particle size (Lewis *et al* 1981).

1.6 Aerosol Testing and Characterisation

A variety of methods and models are available for characterising aerosols, both *in-vitro* and *in-vivo*. The *in-vitro* methods mainly comprise of impaction and impingement, whereas *in-vivo* evaluation and assessment focus on gamma scintigrapghy and pharmacokinetic techniques. This section will review the test procedures and methods used to evaluate:

a) Pharmacodynamic performance (Stevens and Kochuyt 1984, Timsina *et al* 1994, Van Oort 1996, and Hindle and Byron 1996).

b) Pharmacokinetic assessment (Borgstrom *et al* 1996).

c) Gamma scintigraphy (Wilding *et al* 1991, Newman 1993, and Conway *et al* 1997).

1.6.1 Testing Protocol

In-vitro testing of pharmaceutical inhalers has been going through a state of change and harmonisation. There has been a steady effort to standardise the testing conditions across the various pharmacopoeias. The need for change was brought about by the increasing number of DPIs on the market all with varying device resistance. Newman *et al* (1989, 1994a), and Vidgren *et al* (1988) had shown that the flow rate at which a patient inhales through a powder inhaler significantly affects the amount of drug reaching the lung. Clark and Hollingworth (1993), Olsson and Asking (1994) and Hindle *et al* (1994) carried out a series of experiments to determine the relationship between device resistance and the maximum inhaled flow rate. It was found that the maximum pressure drop developed by the chest muscles of adults with respiratory disease, when inhaling through a DPI at peak inspiratory flow rate was in the region of 4kPa (40.8cm H_2O). The following equation was proposed by Clark and Hollingworth (1993): -

$$\sqrt{\Delta P} = Q_D . R_D \qquad \textbf{Equation 4}$$

Where, ΔP is the pressure drop across the device, Q_D is the flow rate through the device, and R_D is the device resistance. Further detail on the testing procedure is given by Ganderton (1996), Olsson *et al* 1998a, Medicines Control Agency (1998) and EP supplement (1999). Hence, drug delivery from DPIs should be determined at an airflow rate equivalent to a 4kPa pressure drop across the device. If the flow rate (required to produce a pressure drop of 4kPa) is greater than $100Lmin^{-1}$, as is the case for low resistance inhalers, then the test should be performed at $100Lmin^{-1}$. Figure 12 and Figure 13 show some of the typical experimental apparatus used to carry out such tests. These apparatus were used in the *in-vitro* aerosol investigations undertaken in this study. Some of the investigations were performed at $60Lmin^{-1}$, which was considered representative of flow rates achievable by patients (BP 1993). Other tests were performed according to the procedures described above.

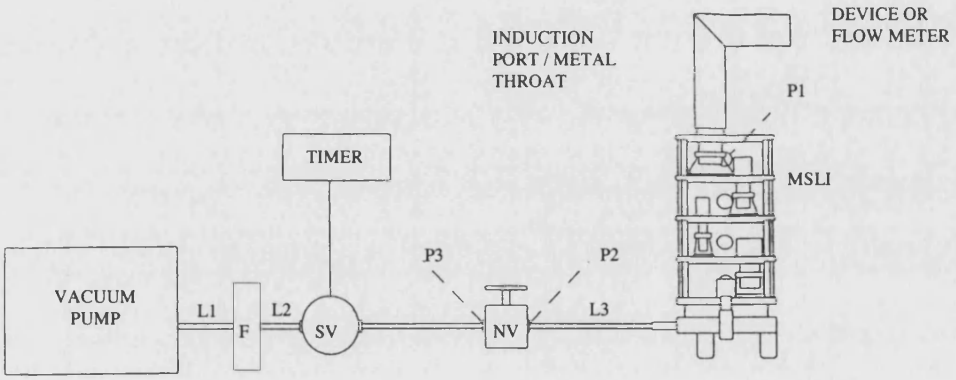

Figure 12: MSLI-Timer-Regulator-Pump Assembly for device testing.

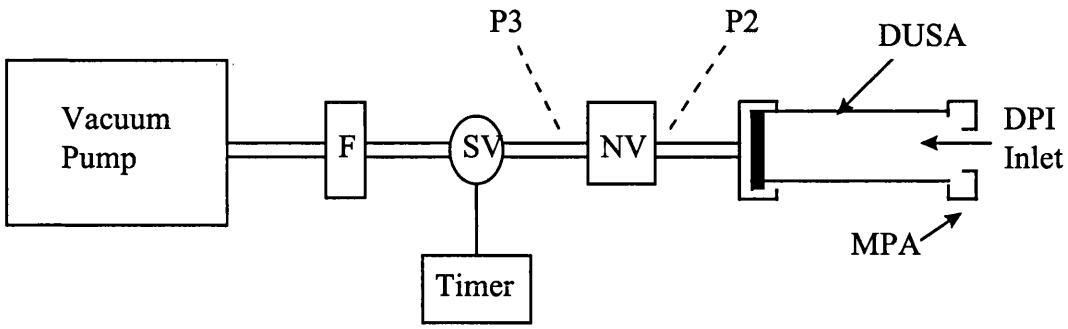

Figure 13: Dose unit sampling apparatus (DUSA) for measuring the uniformity of delivered dose from DPIs.

SV: solenoid valve NV: needle valve F: pump protection filter

MPA: mouth piece and adaptor

P1: Pressure reading for determination of test flow rate (determined using the Hastings Mass Flow Meter, HFM 201, Teledyne Brown Engineering, Hastings Instruments, VA, USA) with a differential pressure transducer (Digitron Instrumentation, Technology House, Herts., UK). Flow rate is adjusted with a needle valve so that P1 is 4kPa.

P2/P3: Pressure reading points for critical flow examination with an absolute transducer (Digitron Instrumentation, Technology House, Herts., UK). The ratio of P3/P2 should be ≤ 0.5 for critical flow.

L1, L2, and L3: are vacuum tubing with internal diameters of at least 10mm. L1 and L2 should be as short as possible whereas L3 should be 30-40cm in length.

1.6.2 *In-Vitro* Methods

In-vitro methods of aerosol characterisation are primarily used to evaluate prototype or new delivery systems, prior to first human use. Testing is rapid, when compared with *in-vivo* assessments and provides vital information on device / system performance and gives a good indication as to how the device / system in question will fair in clinical trials. The techniques used are wide and varied and the models / instrumentation utilised is based on the anatomical

structure of the human airways, be it loosely in some cases. The two methods used throughout this study were the TSI and the MSLI.

1.6.2.1 The Twin-Stage Impinger (TSI)- BP Apparatus A

The TSI is Apparatus A of the British Pharmacopoeia (BP) (1998), Appendix XVIIC, and is a glass, two-stage separating device developed by Hallworth (1987). The TSI was based on the multi-stage liquid impinger (MSLI) developed by May (1966). Stage 1 contains 7ml of test solution (often, mobile phase for HPLC analysis), and stage 2, contains 30ml of test solution. The apparatus is usually calibrated for operation at 60L min^{-1} although higher flow rates may be used. The first impaction point is the glass throat. The particles that do not impact on the throat remain entrained in the air-stream and enter stage 1 of the device, which has a cut-off diameter of 6.4μm at 60L min^{-1}, with a jet diameter of 14mm. The cut-off diameter is predicted by the following equation: -

$$ECD_{50\%} = X\frac{W^{3/2}}{F^{1/2}} \qquad \textbf{Equation 5}$$

Where: ECD= effective cut-off diameter (i.e. the particle size for 50% retention of unit density spheres of equivalent settling rate in air), X= a constant, 30 for TSIs, W= Jet diameter in cm, F= Flow rate (L min^{-1}).

The above equation developed by Hallworth (1987) can be used to calculate the ECD at other flow rates and jet diameters. Therefore, as jet size increases the cut-off diameter decreases.

Stage 1 Jet Diameter (mm)	Calculated $ECD_{50\%}$ (μm)	As measured by AEA Technology (μm)
3.9	1.33 @ 30L min^{-1}	1.3
6.9	3.14 @ 30L min^{-1}	3.2
9.7	5.20 @ 30L min^{-1}	6.6
10.9	6.23 @ 30L min^{-1}	7.3
11.6	4.80 @ 60L min^{-1}	5.3
13.4	5.20 @ 80L min^{-1}	5.37
14.0	6.42 @ 60L min^{-1}	N/A

Table 3: Table showing stage 1 jet-diameter versus TSI cut-off diameters at various flow rates

Particles <6.4μm impact on to stage 2, and constitute the respirable fraction. The result is expressed as the amount of drug collected in stage 2 as a percentage of the total amount of drug emitted from the device.

Although originally developed for pMDIs, the TSI can also be used for DPIs. The advantage of the TSI is that analyses are quick, easy and informative. However, the disadvantage is that the TSI only separates the aerosol into two size ranges, and hence the information concerning aerosol cloud quality is not as detailed as the Andersen impactor or the multi-stage liquid impinger.

1.6.2.2 The Multi-Stage Liquid Impinger (MSLI)

The original MSLI was constructed by May (1966) and later modified to a glass 4-Stage impinger for pharmaceutical use by Bell *et al* (1973). The underlying principles and the mode of action of the MSLI is essentially similar to the Andersen cascade impactor. The 4-stage impinger consists of three stages and an after-filter (stage 4) with cut-off diameters of 13, 6.8, 3.1, and <3.1μm respectively, when operated at 60L min^{-1}. Until 1995, the glass 4-stage impinger together with a glass / metal throat was the only model in use, but Olsson (1995), introduced an extension to the apparatus by the addition of a new stage. This additional stage has a cut-off diameter of 1.7μm at 60L min^{-1} flow rate and is inserted between stage 3 and the

after-filter of the original 4-stage apparatus. The 5-stage impinger's cut-off diameters are shown in Table 4 (Olsson 1995).

Cut-Off Diameters (μm)					
Flow Rate	Stage 1	Stage 2	Stage 3	Stage 4	Stage 5 (After-filter)
$60Lmin^{-1}$	>13.00	6.80	3.10	1.70	0.00
$90Lmin^{-1}$	>10.61	5.55	2.53	1.39	0.00
$100Lmin^{-1}$	>10.07	5.27	2.40	1.32	0.00

Table 4: MSLI cut-off diameters at different flow rates.

An ideal impaction stage has an inverse square root function of the flow (Lodge and Chan 1986).

$ECD_{50\%.Q} = a(Q/60)^b$ **Equation 6**

Where Q= flow rate (L min^{-1}), a= $ECD_{50\%}$ at 60L min^{-1}) and b= an exponent describing the power of the flow rate dependency. The equation can be simplified since the estimation of b is close to the theoretical value, -1/2 (i.e. inverse square root). Therefore the equation becomes:

$$ECD_{50\%.Q} = \frac{1}{a\sqrt{Q/60}}$$ **Equation 7**

The addition of the extra stage was necessitated by the fact that percent cumulative undersize plots obtained via the 4-stage apparatus had only two points on the graph in the respirable fraction particle size range, whereas with the 5-stage impinger, stages 3, 4, and 5 are all part of the respirable fraction (therefore three points on the curve) and contain size ranges of particles capable of deep-lung penetration. Hence, the 5-stage impinger offers better discrimination between particle sizes and provides more comprehensive aerosol data and characterisation. The collection plates at each stage are made of sintered glass, which is wetted with 20ml of mobile phase, prior to aerosol actuation. Upon actuation air passes through the nozzles, over the collection plate and onto the next stage. Particles which impact on the collection plate are

retained. The airflow through the device is usually at 60L min^{-1}, although other flow rates can be used, provided the apparatus has calibration data for those flow rates or the cut-off diameter data is accepted. Once the desired number of actuations have been made, the after-filter is removed and sonicated in 20ml of mobile phase. An additional 5ml of mobile phase is used to wash the jet leading to stage 1. This ensures that any particles on the inside of the jet are washed into stage 1. Therefore, stage 1 usually contains a total of 25ml of mobile phase. The impinger is then swirled for 10 minutes to ensure that all particulate matter is removed from the walls of the apparatus and that all drug particles are in solution. The ceiling of each stage is also wetted by the mobile phase to collect any particles which may have 'bounced-off' the collection plate and impacted on the surface above. Once all of the described procedures are complete, an aliquot from each stage (and also an aliquot from the solution used to rinse the glass throat) is taken and analysed for drug content, usually using HPLC along with an internal standard. If an internal standard is not used then it is necessary to wash all the drug out of each stage.

Although the 5-stage impinger is robust, reliable, produces more data, and provides more complete aerosol characterisation, it does have the following potential disadvantages:

a) The instrument is expensive to purchase and requires maintenance.

b) The analysis procedure is time consuming and labour intensive.

c) When sonicated, the solution in stage 5 usually becomes cloudy and needs to be filtered, prior to HPLC analysis.

d) The grade efficiencies for successive cut-off diameters are lower than between stage 1 and 2 of the TSI.

e) When analysis is complete, the instrument needs to be washed in water, rinsed with methanol and left to dry in an oven, which is time consuming.

1.6.2.3 Other *In-Vitro* Methods

Other Methods of testing include the Andersen Cascade Impactor (ACI), The Marple-Miller Impactor (MMI) and apparatus B (BP (1993), Appendix XVIIC)-the Metal Impinger. These instruments are outside the scope of this report, as they were not used in the study of SAPL.

1.6.2.4 Parameters Used to Describe *In-Vitro* Aerosol Performance

The following parameters are used in this report to describe the performance of an aerosol during *in-vitro* testing.

Parameter	Explanation
Emitted Dose (ED)	Can be expressed as a mass or percentage and refers to the amount of drug expelled by the device and recovered from the sampling apparatus.
Fine Particle Dose (FPD)	Expressed as a mass, and refers to the portion of the emitted dose which is potentially in the respirable range (1-≤5μm).
Fine Particle Fraction (FPF)	Expressed as a percentage, calculated by dividing the FPD by the emitted dose. Stage 2 of the apparatus A and stages 3, 4, and 5 of the MSLI usually comprise the FPF and FPD.

Table 5: Table describing the various *in-vitro* aerosol performance parameters.

1.7 *In-Vivo* Methods

Prototype or new delivery systems can be tested *in-vitro* using the techniques described earlier. However, it is critical that characteristics of new devices or drug presentations be assessed using *in-vivo* lung deposition and / or drug release studies. To some extent, animal models aid the *in-vivo* evaluation of new systems / drugs (Current Perspectives in Inhaled Drug Therapy (1994). However, over the past decade, there has been a growing tendency for new delivery systems to be tested in human subjects, where possible, in phase I clinical trials (Newman 1993, and Davis 1991). This trend is a direct result of companies wanting to get their product on the market as quickly as possible, or to make early cost-saving decisions on products and drugs which will not reach the market.

In-vivo techniques include gamma scintigraphy, Positron-Electron Tomography (PET), and Magnetic Resonance Imaging (MRI). These techniques are outside the scope of this report and further details can be found elsewhere Newman 1993, 1995, 1996, Gerrity 1994, Conway *et al* 1997.

1.8 Aims of the Study

On the outset, the aim of the study was to develop a system for delivering SAPL as a dry powder for the treatment of ARDS and neonatal RDS. The conventional system at the time had consisted of administering SAPL as an intra-tracheal suspension and a powder alternative was investigated. However, the direction of the research changed dramatically in early 1997, when a number of publications indicated that surfactant therapy might be applicable in asthma. As a result, encouraged by these findings, a development program was undertaken to test the hypothesis that surfactants may be therapeutic in the treatment of asthma. Thus, research focussed on characterisation of SAPL powder and investigation of various formulation and delivery avenues. More specifically, the objective was to evaluate the potential of various types of SAPL powder (ranging from a freeze-dried sterile product to a non-freeze-dried micronised material) as dry powder formulations. Deposition profiles of various powder formulations were obtained using conventional capsule technology and delivery systems. These profiles were compared against those obtained from novel delivery systems, developed during the course of this research with the aim of selecting a definitive system that may be used in clinical trials. These new delivery systems included: a dry powder aerosol generator and an inhalation system designed to deliver large quantities of SAPL into the lungs.

Publications indicating the possible use of surfactant in the treatment post-surgical adhesions in adults were also prominent, with some dating back to early 1980's. Thus, the secondary aim of the project was to develop a concept system whereby SAPL could be used for this indication. This delivery system utilised pressurised medical grade carbon dioxide as a propellant to aerosolise and expel freeze-dried SAPL from a pre-filled vial. The ultimate aim

was to use this device in clinical trials for efficacy testing of SAPL for post-surgical adhesions.

Chapter 2

Materials and General Characterisation

2 Materials and General Characterisation

Characterisation of SAPL and the various materials used throughout the study is given below. It must be stressed that various different types of SAPL were used:

a) Freeze-dried, sterile SAPL (abbreviated to FDS) packed into small crimped vials with a nominal weight of 100mg - As described in the section 1.2.2.5.2 Artificially Derived Surfactants), page 30.

b) Micronised and unmicronised SAPL (abbreviated to MS and UMS respectively), sterile, received in glass containers as bulk powder, manufactured without the freeze-drying process. SAPL was micronised at Micro-Macinazione SA (Micro-Grinding Ltd), Switzerland, using their patented Chrispro®-Jetmills. The details of the micronisation procedure are given in section 2.2.6.1 Micronisation of SAPL), page 113.

c) FDS labelled with a fluorescent probe (see section 3 Fluorescent Labelling of FDS, page 121). Micronised and unmicronised, labelled forms of FDS are abbreviated to MLFDS and UMLFDS respectively. A control was also used during the labelling process, abbreviated to CFDS. The micronisation of the labelled material (MLFDS) was done so by fluid-energy milling using the Gem-T air pulveriser, Glen-Creston, Stanmore, UK. (see section page 116).

2.1 Formulation / Analytical Materials

Product	Supplier
α-Lactose Monohydrate (Lactochem)	Borculo Whey Products Ltd., Chester, UK
Dansyl Chloride	Sigma Chemical Co., Poole, UK.
Dichloromethane (GPR)	Fisons Scientific Equipment, Loughborough, UK
DL-α-Phosphatidylcholine, Dipalmitoyl (DPPC)	Sigma Chemical Co., Poole, UK.
Hard Gelatine Capsules	Davcaps Ltd., Herts., UK
Lecithin	The Lecithin People, Clwyd, Wales, UK
L-α- Phosphatidyl-DL-Glycerol (PG)	Sigma Chemical Co., Poole, UK.
Methanol and Chloroform (HPLC grade)	Fisons Scientific Equipment, Loughborough, UK
Magnesium Sulphate (GPR)	BDH Chemicals
n-Octadecyl dansylamide	Synthesised at Bath University
Octadecylamine (Stearylamine)	Sigma Chemical Co., Poole, UK.
Phosphorous Pentoxide	BDH Chemicals
Propan-2-ol and Cyclohexane	Fisons Scientific Equipment, Loughborough, UK
Sorbolac 400 (fine lactose) (Microtose)	Meggle, Germany.
Triethylamine (GPR)	Sigma, Poole, UK.

Table 6: List of the various materials, powders and solvents used throughout the study.

2.2 Characterisation of Materials

The general characterisation tests for the materials to be used throughout the study are outlined below.

2.2.1 Particle Size Analysis

Particle size analyses of all materials were carried out using two different types of equipment. Firstly, the Malvern Mastersizer X (Malvern Instruments Ltd., Malvern, UK) was used to characterise powders in various solvents or using the dry powder option available on the machine. Secondly, the Amherst Process Instruments (API) Aerosizer® (mach2 V6.04) powder analysis system fitted with API Aero-Disperser™ accessory was used to characterise all the powders used throughout.

2.2.1.1 Malvern Analysis (Laser Light Diffraction)

Introduction

Low Angle Laser Light Scattering (LALLS) methods involving laser light scattering are available to give information about particle size distributions of therapeutic aerosols. The physical principle of LALLS particle size analysis uses the light scattered in the near forward direction (Fraunhofer or Mie diffraction) with respect to the incident light (Kraut *et al* 1990, Kaye 1999). Fraunhofer diffraction theory (Annapragada and Adjei 1996) can be applied to particles that are significantly larger than the wavelength of illuminating light. By also incorporating Mie diffraction theory (Diffraction Training Manual (1993), Malvern Instruments Ltd., Malvern, UK), which relates to light scattered by large molecules and nano-particles at right angles to the incident beam, the particle sizing instruments can measure, accurately, particle sizes between 0.1-2000μm. Particle sizing of DPI devices and powders can be carried out using a special dry powder feeder with an external de-agglomerating

accessory. In order to measure particle size distributions in saturated suspensions, pMDIs and nebulised solutions, the refractive index and density of the test material need to be inputted into the instrument, before a meaningful answer can be attained. The problem with LALLS is that a lot of material is often needed to generate a result, this may not be viable if material is in short supply. Clark (1995b) has shown laser diffraction to be a more reliable and accurate measure of testing aerosol clouds generated by medical nebulisers. The results obtained using a Malvern Mastersizer X (Malvern Instruments Ltd., Malvern, UK), were correlated with published and empirical deposition models. The results showed that the diffraction technique measures size parameter relevant to clinical performance of the nebuliser, and that the correlation between the published and the attained data was high.

This section outlines the methods used to characterise the various forms of SAPL and the Lactochem-lactose used throughout the mixing studies. Results are tabulated with the conditions per analysis given at the bottom of the table.

Method 1:Use of a Dry Powder Feeder

A small spatula full of the sample was introduced into the apparatus via a glass adapter, mounted at the inlet leading to the lens. A high-powered vacuum cleaner capable of achieving approximately 180Lmin^{-1} flow rate was attached to the outlet at the back of the Mastersizer X. Once switched on, the instrument took both background and electrical readings before measuring the size of the powder entrained into the air-stream. The amount of sample added was just adequate to give an obscuration value of between 3-25% and the particle size, by volume, was calculated. A total of 10 measurements per sample were taken and the particle size, by volume, calculated and transported to a spreadsheet via the use of a macro program.

Method 2:Use of a Small Volume Stirred Cell

The liquid apparatus (MSX1 small volume unit) had a capacity of 20ml. A suitable dispersant with or without a suspending agent was added to the cell, and circulated via a small magnetic flee. Both background and electrical readings were taken before a filtered, saturated representation of each sample was introduced into the cell, drop-wise using a Pasteur pipette. Sonication of some samples was necessary to reduce or eliminate agglomeration. A 0.1% w/v solution of lecithin in cyclohexane was used as the suspending agent and dispersant respectively. The other solvent used during the measurements was acetone. For sonication times, temperature of the sonic bath, and other details, refer to the experimental conditions outlined in the individual tables.

Operating Conditions and Results

Particle Size: Calculated by Volume. Model used: Polydisperse.
Air-Supply: vacuum cleaner, Dyson, Model DC01.
Measuring Vessel: Small volume stirred cell (MSX1), manual dry powder feeder.
Lens Used: 100mm diameter (measurement range: 0.2-180μm) or 300m diameter (range: 1.2-600μm). Typical Laser Obscuration: 17-25%.

			Particle Size (μm)		
Sample ID	Dispersant or Solvent	Suspending Agent (w/v)	D(0.1)	D(0.5)	D(0.9)
Lactochem Lactose (63-90μm Fraction- prepared by sieve analysis)	Air	None	26.4 (±4.16)	84.3 (±0.5)	130.4 (±0.5)

Table 7: Particle size analysis results for lactose using the dry powder feeder n=10.

Values in brackets indicate standard deviation.

Detailed tables can be found in Appendix 2: Detailed Particle Size Analysis Tables of SAPL Powders by Laser Light Diffraction (Malvern Analysis), page 252. Table 8, below shows a summary of the results obtained.

			Particle Size (μm)		
Sample ID	Dispersant or Solvent	Sonication Time	D(0.1)	D(0.5)	D(0.9)
FDS	Cyclohexane	2 min	3.09	18.6	39.9
	Acetone	2 min	7.27	33.7	66.9
	Air	N/A	25.9	83.3	164.7
UMLFDS	Cyclohexane	2 min	1.51	12.4	64.9
	Acetone	2 min	4.28	53.1	164.6
	Air	N/A	21.2	64.9	140.2
MLFDS	Cyclohexane	2 min	1.61	4.12	8.51
	Acetone	2 min	2.26	19.3	62.4
	Air	N/A	17.8	99.2	168.4
UMS	Cyclohexane	2 min	2.61	13.4	28.2
	Acetone	2 min	8.64	31.6	68.9
	Air	N/A	14.3	78.7	160.9
MS	Cyclohexane	2 min	1.28	2.39	7.62
	Acetone	2 min	4.83	12.7	24.6
	Air	N/A	10.4	61.9	147.8

Table 8: Summary particle size analysis table for various SAPL powders using the Malvern Mastersizer X.

Discussion

The particle sizes of the various SAPL powders have been determined. The general trend is that the particle size measured is dependent on the solvent / dispersant used, sonication time that the sample is subjected to, and the temperature of the sonic bath. Smaller VMDs are obtained for all samples when cyclohexane in combination with lecithin are used compared with solvent alone or samples suspended in air. Presumably, this is because samples are better dispersed in a solvent containing a suspending agent. SEM photos of samples show particle size to be more concordant with results obtained for cyclohexane (with suspending agent) than with acetone. Sonication time of 1-2 minutes seems to optimal to break up the agglomerates of powder.

2.2.1.2 Time-of-Flight Aerosol Beam Spectroscopy (TOFABS)

Introduction

When carrying out Fraunhofer diffraction in liquid media, the particles may be prone to size distribution changes because of dissolution and / or growth during sample preparation (Hindle and Byron 1995). To overcome this problem, powder dispersion equipment capable of dispersing a sample in a gas stream prior to sizing has been developed. This system is commonly called the time-of-flight aerosol beam spectroscopy (TOFABS), one such example is the Aerosizer® (Amherst Process Instruments, MA, USA). This is a laser-based system which measures the time-of-flight of a given particle across a measurement zone, and determines size distributions according to the aerodynamic principles described by Niven (1993). Powder is first fluidised by a combination of pulsed jet air and carrier gas. Particles are transported to a computer-controlled disperser and mixed and further diluted by sheath air and subjected to a pressure drop. The resultant shear force assists in particle de-aggregation and the particles are fed into the Aerosizer® for time-of-flight analysis. The time taken for particles to traverse two laser beams is measured. The data collected can be converted to either volume or number based frequency distributions and can be displayed as functions of aerodynamic or geometric diameter

Method

A small amount of powder, approximately 100mg was placed into the disperser cup. Combinations of pulsed jets of air from an external power source and carrier air were used to fluidise the powder. Once fluidised the samples were de-agglomerated within the Aero-Disperser™ and fed into the Aerosizer® for time of flight analysis. The parameters in Table 9, page 80 have been investigated by Niven (1993), and Hindle and Byron (1995) and have been optimised in this study to give the best possible results.

Parameter	Function
Sample Run Time	Controls duration of powder de-agglomeration and particle counting.
Shear Force	Controls shear force applied to particles within the Aero-disperser™ before being fed into the Aerosizer®.
Feed Rate	Controls and maintains the target count rate.
Pin Vibration	Causes the pin to dither so as to prevent power accumulation
Deagglomeration	Selects airflow pattern carrying powder from sample cup to disperser.

Table 9: Showing the Aero-Disperser™ variables and their functions

Operating Conditions / Instrument Settings

Shear Force range(psi): 0-5.0 Shear Tolerance: unchanged

Feed Rate range: 2000-10000 particles per second Pin Vibration: On

Run Time: 100secs Deagglomeration: High (H) and constant.

Sum of Channels: Total number if particles counted

Regularisation: Low Gaussian Extension: Off

Results

Table 10, page 81, shows the summary results for the various SAPL powder obtained using TOFABS. In each case combinations of low shear / high shear and low feed rate / high feed rate results are displayed.

Parameter						Aerodynamic Diameter (VMD) (μm) (% under size)		
Sample ID	Sum of Channels	Shear Force (psi)	Feed Rate	Deag (H)	Run Time (sec)	5%	50%	95%
FDS	111292	5.0	3000	H	100	7.22	18.6	38.2
FDS	142567	4.5	10000	H	100	7.95	20.0	41.9
FDS	45054	2.0	3000	H	100	11.3	44.3	63.0
FDS	82641	2.0	10000	H	100	13.1	46.6	66.2
UMLFDS	156525	4.5	3000	H	100	5.59	13.5	21.3
UMLFDS	107972	4.5	10000	H	100	7.62	24.1	39.5
UMLFDS	96161	2.0	3000	H	100	10.9	40.2	60.4
UMLFDS	23901	2.0	10000	H	100	12.7	37.9	61.7
MLFDS	323820	4.5	3000	H	100	2.59	5.02	13.9
MLFDS	134626	4.5	10000	H	100	3.42	7.54	15.7
MLFDS	84251	2.0	3000	H	100	13.4	22.6	48.9
MLFDS	36844	2.0	10000	H	100	14.8	24.3	52.3
UMS	202347	4.5	3000	H	100	9.16	18.6	33.9
UMS	168236	4.5	10000	H	100	12.8	34.0	56.2
UMS	71365	2.0	3000	H	100	18.6	50.3	85.4
UMS	51002	2.0	10000	H	100	19.2	64.2	85.4
MS	178424	4.5	3000	H	100	2.12	3.64	5.13
MS	122454	4.5	10000	H	100	2.24	4.06	6.17
MS	63889	2.0	3000	H	100	3.95	7.26	10.9
MS	49224	2.0	10000	H	100	4.34	8.69	13.8

Table 10: Particle size analysis using the Aerosizer® coupled to the Aero-Disperser™. Results show volume and number based aerodynamic particle size for various SAPL powders.

Key: Sum of chan.: sum of channels, Deag H: Deagglomeration high and constant.

The results above are represented graphically in Figure 14, Figure 15, and Figure 16 on pages 82 and 83.

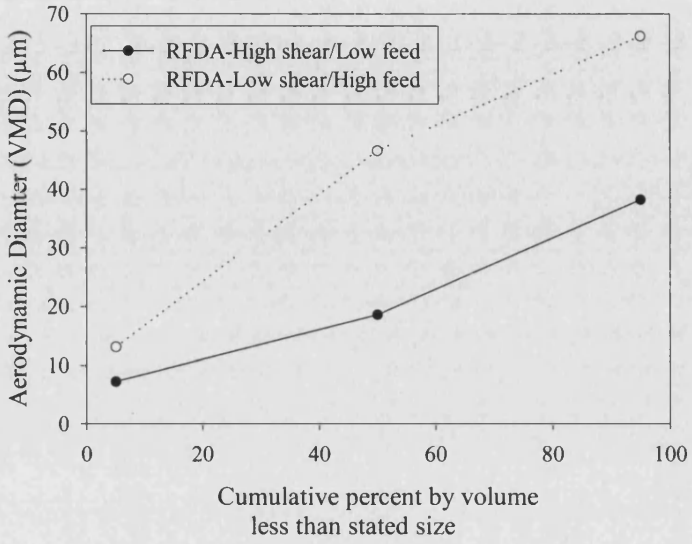

Figure 14: Measured cumulative percent by volume less than stated size vs. Aerodynamic diameter FDS measured under high shear/low feed and low shear/high feed conditions.

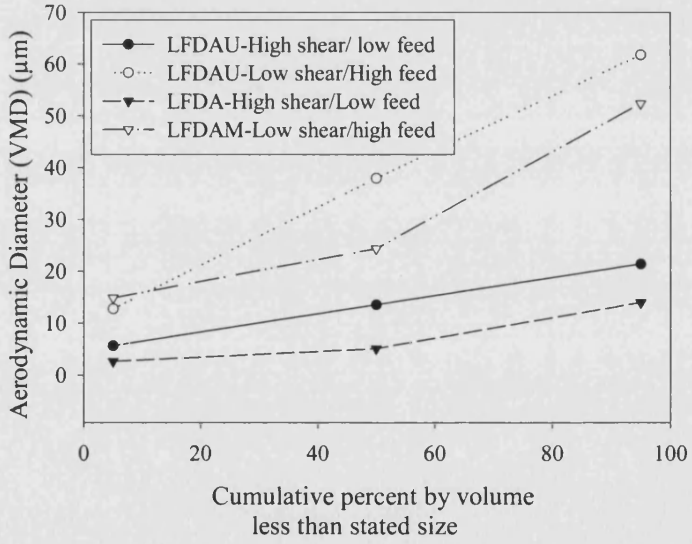

Figure 15: Measured cumulative percent by volume less than stated size vs. Aerodynamic diameter LFDSU and LFDSM measured under high shear/low feed and low shear/high feed conditions.

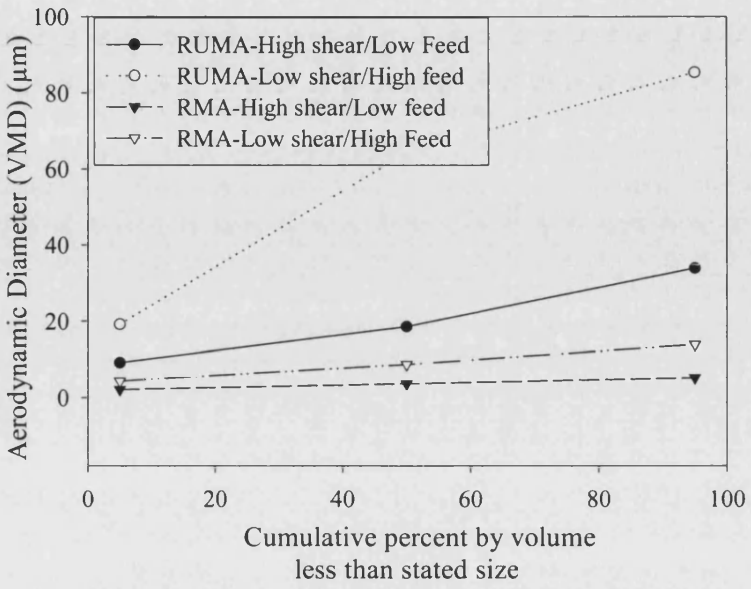

Figure 16: Measured cumulative percent by volume less than stated size vs. Aerodynamic diameter for UMS and MS measured under high shear/low feed and low shear/high feed conditions.

Discussion

The volume median diameters of SAPL powders have been determined. Particle size obtained by this technique seems to be dependent on the applied shear force, the feed rate, and whether or not high deagglomeration is used. Generally for cohesive powders, shear force should be as high as possible, and in this study the lowest VMD results were obtained when this was the case. The feed rate should also be as high as possible, but in this case the instrument had difficulties in supplying adequate sample into the aerosizer at higher feed rates, due to the cohesiveness of the powder. Thus, more concordant results were obtained at lower feed rates coupled with high shear forces. Sample run-time is of secondary importance in this case, since the compressor (supplying the incoming air) reaches maximum capacity before the entire sample is analysed. Run-time of 100 seconds conveniently coincided with the capacity of the compressor.

2.2 2 Microscopy

Introduction

Optical techniques allow for the study of particle size and shape, and have been used extensively in the pharmaceutical sciences for acquiring information during drug development. Effects of micronisation and spray drying on compounds (Vidgren *et al* 1989), surface modifications of drug particles (Hickey *et al* 1992), and evaluation of carried based inhalation systems (Lucas *et al* 1997) are examples of the type information that can be attained.

Scanning electron microscopy (SEM) was used to assess the powders used throughout the study. SEM analysis allowed a detail look at the raw material and the uniformity of the various blends made throughout the study.

2.2.2.1 Scanning Electron Microscopy (SEM)

Introduction

Scanning electron microscopy utilises a fine beam of electrons to bombard the surface of test materials, which cause secondary electrons to be emitted from the atoms in the sample surface, subsequent detection and processing of these electrons form the image (Beckett and Read 1986). Samples for SEM analysis need to be dry, mechanically stable, non-volatile and electrically conducting. However, most pharmaceuticals do not posses these properties. Therefore, it becomes necessary coat samples with a thin layer of gold to aid imaging and dissipation of electrical charge from the sample surface. If the coated surface is damaged during analysis due to excessive build up and accumulation of electrons, or when imaging hydrated or thermo-liable compounds, then sample charging can occur which leads to distortion and subsequent loss of resolution of the image (Beckett and Read 1986). To overcome these difficulties, variants of SEM have been developed namely, low-temperature

(LTSEM) and Environmental (ESEM). LTSEM allows imaging of the sample under reduced temperatures while maintaining the integrity of hydrated or delicate materials (Babic *et al* 1996). With ESEM, samples may be imaged in their natural state without prior sample preparation. This is possible because rather than operating just under vacuum (like conventional SEM), ESEM uses a differential pumping system to segregate the environment within the specimen chamber from other parts of the instrument.
This section outlines the instrumentation methods used during the acquisition of the SEM images of the various forms of SAPL.

Method

The powders under analysis were examined for particle shape, surface characteristics, and, in some cases, in evaluating the efficiency of an ordered mix using SEM. A representative sample of powder was mounted on aluminium specimen stubs using carbon-coated adhesive fixers. A thin, conductive layer of gold was evaporated onto the sample surface using a sputter coater for five minutes (Model: S150B, Edwards High Vacuum, Crawley, UK). The prepared specimens were examined using a JEOL 6310 SEM (Japanese Electron Optics Ltd., Tokyo, Japan). Typical Instrumentation Settings: Operating Voltage: 5-10 kV, Spot Size: 12.

Results

Figure 17 through to Figure 25, pages 86 to 89 show the electron photomicrographs obtained for FDS, UMLFDS, MLFDS, UMS, MS, and the label respectively. The interpretation of the images is given in the discussion / conclusion part of this section.

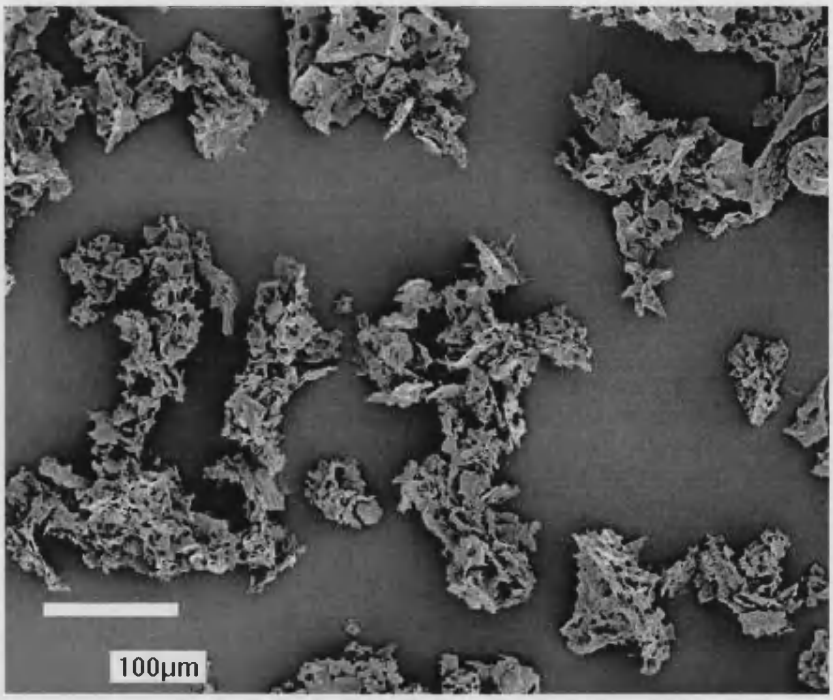

Figure 17: Scanning Electron Photomicrograph of FDS at x500 magnification.

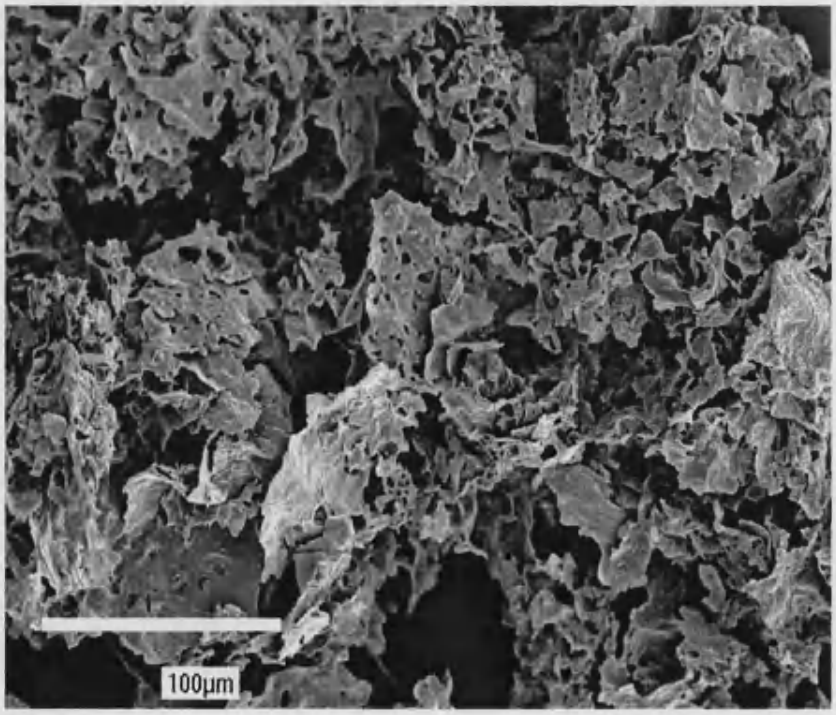

Figure 18: Scanning Electron Photomicrograph of FDS at x1500 magnification.

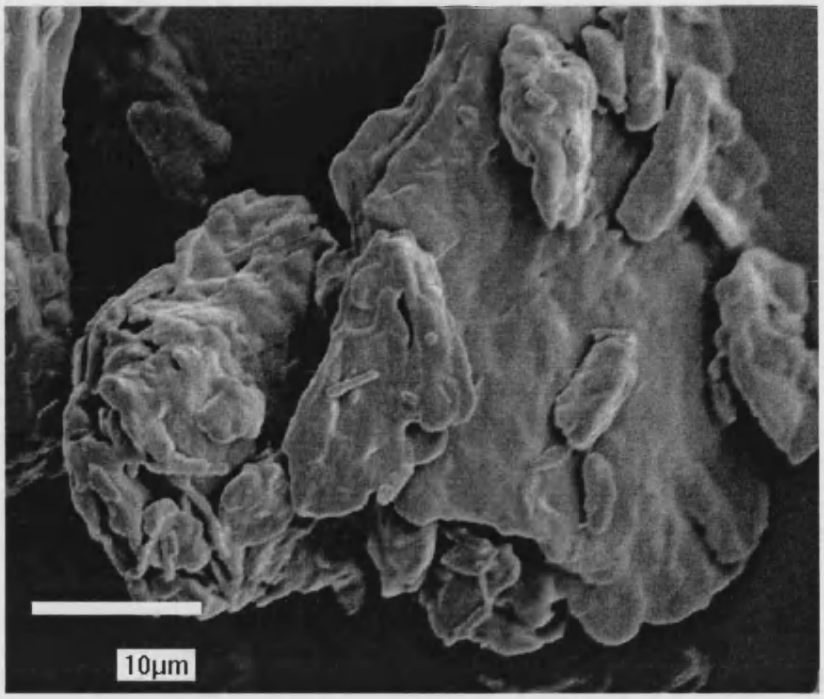

Figure 19: Scanning Electron Photomicrograph of UMLFDS at x2500 magnification.

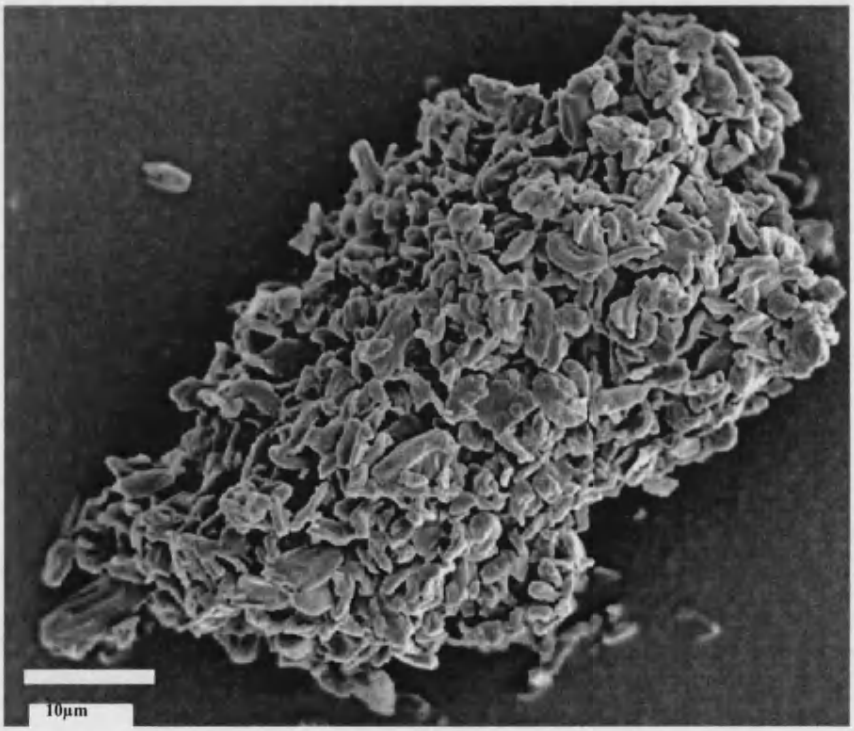

Figure 20: Scanning Electron Photomicrographs of MLFDS at x3000 magnification.

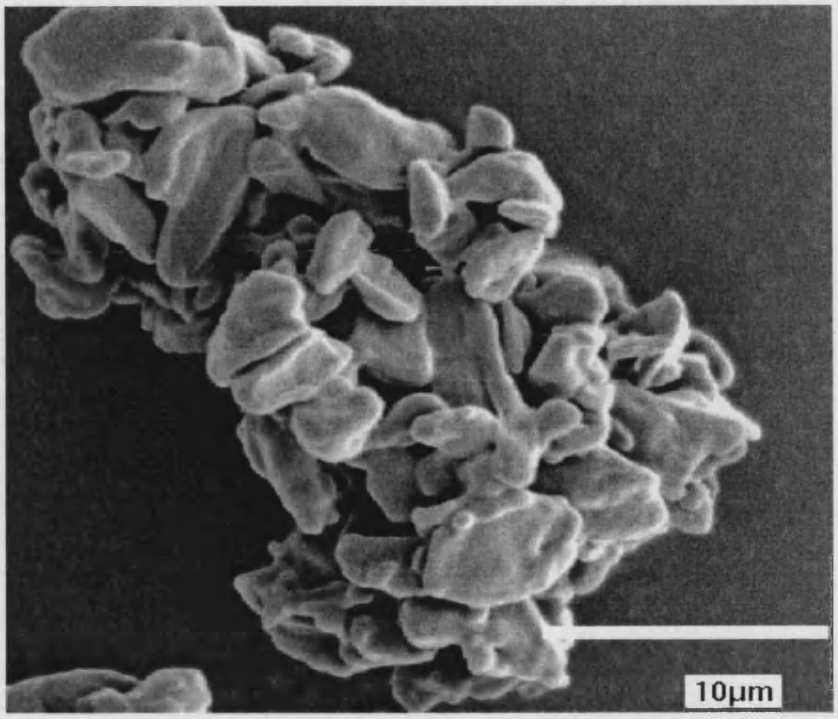

Figure 21: Scanning Electron Photomicrographs of MLFDS at x4500 magnification.

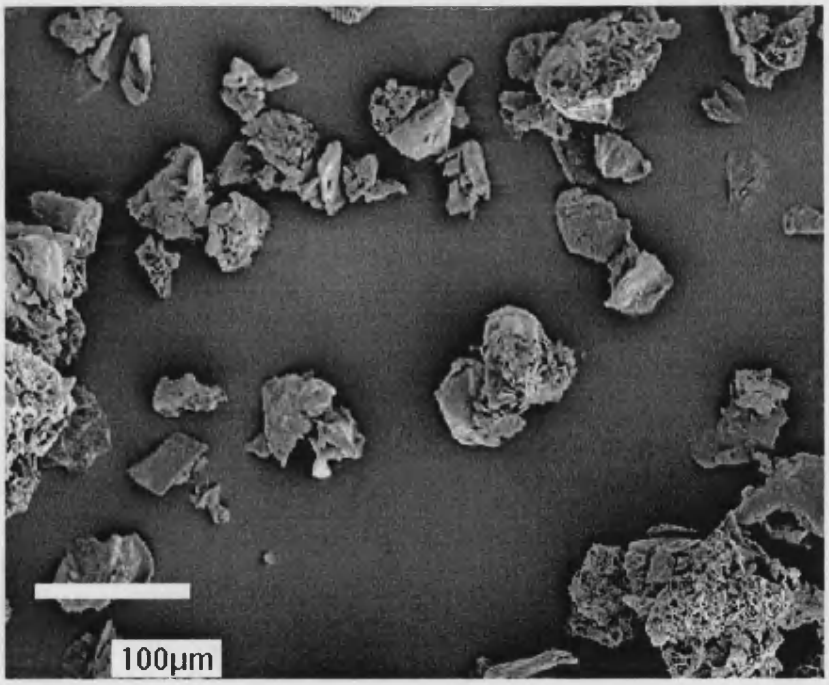

Figure 22: Scanning Electron Photomicrograph of UMS at x300 magnification.

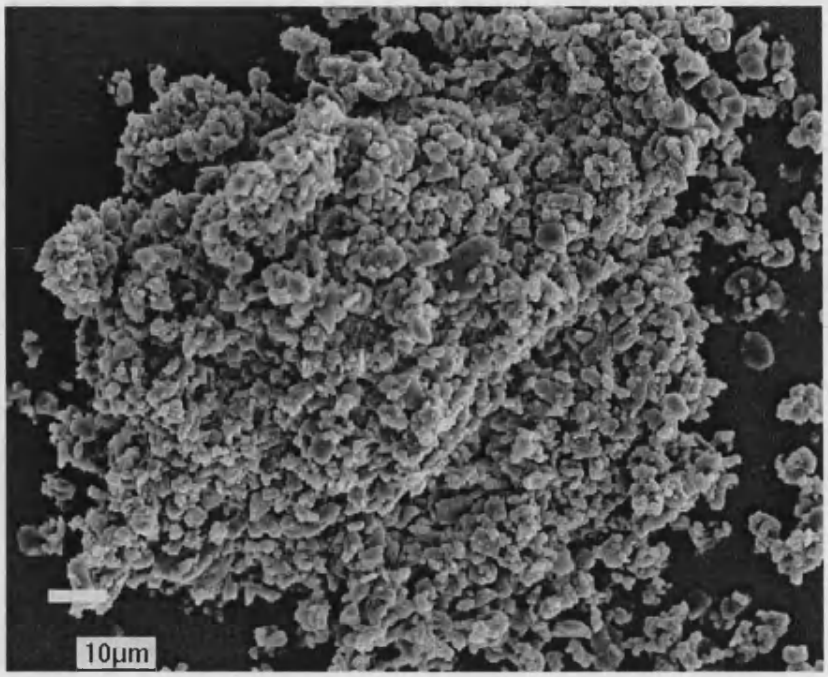

Figure 23: Scanning Electron Photomicrograph of MS at x1000 magnification.

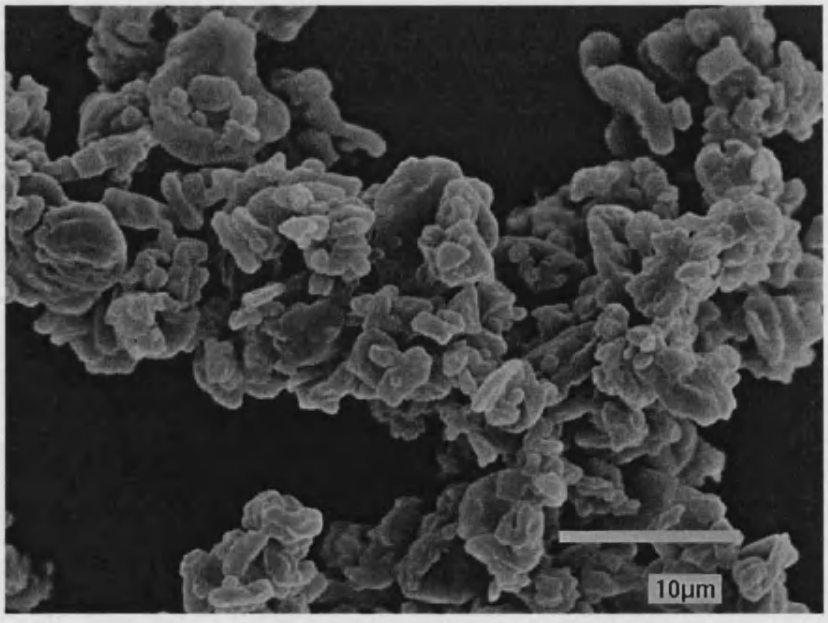

Figure 24: Scanning Electron Photomicrograph of MS at x5000 magnification.

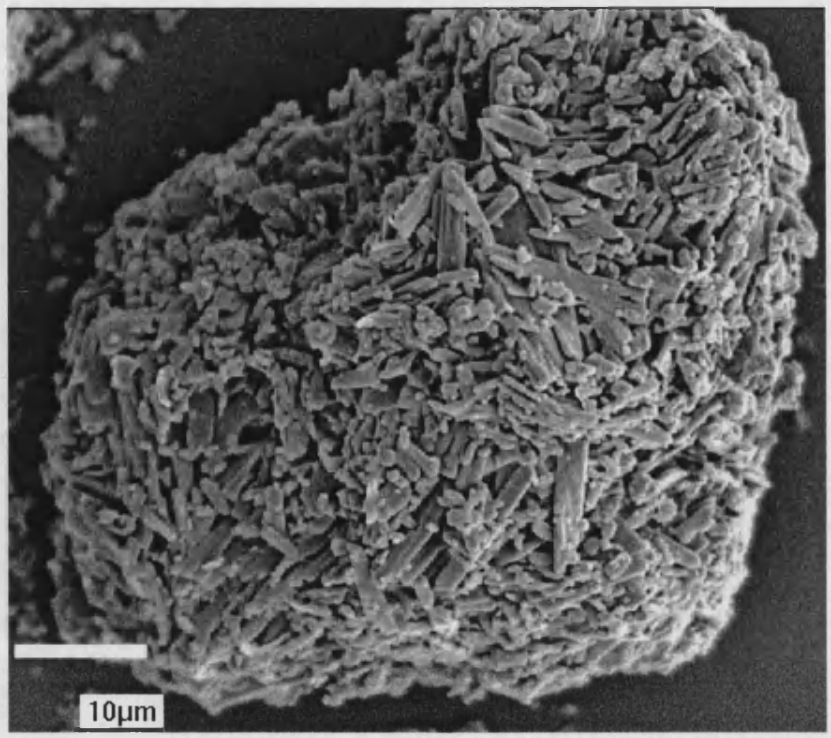

Figure 25: Scanning Electron Photomicrograph of n-Octadecyl Dansylamide (the label) at x1500 magnification.

Discussion

The various SEM photographs of SAPL have been presented. FDS images (Figure 17 and Figure 18, page 86) suggest highly amorphous particles, existing as aggregates of no definitive size. When subjected to the labelling procedure (see section 3 Fluorescent Labelling of FDS, page 121) and subsequent micronisation (see section 2.2.6.1 Micronisation of SAPL, page 113) these particles are no longer amorphous, rather they are more defined in nature, as shown in the photomicrographs of UMLFDS and MLFDS (Figure 19, Figure 20, and Figure 21, pages 87 and 88). Photomicrographs of UMS (Figure 22, pages 88) show large, irregularly shaped particles, which are reduced in size upon micronisation as shown in the images of MS (Figure 23 and Figure 24, page 89). Photomicrographs of the label (n-ocatdecyl dansylamide, Figure 25, page 90) show particles that are long and needle-like with a wide size distribution range.

2.2.3 Density Measurements

Powder flow properties of SAPL were assessed from Carr's Index and Hausner ratio values derived from bulk and true density measurements. Bulk density (also called poured or fluff density), is a characteristic of a powder system, rather than individual particles. The bulk density of powder is always less than the true density of its component particles, because the powder contains interparticle pores or voids. Therefore, whereas there is only one true density, there can be many bulk densities, depending on the way particles are packed and the bed porosity.

Tapped density is also known as equilibrium or consolidated bulk density. It can be used to follow the change in packing that occurs when void space diminishes and consolidation occurs. As the powder is tapped the density increases from an initial bulk density D_o to a final value D_f. This ratio can be used to assess the quality of powder flow. Carr's index gives an indication of percentage compressibility of a powder arch or bridge strength and assigns an index of flowability to the sample. Hausner ratio is simply a ratio of tapped density divided by the bulk density.

2.2.3.1 Tapped / Bulk Density

Method

A known weight of sample was accurately weighed into a 25cm^3 measuring cylinder. The initial volume occupied by the sample was recorded and the cylinder was placed onto a jolting volumeter (Stampf volumeter STAV 2003, Rhein, Germany). The volume of powder was measured after 500 taps and the various parameters below in Table 12 were calculated. Three determinations were made for each sample.

Calculations / Tables

$$Bulk\ Density = \frac{Sample\ Wt.}{Initial\ Vol.} \qquad Tapped\ Density = \frac{Sample\ Wt.}{Final\ Vol.}$$

$$Carr's\ Index = \frac{Tapped - Bulk}{Tapped} X100 \qquad Hausner\ Ratio = \frac{Tapped}{Bulk}$$

Carr's Index (%)	Hausner Ratio	Type of Flow
5-15		Excellent
12-16	<1.25	Good
18-21		Fair to Passable
23-35	>1.25	Poor
33-38		Very Poor
>40		Extremely Poor

Table 11: Table of Carr's Index and Hausner Ratio as an Indication of Powder Flow Properties.

Results

Sample ID	Sample Wt (g)	Initial Vol (cm^3)	Final Vol (cm^3)	Mean Bulk Density (g/cm^3)	Mean Tapped Density (g/cm^3)	Mean Carr's Index	Mean Hausner Ratio
FDS-1	0.456	12.05	8.10	0.0367	0.0552	33.3	1.50
FDS-2	0.429	11.83	7.88	±0.001	±0.001	±0.4	±0.01
FDS-3	0.435	11.90	7.91				
MLFDS-1	7.042	14.11	11.95	0.500	0.594	15.8	1.19
MLFDS-2	6.942	13.80	11.65	±0.002	±0.004	±0.7	(±0.01
MLFDS-3	6.870	13.79	11.51				
UMS-1	11.828	43.3	37.1	0.275	0.322	14.6	1.17
UMS-2	12.090	44.1	37.6	±0.003	±0.003	±0.3	±0.01
UMS-3	12.425	44.7	38.2				
MS-1	4.561	13.3	11.1	0.342	0.403	15.3	1.18
MS-2	4.688	13.8	11.8	±0.008	±0.014	±1.082	±0.015
MS-3	4.692	14.0	11.9				

Table 12: Bulk density and flow characteristics of various forms of SAPL.

Mean Hausner ratio of 1.50 and a Carr's index of 33.3 for FDS indicate poor flow. The values 1.19 and 15.8 for LFDS indicate good flow. UMS and MS show good flow properties before and after micronisation.

2.2.3.2 True Density

Method

This was determined by helium pycnometry using a true density measuring apparatus (AccuPyc 1330 V2.01, Micromeritics, USA). A sample of SAPL was weighed into small, cylindrical aluminium container such that the sample occupied about two thirds of the container. The container was placed into the apparatus and the system was purged and equilibrated using a helium source. All analyses were carried out in triplicate and an average of ten readings per sample was taken.

Run conditions / Instrument settings:

Chamber temperature: 29.8°C	Cell Volume: 12.1274cm^3
Number of Purges: 10	Equilibration rate: 0.0100 psig/min
Expansion Volume: 8.3523	Number of readings per sample: 10

Results

A summary of the true density results for SAPL is shown below in Table 13.

Sample ID	Sample Wt (g)	Sample Volume (cm^3)	Density (g/cm^3)	Mean Density (g/cm^3)
FDS-1	0.9573	0.8797	1.0882	1.088
FDS-2	0.9622	0.8815	1.0870	(±0.001)
FDS-3	0.9648	0.8824	1.0890	
MLFDS-1	2.2279	2.0799	1.0722	1.072
MLFDS-2	2.1894	2.0642	1.0715	(±0.0004)
MLFDS-3	2.0272	2.0715	1.0719	
UMS-1	2.143	2.0842	1.0784	1.077
UMS-2	2.264	2.1030	1.0749	(±0.002)
UMS-3	2.094	2.0805	1.0766	
MS-1	2.501	2.4220	1.0806	1.080
MS-2	2.488	2.4125	1.0790	(±0.001)
MS-3	2.529	2.4352	1.0814	

Table 13: Table showing the true density values for SAPL.

Values in brackets indicate standard deviation, n=3.

There seems to be no apparent differences in true density values for the various types of SAPL.

2.2.4 Structural Characterisation

This section looks at the X-ray diffraction patterns of the various forms of SAPL to ascertain any differences between the samples in question. The theory is described briefly as well as the methods used to characterise SAPL.

2.2.4.1 X-ray Powder Diffraction (XRPD)

XRD diffraction patterns are produced when fast-moving electrons impinge on matter (Klug and Alexander 1974). The phenomena resulting from the deceleration of such electrons are very complex, and x-rays result from two general types of interaction of the electrons with the atoms of the target material. A high-speed electron may strike and displace a tightly bound electron deep in the atom near the nucleus, thereby ionising the atom. When a certain inner shell of an atom has been ionised in this manner, an electron from an outer shell may fall into the vacant space, with the resulting emission of an x-ray characteristic of the atom involved. Such production of x-rays is a quantum process. The phenomenon of x-ray diffraction by crystals result from a scattering process in which x-rays are scattered by the electrons of the atoms without change in wavelength. A diffracted beam is produced by such scattering only when certain geometrical conditions are satisfied, which may be expressed in either of two forms, the Bragg law or the Laue equations, explained elsewhere (Klug and Alexander 1974). The resulting diffraction pattern of a crystal, comprising both the position and intensities of the diffraction effects, is a fundamental physical property of the substance, serving not only for its speedy identification but also for the complete elucidation of its structure. The essential features of the powder diffraction technique include a narrow beam of monochromatic x-rays impinging upon a crystalline powder composed of fine, randomly orientated particles. Under these conditions all the diffracted rays from sets of planes of spacing generates a cone of semi-apex angle 2θ. A pattern of concentric rings is produced by those cones of diffracted rays that intersect a film placed perpendicular to the undeviated beam, a detailed account of the theory is given elsewhere (Klug and Alexander 1974).

Method

Small (35mm x 35mm), square aluminium plates (1mm thick) with a 20mm x 15mm window towards the top of the plate, were used as sample holders. A 20mm x 25mm slide was used as a support during measurements to ensure the sample did not fall out. A small, representative, quantity of the sample was evenly placed into the window such that the entire area was covered, without voids. Care was taken not to compress the powder during the above procedure. A second slide was used to cover the powder bed, and the sample was place into the diffractometer (Philips PW 1820/00 computer controlled vertical diffractometer, PW1710/00 microprocessor diffractometer control, equipped with PW 1877 PC-APD version 3.5b diffraction software) with for analysis. Data was generated in the Materials Science Department, University of Bath. Interpretation of the results was carried out in association with various members of the same department.

Operating Conditions / Instrument Settings

Tube Anode: Copper	Generator (4kW, Philips PW 1730/00), Tension: 40kV
Generator Current: 25mA	Wavelength Alpha 1 [A°]: 1.54060
Wavelength Alpha 2 [A°]: 1.54439	Intensity ratio: (Alpha 1/Alpha 2): 0.500
Divergence Slit: Automatic	Irradiated Length: 12mm
Monochromator Used: None	Start Angle (°2θ): 5.010
End Angle (°2θ): 89.950	Step Size (°2θ): 0.020
Time per Step: 0.5secs	Type of Scan: Continuous

Results

Table 14 shows the results obtained and expressed as an average of three runs. Only FDS, UMLFDS, MLFDS, and a control sample were analysed. The purpose of the experiment was to see if the labelling procedure (see 3 Fluorescent Labelling of FDS, page 121) used had altered the structure of the material. UMS and MS were not analysed because they had not undergone any labelling procedure.

Sample Details	Angle (°2θ)	Number of Peaks	d-Value α1 (Å)	Relative Intensity (%)
FDS	6.175	4	14.301	8.5
	9.165		9.6415	2.4
	12.110		7.3026	1.9
	20.890		4.2490	100.0
SAPL-Control (used during labelling)	6.200	4	14.244	14.7
	9.335		9.4663	3.1
	12.330		7.1728	3.1
	21.035		4.2200	100.0
MLFDS	6.210	5	14.221	6.0
	9.200		9.6049	1.8
	12.270		7.2077	1.5
	21.115		4.2042	100.0
	36.830		2.4384	1.3

Table 14: X-ray diffraction results for various forms of SAPL.

The values are an average of three runs per sample (n=3).

N.B. Under the measured conditions the diffracted rays from different sets of planes of spacing generates a cone of semi-apex angle 2θ. A pattern of concentric rings is produced by those cones of diffracted rays that intersect a film placed perpendicular to the undeviated beam, a detailed account of the theory is given elsewhere (Klug and Alexander 1974). The d-spacing values represent the space between orders in the crystalline matrix of the sample. Thus, bigger the number, greater the spacing between planes of crystals.

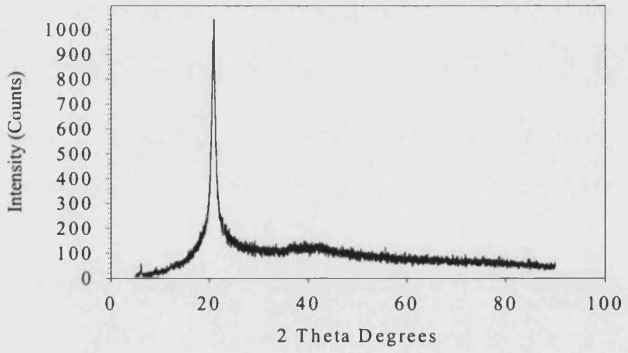

Figure 26: X-ray diffractogram of FDS.

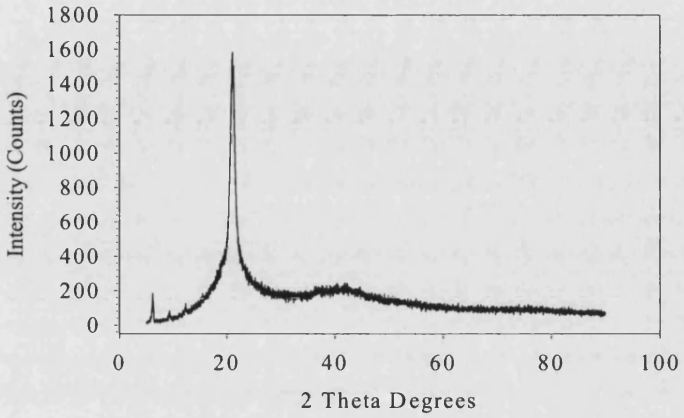

Figure 27: X-ray diffractogram of SAPL-Control

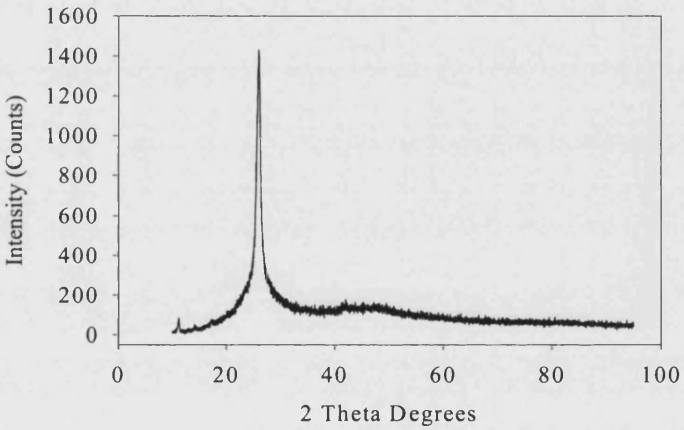

Figure 28: X-ray diffractogram of MLFDS.

Discussion

When the above diffractograms are compared, a characteristic main peak at (°2θ) ~21.0 can be seen. The broadness of this peak, may arise from very small crystallite size, or lattice distortion, or both. For a polycrystalline specimen (i.e. most organic compounds) consisting of sufficiently large and free crystallites, diffraction theory predicts that the lines of the

powder pattern will be exceedingly sharp (Klug and Alexander 1974). Thus, the broad peak coupled with the noisy baseline of the diffractograms is indicative of the amorphous nature of most organic material, which tend to be semi-crystalline in nature. In addition, SAPL is a freeze-dried material and an artefact of the process is usually the production of amorphous material, which are produced as a direct result of the lyophilisation process itself, namely the non-discriminative way in which the water is extracted (Craig *et al* 1999). In addition to the peak at (°2θ) ~21.0, there are also common peaks at (°2θ) ~6.2 and 9.2, between the raw material and the materials which had undergone the labelling process. The differences in the values between the samples can be attributed to the measurement error associated with the technique, typically about 10% (Klug and Alexander 1974). The only difference between the treated (i.e. materials which have been through the labelling process) material and the raw product are the peaks which can be seen at (°2θ) ~12.2 and 36.8(for MLFDS only). These peaks are of low relative intensity and are possible artefacts of the labelling process, possibly due to the residual chloroform left from the vacuum drying employed during the procedure.
In conclusion, the labelling procedure has not produced any significant change in the chemical composition of SAPL.

2.2.5 Analytical Methods

The two analytical techniques used in the separation and quantification of the various forms of SAPL were HPLC and fluorimetry. The various experimental aspects of each technique and the justification for use on SAPL are outlined below.

2.2.5.1 HPLC Detection of MS

The two components of MS, Phosphatidylgylcerol (PG) and Dipalmitoylphosphatidylcholine (DPPC), used during the *in-vitro* deposition experiments were separated and quantified by HPLC. Professor John Harwood and his team at Cardiff University, School of Biomedical Sciences originally developed the method used. Thus, in order to use this method in the

present study, site-to-site transfer of the method was instigated. Full method validation was not undertaken, rather, linearity and repeatability experiments were carried out to assess the response of the detector and the performance of the HPLC equipment. The only unusual aspect of the method was the detection technique employed. A non-selective 'universal' detector (PL-ELS 1000, evaporative light scattering or mass detector, Polymer Laboratories Ltd., Shropshire, UK) was used as the detection method (see Figure 29).

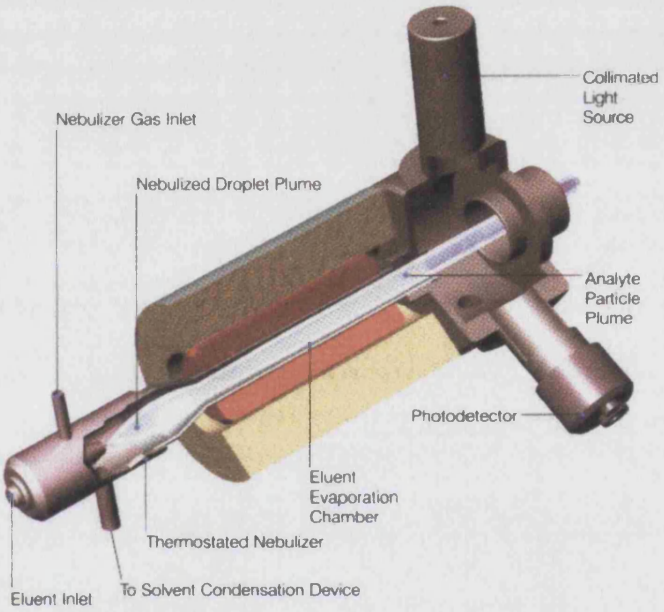

Figure 29: A picture of the PL-ELS 1000 mass detector.

PL-ELS 1000 is a unique and highly sensitive detector for non-volatile solutes in a volatile liquid stream. The solvent containing the solute material is nebulised and carried by a gas flow through an evaporating chamber. The solvent is volatilised, leaving a mist of solute particles that scatter light to a photosensitive device. The signal is amplified and a voltage output results. The output is directly related to the mass of the solute particles passing through the light, hence the name mass detector.

Chromatographic Conditions

Column: 250 x 4.6mm LiCN (10μm packing, Hi-Chrom Ltd, UK) with a guard column 13mm x 8mm (10μm packing, Hi-Chrom Ltd, UK).

Column Temp: Ambient Injection Volume: 20μl Flow Rate: 1.0ml/min

Run time: 8 minutes Retention times: PG 2.7min, DPPC 3.8min

Pump: Jasco intelligent HPLC pump, model PU980 (Jasco Ltd., Essex, UK)

Sampler: Jasco intelligent sampler, model PAS950

Mobile Phase: Methanol (HPLC grade, Fisons Scientific Equipment Ltd., UK)

Software: Borwin chromatography software V1.22 (JMBS, Grenoble, France)

Detector: PL-ELS 1000, software version V1.1

Detector settings: N_2 Inlet pressure: ~50psi, Evaporator Temp: 80°C, nebuliser Temp: 80°C, Gas Flow: 0.7 SLM (standard litres per minute), Exhaust Temp: 50°C

Standard Preparation

DPPC and PG standards were stored at -20°C, prior to use. Three stock solutions were prepared by accurately weighing approximately 70mg of DPPC and 30mg of PG into a 100ml volumetric flask to produce a solution of 700/300μg/ml of DPPC and PG respectively. Two sets of five dilutions were prepared from each of the three stock solutions (see Figure 30, page 102) making sure that in each case the ratio of PG: DPPC were maintained at 0.429. This ratio of 0.429 is the ratio of the two phospholipids within SAPL.

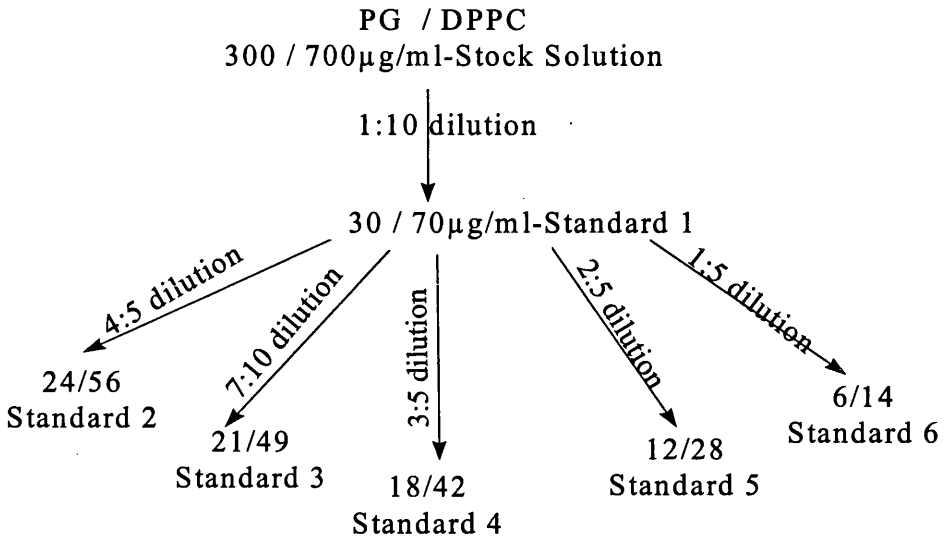

Figure 30: Stock solution dilution procedure for PG and DPPC.

Stock Solution	Wt. DPPC (mg)	Wt PG (mg)
A	70.1	30.1
B	70.0	30.0
C	69.9	29.9

Table 15: Stock solutions and weights of standards used in the linearity experiments.

Linearity Experiments

Six sets (two groups from each stock solution) of six standards were injected (5 times per sample) and the areas of the two components determined by integration. The integrated areas were then expressed as % areas and % PG was adjusted by multiplying with a correction factor, before the phospholipid ratio of the two components was calculated. A correction was employed to account for the sensitivity of the HPLC equipment to PG. This was necessary because in the original method development, various known quantities of DPPC and PG were analysed and also to adjust the % ratio of the PG and DPPC peaks so as to maintain the fixed ratio of 0.429 present in each of the standards.

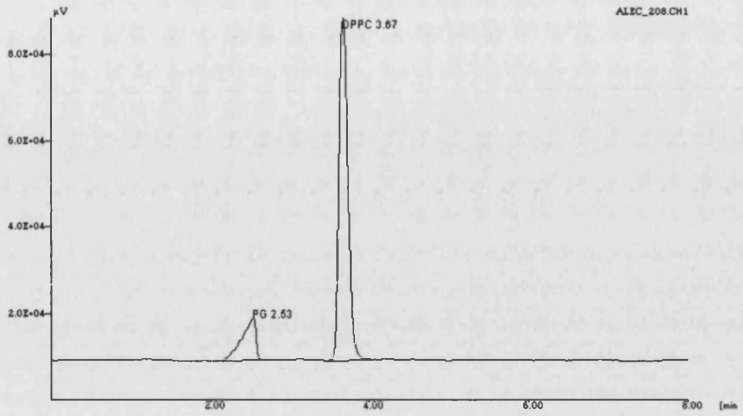

Figure 31: Specimen HPLC chromatogram showing the two components of SAPL.

Stk /Std No.	Dil. Set	Mean PG Area	Mean DPPC Area	PG C.F.	Mean Corr. PG Area
A1	1	108607±6082	553562±30999	1.83	198651±11124
	2	107135±5785	555014±32191	1.85	198645±10727
A2	1	81152±4058	374074±19826	1.68	136568±6828
	2	80553±4189	376000±20304	1.70	136966±7122
A3	1	68941±3171	294242±15889	1.58	108955±5012
	2	68765±2957	293126±14949	1.58	108567±4668
A4	1	55698±2339	223510±11176	1.50	83762±3518
	2	55081±2203	221047±11494	1.50	82838±3314
A5	1	31555±1262	123831±5572	1.48	46616±1865
	2	31543±1293	121907±5364	1.46	46035±1887
A6	1	13278±491	34200±1402	1.07	14243±527
	2	13114±446	34118±1365	1.08	14170±482
B1	1	110468±6510	558319±30149	1.82	200636±11838
	2	109340±6777	555942±43363	1.83	199585±12574
B2	1	83363±4752	376605±20713	1.66	137990±7865
	2	84167±4798	375064±24379	1.64	137769±7853
B3	1	67990±2924	294734±14737	1.60	108817±4679
	2	69008±2829	296762±16915	1.59	109731±4499
B4	1	54883±2415	222424±12678	1.52	83192±3660
	2	56348±2141	223101±11601	1.49	83835±3180
B5	1	31746±1302	120990±4961	1.44	45821±1879
	2	32095±1027	121738±5478	1.44	46150±1477
B6	1	13092±458	34710±1388	1.10	14341±502
	2	13242±437	35460±1454	1.10	14611±482

Table 16: Table showing the HPLC areas obtained for stock solutions A and B, dilution sets 1 and 2.

Stk /Std No.	Dil Set	Mean PG Area	Mean DPPC Area	PG C.F.	Mean Corr. PG Area
C1	1	112064±6276	559342±42510	1.80	201422±11280
	2	110967±6103	557618±47955	1.81	200576±11032
C2	1	86014±4731	378205±20045	1.62	139266±7660
	2	84649±4402	376±30484	1.63	138299±7192
C3	1	69113±3387	297301±16054	1.59	109924±5386
	2	68385±3146	296435±21640	1.60	109446±5035
C4	1	58135±2442	223611±12299	1.45	84524±3550
	2	57946±2723	222755±15593	1.45	84210±3958
C5	1	33266±1497	122282±5992	1.40	46664±2100
	2	32317±1487	121371±7040	1.43	46106±2121
C6	1	13558±420	36314±1743	1.10	14962±464
	2	13256±398	35348±1661	1.10	14581±437

Table 17: Table showing the HPLC areas obtained for stock solution C, dilution sets 1 and 2.

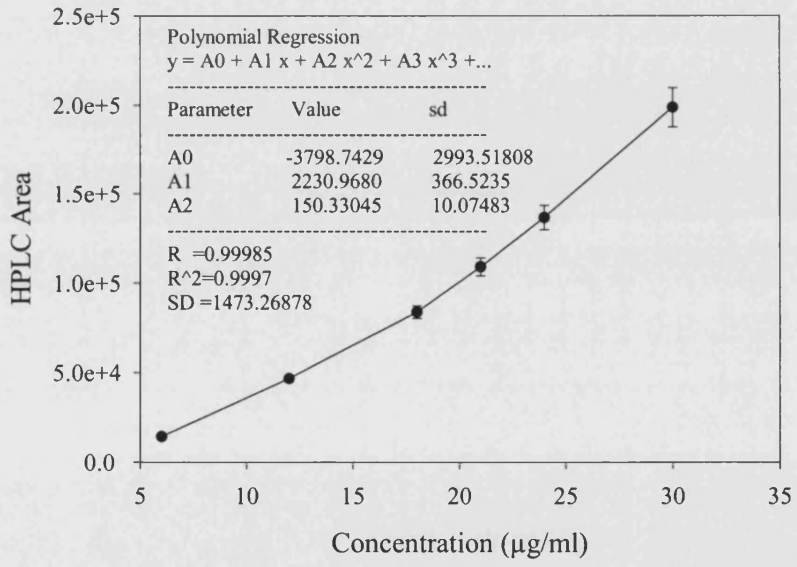

Figure 32: A graph showing an example of the Binomial relationship between standard concentration and HPLC area.

The graph is a plot of concentration versus corrected PG HPLC area for stock A, dilution set 1.

Similar calibration curves were obtained for the other stock solutions and dilution sets. These all showed a binomial relationship ($y=A0+A1x+A2x^2+.....Etc.$) with increasing standard concentration. The parameters obtained from these graphs are summarised below. Regression analysis was performed using Microcal® Origin v2.94 (Microcal Software Inc., MA, USA).

Parameter / Stock	Dil Set	PG Value (±SD)	DPPC Value (±SD)	Dil Set	PG Value (±SD)	DPPC Value (±SD)
A0-Stk A	1	-3799(±2994)	-7717(±11680)	2	-3449(±3297)	-6015(±12171)
A1-Stk A	1	2231(±337)	2020(±613)	2	2118(±404)	1824(±639)
A2-Stk A	1	150(±10.1)	85.5(±7.22)	2	154(±11.1)	88.4(±7.52)
R-Stk A	1	0.99985	0.99971	2	0.99982	0.99969
R^2-Stk A	1	0.99970	0.99942	2	0.99964	0.99938
SD-Stk A	1	1473	5748	2	1623	5990
A0-Stk B	1	-2668(±3159)	-4967(±10243)	2	-3600(±2672)	-5990(±9524)
A1-Stk B	1	1971(±387)	1747(±537)	2	2194(±327)	1895(±500)
A2-Stk B	1	160(±9.06)	89.9(±6.33)	2	153(±8.99)	87.5(±5.89)
R-Stk B	1	0.99984	0.99978	2	0.99988	0.99981
R^2-Stk B	1	0.99967	0.99956	2	0.99976	0.99962
SD-Stk B	1	1554	5041	2	1315	4687
A0-Stk C	1	-2825(±3030)	-4099(±10046)	2	-3280(±2614)	-5306(±9782)
A1-Stk C	1	2110(±371)	1791(±527)	2	2125(±320)	1817(±513)
A2-Stk C	1	157(±10.2)	89.4(±6.21)	2	156(±8.80)	88.8(±6.05)
R-Stk C	1	0.99985	0.99979	2	0.99989	0.99980
R^2-Stk C	1	0.99970	0.99958	2	0.99978	0.99960
SD-Stk C	1	1491	4944	2	1286	4814

Table 18: Table summarising the polynomial relationship between standard concentration and detector response in the linearity experiments.

Statistics

The Bartlett test and Student's t-test, as outlined in section 2.3, page 118, were performed on the binomial constants A0, A1, and A2 obtained from the graphs to ascertain inter and intra sample variation. The Bartlett and T-test at results obtained are shown in Table 19, page 58.

	χ^2-Value	Degrees of Freedom	Probability	Significant Difference
A0	0.427	11	>0.9999	No
A1	1.422	11	0.9997	No
A2	187.9	11	<0.005	Yes

Table 19: Table showing the Bartlett test values for binomial constants A0, A1, and A2 obtained from the statistical analysis of MS-HPLC linearity experiments.

	DOF	T-value for A0 at p=0.05					
		PG	Prob.	Significant Difference	DPPC	Prob.	Significant Difference
Stock A-Set 1/2	8	0.079	0.470	No	0.101	0.461	No
Stock B-Set 1/2	8	0.225	0.414	No	0.073	0.472	No
Stock C-Set 1/2	8	0.114	0.456	No	0.086	0.467	No
		T-value for A1 at p=0.05					
Stock A-Set 1/2	8	0.215	0.418	No	0.221	0.415	No
Stock B-Set 1/2	8	0.440	0.336	No	0.202	0.423	No
Stock C-Set 1/2	8	0.031	0.488	No	0.035	0.487	No
		T-value for A2 at p=0.05					
Stock A-Set 1/2	8	0.267	0.398	No	0.278	0.394	No
Stock B-Set 1/2	8	0.548	0.293	No	0.278	0.394	No
Stock C-Set 1/2	8	0.074	0.471	No	0.069	0.473	No

Table 20: Table showing the T-test values obtained for the binomial factors A0, A1 and A2 from the statistical analysis of MS-HPLC linearity experiments.

Repeatability Experiments

The precision of the method was measured by performing five injections of a standard solution (30/70µg/ml) and calculating the relative standard deviation of the peak areas obtained. The results are given in Table 21, page107.

Injection Number	PG Area	PG retention Time (Min)	DPPC Area	DPPC Retention Time (Min)
1	110416	2.53	558507	3.66
2	110995	2.53	557121	3.67
3	110403	2.53	559493	3.66
4	111449	2.53	556914	3.66
5	111263	2.53	559637	3.67
Mean	110905	Mean	558334	
SD	480	SD	1281	
RSD(%)	0.433	RSD(%)	0.229	

Table 21: Repeatability of injection for standard 1 (30/70µg/ml PG:DPPC).

Sample Measurement

Following calibration of the SAPL assay, determination of the concentration of the active in unknown solutions was undertaken as described below.

The six standards were prepared as described earlier. These solutions were injected in duplicate at the beginning of a run, prior to unknown samples. The unknown samples were prepared and diluted according to the methods given for the various deposition studies undertaken, such that they fell within the standard range. The test samples were also injected in duplicate. The concentrations of SAPL in the unknown solutions were calculated by solving the quadratic equations of the standard curves using a mathematics programme (Maple© V, Release IV, The Power Edition, Waterloo Maple Inc., Canada) as shown below. The values in the equation below are for stock solution A, dilution set 1, from Figure 32, page 104.

$$y = -3799 + 2231X + 150.3X^2 \qquad \text{Equation 8}$$

solution:

$$\underset{\mathbf{A}}{\frac{-11155}{1503}} + \underset{\mathbf{B}}{\frac{1}{1503}} \underset{\mathbf{C}}{\sqrt{181532995 + 15030y}} \ldots, \frac{-1155}{1503} - \frac{1}{1503}\underset{\mathbf{D}}{\sqrt{181532995 + 15030y}}$$

Thus, by taking the positive values from the above equation, labelling them A, B, C and D and incorporating the values into a spreadsheet, equation 9 can be used to calculate the concentration of the unknown samples in the individual deposition profiles. Examples of this process as well as raw data are given in Appendix 13: MS Testing and Stability Study Raw HPLC Data, page 271.

Concentration= A+B*sqrt(C+D*HPLC Area) **Equation 9**

Discussion

Statistical analysis and the method outlined show that this technique for quantifying SAPL is appropriate for use in this study.

2.2.5.2 Fluorimetric Detection of LFDS

A full account of the labelling procedure, reasons for labelling and subsequent identification and characterisation of LFDS is given in section 3 Fluorescent Labelling of FDS, page 121. This section describes the fluorimetric method developed to quantify LFDS.

Standard Preparation

Three stock solutions were prepared by accurately weighing approximately 200mg of LFDS, containing 1% label (i.e. 2mg total weight), into a 100ml volumetric flask to produce a stock solution with a label content of 20μg/ml, dissolved in methanol (HPLC grade). Three sets of subsequent dilutions were prepared from each of the three stock solutions (see Figure 33, page 109) to produce six standards, ranging from 0.05 to 08μg/ml from which the calibration curves were constructed.

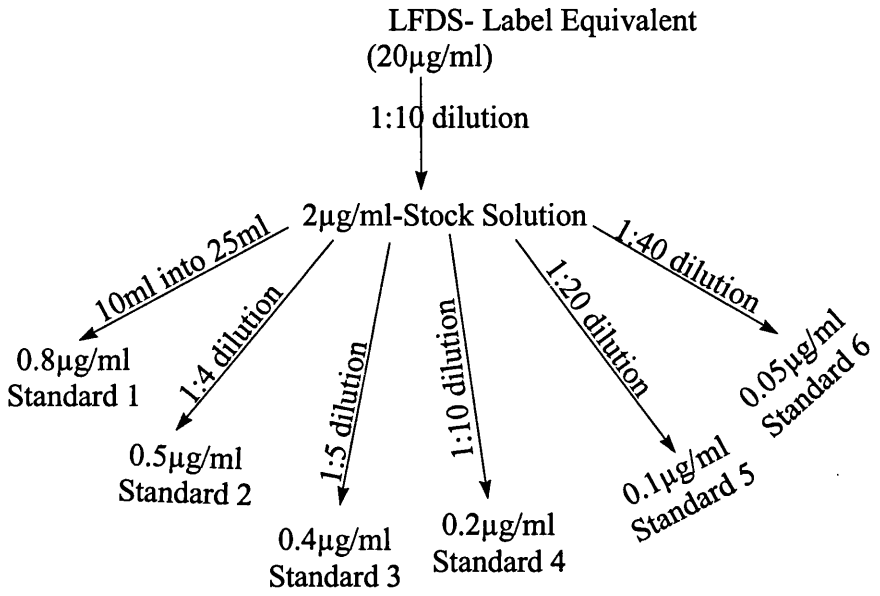

Figure 33: Stock solution dilution procedure for LFDS.

Stock Solution	Wt. of LFDS (mg)	Label Nominal Content (µg)
A	200.18	2.18
B	200.25	2.25
C	200.40	2.40

Table 22: Stock solutions and weights used in the construction of the fluorimetric calibration curve.

Detection of Excitation and Emission Wavelengths

The standard solutions were scanned using a Hitachi F2000 Fluorimeter, Hitachi Ltd., Japan. The scan conditions are given below:-

Scan speed: Fast Scan step: 10nm Sensitivity: High

Excitation slit: 10nm Emission slit: 10nm Excitation scan range: 200-450nm

Emission Scan range: 400-600nm

Preliminary settings were such that a coarse scan was carried out for both excitation and emission. The instrument was then set at a lower scan speed and both the excitation and emission wavelengths were determined more accurately. The excitation (Ex) and emission (Em) was found to be 345nm and 482nm respectively, see Figure 34, page 110.

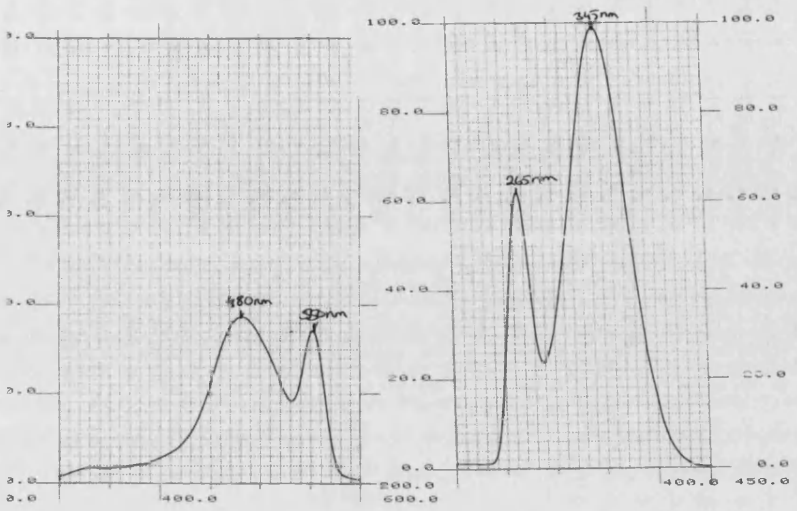

Figure 34: A specimen spectrum showing the λ_{max} obtained for n-octadecyldansylamide by fluorimetric Analysis.

The standard solutions were then measured at the above wavelengths and the relative intensities of the samples were determined. Methanol was used as the blank.

Stock / Std No.	Conc. (µg/ml)	Dilution Set	Relative. Intensity (%)	Dilution Set	Relative Intensity (%)	Dilution Set	Relative Intensity (%)
A1	0.05	1	6.42	2	6.44	3	6.40
A2	0.1	1	12.9	2	12.9	3	12.8
A3	0.2	1	25.7	2	25.6	3	25.6
A4	0.4	1	51.3	2	51.5	3	51.3
A5	0.5	1	63.8	2	63.8	3	63.7
A6	0.8	1	101.8	2	101.8	3	101.6
B1	0.05	1	6.41	2	6.41	3	6.40
B2	0.1	1	12.7	2	12.7	3	12.8
B3	0.2	1	25.5	2	25.3	3	25.5
B4	0.4	1	50.4	2	50.6	3	50.5
B5	0.5	1	63.6	2	63.5	3	63.3
B6	0.8	1	101.3	2	101.4	3	101.3
C1	0.05	1	6.41	2	6.45	3	6.42
C2	0.1	1	12.6	2	12.8	3	12.9
C3	0.2	1	25.2	2	25.1	3	25.0
C4	0.4	1	49.9	2	49.8	3	49.7
C5	0.5	1	62.3	2	62.5	3	62.4
C6	0.8	1	102.4	2	102.2	3	102.1

Table 23: LFDS standard solutions and corresponding relative intensities for dilutions sets 1, 2 and 3.

The calibration curves for the above data all show a linear relationship with increasing concentration.

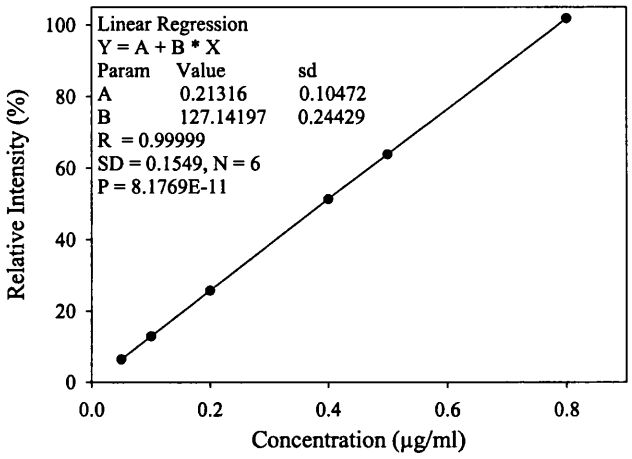

Figure 35: A specimen calibration plot of standard concentration versus relative intensity

Stock	Dil	Slope	Slope SD	Intercept	Intercept SD	Correlation Coefficient
A	1	127.1	0.2443	0.2132	0.1047	0.99999
A	2	127.2	0.3676	0.2182	0.1576	0.99998
A	3	127.0	0.3141	0.1803	0.1346	0.99999
B	1	126.5	0.3260	0.11821	0.1398	0.99999
B	2	126.7	0.1691	0.05047	0.07247	0.99999
B	3	126.3	0.1773	0.1617	0.07601	1.00000
C	1	127.4	1.243	-0.3919	0.5329	0.99981
C	2	127.1	1.140	0.2904	0.4886	0.99984
C	3	126.9	1.200	0.2869	0.5144	0.99982

Table 24: Table summarising the various parameters obtained from the calibration plots for the three sets of LFDS standards.

Statistics

Statistical analysis on the slopes of the above results was performed using the Bartlett test as outlined section 2.3 Statistical Analysis, page 118. The test indicated no significant differences between the three standards and three dilutions per set (χ^2= 0.527, p= 0.9998). With the exception of A1, the intercepts passed through zero within ±2 SDs and RSDs for the slopes were ≤4.4%, indicative of good linearity.

Sample Measurement

Following calibration of the SAPL assay, determination of the concentration of the active in unknown solutions was undertaken as described below.
The six standards were prepared as described earlier. These solutions were measured and a standard curve constructed for each separate analysis. The unknown samples were prepared and diluted according to the methods given for the various deposition studies undertaken, such that they fell within the standard range. The concentrations of SAPL in the unknown solutions were calculated by substituting the equations of the standard curves into a spreadsheet. A more precise account of this process is given in the individual deposition studies profiles (see section 4 Deposition Studies of MLFDS, page 135).

2.2.6 General / Other Methods

This section outlines the various miscellaneous techniques used in the characterisation and processing of SAPL. These include micronisation, surface area analysis, and moisture analysis.

2.2.6.1 Micronisation of SAPL

Micronisation of raw, freeze-dried labelled SAPL (FDS) was carried at out by fluid-energy milling using the Gem-T air pulveriser, Glen-Creston, Stanmore, UK. Micronisation of Raw SAPL (manufactured without the freeze drying process) was carried out at Micro-Macinazione SA (Micro-Grinding Ltd), Switzerland, using their patented Chrispro®-Jetmill.

Method 1- Using the Gem-T Air Pulveriser

Samples were fed into the micronisation chamber using a small vibrating spatula, via small feed-orifice located at the side of the instrument. The feed-rate was varied according pressure differences between the inlet and the outlet valve of the instrument. Inlet valve operating pressure was 100psi, and the outlet valve pressure was 80psi, therefore, creating a 20psi net pressure difference in the flow of air towards the micronisation chamber. This pressure difference was used to entrain the sample to the micronisation chamber. The micronised samples were collected in a glass collection jar, removed, weighed and the efficiency of the procedure calculated. Typically, the process was about 65% efficient, and sample loss was due to:

a) Sample adhering to the various internal components of the mill.
b) Sample loss during transfer after the micronisation process.
c) Ultrafine particles not heavy enough to fall into the collection jar being collected in the relief bag required for the escaping air from the system.

Method 2- Using the Chrispro®-Jetmill

Chrispro® jetmill, model MC50, was used to micronise SAPL in a class 10,00 laboratory supplied with filtered air. The humidity (<10%) and temperature (18-20°C) of the room was controlled. A glove-box was specially constructed to house the equipment and to produce micronised material suitable for inhalation. The procedure was carried out under a stream of nitrogen, filtered through a 0.2μm filter, and all air was eliminated from the system. Standard

bacterial swab tests were carried out to ensure the conditions met the criteria necessary to produce inhalation quality material. The operating conditions were:

Air Consumption at 7bar: 0.41Nm^3/min.

Sample Feed-Rate: 0.05-1kg/h Projected particle size range: 0.5-10μm

Efficiency: ~70%, losses due to reasons explained above.

2.2.6.2 Surface Area Analysis (BET Multi-Point)

In the pharmaceutical industry, surface area is becoming more important in the characterisation of materials during development, formulation, and manufacturing (Webb and Orr 1997). The surface area of a solid provides information about the void spaces on the surfaces of individual particles or aggregates of particles (Parrott 1970). This is important because factors such as chemical activity, adsorption, dissolution, and bioavailability of the drug may depend on the surface of the solid. The adsorption of inert gases onto solid materials represents the most widely used method for the determination of surface area. The Brunauer, Emmett, and Teller (BET) method is generally used for gas adsorption surface area measurements. The BET method is based on the monolayer adsorption of an inert gas onto the solid surfaces at reduced temperatures, nitrogen is used as the adsorbate gas for most samples. The way in which a material adsorbs a gas is referred to as an adsorption isotherm, and there are five typical adsorption isotherms. The isotherm shapes reflect specific conditions for adsorption, such as pore size and heats of adsorption, and the most common isotherm type is the type II isotherm (used in BET measurements). BET theory is an extension of Langmuir's theory of monolayer gas adsorption on surfaces (Lowell and Shields 1984). BET theory takes into account the formation multilayers on surfaces (Webb and Orr 1997), and relates condensation rate of gas molecules onto an adsorbed layer and the evaporation rate from that layer for an infinite number of layers. The linear form of the relationship is called the BET equation.

$$\frac{P}{V(P_0 - P)} = \frac{1}{V_m C} + \frac{C-1}{V_m C}\left[\frac{P}{P_0}\right] \qquad \textbf{Equation 10}$$

(i.e. Y= C + mX)

where V= Volume of gas adsorbed at pressure P.

P= Partial pressure of adsorbate.

V_m= Volume of gas adsorbed in monolayer.

P_0= Saturation Pressure of adsorbate at experimental temperature.

C= BET constant exponentially relating the heats of adsorption and condensation of the adsorbate.

The BET theory assumes that all adsorption sites are energetically equivalent, which is not the case for normal samples. The BET model also ignores lateral adsorbate interactions on the surface, and assumes that the heat of adsorption for the second layer and above is equal to the heat of liquefaction.

Method

Samples were weighed into glass bulbs, and degassed (FlowPrep 060 Degasser, Micromeritics, Particle Technology Instruments, GA, USA) under the conditions given below to remove pre-adsorbed gasses and vapours from the solid surface. Higher degassing temperatures were avoided to minimise sample degradation and dehydration. Samples were re-weighed and the values were used for subsequent surface area measurements (Gemini 2360 V5.00 (Micromeritics, Particle Technology Instruments, GA, USA).

Operating Conditions

Evacuation Time: 1min

Equilibration Time: 5 or seconds

Saturation Pressure 760mmHg

De-gassing period: 24hrs

De-gassing temperature: 50°C

Results

Table 25 below shows the various parameters obtained from the BET measurements.

Sample ID	Sample Wt (g)	SA (m^2/g)	Slope ($1/cm^3$)	Y Intercept	BET Constant	V_m (cm^3)	R
FDS	1.576	0.435	9.28	0.718	14.0	0.100	1.000
MLFDS	0.971 (±0.023)	0.718 (±0.008)	5.54 (±0.155)	0.341 (±0.050)	14.6 (±0.118)	0.163 (±0.004)	0.9998
UMS	1.568 (±0.060)	0.510 (±0.008)	7.96 (±0.130)	0.580 (±0.019)	14.7 (±0.415)	0.117 (±0.003)	0.9995
MS	1.720 (±0.072)	3.0784 (±0.025)	1.33 (±0.721)	0.0876 (±0.057)	16.1 (±0.469)	0.707 (±0.006)	0.9994

Table 25: BET parameters obtained on the Gemini 2360 V5.00 (Micromeritics, Particle Technology Instruments, GA, USA) for various forms of SAPL, n=3.

Discussion

Results of the surface area measurements show clear differences between the various samples analysed. Generally, as expected, the surface area of the micronised material is greater than non-micronised samples. However, the technique may be underestimating the surface area of the micronised material since firmly agglomerated particles may hinder or prevent nitrogen from penetrating the surfaces of every individual particle.

2.2.6.3 Moisture Analysis of SAPL

Method

Moisture determinations were carried out using Karl-Fischer (KF) analysis (Metrohm 684 Karl-Fischer Coulometer, Hensau, Switzerland). A mixture of chloroform: methanol (Ratio 1:2 v/v) was prepared and used as the solvent. 0.5ml of the solvent was injected through the septum of the KF chamber a total of 10 times, using a high precision gas chromatography

syringe (Hamilton Gastight 1700 syringe, Hamilton Company, Nevada, USA). The average of ten readings were used to calculate the water content of the solvent in μg, and this was used as the blank value in subsequent measurements. Approximately 20-40mg of the sample was weighed and dissolved in the mixture to give 0.5mg/ml solution, of which five 0.5ml aliquots were injected. By multiplying the concentration of the solution with the volume, the amount of sample injected (in mg) was calculated. This figure was inputted into the instrument and % water content for the sample was obtained.

Instrument settings and Calculations

Drift (μg/min)= 0.0006, Delay (s)= 5, Extraction time (min)= 1

$$\%water = \frac{M(H_20 - Blank)}{Sample}$$ **Equation 11**

Results

	FDS Pre-Micro	FDS Post-Micro	LFDS	LMFDS	UMS	MS
% Moisture	3.40 (±0.10)	5.20 (±0.14)	3.25 (±0.04)	3.43 (±0.05)	4.18 (±0.09)	4.42 (±0.15)

Table 26: Percentage moisture content values for various forms of SAPL, pre and post micronisation. Values in brackets indicate standard deviation, n=5.

Discussion

The results show that the indigenous moisture of the various forms of SAPL, before any processing, are very similar with values of 3.40, and 4.18% for FDS and UMS respectively. The micronisation procedure appears to increase the moisture content slightly, but not enough to cause any undue concern.

2.2.6.4 Mixing Techniques

Preliminary, geometric and ad-hoc hand blending techniques using a pestle and mortar yielded poor content uniformity results. Also, the mechanical stress caused by hand blending raised questions as to the stability of SAPL during the mixing process. Thus, this type of blending was discontinued. Turbulent tumbling mixing using the Turbula T2C (Bachofen, Basel, Switzerland) also produced blends with poor content uniformity. The probable cause of this was due to low shear achieved by this type of mixing. Hence, only the high-shear blending techniques described below was employed.

MLFDS was mixed with coarse Lactochem-lactose (63-90μm, see Figure 105, page 269). The powders were mixed using a rotary bladed blender (Kenwood Mini Chopper, CH100, Kenwood Ltd., Hants., UK) at a constant blade speed. At various intervals (every minute) the mixing procedure was halted, the powder adhering to the sides of the chamber and the blade face was removed using a soft brush. The benefit of this procedure was two-fold. Firstly, constant mixing caused the blender to overheat. Thus, stopping periodically allowed the blender to cool-down. Secondly, adhered powder was introduced back to the bulk powder bed to ensure uniform mixing. When producing ternary blends of SAPL with coarse and fine lactose combinations, the two components were pre-blended for a period ten minutes. Following this, the drug was introduced to the system and the blending was continued until acceptable content uniformity values (i.e. <5% RSD) were obtained. The size of the blends varied between ten and forty grams depending upon the study. The optimum mixing time of each blend was determined by carrying out content uniformity experiments.

2.3 Statistical Analysis

The theory of statistics is based on probability (Bolton 1996). Probability distribution is a mathematical function that assigns probabilities for outcomes in its domain. The normal distribution is the basis of modern statistical theory and methodology. The chief reason for this is the central limit theorem, which shows that means of samples from virtually all

probability distributions tend to be normal for large sample sizes. Probability distributions used in statistical analyses are based on normal distribution and include the t and chi-square distributions.

2.3.1 Analysis of Variance (ANOVA)

This is perhaps the most powerful statistical stool and is a general method for analysing data from designed experiments, whose objective is to compare two or more group means. The statistics packaged used to analyse the results throughout this report was Minitab® for Windows, V 10.2, Minitab Inc., PA, USA. There are two types of anova:

a) One-Way: only looks at the differences in group means
b) Two-Way: may look at other variables apart from means (e.g. different treatments of the groups).

Only the one-way anova was used to assess the results throughout this report. P and F values were obtained, where P was the probability and F was an indication of actual variation in group averages devided by the expected variation in group averages. To put it another way, F is the value obtained when the error within the group is divided by the error between the averages. Thus, F is greater than or equal to 1, and larger the F value more the error associated within the group.

2.3.2 Student's t-Test

The t distribution is an extremely important distribution and is a special case of ANOVA in which only two means are compared. The t-test formula used in the statistical analysis throughout the report to to check for intra-group variability is given below:

$$t = \frac{slope1 - slope2}{(sd_1^2 + sd_2^2)^{1/2}}$$ **Equation 12**

at $(n_1+n_2)-4$, where n_1= number of points on line 1 and n_2= number of points on line 2.

2.3.3 Chi-Square (Bartlett) Test

Chi-square distribution is another important probability distribution and may be derived from normally distributed variables, defined as the sum of squares of independent normal variables, each of which has mean 0 and standard deviation 1. Thus, when more than two estimates of a parameter P are tested for equality, the following statistic is used:-

$$B = \frac{\Sigma(pi - \bar{P})^2}{\hat{(\sigma)}^2} \qquad \textbf{Equation 13}$$

Where: $\hat{(\sigma)}^2 = \frac{n_1 S_1^{\,2} + n_2 S_2^{\,2} \ldots\ldots n_n S_n^{\,2}}{n_1 + n_2 + \ldots\ldots n_n}$ **Equation 14**

Where S_1, S_2 etc. are the standard deviations associated with the estimates P_1, P_2 etc. and n_1, n_2 etc. are the number of observations used in determining the estimates. If the estimates all come from the same normal distribution then the above equation will have a χ^2 distribution with N-1 degrees of freedom where N is the number of estimates.

Chapter 3

Fluorescent Labelling of FDS

3 Fluorescent Labelling of FDS

The various sections and sub-sections below are intended to give a systematic insight into the properties and behaviour of SAPL powder.

3.1 Reasons for Labelling

SAPL has no UV chromophore and cannot be detected by UV analysis. Attempts were made to quantify the material with atomic absorption (AA), refractive index (RI) analysis, and by fluorescence. AA analysis was undertaken in attempt to quantify SAPL indirectly by measuring the levels of calcium (Ca^{2+}) and sodium (Na^{+}) present within freeze-dried samples. Samples were dissolved in methanol (0.5-10mg/ml) and measured using air/acetylene, nitrous oxide/acetylene, and nitrous oxide only as the fuel sources. AA was not used as the detection method, however, since the levels of Ca^{2+} and Na^{+} were different from batch to batch, and the material was poorly soluble in aqueous solutions. RI analysis (Abbe refractometer, Bellingham & Stanley Ltd, London) of varying concentration (0.01-0.5mg/ml) of SAPL, dissolved in chloroform, showed that the technique was not sensitive enough to be used as the detection method. A full range scan using a fluorescence spectrophotometer (Shimadzu RF540, Simadzu Ltd., Tokyo, Japan) revealed a concentrated solution of SAPL to be only very slightly fluorescent, too small to be quantifiable in any deposition study profiles. Thus, in order to quantify FDS in the various deposition studies undertaken, it was necessary to label the material with a fluorescent agent (n-octadecyl dansylamide-1%w/w).

A full account of the synthesis of the label, the labelling procedure, identification of labelled material, and an experiment to evaluate the uniform distribution of the label within SAPL is described in this section.

3.1.1 Preparation of the Label (n-Octadecyl Dansylamide)

The fluorescent label, n-octadecyl dansylamide, (see Figure 98, page 263 for structure and physico-chemical properties) was synthesised by reacting equal quantities (1.35g) of octadecylamine (see Figure 97, page 263) and dansyl chloride (see Figure 96, page 263), both dissolved in dichloromethane. Triethylamine (700mg) was used to remove excess hydrochloric acid (HCl) from the reaction. The presence of the final product was established by thin layer chromatography. A drop of all the components used in the synthesis was placed near one edge of the plate and their positions marked with a pencil. The sample solvent was then evaporated and the plate was placed in a closed glass container with one end immersed into the developing solvent (hexane:ethyl acetate (1:1)). The plate was then removed, dried and sprayed with ninhydrin to reveal the spots on the plate.

Once the final product was identified, magnesium sulphate and 1M HCl were then added to remove residual water and excess triethylamine respectively. Identification of the final product was established using nuclear magnetic resonance (NMR) (see 3.1.3 NMR Identification of the Label, FDS, and FDS-Control) and hot-stage microscopy. The melting point of n-octadecyl dansylamide was found to be 70-72°C, this compared with 69.5-71°C, which was the quoted literature value for the compound, Bergbreaker (1990).

3.1.2 Labelling Procedure

SAPL (5g) and 1% w/w (50mg) of the label were dissolved in a minimum amount of chloroform, stirred thoroughly and filtered to remove any impurities. The solvent was removed using a rotary evaporator. The labelled SAPL was collected and identified via NMR and Mass Spectometry with the help of Dr Mike Threadgill and his group, University of Bath, School of Pharmacy and Pharmacology.

3.1.3 NMR Identification of the Label, FDS, and FDS-Control

Figure 36 shows a ^{1}H NMR trace of n-octadecyl dansylamide. The trace was produced using the method outlined below.

The samples were dissolved in deuteriated chloroform ($CDCl_3$) and a small amount was placed into NMR sample tubes for analysis. The NMR instrument used for both ^{1}H and ^{13}C analysis had field strength of 400MHz (JEOL EX 400, Japan).

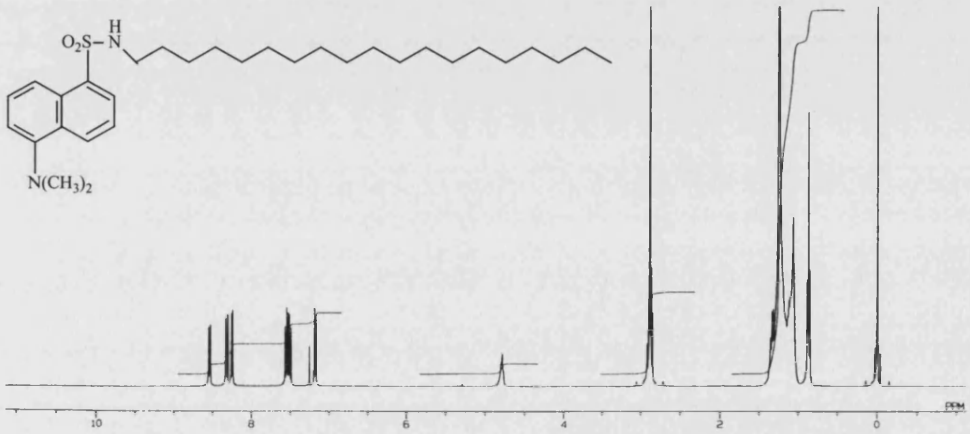

Figure 36: ^{1}H NMR trace of n-octadecyl dansylamide.

The peak at 0ppm is TMS (reference solvent). The singlet at δ0.8-0.9ppm is due to the terminal CH_3 group at the end of the long alkyl chain. All other CH_2 groups within the compound are represented by the wide multiplet seen between δ1-1.5ppm. The peak at δ2.9ppm is due to two methyl groups next to nitrogen at the bottom of the aromatic ring as well as the CH_2 group next to the Nitrogen at the beginning of the long alkyl chain. The peak at δ4.7ppm is due to the NH coupling. The peaks between δ7.2 to δ8.6ppm are due to the various aromatic protons. The reason for the wide range is that some are affected by the hetero-atoms far more than others.

Figure 37, page 124 shows the ^{13}C NMR trace of n-octadecyl dansylamide. The peak at 14ppm is due to terminal carbon on the methyl group on the long alkyl chain portion of the label. The peak at 22.7ppm belongs to the carbon present in CH_2 groups in the alkyl chain portion of the label.

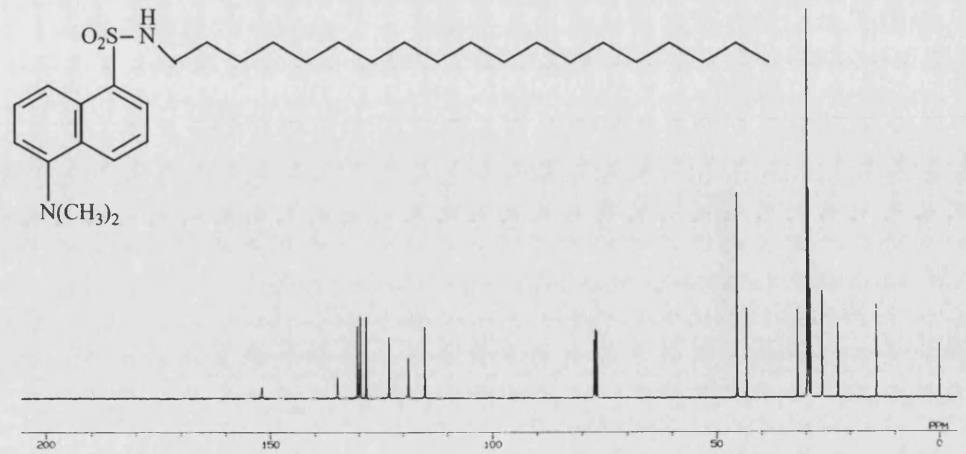

Figure 37: ^{13}C NMR trace of n- ocatdecyl dansylamide.

The multiple peaks between 26.4 and 32.0 belong to other carbons, which make up CH_2 groups within the structure. The N-CH_2 coupling produces the peak at 43.2. The peak at 45.4 is due to two carbons on the Methyl groups, which are attached to the Nitrogen at the bottom of the aromatic ring. The multiple peaks between 76.7 and 77.3 belong to Chloroform, which is the solvent used to prepare the material for analysis. The aromatic carbon groups are given between 115.2 and 130.3. Quaternary carbons within the structure are represented by the peaks at 134.8 and 151.9. Figure 38, below, shows the ^1H NMR trace of FDS (see Figure 1, page 13 for structure) and FDS control. FDS control is material that has undergone the labelling procedure, but without the label being introduced into the process.

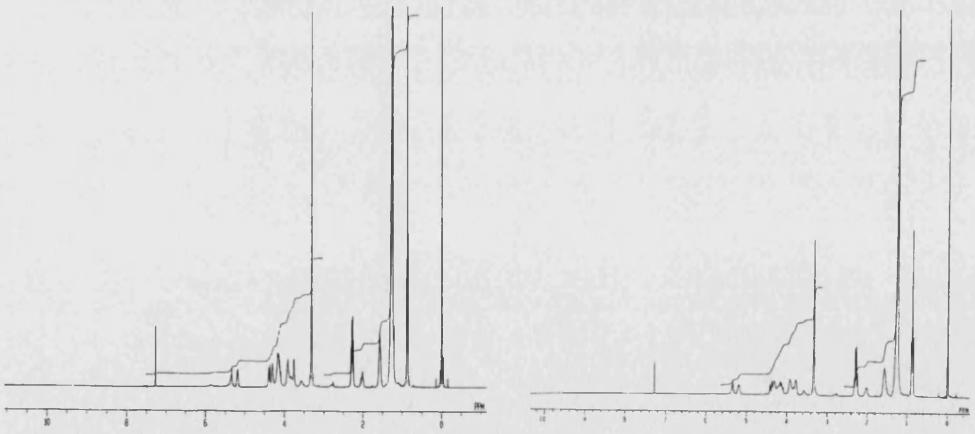

Figure 38: ^1H NMR trace of FDS and FDS-Control.

The peak at approximately δ0.5ppm are due to the methyl groups from the DPPC and possibly from the terminal methyl groups at the end of the fatty chains attached to PG on positions R_1 and R_2. The broad series of multiplets at δ1.2 to δ1.35 are due to the various CH_2 groups in both the DPPC and PG. The broadness of the peak is due to the various environments that the CH_2 groups are under. The peak at δ1.6ppm is due to the O=C-CH_2-CH_2 couplings. The quartet at δ2.4ppm is probably due to the various O=C-CH_2 couplings throughout both DPPC and PG. The triplet at δ3.3ppm is due to the N-$(CH_3)_3$ interactions. The multiple of peaks from δ3.5 to 4.4ppm are due to the various CH_2s connected to oxygen throughout both the structures.

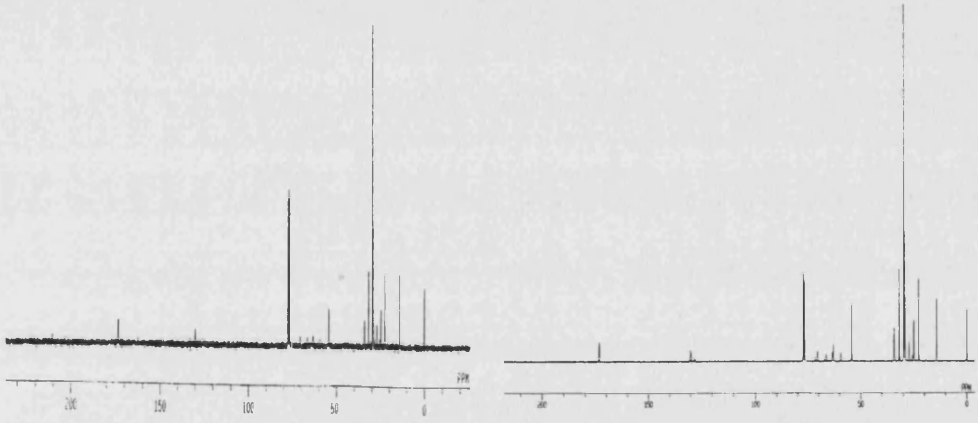

Figure 39: ^{13}C NMR traces of FDS and FDS -control

The peak at 14.1ppm is due to the presence of end methyl groups within the structures. The peaks from 22.6 to 34.3ppm are due to the various CH_2 groups. The peak at 54.4ppm is due to ternary nitrogen connected to three methyl groups. The peak at 59.4ppm is due to the CH_2-N bond. The various peaks at 63.0 to 66.4ppm are due to the CH_2 structures attached to oxygen. The peaks at 70.4 and 70.5ppm are possibly due to CH-OH interactions. The peaks at 77.0 to 77.3 are due to the chloroform used in preparing NMR samples. The peak at 174ppm is probably due to C=O interactions.

Discussion

The identification of n-octadecyl dansylamide (label) has been confirmed. The identical traces obtained for both FDS and FDS-control show that the sample does not undergo any chemical changes during the labelling process.

3.1.4 Mass Spectrometric Identification of the Label, FDS, and FDS-Control

Mass spectra were recorded on VG7070 and VG Autospec instruments at the Mass Spectrometry Service, University of Bath. Fast-Atom Bombardment (FAB) spectra presented in this section were obtained using *m*-nitrobenzyl alcohol (*m*-NBA) as the matrix. Intrepretation of the spectra were carried out in collobartion with Dr Mike Threadgill and his research group, University of Bath, School of Pharmacy and Pharmacology.

In each of the spectra presented, there are two traces. The top trace shows the various positive fragments of the sample in question, whilst the bottom trace shows the main ions of the sample.

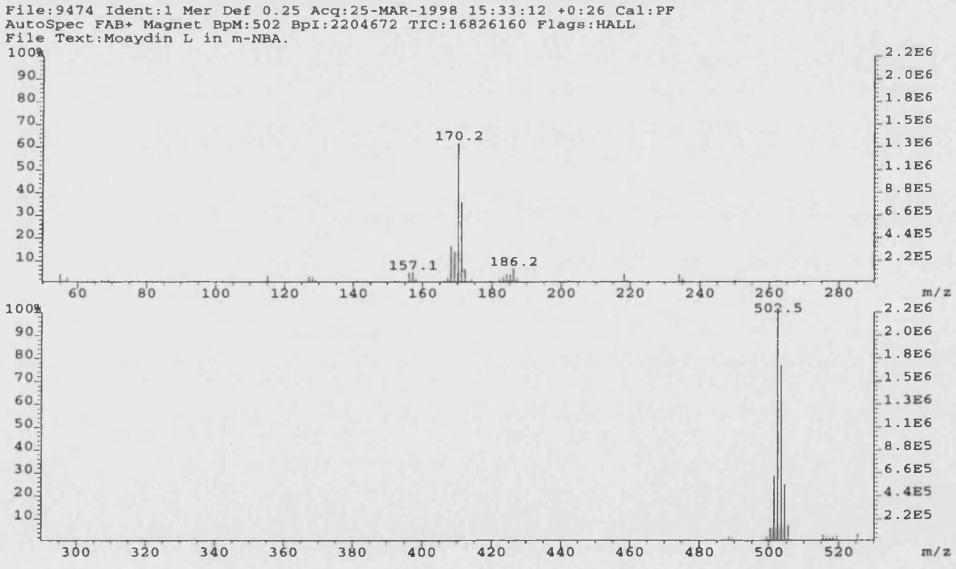

Figure 40: Fast Atom Bombardment (FAB) of positive ions (FAB+) of the label.

The bottom trace shows the main ions whilst the top trace shows the various positive fragments of the label.

Result: m/z 502.5 [(M+H)+ 100%] is the n-octadecyl danyslamide peak.

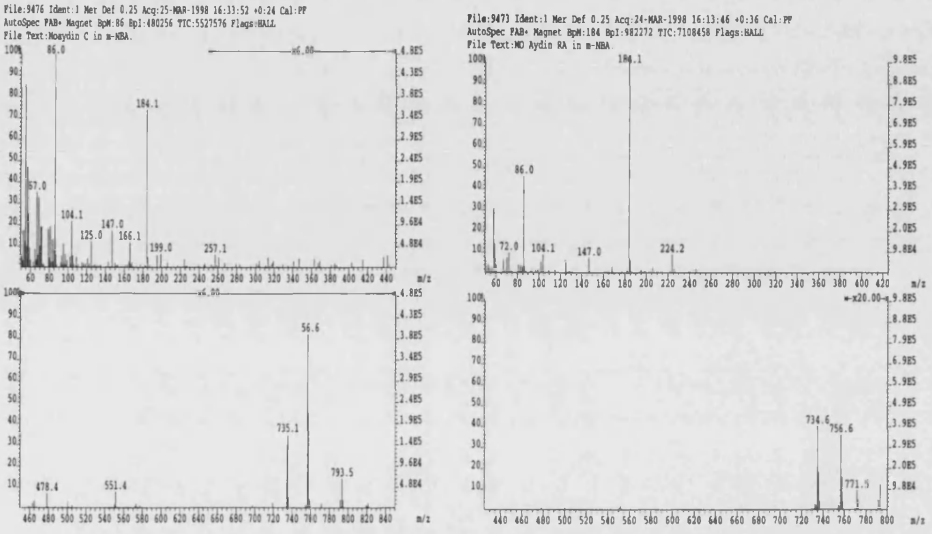

Figure 41: Fast Atom Bombardment (FAB) of positive ions (FAB+) of FDS-Control (left) and FDS (right).

The left trace can be interpreted as follows: m/z 735.1 [(M+H)+ 70%] is the DPPC whilst m/z 793.5 [(M+H)+ 30%] is the PG. The peak at 756.6 is DPPC + Sodium, this is an artefact of the measuring process when sodium from the atmosphere is measured along with the main fragment to produce a pseudo peak. Similarly, the right trace results are: m/z 734.6 [(M+H)+ 70%] is the DPPC whilst m/z 771.5 [(M+H)+ 30%] is the PG. The peak at 756.6 is DPPC+ Sodium.

3.1.5 Experiment to Prove the Uniform Distribution of the Label within FDS

The introduction of the label (n-octadecyl dansylamide) into FDS was carried out in solution, as described earlier. The solution was then evaporated off to leave the solid material behind. To assess the quantity and distribution of the label within FDS, an experiment was devised to evaluate the uniformity of the labelling process.

Standard Preparation

Six standards of the label were prepared and measured by a fluorescence spectrophotometer, as described in section 2.2.5.2 Fluorimetric Detection of LFDS, page 108, to produce the table below. Methanol (HPLC grade) was used as the blank during measurements.

Standard No.	Concentration (µg/ml)	Relative Intensity (%)
1	0.8	100.8
2	0.5	62.8
3	0.4	52.0
4	0.2	26.6
5	0.1	14.1
6	0.05	7.1

Table 27: Table showing the six standards of n-octadecyl dansylamide used to produce the calibration curve.

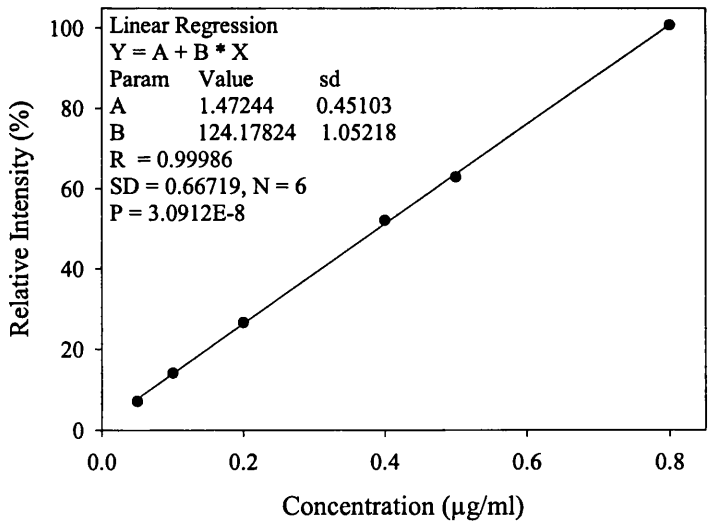

Figure 42: Calibration curve of n-octadecyl dansylamide.

Method

Twenty samples of approximately 20mg (~0.2mg or 200μg label by weight) of LFDS were accurately weighed, using a small glass weighing boat, and washed into a 50ml volumetric flask with methanol and adjusted to volume. This gave a 40μg/ml solution of the label that was further diluted with the methanol (1:10) to give a 4μg/ml test sample.

Results

The equation of the straight line of the calibration curve was taken and incorporated into Table 28, to give the concentration of the unknown samples. The corrected intensities take into account the fluorescence of the blank.

Sample Wt. (mg)	Relative Intensity (%)	Corr. Intensity (%)	Conc. (μg/ml)	Corr. Conc. (μg/ml)	Dil. Factor	Label Wt. (μg)
20.27	53.84	53.42	0.415	0.410	500	204.9
19.74	50.20	49.78	0.386	0.391	500	195.5
19.68	50.15	49.73	0.386	0.392	500	195.9
19.60	50.25	49.83	0.386	0.394	500	197.1
19.77	50.85	50.43	0.391	0.396	500	197.9
19.21	50.29	49.87	0.387	0.403	500	201.3
19.53	50.10	49.68	0.385	0.394	500	197.2
19.21	50.55	50.13	0.389	0.405	500	202.4
19.10	50.15	49.73	0.386	0.404	500	201.9
19.36	49.46	49.04	0.380	0.393	500	196.3
20.45	52.62	52.20	0.405	0.397	500	198.3
20.41	52.79	52.37	0.407	0.399	500	199.3
20.62	52.76	52.34	0.407	0.394	500	197.2
20.77	55.10	54.68	0.426	0.410	500	204.9
20.22	52.36	51.94	0.403	0.399	500	199.5
19.63	51.89	51.47	0.400	0.407	500	203.6
19.27	50.09	49.67	0.385	0.400	500	199.8
20.10	51.40	50.98	0.396	0.394	500	196.8
19.66	49.99	49.57	0.384	0.391	500	195.5
19.31	50.87	50.45	0.391	0.405	500	202.7
			Average	0.399		199.4
			SD	0.006		3.12
			RSD(%)	1.6		1.6

Table 28: Relative intensities and corresponding concentrations for 20 samples of LFDS.

3.1.6 Validation of the Labelling Process

In order to validate the labelling process, a solution LFDS was nebulised into a 5-stage liquid impinger, using a Cirrus™ nebuliser and a Nebupump™ compressor, with the set up employed for the deposition studies of radiolabelled SAPL (Figure 77, page 208). Since radiolabelled SAPL has a definitive deposition pattern within the MSLI, it can be used as a reference to evaluate the extent to which the label (n-octadecyl dansylamide) follows the actual drug particles of FDS.

Materials & Equipment

Compressor, Nebupump™ (Carri-Med Ltd, Dorking, UK), maximum output: 6.4L min^{-1}.
Nebuliser: Cirrus™ (maximum output: 3.8L min^{-1}).
Pump: Gast 1023, Rotor Vein, Oil-less, (Bucks., UK).
5-Stage Liquid Impinger, Stage 5 filter: Type A/E glass fibre, 76mm diameter (Gelman Sciences, Mich., USA).
Digital timing unit, Mass flow meter (Hastings Mass Flow Meter, HFM 201, Teledyne Brown Engineering, Hastings Instruments, VA, USA).

Method

Flow rate through the MSLI was set at 60L min^{-1} using the mass flow meter. Each stage of the MSLI was filled with 20ml of HPLC grade methanol. 300mg of LFDS was weighed into a 10ml volumetric flask and dissolved in methanol to produce a 30mg/ml solution. 3ml of the test solution (theoretically containing 1% label, 900μg by weight) was pipetted into the nebuliser. The nebuliser was connected to the MSLI via an adaptor, as shown in Figure 77, page 208. The compressor was connected to the bottom of the nebuliser via vacuum tubing. The timing unit was adjusted so that the by-pass switch was activated, which allowed the pump to work continuously. The pump and the compressor were switched on and the solution was nebulised. It took approximately nine minutes for the chamber empty to dryness. Stage 5

of the MSLI was disconnected from stages 1 to 4 and the MSLI swirled gently to collect droplets that had impacted on the sides and then inverted to wash the ceiling of the apparatus. Stoppers from the four stages were removed and each stage was emptied into 100ml volumetric flasks. Each stage was further washed with methanol to recover as much of the nebulised material as possible and the volumetrics were made up to volume using methanol. The metal throat and silicone adaptor were washed into the same 100ml volumetric flask and made up to volume with methanol. The glass fibre filter from stage 5 was placed into a glass crystallising basin and washed with 20ml of methanol. The solution was poured into a 100ml volumetric and made up to volume with further methanol. The residual liquid left in the nebuliser was washed into a 100ml volumetric falsk and made up to volume using methanol. Both the residual liquid from the nebuliser and stage 5 were further diluted (1:10) such that their intensity readings fell within the standard range. The procedure was carried out in triplicate. The standards were prepared as described earlier (see fluorimetric detection of LFDS, page 108). The relative intensity of the standards and the samples were measured on the Hitachi F2000 fluorimeter, Hitachi Ltd., Japan.

Results

	Intensity (%)	Corr. Intensity (%)	Label Conc. (µg/ml)	Dil. Factor	Total Amount Deposited (µg)	Deposition (%)
Neb	61.3± 0.755	60.5± 0.755	0.474± 0.0059	1000	474.3± 5.94	55.9± 0.699
Tht+Adp	64.5± 2.75	63.7± 2.75	0.499± 0.0216	100	49.9± 2.16	5.88± 0.254
Stg1	38.2± 2.99	37.4± 2.99	0.292± 0.0235	100	29.2± 2.35	3.45± 0.277
Stg2	36.6± 2.88	35.8± 2.88	0.280± 0.0227	100	28.0± 2.27	3.30± 0.267
Stg3	36.5± 3.52	35.7± 3.52	0.279± 0.0276	100	27.9± 2.76	3.29± 0.326
Stg4	51.6± 4.24	50.8± 4.24	0.398± 0.0333	100	39.8± 3.33	4.69± 0.393
Stg5	27.7± 0.529	26.9± 0.529	0.210± 0.0042	1000	210.1± 4.16	24.8± 0.490

Table 29: Distribution of LFDS within an MSLI at 60L min^{-1} flow rate, aerosolised from a Cirrus™ nebuliser using the Nebupump™ compressor operating at 6.4L min^{-1}.

Since 3ml of the test solution (theoretically containing 1% label, 900µg by weight) was pipetted into the nebuliser, the total recovery values can be calculated as shown below in Table 30.

Parameter	Value Obtained or Calculated
Mean Total Recovery (µg)	859.3±13.2
Mean Total Recovery (%)	95.5±1.47

Table 30: Recovery values for LFDS.

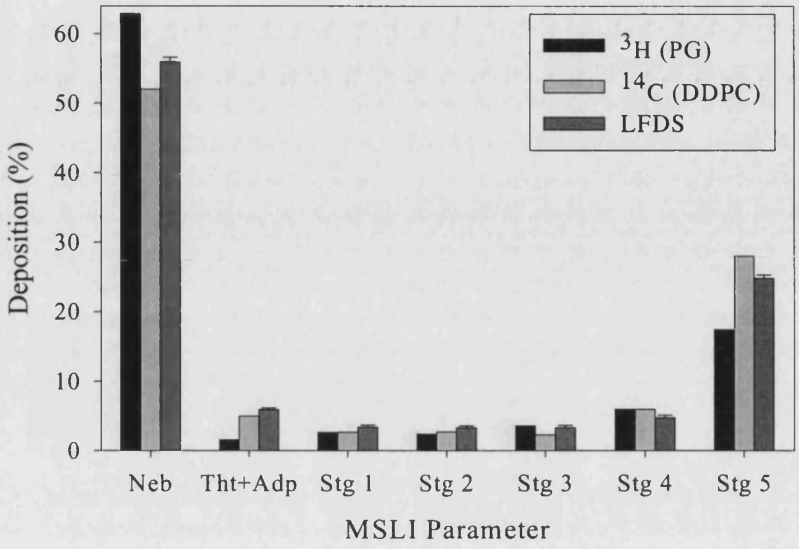

Figure 43: Deposition profiles of LFDS compared againsts radiolabelled PG and DPPC in an MSLI at 60Lmin^{-1} flow rate, aerosolised from a Cirrus^{TM} nebuliser using a Nebupump^{TM} compressor operating at 6.4Lmin^{-1}.

Bars represent the mean + SD of 3 determinations.

3.1.7 General Discussion

Fluorescent labelling as a technique is used in the food industry (Herbert *et al* 1999) as well as for biopharmaceutical and analytical applications, when derivatisation is required for indirect detection of compounds (Gatti *et al* 1995). These applications often incorporate wet chemistry and solid dosage forms are not used. Owing to the difficulties in chemically labelling drug molecules themselves, formulations for pharmaceutical applications are labelled with a gamma ray emitting nuclide like ^{99m}technetium, which forms a complex of radioactive atoms or groups with molecules of the compound (Newman 1996). The isotope has found increasing use in the pharmaceutical industry in the past 10 years for *in-vitro* and *in-vivo* assessments of various delivery systems (Newman 1996). The isotope has a short half-life (6hrs) and can be administered in large doses. The techniques used for labelling DPIs are very

similar to those for pMDIs. ^{99m}TC is used, along with a chelating agent and added to the dry powder in a solvent in which the drug is not soluble (e.g. with terbutaline sulphate, the solvent used is chloroform). The radiolabel permeates the drug particles, and the assessment of the distribution of the radiolabel and drug is made via *in vitro* analysis (such as an MSLI) coupled with scintillation counting (Newman *et al* 1991). Therefore, the drug deposition in the various stages of the apparatus is calculated both via scintillation and MSLI analysis (usually involving HPLC detection) and the two sets of data are compared. Lung deposition of 24% (Vidgren *et al* 1994) and >20% (Newman *et al* 1991) have been achieved using the Easyhaler® and Turbuhaler™ respectively with the authors claiming that ^{99m}TC behaves in the same way as the drug particles. A recent paper by Calmanovici *et al* (1999) stated that exogenous, freeze-dried, natural surfactant, labelled with ^{99m}TC could be used for aerosol lung scintigraphy. Nebulisation studies in animal models showed the biodistribution of the surfactant to be comparable to other radiopharmaceuticals.

A method for attaching the fluorescent label onto SAPL has been presented. The reasons for attaching the label have also been discussed, see page 121. The labelled material has been characterised using standard structure elucidation techniques, which showed that labelled material is not chemically different to the original drug substance. The distribution of the attached probe has been quantified, and deposition profiles of LFDS with those of radiolabelled SAPL have validated the labelling procedure. The reason for choosing a physical association as opposed to chemically labelling SAPL in this study was financial. Adequate funds were not available to pursue the chemical-labelling route. Thus, this raises the question as to whether or not the label behaves in the same way as the drug in the various formulations, especially during the deposition studies when both the drug and label are subjected to high shear forces. The results from content uniformity experiments show that 199.4μg of label are present within a 20mg sample of LFDS, with a relative standard deviation of only 1.6%, suggesting uniform distribution. This, coupled with the validation experiment, comparing the deposition profile of LFDS against chemically labelled SAPL in the MSLI from a nebuliser, suggest that the physical fluorescent probe is behaving in a similar fashion to the drug particles of LFDS.

Chapter 4

Deposition Studies of MLFDS

4 Deposition Studies of MLFDS

This section outlines the various deposition experiments carried out on MLFDS. The average particle size of MLFDS used during the deposition studies was 4.12μm, as determined by LALLS (see section 2.2.1.1 Malvern Analysis (Laser Light Diffraction), page 75). The fluorimetric technique used to quantify the material has been previously described (see section 2.2.5.2 Fluorimetric Detection of LFDS, page 108).

4.1 TSI (Apparatus A) Deposition Profiles

A single dose capsule based device, the Miat Monohaler, was used to assess the *in-vitro* aerosol performance of MLFDS and its various blends with coarse and fine lactose. The Miat Monohaler was chosen for its ease of use and also because when used properly the deaggregating properties of the device is comparable to other DPIs (Pitcairn *et al* 1997). The size three hard gelatine capsules used to deliver MLFDS were stored in a desiccator containing a saturated salt solution of ammonium nitrate (RH 62-67%). This storage condition was chosen because, Konty and Mulski (1989) concluded that if the hard gelatine capsules were stored at <40%RH, they exhibited brittleness at ambient temperature. Konty and Mulski (1989) also concluded that at RH>85% caused the hard gelatine capsules to absorb moisture, thus altering their physical properties.

Method

The *in-vitro* aerosol investigations were performed using vacuum pumps (Gast Manufacturing Inc., Michigan, USA) at 30, 60, and 96.4 $Lmin^{-1}$ (see Table 31, page 136). Flow rate through the device was adjusted via the needle valve using a mass flow meter (Hastings Mass Flow Meter, HFM 201, Teledyne Brown Engineering, Hastings Instruments, VA, USA). The device was not tested at the flow rate equivalent to a 4kPa pressure drop across the device, because the necessary equipment was not available to make such measurements.

Flow Rate	Stage 1 Jet Diameter	Cut-off Diameter (see page 66 for calculation)	Shot time
30.0Lmin^{-1}	9.7mm	6.60µm	8.0secs
60.1Lmin^{-1}	14.2mm	6.55µm	4.0secs
96.4Lmin^{-1}	16.4mm	6.51µm	2.5secs

Table 31: Table showing the conditions used in the TSI (Apparatus A) deposition study of MLFDS.

A size 3 hard gelatine capsule was filled to contain approximately 20mg of MLFDS (~1% label by weight i.e. 0.2mg). The capsule was placed into the chamber of the Miat monohaler (previously stored in an oven at 40°C) and pierced evenly using the four sets of pins on either side of the device, care was taken not to shatter the capsule. The Miat monohaler was coupled with a TSI, containing 7ml and 30ml of HPLC grade methanol in stages 1 and 2 respectively. The shot-time on the timing device was adjusted to deliver a total of four litres of air. Once fired, the capsule and device were washed into separate 50ml volumetric flasks with methanol and adjusted to volume. Stage 1 and throat (plus adaptor) of the TSI were washed into 100ml volumetric with the mixture and diluted so as their intensity reading from the fluorimeter fell within the standard range. Stage 2 was washed into a 50ml volumetric and adjusted to volume, and diluted such that the relative intensities of the unknown samples fell within the standard range, details of the dilutions are given in individual deposition tables within this section. The relative intensity of the standards (see page 108 for preparation) and the samples were measured on the Hitachi F2000 fluorimeter, Hitachi Ltd., Japan.

4.1.1 Drug Only

Table 32 and Table 33, page 137 show the results obtained for MLFDS at 30.0, 60.1, and 96.4Lmin^{-1} respectively.

Parameter	FR	Capsule	Device	Stage 1	Stage 2
Measured Intensity (%)	30.0	39.3±4.49	16.3±2.65	9.6±0.347	14.4±1.38
	60.1	29.3±0.175	7.60±1.19	11.2±0.100	38.9±0.912
	96.4	27.7±3.25	6.48±1.34	9.09±0.344	44.3±4.48
Corrected Intensity (%)	30.0	38.3±4.49	15.2±2.65	8.6±0.347	13.4±1.38
	60.1	28.0±0.175	6.40±1.19	10.0±0.100	37.7±0.912
	96.4	26.7±3.25	5.44±1.34	8.05±0.344	43.2±4.48
Conc. (µg/ml)	30.0	0.607±0.070	0.248±0.041	0.144±0.005	0.219±0.021
	60.1	0.410±0.003	0.089±0.018	0.141±0.001	0.553±0.014
	96.4	0.426±0.051	0.095±0.021	0.136±0.005	0.684±0.070
Dilution Factor	30.0	50	50	1000	50
	60.1	50	50	1000	50
	96.4	50	50	1000	50
Amount Deposited (µg)	30.0	30.4±3.50	12.4±2.05	143.8±5.41	10.9±1.05
	60.1	20.5±0.150	4.40±0.882	141.4±1.49	27.7±0.677
	96.4	21.3±2.53	4.80±1.05	135.7±5.3	34.2±3.48
(%) Deposited	30.0	15.3±1.41	6.27±1.18	72.8±2.64	5.54±1.19
	60.1	10.6±1.57	2.39±0.939	72.9±2.55	14.3±1.71
	96.4	11.1±1.26	2.50±0.790	69.5±2.22	16.9±1.48

Table 32: Summary table of TSI deposition data for MLFDS at 30.0, 60.1, and 96.4Lmin^{-1}, n=10.

Table 33 was constructed from the results obtained above, in Table 32.

Parameter	Value Obtained or calculated @ 30.0Lmin^{-1}	Value Obtained or calculated @ 60.1Lmin^{-1}	Value Obtained or calculated @ 96.4Lmin^{-1}
Mean Total Recovery	197.5µg(±8.20)	194.0µg(±3.52)	196.0µg(±4.04)
Mean Total Recovery	99.0%(±2.52)	97.3%(±2.45)	98.3%(±1.29)
Mean Emitted Dose	149.4µg(±5.44)	168.5µg(±4.81)	165.5µg(±3.94)
Mean Emitted Dose	78.4%(±1.79)	87.2%(±0.302)	86.5%(±1.56)
Mean FPD	10.6µg(±2.06)	27.6µg(±2.58)	33.4µg(±3.28)
Mean FPF	7.06%(±0.570)	16.4%(±1.27)	20.2%(±1.86)
Mean Fill Weight	20.7mg(±1.10)	20.1mg(±0.252)	20.5mg(±0.497)

Table 33: Summary table of various parameters calculated from TSI deposition data for MLFDS at 30.0, 60.1, and 96.4 Lmin^{-1}, n=10.

The distribution of MLFDS within the TSI as well as the mean emitted dose and fine particle dose are displayed graphically on page 138.

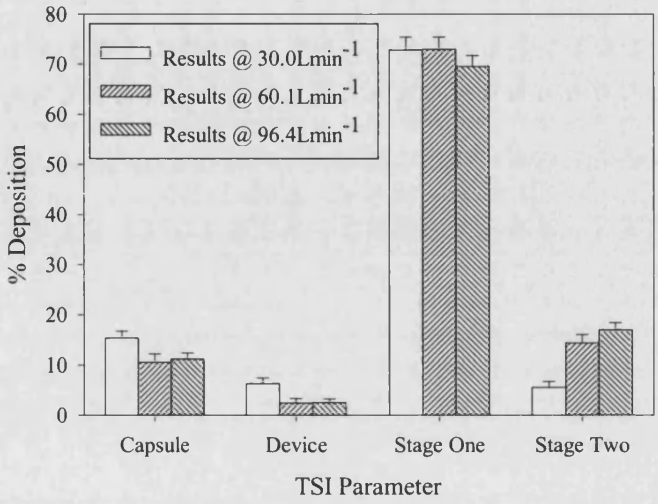

Figure 44: Distribution of MLFDS within Apparatus A at different flow rates. Bars represent the mean + SD of 10 determinations.

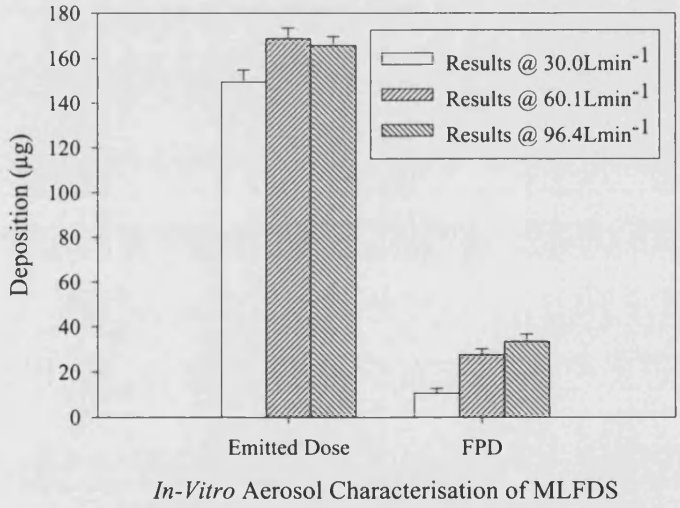

Figure 45: Emitted dose and fine particle dose of MLFDS at different flow rates. Bars represent the mean + SD of 10 determinations.

Statistics

One-way analysis of variance on the emitted dose (ED) of MLFDS at 30, 60.1, and 96.4Lmin^{-1} showed significant differences ($F=169.2$, $p<0.001$). Fisher's pairwise comparisons revealed that the ED at 30Lmin^{-1} was significantly different from those at 60.1 and 96.4Lmin^{-1}. Significant differences were also observed ($F=209.4$, $P<0.001$) for the FPD values for MLFDS at the three flow rates, when one-way analysis of variance was carried out.

4.1.2 Binary Blends

Three different blends of MLFDS and lactose were prepared (as described below) using the rotary bladed blender (Kenwood Mini Chopper, CH100, Kenwood Ltd., Hants., UK) employing the mixing techniques outlined earlier (see 2.2.6.4 Mixing Techniques, page 118). The blends were tested for content uniformity and the optimum mixing time for each blend was determined. The deposition profiles of the blends were then obtained using the TSI at 60 and 96.4 L min^{-1} using the Miat monohaler and size three hard gelatine capsules, as described on page 135. The relative intensity of the standards (see 2.2.5.2 Fluorimetric Detection of LFDS, page 108 for preparation) and the samples were measured on the Hitachi F2000 fluorimeter, Hitachi Ltd., Japan.

Blend ID	Blend Size	MLFDS (% w/w)	Lactose (% w/w)	Lactose Type
A	10g	10	90	Coarse (63-90μm) Fraction
B	10g	10	90	Fine (Microtose) (<10μm)
C	10g	5	95	Coarse (63-90μm) Fraction

Table 34: Table showing the details of the various binary blends of MLFDS with coarse and fine lactose.

Blends A, B, and C contain ~1% label by weight. This equates to 40μg of label (total) in blends A / B, and 20μg for C for a 40mg load capsule. Thus, to make the analysis easier and to make blend C comparable with A and B, a capsule load of 80mg was chosen for blend C. The scale of scrutiny of the content uniformity tests was set at 20mg due to sample shortage,

but the final fill weight of the capsules to be tested were 40mg (blends A and B) and 80mg (blend C).

Content uniformity Experiments

In order to determine the optimum mixing time for each of the above blends, the blender was stopped periodically and ten representative samples from the blend were removed. This was done by first placing the whole powder bed onto a piece of paper, dividing it into nine sections and taking ~20mg from each section and an additional 20mg randomly. Samples were placed into 50ml volumetric flasks and made up volume with methanol. The results of this procedure are shown below. The pre-set criteria for a blend to be acceptable was that it must have had a corrected concentration (μg/ml) RSD of <5%. Table 35, below, summarises the results obtained. For more detailed results please refer to Appendix 3: Content Uniformity Experiments for Binary Blends of MLFDS, page 255.

Blend ID	Mix-Time (min)	Average Conc. (μg/ml)	Expected Conc.(μg/ml)	SD	RSD (%)
A	5	0.370	0.4	0.046	12.7
A	10	0.397	0.4	0.027	7.0
A	15	0.394	0.4	0.018	4.6
B	5	0.401	0.4	0.023	6.0
B	10	0.400	0.4	0.021	5.3
B	15	0.407	0.4	0.016	4.1
C	5	0.212	0.2	0.032	15.5
C	10	0.215	0.2	0.015	7.2
C	15	0.208	0.2	0.009	4.6

Table 35: Mixing time versus average concentration (n=10) values for MLFDS binary blends A, B, and C.

SEM Photomicrographs on pages 141 and 142 show examples from the three blends.

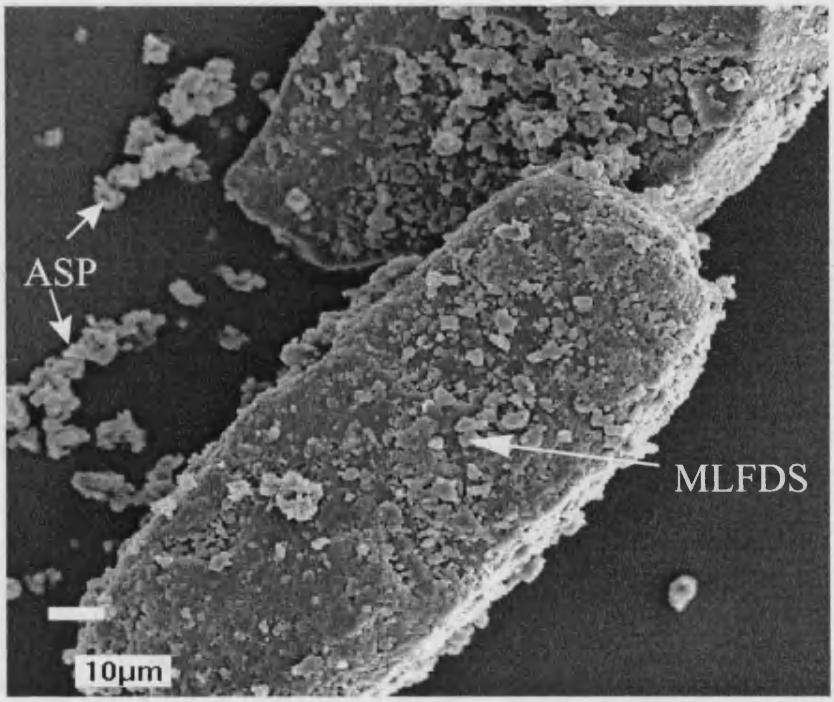

Figure 46: SEM photomicrograph of MLFDS binary blend A at x2500 magnification, mix time: 15min.

Key: ASP: Aggregated SAPL Particle

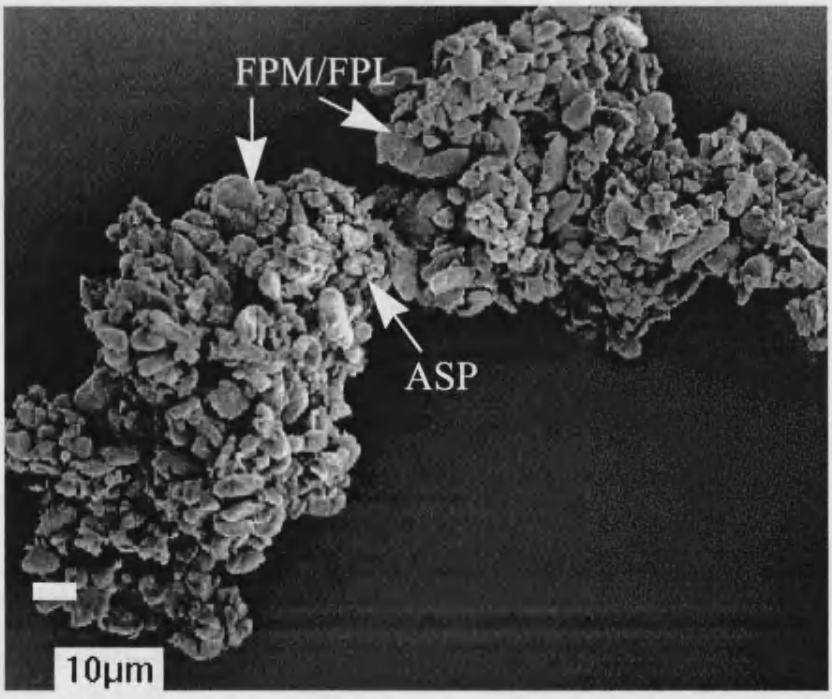

Figure 47: SEM photomicrograph of MLFDS binary blend B at x3000 magnification, mix time: 15min.

Key: ASP: Aggregated SAPL Particle FPM/FPL: Fine Particle Multiplet / Lactose

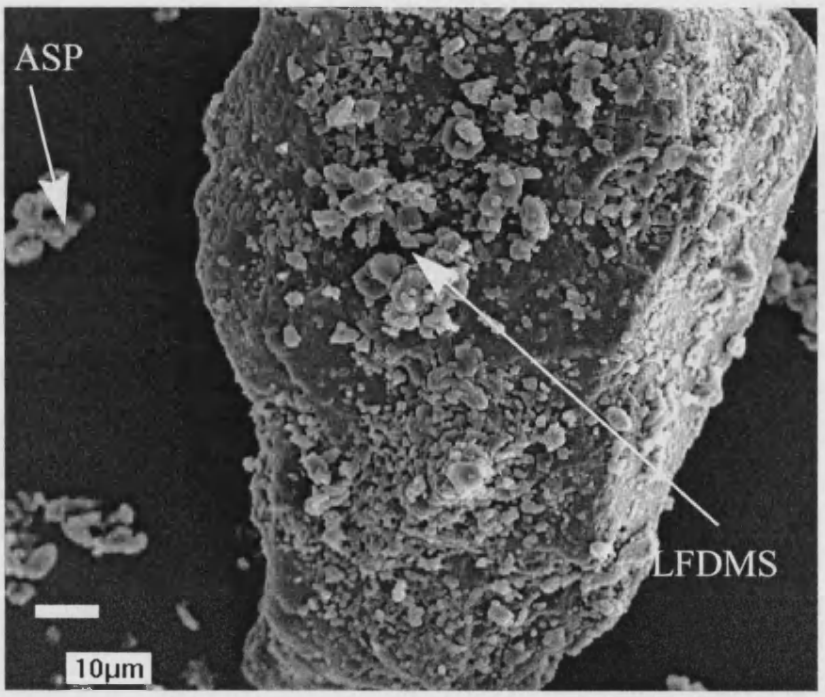

Figure 48: SEM photomicrograph of MLFDS binary blend C at x2200 magnification, mix time: 15min.

The SEM pictures above show examples of the photographs obtained for the different blends. As outlined in the introduction (see mixing theory, page 46), carrier-based systems inevitably contain combinations of drug-drug-carrier and drug-carrier-drug associations. These characteristics are also exhibited in the SEMs above.

Deposition Study Method

The *in-vitro* aerosol conditions and method employed were the same as those outlined in section 4.1. Flow rates of 60 ($ECD_{50\%}$ 6.55µm, stage 1 jet 14.2mm, shot time 4.0secs) and 96.4 $Lmin^{-1}$ ($ECD_{50\%}$ 6.51µm, stage 1 jet 16.4mm, shot time 2.5secs) were used.

Results

The tables below show the TSI deposition data obtained for blends A, B and C at 60.0 and 96.4 $Lmin^{-1}$.

Parameter	FR	Blend ID	Capsule	Device	Stage 1	Stage 2
Measured Intensity (%)	60.0	A	3.43(±0.546)	3.16(±0.597)	21.1(±0.382)	4.26(±0.303)
		B	1.85(±0.085)	1.93(±0.080)	17.6(±0.456)	3.93(±0.085)
		C	3.07(±0.201)	3.02(±0.184)	19.8(±0.461)	3.74(±0.068)
Corrected Intensity (%)	60.0	A	2.27(±0.546)	2.04(±0.597)	17.0(±0.382)	2.96(±0.303)
		B	1.26(±0.085)	1.34(±0.080)	17.0(±0.456)	3.34(±0.085)
		C	1.61(±0.201)	1.56(±0.184)	18.3(±0.461)	2.27(±0.068)
Conc. (µg/ml)	60.0	A	0.05(±0.001)	0.04(±0.001)	0.329(±0.01)	0.058(±0.01)
		B	0.02(±0.002)	0.023(±0.02)	0.350(±0.01)	0.066(±0.02)
		C	0.04 (±0.003)	0.04(±0.003)	0.33(±0.008)	0.05(±0.001)
Dilution Factor	60.0	A B C	50	50	100	50
Amount Deposited (µg)	60.0	A	2.26(±0.050)	2.03(±0.050)	32.9(±0.521)	2.92(±0.064
		B	1.09(±0.100)	1.17(±0.100)	34.4(±0.690)	3.23(±0.032)
		C	2.10(±0.150)	2.06(±0.147)	32.9(±0.976)	2.67(±0.045)
(%) Deposited	60.0	A	5.62(±1.12)	5.06(±1.24)	82.1(±2.62)	7.28(±1.66)
		B	2.73(±0.825)	2.94(±0.762)	86.2(±2.58)	8.09(±1.72)
		C	5.30(±1.36)	5.19(±1.47)	82.8(±2.33)	6.73(±1.39)

Table 36: Summary table of TSI deposition data for MLFDS binary blends A, B, and C at 60.0$Lmin^{-1}$. Values in brackets indicate standard deviation, n=10.

Parameter	FR	Blend ID	Capsule	Device	Stage 1	Stage 2
Measured Intensity (%)	96.4	A	3.63(±0.397)	3.05(±0.572)	20.7(±0.577)	5.19(±0.119)
		B	1.47(±0.056)	1.52(±0.118)	17.1(±.065)	5.1(±0.062)
		C	2.87(±0.204)	2.83(±0.081)	19.4(±0.210)	5.34(±0.119)
Corrected Intensity (%)	96.4	A	2.81(±0.397)	2.23(±0.572)	19.9(±0.577)	4.37(±0.119)
		B	0.89(±0.056)	0.94(±0.118)	16.5(±0.065)	4.52(±0.062)
		C	1.41(±0.204)	1.36(±0.081)	17.9(±0.210)	3.87(±0.119)
Conc. (µg/ml)	96.4	A	0.05(±0.001)	0.04(±0.001)	0.321(±0.01)	0.078(±0.02)
		B	0.02(±0.001)	0.02(±0.002)	0.336(±0.01)	0.092(±0.01)
		C	0.04(±0.004)	0.04(±0.001)	0.325(±0.04)	0.08(±0.002)
Dilution Factor	96.4	A B C	50	50	100	50
Amount Deposited (µg)	96.4	A	2.77(±0.053)	2.24(±0.054)	27.4(±1.18)	3.76(±1.27)
		B	0.88(±0.051)	0.93(±0.114)	33.3(±1.28)	4.54(±0.507)
		C	1.94(±0.206)	1.94(±0.053)	32.4(±4.02)	4.07(±0.106)
(%) Deposited	96.4	A	6.57(±1.06)	5.47(±1.68)	78.4(±2.53)	9.55(±1.94)
		B	2.23(±0.923)	2.36(±0.983)	83.9(±2.74)	11.5(±2.06)
		C	4.82(±1.02)	4.72(±1.16)	80.4(±2.66)	10.1(±2.17)

Table 37: Summary table of TSI deposition data for MLFDS binary blends A, B, and C at 96.4Lmin^{-1}. Values in brackets indicate standard deviation, n=10.

Table 36, page 143 was use to produce the data below in Table 38.

Parameter	Blend A	Blend B	Blend C
Mean Total Recovery (μg)	40.6(±1.43)	40.7(±1.06)	39.8(±1.43)
Mean Total Recovery (%)	101.0(±2.07)	100.9(±1.53)	98.2(±2.12)
Mean Emitted Dose (μg)	35.2(±1.69)	37.6(±1.70)	36.4(±1.73)
Mean Emitted Dose (%)	89.3(±1.39)	94.3(±1.38)	91.5(±1.920)
Mean FPD (μg)	2.87(±0.235)	3.23(±0.309)	2.97(±0.551)
Mean FPF (%)	8.14(±1.13)	8.58(±1.15)	8.16(±1.17)
Mean Fill Weight (mg)	40.7(±1.6)	40.8(±1.47)	80.6(±1.42)

Table 38: Summary table of various parameters calculated from TSI deposition data for MLFDS binary blends A, B, and C at 60.0Lmin^{-1}.

Table 37, page 144 was used to produce the data below in Table 39.

Parameter	Blend A	Blend B	Blend C
Mean Total Recovery (μg)	40.8(±1.56)	40.0(±1.10)	40.4(±1.33)
Mean Total Recovery (%)	100.3(±1.06)	100.3(±1.460)	101.3(±1.20)
Mean Emitted Dose (μg)	34.9(±1.90)	37.8(±1.34)	36.5(±1.21)
Mean Emitted Dose (%)	88.0(±1.53)	95.4(±1.48)	90.5(±1.32)
Mean FPD (μg)	3.79(±0.12)	4.54(±0.87)	4.07(±0.86)
Mean FPF (%)	10.9(±1.27)	12.0(±1.16)	11.2(±1.24)
Mean Fill Weight (mg)	41.3(±1.4)	40.4(±1.25)	80.2(±1.35)

Table 39: Summary table of various parameters calculated from TSI deposition data for MLFDS binary blends A, B, and C at 96.4Lmin^{-1}.

The distributions of MLFDS binary blends within the TSI, as well as the mean emitted dose and fine particle doses are displayed graphically in Figure 49 and Figure 50, page 146 and summarised in Figure 51, page 147.

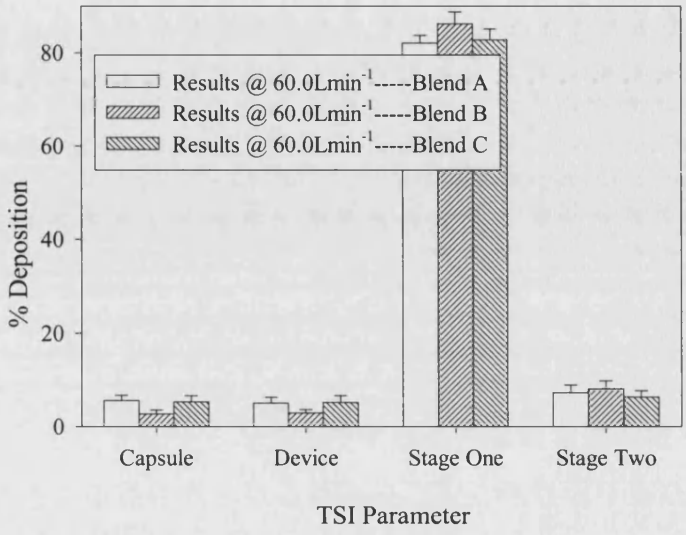

Figure 49: Distribution of MLFDS binary blends A, B and C within Apparatus A at 60.0Lmin^{-1}. Bars represent the mean + SD of 10 determinations.

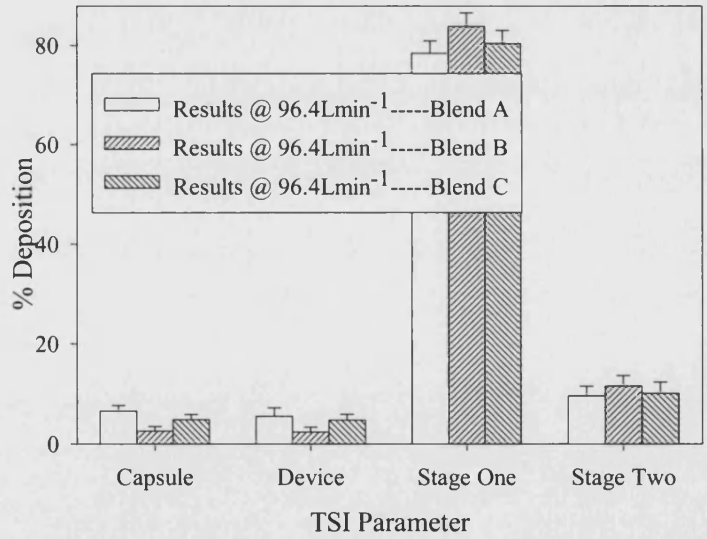

Figure 50: Distribution of MLFDS binary blends A, B and C within Apparatus A at 96.4Lmin^{-1}. Bars represent the mean + SD of 10 determinations.

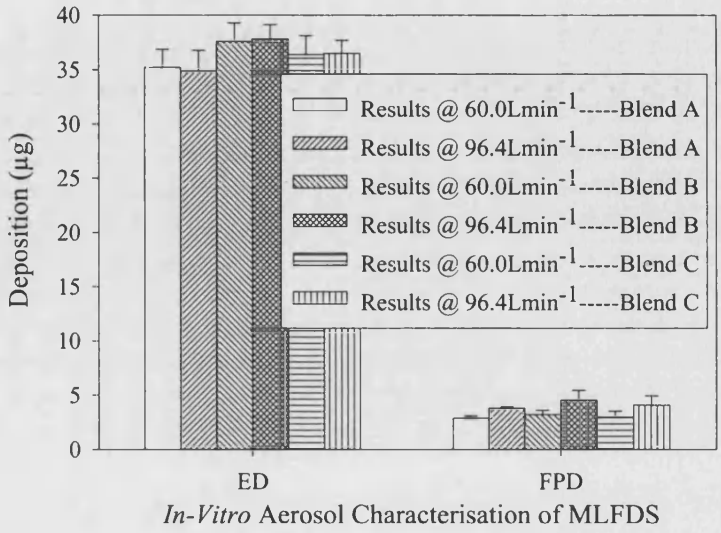

Figure 51: Emitted dose and fine particle dose of MLFDS binary blends A, B and C at 60 and 96.4Lmin^{-1}. Bars represent the mean + SD of 10 determinations.

Statistics

One-way analysis of variance on the ED of MLFDS binary blends A, B, and C 60.0Lmin^{-1} showed significant differences (F=5.88, p=0.008). Significant difference in the ED was also observed at 96.4Lmin^{-1} (F=9.57, p=0.001). Fisher's pairwise comparisons revealed that the ED of blend A was significantly different to that of blends B and C.

No significant differences were observed (F=2.25, p=0.125) for the FPD values for MLFDS binary blends A, B, and C 60.0Lmin^{-1} when one-way analysis of variance was carried out. Similarly, no significant (F=2.88, p=0.073) differences in FPD results at 96.4Lmin^{-1} were observed.

4.1.3 Ternary Blends

A ternary blend of MLFDS, coarse lactose (63-90μm), and fine lactose (microtose)(ratio 5: 90:5 % w/w) was prepared using the rotary bladed blender (Kenwood Mini Chopper, CH100, Kenwood Ltd., Hants., UK) employing the mixing techniques outlined earlier (see section 2.2.6.4 Mixing Techniques, page 118). The content uniformity of the blend was assessed at various time intervals and is outlined in Table 40, page 149. The deposition profiles of the blend obtained using the TSI (Apparatus A) at 60 and 96.4 L min^{-1} using the Miat monohaler and size three hard gelatine capsules, as described on page 135. The relative intensity of the standards (see page 108) and the samples were measured on the Hitachi F2000 fluorimeter, Hitachi Ltd., Japan.

MLFDS contains ~1% label by weight. This equates to 40μg of label (total) in blends A / B, and 20μg for C for a 40mg load capsule. Thus, to make the analysis easier and to make blend C comparable with A and B, a capsule load of 80mg was chosen for blend C. The scale of scrutiny of the content uniformity tests was set at 20mg due to sample shortage, but the final fill weight of the capsules to be tested were 40mg (blends A and B) and 80mg (blend C).

Content uniformity Experiments

In order to determine the optimum mixing time for each of the above blends, the blender was stopped periodically and ten representative samples from the blend were removed. This was done by first placing the whole powder bed onto a piece of paper, dividing it into nine sections and taking ~40mg from each section and an additional 40mg randomly. Samples were placed into 50ml volumetric flasks and made up volume with methanol. The pre-set criteria for a blend to be acceptable was that it must have had corrected concentration (μg/ml) RSD of <5%. Table 40, below, summarises the results obtained. For more detailed results please refer to Appendix 4: Content Uniformity Experiments for Ternary Blends of MLFDS, page 258.

Mix-Time (min)	Average Conc. (µg/ml)	Expected Conc.(µg/ml)	SD	RSD (%)
5	0.397	0.4	0.0247	6.2
10	0.406	0.4	0.0208	5.1
20	0.405	0.4	0.0196	4.9

Table 40: Mixing time versus average concentration (n=10) for a ternary blend of MLFDS, coarse lactose, and fine lactose (5:90:5% w/w).

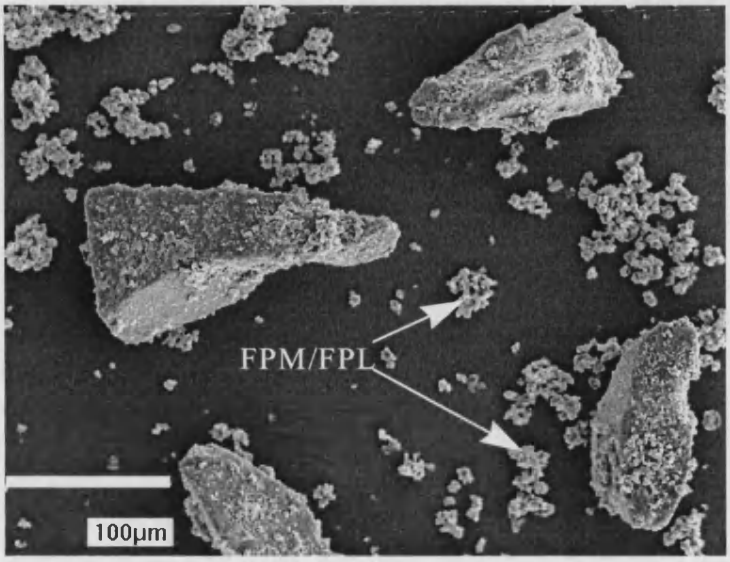

Figure 52: SEM photomicrograph for a ternary blend of MLFDS, coarse lactose, and fine lactose (5:90:5% w/w) at x1500 magnification, mix time: 20min.

Key: FPM / FPL: Fine Particle Multiplet / Lactose.

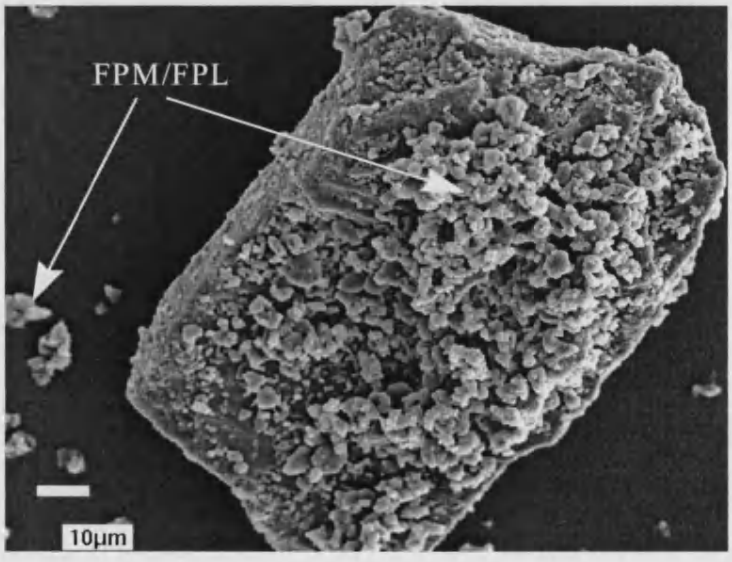

Figure 53: SEM photomicrograph for a ternary blend of MLFDS, coarse lactose, and fine lactose (5:90:5% w/w) at x2500 magnification, mix time: 20min.

The SEM pictures, on page 149, show examples of the photomicrographs obtained for the ternary blends of SAPL. As outlined in the introduction (see section 1.4.2.2.1 Mixing Theory, page 45), carrier-based systems contain various combinations of carrier-drug-carrier associations. These characteristics are also exhibited. More specifically, the images contain FPM and FPL aggregates as well the normal ordered mixing that takes place between the drug and the carrier. The associations vary in size from a few aggregated particles to a large mass. It should also be noted that particles adhered to coarse lactose are not done so in a uniform fashion. Rather, layers of particles adhering both to the carrier and each other are present.

The *in-vitro* aerosol conditions and method employed were the same as those outlined in section 4.1. Flow rates of 60 ($ECD_{50\%}$ 6.55μm, stage 1 jet 14.2mm, shot time 4.0secs) and 96.4 $Lmin^{-1}$ ($ECD_{50\%}$ 6.51μm, stage 1 jet 16.4mm, shot time 2.5) were used.

Results

Table 41, below, shows the TSI deposition data obtained for a ternary blend of MLFDS, coarse lactose, and fine lactose at 60.0 and 96.4 $Lmin^{-1}$.

Parameter	FR	Capsule	Device	Stage 1	Stage 2
Measured Intensity (%)	60.0	1.57(±0.230)	1.44(±0.228)	17.8(±1.31)	4.29(±0.964)
	96.4	1.32(±0.273)	1.46(±.0.274)	17.0(±1.05)	5.36(±0.623)
Corrected Intensity (%)	60.0	0.980(±0.230)	0.850(±0.228)	17.2(±1.31)	3.70(±0.964)
	96.4	0.736(±0.273)	0.878(±0.274)	16.4(±1.05)	4.77(±0.623)
Conc. (μg/ml)	60.0	0.016(±0.004)	0.014(±0.005)	0.356(±0.006)	0.073(±0.006)
	96.4	0.0152(±0.002)	0.018(±0.002)	0.335(±0.005)	0.097(±0.005)
Dilution Factor	60.0	50	50	100	50
	96.4				
Amount Deposited (μg)	60.0	0.813(±0.242)	0.683(±0.258)	35.3(±0.608)	3.64(±0.331)
	96.4	0.754(±0.185)	0.897(±0.183)	33.2(±0.561)	4.84(±0.254)
(%) Deposited	60.0	2.01(±0.587)	1.69(±0.599)	87.3(±3.95)	9.00(±1.86)
	96.4	1.90(±0.439)	2.24(±0.635)	83.7(±4.67)	12.2(±1.55)

Table 41: Summary table of TSI deposition data for a ternary blend of MLFDS, coarse lactose, and fine lactose (5:90:5% w/w) at 60.0 and 96.40$Lmin^{-1}$, n=10.

Parameter	Value Obtained or calculated @60.0Lmin^{-1}	Value Obtained or calculated @96.4Lmin^{-1}
Mean Total Recovery (µg)	40.7(±0.602)	40.0(±0.661)
Mean Total Recovery (%)	101.5(±2.15)	99.8(±1.37)
Mean Emitted Dose (µg)	38.9(±1.92)	38.1(±1.70)
Mean Emitted Dose (%)	96.3(±1.89)	95.8(±1.45)
Mean FPD (µg)	3.64(±0.771)	4.84(±0.524)
Mean FPF(%)	9.00(±1.63)	12.7(±1.03)
Mean Fill Weight (mg)	80.7(±0.949)	80.6(±0.478)

Table 42: Summary table of various parameters calculated from TSI deposition data for a ternary blend of MLFDS, coarse lactose, and fine lactose (5:90:5% w/w) at 60.0 and 96.4Lmin^{-1}, n=10.

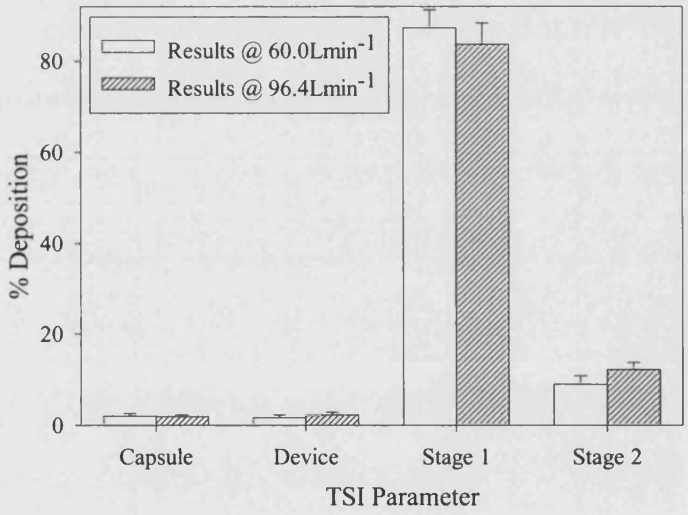

Figure 54: Distribution of a ternary blend of MLFDS, coarse lactose, and fine lactose (5:90:5% w/w) at 60.0 and 96.4Lmin^{-1}.

Bars represent the mean + SD of 10 determinations.

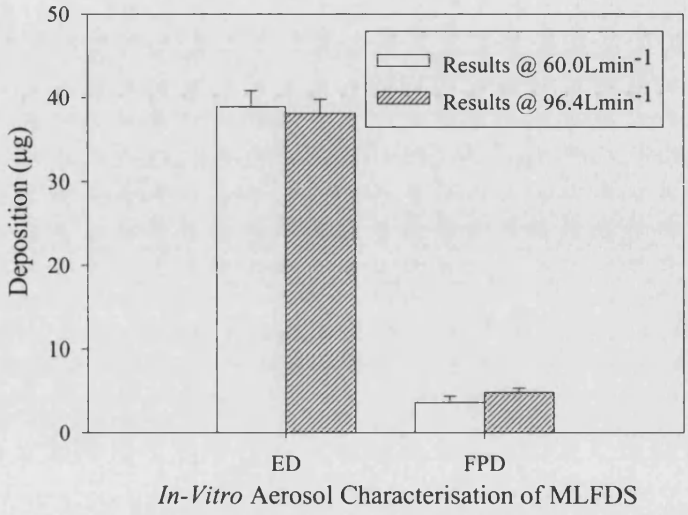

Figure 55: Emitted dose and fine particle dose of a ternary blend of MLFDS, coarse lactose, and fine lactose (5:90:5% w/w) at 60.0 and 96.4Lmin^{-1}.

Bars represent the mean + SD of 10 determinations.

Statistics

One-way analysis of variance on the ED of MLFDS ternary blend at 60.0 and 96.4Lmin^{-1} revealed no significant differences ($F=1.03$, $p=0.324$). However, there was a significant difference ($F=37.9$, $p=<0.001$) in the FPD at the two flow rates.

4.1.4 General Discussion

The preparation of the various blends of MLFDS, their content uniformity, and subsequent deposition profiles under two different conditions has been presented. Table 43 and Table 44, page 153 summarise the findings.

Parameter	Summary TSI Results at 60.0Lmin^{-1}				
	Drug-Only	Binary Blend A	Binary Blend B	Binary Blend C	Ternary Blend
ED(µg)	168.5(±4.81)	35.2(±1.69)	37.6(±1.70)	36.4(±1.73)	38.9(±1.92)
FPD(µg)	27.6(±2.58)	2.87(0.235)	3.23(0.309)	2.97(0.551)	3.64(±0.771)
FPF(%)	16.4(±1.27)	8.14(±1.13)	8.58(±1.15)	8.16(±1.17)	9.00(±1.63)
Fill Wt (mg)	20.1(±0.252)	40.7(±1.60)	40.8(±1.47)	80.6(±1.42)	80.7(±0.949)

Table 43: Summary TSI results obtained for MLFDS and its various blends at 60.0Lmin^{-1}, n=10.

Parameter	Summary TSI Results at 96.4Lmin^{-1}				
	Drug-Only	Binary Blend A	Binary Blend B	Binary Blend C	Ternary Blend
ED(µg)	165.5(±3.94)	34.9(±1.90)	37.8(±1.34)	36.5(±1.21)	38.1(±1.70)
FPD(µg)	33.4(±3.28)	3.79(±0.12)	4.54(±0.87)	4.07(±0.86)	4.84(±0.524)
FPF(%)	20.2(±1.86)	10.9(±1.27)	12.0(±1.16)	11.2(±1.24)	12.7(±1.03)
Fill Wt (mg)	20.5(±0.497)	41.3(±1.4)	40.4(±1.25)	80.2(±1.35)	80.6(±0.478)

Table 44: Summary TSI results obtained for MLFDS and its various blends at 96.4Lmin^{-1}, n=10.

It must be noted that the above results are the distribution of the label within the TSI and not the drug itself. Since the label is only present at 1% (w/w) within each capsule, the final values need to be multiplied by 100 in order to make the results applicable for the drug itself. In addition, the values have been normalised to make all the results directly comparable. Therefore, the revised summary tables are as shown below.

Parameter	Summary TSI Results at 60.0Lmin^{-1}				
	Drug-Only	Binary Blend A	Binary Blend B	Binary Blend C	Ternary Blend
ED(mg)	3.34	3.48	3.72	3.60	3.85
FPD(mg)	0.546	0.284	0.320	0.294	0.360
FPF(%)	16.4	8.15	8.59	8.16	9.36
Fill Wt (mg)	20.1	40.7	40.8	80.6	80.7

Table 45: Modified, Summary TSI results obtained for MLFDS and its various blends at 60.0Lmin^{-1}.

Parameter	Summary TSI Results at 96.4Lmin^{-1}				
	Drug-Only	Binary Blend A	Binary Blend B	Binary Blend C	Ternary Blend
ED(mg)	3.28	3.46	3.74	3.61	3.77
FPD(mg)	0.661	0.375	0.449	0.403	0.479
FPF(%)	20.2	10.9	12.0	11.2	12.7
Fill Wt (mg)	20.5	41.3	40.4	80.2	80.6

Table 46: Modified, summary TSI results obtained for MLFDS and its various blends at 96.4Lmin^{-1}.

The results for the modified results show the following:

a) The drug-only formulation performs best, in terms of FPD and FPF, but is the worst at actually emptying from the capsule.

b) There seems to be no appreciable differences in the performances of the various binary blends and the ternary blend.

Blend ID	FR	ANOVA ED		ANOVA FPD		Fisher's Pairwise Significance?
		P-value	F-value	P-Value	F-Value	
Drug Only	30.0 60.0 96.4	<0.001	169.2	<0.001	209.4	Yes, results at 30 are significantly different from those at 60 & 96.4
BB-A BB-B BB-C	60.0	0.008	5.88	0.125	2.25	No, significant differences were observed
BB-A BB-B BB-C	96.4	0.001	9.57	0.073	2.88	ED values of BB-A significantly different to that of BB-B and BB-C
TB	60.0 96.4	0.324	1.03	<0.001	37.9	FPD values significantly different at the two flow rates

Table 47: Summary TSI statistics for LFDS and its various blends at 30, 60, and 96.4Lmin^{-1}.

Key: BB= Binary Blend, TB= Ternary Blend, FR= Flow Rate.

From the various statistical analyses carried out at the end of each sub-section and summarised in Table 47, it can be concluded that for the drug-only formulation, ED is dependent on flow rate. At low flow rates ($30Lmin^{-1}$) the capsule does not empty efficiently. In addition, because of the cohesive nature of MLFDS, FPD only increases with increasing flow rate and turbulence within the capsule. The binary blends of MLFDS showed no significant differences in ED at $60Lmin^{-1}$ (3.48, 3.72, and 3.60% respectively for blends A, B, and C) but did so at $96.4Lmin^{-1}$ (3.46, 3.74, and 3.61% respectively for blends A, B, and C). This difference at $96.4Lmin^{-1}$ is unexpected and marginal and one possible explanation is that the ED of blend A (10% MLFDS: 90% coarse lactose) is lower than it ought to be. FPD values of MLFDS binary blends are concordant and not statistically different. As with the binary blends, the ED of the ternary blend was equally good at 60 and $96.4Lmin^{-1}$. However, the higher flow rate produced a higher FPD, as expected. Although direct comparison of the above data is not possible with other powdered surfactant studies (because no published data exists), comparisons can be made against standard powder formulations. A study carried out by Zeng *et al* (1999) on ternary mixtures of salbutamol sulphate (5.8μm), coarse lactose (90.8μm), intermidiate (15.9μm), and fine lactose (5μm) using the TSI at 60 and 90 $Lmin^{-1}$ via the Rotahaler™ and employing various mixing sequences produced a FPF value in excess of the 12.7% obtained in this study. Srichana *et al* (1998) investigated the effect of the resistance of the device and the influence of powder formulation on the deposition of drug and carrier for formulations of salbutamol. Results showed FPF values of ~20% for several devices tested at differing flow rates.

4.2 MSLI Deposition Profiles

Deposition studies of MLFDS and its various blends were performed using the 5-stage liquid impinger (as described in section 1.6 Aerosol Testing and Characterisation, page 63). Both the instrument and the testing protocols outlined by the EP supplement (1999) are given in more detail in the above-mentioned section. A brief description of the method is presented below.

The Miat monohaler (as described on page 135) was used to assess the *in-vitro* aerosol performance of MLFDS and its various blends with lactose. The size 3 hard gelatine capsules used to deliver MLFDS were stored in desiccator containing a saturated salt solution of ammonium nitrate, for the reasons given on page 135.

4.2.1 Drug Only

The deposition studies were performed at 92.0Lmin^{-1} (see below for cut-off diameters), which corresponded to a 4kPa pressure drop between the atmosphere and stage one of the MSLI (P1). Determination of sonic flow revealed values of 815 and 338mBar for P2 and P3 respectively, ratio P3/P2: 0.41, therefore sonic flow.

Cut-Off Diameters (μm)					
Flow Rate	Stage 1	Stage 2	Stage 3	Stage 4	Stage 5
92.0Lmin^{-1}	>10.50	5.49	2.50	1.37	0.00

Table 48: The MSLI cut-off diameters at 92.0Lmin^{-1} flow rate as used in the *in-vitro* characterisation of MLFDS.

Each stage of the MSLI was filled with 20ml of HPLC grade methanol. Five accumulative capsules containing ~20mg of MLFDS (~1% label by weight, i.e. 1mg total label weight) were fired into the system (shot time: 2.61secs), using the Miat monohaler. The procedure was carried out in triplicate. The five capsules and the device were washed with methanol after each firing into 50ml volumetric flasks and made up to volume. Once the firing sequence was complete, the adaptor and throat were washed into 50ml and 100ml volumetric flasks respectively and adjusted volume with methanol. Stage 1 jet was washed with 5ml of methanol to ensure that any particulates in the jet were washed down into stage 1. Stage 5 (after-filter) of the apparatus was removed and the filter paper was sonicated in 20ml of methanol for 1 minute, ensuring that drug particles on the filter went into solution. The MSLI apparatus was then gently swirled and rotated to recover any drug particles from the walls of the apparatus. The apparatus was then turned up side down to carefully wet the ceiling of each stage and, thus, recover any drug particles that may have impacted onto the ceiling. The

swirling motion was carried out for a period of 10 minutes to ensure all drug particles had gone into solution. Stages 1 to 5 were all sonicated for 2 minutes and made up to 100ml with methanol. The throat and stage 1 were diluted further (1:10) so as their intensity reading from the fluorimeter fell within the standard range. The standards were prepared as described earlier (see fluorimetric detection of LFDS, page 108). The relative intensity of the standards and the samples were measured on the Hitachi F2000 fluorimeter, Hitachi Ltd., Japan.

Results

	Intensity (%)	Corr. Intensity (%)	Label Conc. (µg/ml)	Dil. Factor	Total Amount Deposited (µg)	Amount Deposited Per Shot (µg)	Deposition (%)
Cap	27.0 (±1.55)	25.9 (±1.55)	0.378 (±0.026)	50	18.9 (±1.35)	3.78 (±0.272)	1.98 (±0.722)
Dev	26.6 (±0.370)	25.5 (±0.370)	0.372 (±0.024)	50	18.6 (±1.20)	3.72 (±0.24)	1.94 (±0.831)
Adp	17.8 (±1.32)	16.7 (±1.32)	0.241 (±0.019)	50	12.0 (±0.954)	2.41 (±0.191)	1.26 (±0.620)
Tht	31.5 (±2.98)	30.4 (±2.98)	0.444 (±0.047)	1000	444.4 (±47.3)	88.9 (±9.46)	46.5 (±3.68)
Stg1	18.6 (±1.56)	17.5 (±1.56)	0.253 (±0.020)	1000	252.7 (±20.1)	50.6 (±4.02)	26.5 (±2.41)
Stg2	54.6 (±3.09)	53.5 (±3.09)	0.788 (±0.094)	100	78.8 (±9.4)	15.8 (±1.88)	8.24 (±1.82)
Stg3	42.6 (±2.75)	41.5 (±2.75)	0.609 (±0.199)	100	61.0 (±19.9)	12.2 (±3.98)	6.38 (±1.23)
Stg4	36.9 (±2.52)	35.8 (±2.52)	0.525 (±0.140)	100	52.5 (±14.1)	10.5 (±0.395)	5.49 (±1.47)
Stg5	12.7 (±0.926)	11.6 (±0.926)	0.165 (±0.055)	100	16.5 (±5.53)	3.30 (±1.11)	1.73 (±0.717)

Table 49: Summary table of MSLI deposition data for MLFDS at 92.0Lmin^{-1}, n=15.

Parameter	Value Obtained or calculated
Mean Total Recovery (µg)	191.1(±2.78)
Mean Total Recovery (%)	95.8(±1.42)
Mean Emitted Dose (µg)	183.6(±4.92)
Mean Emitted Dose (%)	96.1(±1.35)
Mean FPD (µg)	26.0(±1.97)
Mean FPF (%)	14.2(±2.59)
Mean Fill Weight (mg)	20.2(±1.2)

Table 50: Summary table of various parameters calculated from MSLI deposition data for MLFDS at 92.0 Lmin^{-1}.

The results expressed are the values obtained per shot, values in brackets indicate standard deviation, n=15.

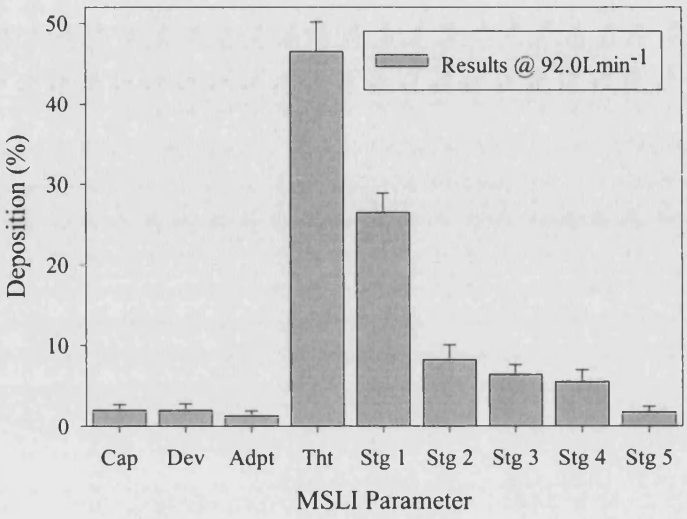

Figure 56: Distribution of MLFDS within the MSLI at 92.0Lmin^{-1}.

Bars represent the mean + SD of 15 determinations.

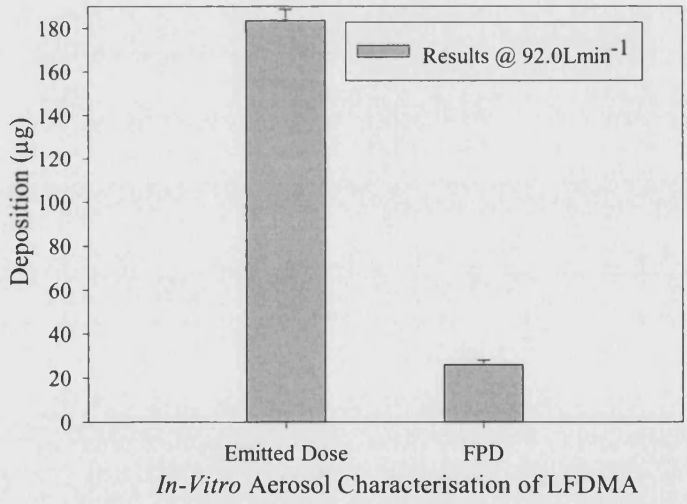

Figure 57: Emitted dose and fine particle dose of MLFDS within the MSLI at 92.0Lmin^{-1}.

Bars represent the mean + SD of 15 determinations.

4.2.2 Binary Blends

Three different blends of MLFDS and lactose (see below), were prepared as described on page 118 using the rotary bladed blender (Kenwood Mini Chopper, CH100, Kenwood Ltd., Hants., UK).

Blend ID	Blend Size	MLFDS (%w/w)	Lactose (%w/w)	Lactose Type
A	10g	10	90	Coarse (63-90μm) Fraction
B	10g	10	90	Fine (Microtose) (<10μm)
C	10g	5	95	Coarse (63-90μm) Fraction

Table 51: Table showing the details of the various binary blends of MLFDS with coarse and fine lactose.

The blends were tested for content uniformity and the optimum mixing time for each blend was determined, as previously outlined on page 139. The deposition profiles of the blends were then obtained using the MSLI method as described on page 156. Five accumulative capsules containing ~1% label by weight (i.e. 200μg of label (total) in blends A, B, and C for a 40mg and 80mg load capsules respectively) were fired into the system (shot time: 2.61secs), using the Miat monohaler. The procedure was carried out in triplicate. The relative intensity of the standards (see page 108 for preparation) and the samples were measured on the Hitachi F2000 fluorimeter, Hitachi Ltd., Japan.

Results

Table 52, page 161 is a summary table of MSLI deposition data for MLFDS blend A at 92.0Lmin^{-1}. Values in brackets indicate standard deviation, n=15.

	ID	Int.(%)	Corr. Int. (%)	Label Conc. (μg/ml)	Dil. Fac.	Total Amount Deposited	Amount Deposited Per Shot (μg)	Dep (%)
Cap	A	28.7 (1.56±)	27.6 (±1.56)	0.387 (±0.157)	10	3.87 (±1.57)	0.775 (±0.314)	2.01 (±0.738)
Dev	A	29.6 (±1.91)	28.5 (±1.91)	0.400 (±0.174)	10	4.00 (±1.74)	0.801 (±0.348)	2.08 (±0.644)
Adp	A	10.9 (±0.835)	9.81 (±0.835)	0.132 (±0.064)	10	1.32 (±0.645)	0.263 (±0.129)	0.684 (±0.218)
Tht	A	20.3 (±1.39)	19.2 (±1.39)	0.267 (±0.002)	200	2.67 (±0.403)	0.533 (±0.080)	1.39 (±0.269)
Stg1	A	32.3 (±2.34)	31.2 (±2.34)	0.439 (±0.096)	200	87.8 (±19.2)	17.6 (±3.84)	45.6 (±6.36)
Stg2	A	24.8 (±2.33)	23.7 (±2.33)	0.331 (±0.124)	20	66.3 (±9.09)	13.3 (±0.496)	34.4 (±6.84)
Stg3	A	50.1 (±3.08)	49.0 (±3.08)	0.695 (±0.169)	20	13.9 (±3.38)	2.78 (±0.676)	7.22 (±1.36)
Stg4	A	36.3 (±2.98)	35.2 (±2.98)	0.497 (±0.156)	20	9.94 (±3.12)	1.99 (±0.624)	5.16 (±1.01)
Stg5	A	11.4 (±2.41)	10.3 (±2.41)	0.139 (±0.033)	20	2.78 (±0.664)	0.555 (±0.133)	1.44 (±0.330)

Table 52: Summary table of MSLI deposition data for MLFDS blend A at 92.0Lmin^{-1}.

Table 53, page 162 is a summary table of MSLI deposition data for MLFDS blend B at 92.0Lmin^{-1}. Values in brackets indicate standard deviation, n=15.

	ID	Int. (%)	Corr. Int. (%)	Label Conc. (μg/ml)	Dil. Fac.	Total Amount Deposited (μg)	Amount Deposited Per Shot (μg)	Deposition (%)
Cap	B	27.6 (±2.88)	26.5 (±2.88)	0.372 (±0.105)	x10	3.72 (±1.05)	0.743 (±0.216)	1.92 (±0.313)
Dev	B	29.3 (±3.01)	28.2 (±3.01)	0.396 (±0.091)	x10	3.96 (±0.916)	0.792 (±0.183)	2.05 (±0.301)
Adp	B	11.4 (±1.46)	10.3 (±1.46)	0.139 (±0.037)	x10	1.39 (±0.371)	0.278 (±0.074)	0.717 (±0.224)
Tht	B	20.6 (±1.71.)	19.5 (±1.71)	0.271 (±0.006)	x200	2.71 (±1.26)	0.542 (±0.252)	1.40 (±0.404)
Stg1	B	32.0 (±3.26)	30.9 (±3.26)	0.435 (±0.065)	x200	87.0 (±13.1)	17.4 (±2.61)	44.9 (±6.30)
Stg2	B	25.3 (±2.09)	24.2 (±2.09)	0.339 (±0.102)	x20	67.7 (±2.04)	13.5 (±0.408)	35.0 (±6.01)
Stg3	B	50.7 (±4.49)	49.6 (±4.49)	0.703 (±0.233)	x20	14.1 (±4.66)	2.81 (±0.932)	7.27 (±1.86)
Stg4	B	36.9 (±3.64)	35.8 (±3.64)	0.505 (±0.107)	x20	10.1 (±2.14)	2.02 (±0.428)	5.22 (±1.42)
Stg5	B	11.8 (±1.06)	10.7 (±1.06)	0.145 (±0.042)	x20	2.89 (±0.840)	0.578 (±0.168)	1.49 (±0.023)

Table 53: Summary table of MSLI deposition data for MLFDS blend B at 92.0Lmin^{-1}.

Table 54, page 163 is a summary table of MSLI deposition data for MLFDS blend C at 92.0Lmin^{-1}. Values in brackets indicate standard deviation, n=15.

	ID	Int. (%)	Corr. Int. (%)	Label Conc. (µg/ml)	Dil. Fac.	Total Amount Deposited (µg)	Amount Deposited Per Shot (µg)	Deposition (%)
Cap	C	27.6 (±2.84)	26.5 (±2.84)	0.372 (±0.107)	x10	3.72 (±1.07)	0.743 (±0.214)	1.90 (±0.206)
Dev	C	28.3 (±2.28)	27.2 (±2.28)	0.382 (±0.146)	x10	3.82 (±1.46)	0.763 (±0.292)	1.95 (±0.350)
Adp	C	10.6 (±1.10)	9.5 (±1.10)	0.127 (±0.053)	x10	1.27 (±0.535)	0.255 (±0.107)	0.649 (±0.183)
Tht	C	20.1 (±1.82)	19.0 (±1.82)	0.264 (±0.009)	x200	2.64 (±0.917)	0.528 (±0.183)	1.35 (±0.126)
Stg1	C	33.6 (±3.53)	32.5 (±3.53)	0.458 (±0.016)	x200	91.6 (±3.22)	18.3 (±0.644)	46.7 (±4.60)
Stg2	C	24.5 (±2.62)	23.4 (±2.62)	0.327 (±0.104)	x20	65.4 (±2.08)	13.1 (±0.416)	33.4 (±4.01)
Stg3	C	49.1 (±5.21)	48.0 (±5.21)	0.680 (±0.182)	x20	13.6 (±3.64)	2.72 (±0.728)	6.94 (±1.16)
Stg4	C	39.1 (±3.60)	38.0 (±3.60)	0.537 (±0.061)	x20	10.7 (±1.22)	2.15 (±0.244)	5.48 (±1.38)
Stg5	C	13.3 (±1.71)	12.2 (±1.71)	0.166 (±0.050)	x20	3.32 (±1.00)	0.664 (±0.200)	1.69 (±0.365)

Table 54: Summary table of MSLI deposition data for MLFDS blend C at 92.0Lmin^{-1}.

Parameter	Blend A	Blend B	Blend C
Mean Total Recovery (µg)	38.5(±3.06)	38.7(±2.72)	39.2(±2.86)
Mean Total Recovery (%)	96.6(±2.88)	97.0(±2.14)	98.3(±2.60)
Mean Emitted Dose (µg)	36.9(±3.11)	37.2(±2.57)	37.7(±2.89)
Mean Emitted Dose (%)	95.9(±2.53)	96.0(±2.40)	96.2(±3.23)
Mean FPD (µg)	5.32(±0.926)	5.41(±1.15)	5.53(±1.31)
Mean FPF (%)	14.4(±1.35)	14.6(±1.48)	14.7(±1.73)
Mean Fill Weight (mg)	40.3(±1.2)	39.9(±1.4)	80.4(±1.9)

Table 55: Summary table of various parameters calculated from MSLI deposition data for blends A, B, and C at 92.0Lmin^{-1}.

The results expressed are the values obtained per shot, values in brackets indicate standard deviation, n=15.

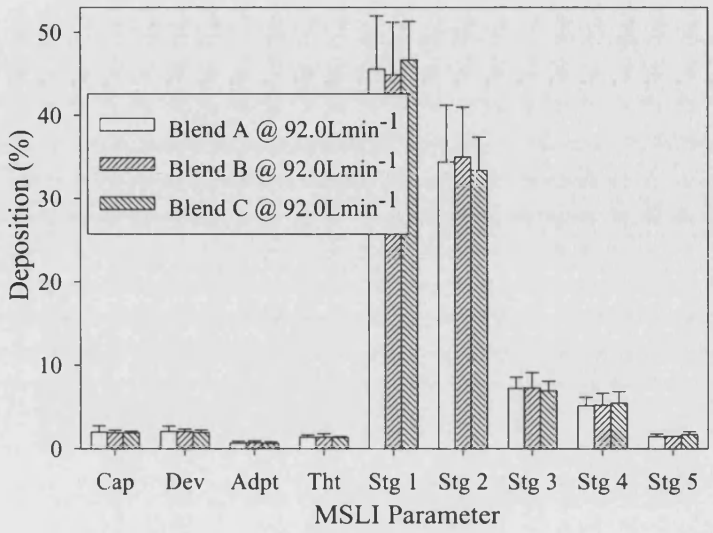

Figure 58: Distribution of blends A, B, and C within the MSLI at 92.0Lmin^{-1}.

Bars represent the mean + SD of 15 determinations.

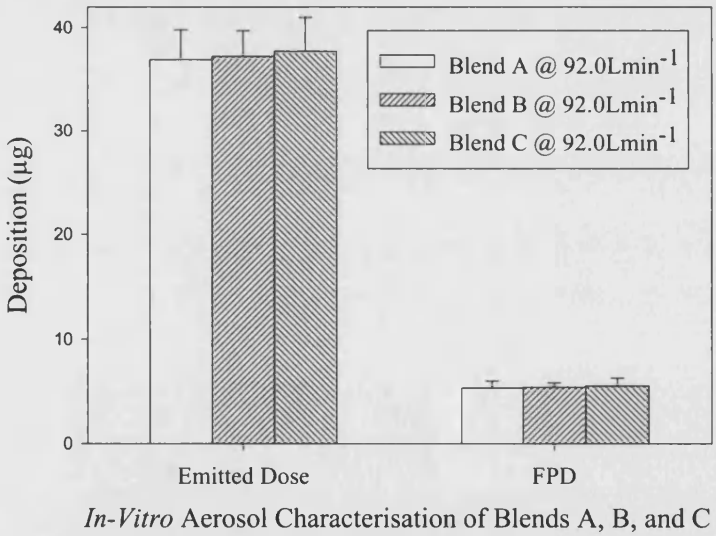

Figure 59: Emitted dose and fine particle dose of blends A, B, and C at 92.0Lmin^{-1}.

Bars represent the mean + SD of 15determinations.

Statistics

One-way analysis of variance on the ED of MLFDS binary blends A, B, and C showed no significant differences (F=0.23, p=0.799). No significant differences were observed (F=0.09, p=0.911) for the FPD values

4.2.3 Ternary Blends

A ternary blend of MLFDS, coarse lactose (63-90μm), and fine lactose (microtose)(ratio 5:90:5% w/w) as described on page 148 was used in the deposition studies with the MSLI. Refer to page 149 for content uniformity and SEM photomicrographs of the blend.

Method

The deposition profiles of five 80mg accumulative capsules containing ~1% label by weight (i.e. 200μg of label weight total) were fired into the system at 92.0Lmin^{-1}, corresponding to a 4kPa pressure drop across the device as described on page 156. A shot time of 2.61secs was employed, using the Miat monohaler as described on page 135. The procedure was carried out in triplicate. The relative intensity of the standards (see page 108 for preparation) and the samples were measured on the Hitachi F2000 fluorimeter, Hitachi Ltd., Japan.

Results

	Int. (%)	Corr. Int. (%)	Label Conc. (μg/ml)	Dil. Fact.	Total Amount Deposited (μg)	Amount Deposited Per Shot (μg)	Deposition (%)
Cap	27.31 (±2.96)	26.22 (±2.96)	0.367 (±0.093)	10	3.67 (±0.935)	0.735 (±0.187)	1.92 (±0.062)
Dev	23.22 (±2.45)	22.13 (±2.45)	0.309 (±0.026)	10	3.09 (±0.267)	0.617 (±0.053)	1.61 (±0.090)
Adp	8.32 (±1.06)	7.23 (±1.06)	0.0946 (±0.003)	10	0.946 (±0.032)	0.189 (±0.006)	0.493 (±0.106)
Tht	19.42 (±1.99)	18.33 (±1.99)	0.254 (±0.016)	10	2.54 (±0.164)	0.508 (±0.033)	1.32 (±0.426)
Stg1	33.16 (±2.71)	32.07 (±2.71)	0.451 (±0.024)	200	90.3 (±4.85)	18.1 (±0.97)	47.1 (±5.12)
Stg2	24.20 (±2.30)	23.11 (±2.30)	0.323 (±0.019)	200	64.5 (±3.81)	12.9 (±0.762)	33.6 (±2.61)
Stg3	47.14 (±3.29)	46.05 (±3.29)	0.652 (±0.047)	20	13.0 (±0.944)	2.61 (±0.189)	6.80 (±0.735)
Stg4	39.03 (±3.35)	37.94 (±3.35)	0.536 (±0.042)	20	10.7 (±0.847)	2.14 (±0.169)	5.59 (±0.609)
Stg5	12.10 (±1.02)	11.01 (±1.02)	0.149 (±0.009)	20	2.98 (±0.184)	0.596 (±0.037)	1.55 (±0.123)

Table 56: Summary table of MSLI deposition data for a ternary blend of MLFDS, coarse lactose, and fine lactose (5:90:5% w/w) at 92.0Lmin^{-1}.

Values in brackets indicate standard deviation, n=15.

Parameter	Value Obtained or calculated @92.0Lmin^{-1}
Mean Total Recovery (μg)	38.4(±2.14)
Mean Total Recovery (%)	96.2(±1.68)
Mean Emitted Dose (μg)	37.0(±2.66)
Mean Emitted Dose (%)	96.5(±3.09)
Mean FPD (μg)	5.35(±0.427)
Mean FPF(%)	14.4(±1.92)
Mean Fill Weight (mg)	80.2(±1.3)

Table 57: Summary table of various parameters calculated from MSLI deposition data for a ternary blend of MLFDS, coarse lactose, and fine lactose (5:90:5% w/w) at 92.0Lmin^{-1}.

The results expressed are the values obtained per shot, values in brackets indicate standard deviation, n=15.

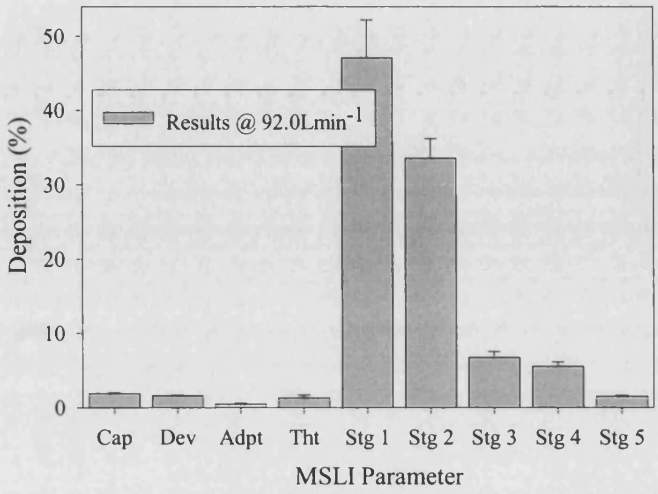

Figure 60: Distribution of a ternary blend of MLFDS, coarse lactose, and fine lactose (5:90:5% w/w) within the MSLI at 92.0Lmin^{-1}.

Bars represent the mean +SD of 15 determinations.

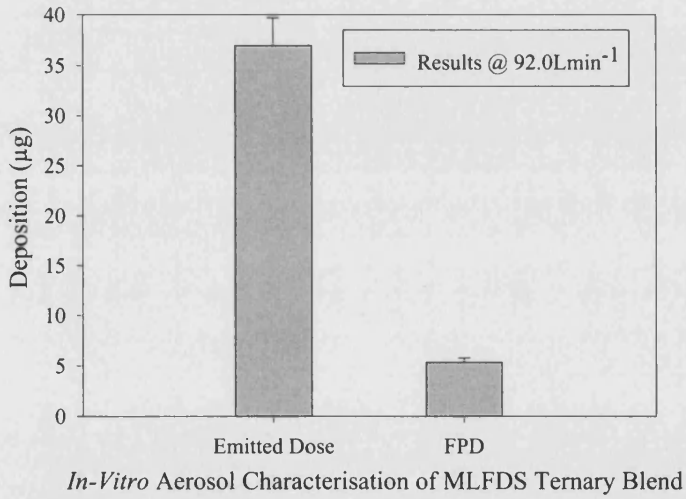

Figure 61: Emitted dose and fine particle dose of a ternary blend of MLFDS, coarse lactose, and fine lactose (5:90:5% w/w) within the MSLI at 92.0Lmin^{-1}.

Bars represent the mean + SD of 15 determinations.

4.2.4 General Discussion

The MSLI deposition profiles of blends of MLFDS, prepared and evaluated for content uniformity on page 156, have been presented in this section. Table 58, below summarises the findings at 92.0Lmin^{-1}.

Parameter	Summary MSLI Results at 92.0Lmin^{-1}				
	Drug-Only	Binary Blend A	Binary Blend B	Binary Blend C	Ternary Blend
ED(µg)	183.6(±4.92)	36.9(±3.11)	37.2(±2.57)	37.7(±2.89)	37.0(±2.66)
FPD(µg)	26.0(±1.97)	5.32(±0.926)	5.41(±1.15)	5.53(±1.31)	5.35(±0.427)
FPF(%)	14.2(±2.59)	14.4(±1.35)	14.6(±1.48)	14.7(±1.73)	14.4(±1.92)
Fill Wt (mg)	20.2(±1.2)	40.3(±1.2)	39.9(±1.4)	80.4(±1.9)	80.2(±1.3)

Table 58: Summary MSLI results obtained for MLFDS and its various blends at 92.0Lmin^{-1}.

It must be noted that the above results are the distribution of the label within the TSI and not the drug itself. Since the label is only present at 1% (w/w) within each capsule, the final values need to be multiplied by 100 in order to make the results applicable for the drug itself. In addition, the values have been normalised to make all the results directly comparable. Therefore, the revised summary table is shown below.

Parameter	Summary MSLI Results at 92.0Lmin^{-1}				
	Drug-Only	Binary Blend A	Binary Blend B	Binary Blend C	Ternary Blend
ED(mg)	3.64	3.65	3.68	3.73	3.66
FPD(mg)	0.515	0.527	0.536	0.547	0.530
FPF(%)	14.2	14.4	14.5	14.7	14.5
Fill Wt (mg)	20.2	40.3	39.9	80.4	80.2

Table 59: Modified, summary MSLI results obtained for MLFDS and its various blends at 92.0Lmin^{-1}.

Results show no appreciable differences between the drug-only and the various formulations. However, the advantage of the drug-only formulations is its ability to deliver a higher total ED and FPD. Statistical analysis on the binary MLFDS systems revealed no significant

differences in the ED and FPD of the three blends. The FPF values on average are about 2% higher than those achieved for the TSI analysis. One possible explanation for this increase could be that the airflow through the MSLI is more conducive to deagglomeration of drug particles.

The data obtained within this section cannot be compared directly against other aerosolised powder surfactant studies using the MSLI because, as yet, there are no such published data within the field with implications for asthma. However, comparison of the data can be made against *in-vitro* (MSLI at 60Lmin^{-1}) and *in-vivo* (scintigraphy) data obtained by Pitcairn *et al* (1997) on a novel asthma drug using a device similar to the Miat Monoler (i.e. Cyclohaler®). Their studies showed FPF values of ~30% for labelled and unlabelled drug, compared with ~14% which was the best obtained in this section using the MSLI at 92Lmin^{-1}. Pitcairn *et al* (1994) looked at the deposition profiles of salbutamol and beclomethasone in an MSLI (at 60Lmin^{-1}) using the Rotahaler® and the Aerohaler®. FPF (particles <6.8μm) values were: Rotahaler®, 6.8 and 5.4%, Aerohaler®, 14.7 and 11.2%, for salbutamol and beclomethasone respectively. Pitcairn *et al* (1994) also reported that significant amount of the powder was retained in the capsule, a trend observed in the present study for MLFDS. Pitcairn *et al* (1997) also looked the performance of the Ultrahaler® for the delivery nedocromil sodium for the prophylaxis of asthma. The effect of different modes of inhalation (slow and fast) from the Ultrahaler® were compared for nedocromil delivery from a pMDI. Results of the study showed that the Ultrahaler® used suboptimally or the pMDI used optimally [mean (SD) lung deposition values of 13.3 (4.8)%, 9.8 (3.5)%, and 7.5 (2.9)%, respectively], Oropharyngeal deposition averaged over 80% of the dose for all three treatment regimens.

In summary, the FPF (~14%) obtained for the various MLFDS formulations in the present study compares favourably to some the above-mentioned standard solid dosage forms, delivered from various devices.

Chapter 5

Deposition Studies of MS

5.0 Deposition Studies of MS

This section outlines the various deposition experiments carried out on MS. The average particle size of MS used during the deposition studies was 2.39μm, as determined by LALLS (see page 75). The HPLC technique used to quantify the material has been previously described (see section 2.2.5.1 HPLC Detection of MS, page 99).

5.1 TSI (Apparatus A) Deposition Profiles

A single dose capsule based device, the Miat monohaler, was used to assess the *in-vitro* aerosol performance of MS. The reasons for choosing the Miat monohaler as the delivery device along with size three hard gelatine capsules has been previously outlined on page 135.

5.1.1 Drug Only

The *in-vitro* aerosol investigations of MS were performed at 30, 60 and 96.4Lmin^{-1} (see Table 60, below). Flow rate through the device was adjusted via the needle valve using a mass flow meter (Hastings Mass Flow Meter, HFM 201, Teledyne Brown Engineering, Hastings Instruments, VA, USA).

Flow Rate	Stage 1 Jet Diameter	Cut-off Diameter	Shot time
30.0Lmin^{-1}	6.9mm	3.2μm	8.0secs
60.0Lmin^{-1}	11.6mm	4.8μm	4.0secs
96.4Lmin^{-1}	16.4mm	6.51μm	2.5secs

Table 60: Table showing the conditions used in the TSI (Apparatus A) deposition study of MS.

A size three hard gelatine capsule was filled to contain approximately 20mg of MS. The capsule was placed into the chamber of the Miat monohaler (previously stored in an oven at 40°C) and pierced evenly using the four sets of pins on either side of the device, care was taken not to shatter the capsule. The Miat monohaler was coupled with a TSI, containing 7ml and 30ml HPLC grade methanol in stages 1 and 2 respectively, via an adaptor. The shot-time on the timing device was adjusted to deliver a total of four litres of air. Once fired, the

capsule and device were washed into separate 50ml volumetric flasks with a minimum amount of HPLC grade methanol and adjusted to volume. Stage 1 and throat (plus adaptor) of the TSI were washed into 100ml volumetric flask with the mixture and diluted so as their concentration fell within the standard range. Stage 2 was washed into a 50ml volumetric flask and adjusted to volume, and diluted accordingly. The standards and the samples were analysed using and chromatographic conditions outlined on page 99. Test sample concentrations were determined by solving the quadratic equations presented by the binomial relationship between the six standards (see Table 18, page105 for example). Once solved, the values obtained were incorporated into a spreadsheet and a final answer was obtained, examples of this process are given in Appendix 13: MS Testing and Stability Study Raw HPLC Data, page 270.

Results

Table 61, below is a summary of the results obtained at 30Lmin^{-1}. For more detailed tables please refer to Appendix 5: Detailed tables for the HPLC analysis of MS-TSI Results, page 258.

Parameter	FR	Capsule	Device	Stage 1	Stage 2
Mean PG Area	30.0	37332 (±1872)	32200 (±3158)	94217 (±2041)	14027 (±1898)
Mean DPPC Area	30.0	111006 (±17237)	96542 (±4039)	256822 (±50730)	64229 (±3347)
PG Conc. (µg/ml)	30.0	2.37 (±0.015)	2.20 (±0.060)	3.70 (±0.163)	1.68 (±0.062)
DPPC Conc. (µg/ml)	30.0	7.95 (±0.483)	7.41 (±0.200)	12.2 (±0.531)	5.76 (±0.193)
Dilution Factor	30.0	100	100	1000	200
Amount of PG Deposited (mg)	30.0	0.237 (±0.015)	0.220 (±0.006)	3.70 (±0.163)	0.336 (±0.012)
Amount of DPPC Deposited (mg)	30.0	0.795 (±0.048)	0.741 (±0.020)	12.2 (±0.531)	1.15 (±0.039)
% MS Deposited	30.0	5.31 (±1.48)	4.95 (±1.02)	82.1 (±3.76)	7.7 (±1.74)

Table 61: Summary table of TSI deposition data for MS at 30.0Lmin^{-1}, n=10.

Table 62 and Table 63, below is a summary of the results obtained at 60Lmin^{-1}. For more detailed tables please refer to Appendix 5: Detailed tables for the HPLC analysis of MS-TSI Results, page 258.

Parameter	FR	Capsule	Device	Stage 1	Stage 2
Mean PG Area	60.0	20408 (±912)	15500 (±1183)	64730 (±1012)	23977 (±1649)
Mean DPPC Area	60.0	80256 (±2148)	54507 (±545)	328735 (±3501)	118227 (±2349)
PG Conc. (µg/ml)	60.0	1.93 (±0.031)	1.58 (±0.017)	3.93 (±0.022)	2.32 (±0.034)
DPPC Conc. (µg/ml)	60.0	6.55 (±0.098)	5.45 (±0.054)	13.0 (±0.072)	7.79 (±0.109)
Dilution Factor	60.0	100	100	1000	200
Amount of PG Deposited (mg)	60.0	0.193 (±0.003)	0.158 (±0.002)	3.93 (±0.022)	0.464 (±0.007)
Amount of DPPC Deposited (mg)	60.0	0.655 (±0.010)	0.545 (±0.005)	13.0 (±0.072)	1.56 (±0.022)
% MS Deposited	60.0	4.14 (±1.05)	3.43 (±0.916)	82.6 (±3.40)	9.9 (±1.19)

Table 62: Summary table of TSI deposition data for MS at 60.0Lmin^{-1}, n=10.

Parameter	FR	Capsule	Device	Stage 1	Stage 2
Mean PG Area	96.4	17182 (±2154)	12659 (±882)	61656 (±1259)	28325 (±1267)
Mean DPPC Area	96.4	71962 (±3412)	44301 (±3112)	295080 (±10015)	125896 (±8933)
PG Conc. (µg/ml)	96.4	1.81 (±0.062)	1.41 (±0.057)	3.73 (±0.060)	2.42 (±0.083)
DPPC Conc. (µg/ml)	96.4	6.16 (±0.194)	4.91 (±0.174)	12.4 (±0.195)	8.11 (±0.266)
Dilution Factor	96.4	100	100	1000	200
Amount of PG Deposited (mg)	96.4	0.181 (±0.006)	0.141 (±0.006)	3.73 (±0.060)	0.484 (±0.017)
Amount of DPPC Deposited (mg)	96.4	0.616 (±0.019)	0.491 (±0.017)	12.4 (±0.195)	1.62 (±0.053)
% MS Deposited	96.4	4.06 (±0.994)	3.22 (±0.867)	82.0 (±3.11)	10.7 (±1.67)

Table 63: Summary table of TSI deposition data for MS at 96.4Lmin^{-1}, n=10.

Table 64, below is summary of the various TSI parameters calculated from the previous three tables.

Parameter	Value Obtained or Calculated @ 30.0Lmin^{-1}	Value Obtained or Calculated @ 60.0Lmin^{-1}	Value Obtained or Calculated @ 96.4Lmin^{-1}
Mean Total Recovery(mg)	19.3(±1.69)	20.1(±3.43)	19.3(±2.87)
Mean Total Recovery(%)	96.3(±4.35)	100.6(±1.72)	96.5(±2.43)
Mean Emitted Dose(mg)	17.3(±1.05)	18.6(±1.30)	17.9(±2.44)
Mean Emitted Dose(%)	89.6(±2.59)	92.4(±1.05)	92.7(±1.78)
Mean FPD(mg)	1.49(±0.210)	1.99(±0.381)	2.07(±0.366)
Mean FPF(%)	7.76(±1.16)	9.87(±0.890)	10.7(±1.69)
Mean Fill Weight(mg)	19.9(±0.4)	20.4(±0.3)	20.3(±0.2)

Table 64: Summary table of various parameters calculated from TSI deposition data for MS at 30.0, 60.0, and 96.4Lmin^{-1}.

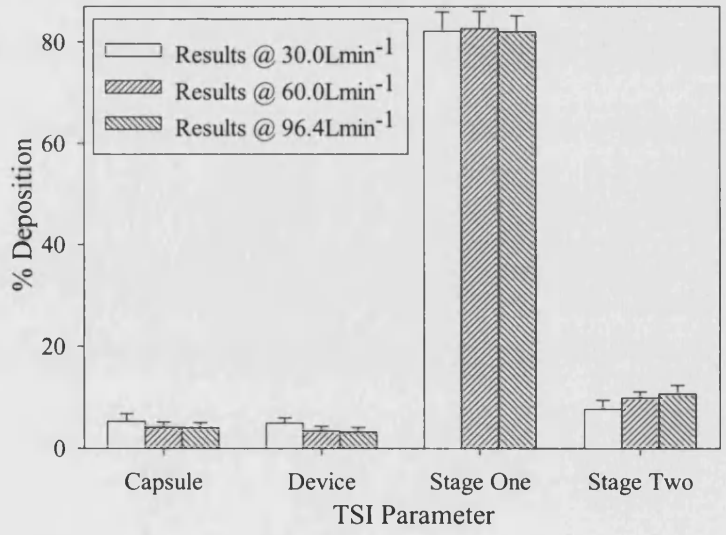

Figure 62: Distribution of MS within Apparatus A at different flow rates.

Bars represent the mean + SD of 10 determinations.

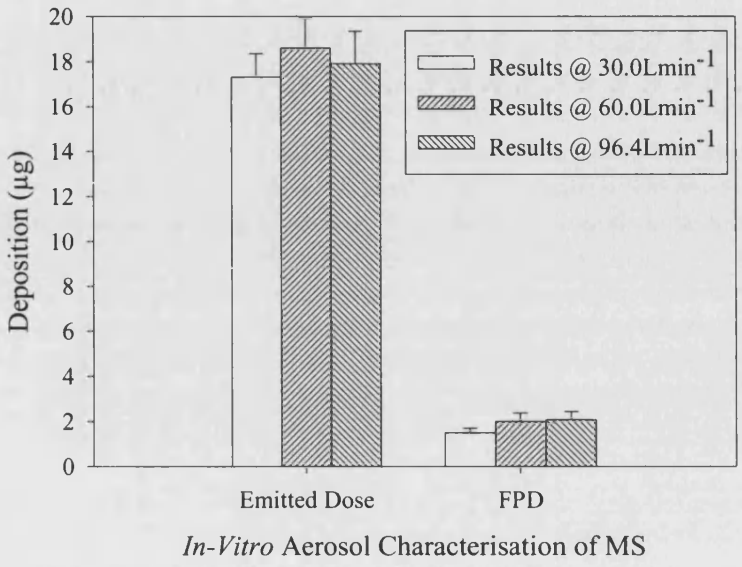

Figure 63: Emitted dose and fine particle dose of MS at different flow rates. Bars represent the mean + SD of 10 determinations.

Statistics

One-way analysis of variance on the ED of MS at 30.0, 60.0 and 96.4Lmin^{-1} showed no significant differences (F=1.58, p=0.225). Significant differences were observed on the FPD of MS at the three flow rates (F=9.07, p=0.001). Fishers pairwise comparisons showed that the FPD of MS at 30Lmin^{-1} was significantly different to the FPDs obtained at the other two flow rates. This is to be expected since at higher flow MS deaggregates better and this in turn leads to increased FPD values.

5.1.2 General Discussion

The TSI deposition profiles of MS at three different flow rates have been presented. The findings show that, as expected, deaggregation of the raw drug is more efficient at higher flow rates. When comparing the FPD and FPF values of MS with those obtained for MLFDS (see Table 65, below and Table 33, page 137 and Table 64, page 173 respectively) it can be seen that the FPD of MS is higher whereas its FPF is marginally lower.

	MLFDS Drug-Only @ 30Lmin^{-1}	MLFDS Drug-Only @ 60Lmin^{-1}	MLFDS Drug-Only @ 96.4Lmin^{-1}	MS @ 30Lmin^{-1}	MS @ 30Lmin^{-1}	MS @ 30Lmin^{-1}
ED	149.4µg	168.5µg	165.5µg	17.3mg	18.6mg	17.9mg
FPD	10.6µg	27.6µg	33.4µg	1.49mg	1.99 mg	2.07 mg
FPF(%)	7.06	16.4	20.2	7.76	9.87	10.7
Fill Wt (mg)	20.7	20.1	20.5	19.9	20.4	20.3

Table 65: Comparative summary table of various parameters calculated from TSI deposition data for MLFDS and MS at 30.0, 60.0, and 96.4Lmin^{-1}

This means that MS empties well from the capsule but does not deaggregate as well as MLFDS. The possible reason for this is that MS has a VMD of 2.39µm compared with 4.12µm for MLFDS. Therefore, a higher FPD is expected but the smaller average size of MS also makes the particles more cohesive and less conducive to deaggregation, hence, the slightly lower FPF. The data obtained within this section cannot be compared directly against other aerosolised powder surfactant studies since there is no such published data within the field with implications for asthma. However, some clinical data on humans does exist from the studies carried out by Kurashima *et al* (1991) and Anzueto *et al* (1997). Kurashima pilot study of surfactant inhalation for the treatment of asthmatic attack utilised nebulised Surfacten® (10mg suspended in 1ml of physiological saline) in a double-blind, placebo-controlled trial. Results showed an 11.7% increase in FVC and a 27.3% increase in FEV_1 in the treated patients when pre and post lung function tests were compared. In a similar, but larger, study Anzueto *et al* (1997) looked at the effect of nebulised Exosurf® for the treatment

of chronic bronchitis. Improvements of 11.4% for FEV_1 and 10.4% for total lung capacity were reported.

5.2 MSLI Deposition Profiles

Deposition studies of MS were performed using the 5-stage liquid impinger (as described on page 63). Both the instrument and the testing protocols outlined by the EP supplement (1999) is given in more detail on page 63. A brief description of the method is presented below.
The Miat monohaler (as described on page 135) was used to assess the *in-vitro* aerosol performance of MS. The size three hard gelatine capsules used to deliver MS were stored in a desiccator containing a saturated salt solution of ammonium nitrate, for the reasons given on page 135.

5.2.1 Drug Only

The deposition studies were performed at 92.0Lmin^{-1} (see below for cut-off diameters), which corresponded to a 4kPa pressure between the atmosphere and stage one of the MSLI (P1). Determination of sonic flow revealed values of 825 and 308mBar for P2 and P3 respectively, ratio P3/P2: 0.37, therefore sonic flow.

Cut-Off Diameters (μm)					
Flow Rate	Stage 1	Stage 2	Stage 3	Stage 4	Stage 5
92.0Lmin^{-1}	>10.50	5.49	2.50	1.37	0.00

Table 66: The MSLI cut-off diameters at 92.0Lmin^{-1} flow rate as used in the in-vitro characterisation of MS.

Each stage of the MSLI was filled with 20ml of HPLC grade methanol. Five accumulative capsules containing ~20mg of MS were fired into the system (shot time: 2.61secs), using the Miat monohaler. The procedure was carried out in triplicate. The five capsules and the device was washed with a minimum amount of methanol after each firing into 50ml volumetric flasks

and made up to volume. Once the firing sequence was complete, the adaptor and throat were washed into a 50ml and 100ml volumetric flask respectively with methanol and adjusted volume. Stage 1 jet was washed with 5ml of methanol to ensure that any particulates in the jet were washed down into stage 1. Stage 5 (after-filter) of the apparatus was removed and the filter paper was sonicated in 20ml of methanol for 1 minute, ensuring that drug particles on the filter went into solution. The MSLI apparatus was then gently swirled and rotated to recover any drug particles from the walls of the apparatus. The apparatus was then turned up side down to carefully wet the ceiling of each stage and, hence, recover any drug particles that may have impacted onto the ceiling. The swirling motion was carried out for a period of 10 minutes to ensure all drug particles had gone into solution. Stages 1 to 5 were all sonicated for 2 minutes and made up to 100ml with methanol. The throat and stage 1 were diluted further so that they fell within the standard range. The standards and the samples were analysed using and chromatographic conditions outlined on page 99. Test sample concentrations were determined by solving the quadratic equations presented by the binomial relationship (refer to Table 18, page 105 for example) between the six standards. Once solved, the values obtained were incorporated into a spreadsheet and a final answer was obtained. Examples of this process as well as the raw data are given in Appendix 13: MS Testing and Stability Study Raw HPLC Data, page 270.

Results

The table below is a summary of the results obtained. For more detailed tables please refer to the appendix (detailed tables for the HPLC analysis of MS- MSLI results).

	Cap	Dev	Adp + Tht	Stg1	Stg2	Stg3	Stg4	Stg5
PG Area	34721 ±4584	32011 ±1728	98426 ±1133	97343 ±2630	90791 ±210	67205 ±2832	48829 ±1400	12928 ±403
DPPC Area	101598 ±1938	91392 ±1110	374757 ±14394	444612 ±10441	412955 ±6003	300356 ±12390	217494 ±1078	53757 ±356
PG Corr. Factor	1.19 ±0.109	1.16 ±0.059	1.44 ±0.031	1.67 ±0.005	1.66 ±0.022	1.64 ±0.008	1.64 ±0.045	1.55 ±0.032
PG Conc. (μg/ml)	9.72 ±0.248	9.22 ±0.025	18.5 ±0.310	19.8 ±0.241	19.1 ±0.113	16.2 ±0.345	13.8 ±0.010	6.59 ±0.041
DPPC Conc.	20.1 ±0.486	19.1 ±0.048	37.5 ±0.619	40.1 ±0.483	38.7 ±0.226	33.0 ±0.688	28.1 ±0.019	14.0 ±0.078
Dilution	100	100	200	1000	200	100	100	100
PG (mg) Deposited	0.972 ±0.025	0.922 ±0.002	3.70 ±0.062	19.8 ±0.241	3.81 ±0.023	1.62 ±0.034	1.38 ±0.001	0.659 ±0.004
DPPC Deposited	2.01 ±0.049	1.91 ±0.005	7.49 ±0.124	40.1 ±0.483	7.73 ±0.045	3.30 ±0.069	2.81 ±0.002	1.40 (±0.008)
% MS Deposited	2.99 ±0.365	2.84 ±0.403	11.2 ±1.38	60.1 ±4.96	11.6 ±1.57	4.94 ±0.546	4.20 ±0.310	2.07 ±0.137

Table 67: Summary table of MSLI deposition data for MS at 92.0Lmin^{-1}, n=15.

Parameter	Value Obtained or calculated
Mean Total Recovery (mg)	99.1(±2.96)
Mean Total Recovery (%)	97.6(±2.45)
Mean Emitted Dose (mg)	93.3(±3.65)
Mean Emitted Dose (%)	94.2(±2.03)
Mean FPD (mg)	11.1(±1.63)
Mean FPF (%)	11.3(±1.79)
Mean Fill Weight (mg)	101.5(±1.8)

Table 68: Summary table of various parameters calculated from MSLI deposition data for MS at 92.0 $Lmin^{-1}$.

The results expressed are the values obtained per shot, values in brackets indicate standard deviation, n=15.

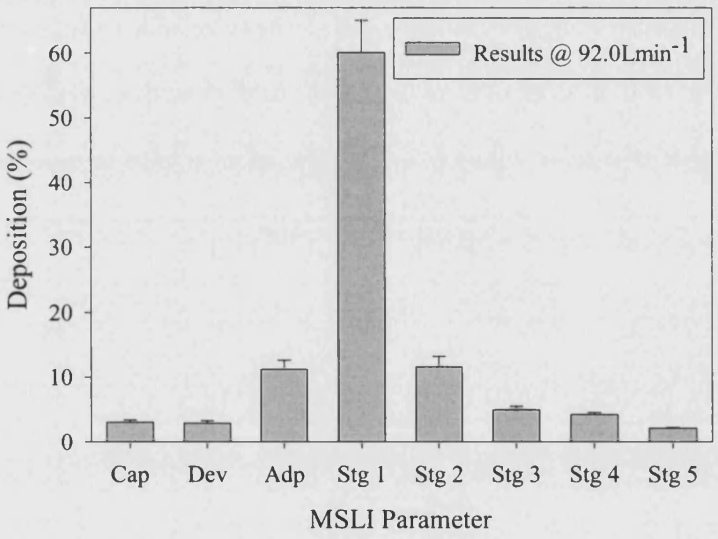

Figure 64: Distribution of MS within the MSLI at 92.0$Lmin^{-1}$.

Bars represent the mean +SD of 15 determinations.

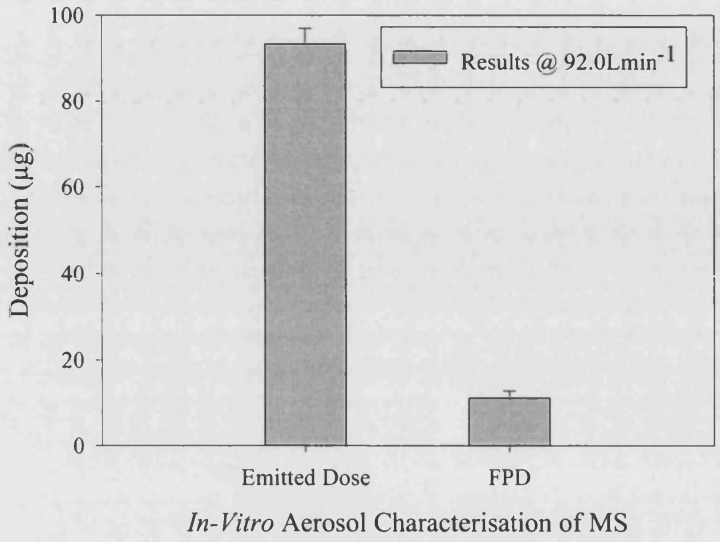

Figure 65: Emitted dose and fine particle dose of MS at 92.0Lmin^{-1}.
Bars represent the mean + SD of 15determinations.

5.2.3 General Discussion

MSLI deposition profile of MS has been presented at 92.0Lmin^{-1} using the Miat monohaler. When comparing the FPD and FPF values of MS with those obtained for MLFDS, the results show the same trend as was seen in the TSI analysis of MS and MLFDS.

Parameter	Summary MSLI Results at 92.0Lmin^{-1}	
	MLFDS Drug-Only	MS
Emitted Dose	183.6(µg) (±4.92)	93.3(µg) (±3.65)
Fine Particle Dose	26.0(µg) (±1.97)	11.1mg (±1.63)
Fine Particle Fraction(%)	14.2(±2.59)	11.3(±1.79)
Capsule Fill Wt (mg)	20.2(±1.2)	101.5(±1.8)

Table 69: Summary Comparison of Aerosol Parameters for LFDS and MS.

This is to say that the FPD of MS is significantly higher than that of MLFDS, but its FPF is lower due to the reasons outlined on page 175.

TSI and MSLI deposition studies of MS using the Miat monohaler and size three gelatine capsules have shown that only modest ED and FPD values are obtained. If SAPL is ever to be marketed as an anti-asthma drug, far greater quantities of it actually need to reach the lungs (i.e. ~100mg). Thus, an alternative approach to delivering the drug was investigated; employing a novel delivery system constructed specifically deliver higher quantities of the drug. This is explained further in the next section.

5.3 A Novel Delivery Device for Asthma

A novel delivery device for the administration of MS is described below. Such a system was necessary since the FPF obtained by other methods of delivery described earlier either yielded poor results, or the change in direction was necessitated because a capsule-based system would be impractical when intending to delivery high-doses (~100mg) of SAPL into the lungs.

5.3.1 Description of the Device

Figure 66, page 182 is the inhalation delivery system for administration of SAPL. It was designed and constructed in colloboration with PA-Consulting (Melbourne, Herts., UK), and intended exclusively for clinical investigations. The system is designed to aerosolise a high-dose of micronised SAPL into a spacer from which the patient in the clinical study may inhale. The early development and component testing was carried out at both Bath University and Melbourne. Full characterisation and subsequent testing of the system and its ability to aerosolise and deliver SAPL was exclusively carried out Bath University.

The system consists of: -

a) A stainless steel spacer with a volume of approximately 4L, from which the patient is intended to breathe.
b) A mesh holder, which aerosolises a sample of MS into the spacer, driven by a regulated supply of medical grade air.

c) A pneumatic assembly that allows the spacer to be connected to and partially evacuated by the pump.

d) A control unit that contains vacuum regulating equipment and the electrical systems necessary to actuate and time the operation of the system.

e) A mounting plate and screen assembly.

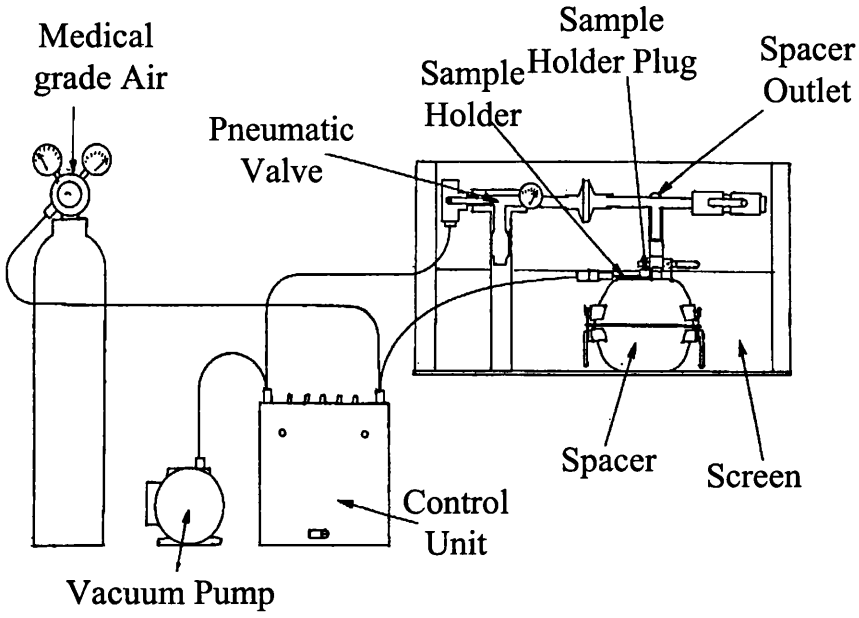

Figure 66: Schematic diagram of the MS Inhalation Delivery System.

5.3.2 Operation of the Device

Samples of micronised MS were previously filled by Penn Pharmaceuticals (Tredegar, Gwent, UK) into 100mg vials in a class 10000 laboratory, supplied with filtered air. The humidity (<10%) and temperature (18-20°C) of the room was also controlled. These measures were taken to minimise moisture absorption from the surrounding atmosphere as outlined on pages 113 and 191. Samples of micronised MS were then transported to Bath University, under controlled conditions (packed using dry-ice), for fine particle assessment.

A photograph of the SAPL delivery device is shown in Figure 67, page 184, part A. Operation if the device is initiated by de-crimping of the vial and introducing the sample into

the mesh holder. Once the sample is loaded (see Figure 67, part B), the mesh holder is placed on top of the spacer (Figure 67, part C). The spacer is sealed by depressing the handles until fixed in the downward position. The pressure inside the spacer is reduced (-0.5bar) by the regulated vacuum system. The powder is then aerosolised and injected into the spacer by actuating the compressed air supply (400kPa) using the control unit (see Figure 67, part D). The spacer is then vented to atmosphere (see Figure 67, part E), the inlet valve is opened to atmosphere (see Figure 67, part F) and the aerosolised cloud is characterised by pulling a pre-set volume of air (4L) through the spacer into an MSLI. The mesh holder is weighed pre and post firing to determine the mass delivered into the spacer. Once the firing is complete, the spacer is dismantled as shown in Figure 67, part G.

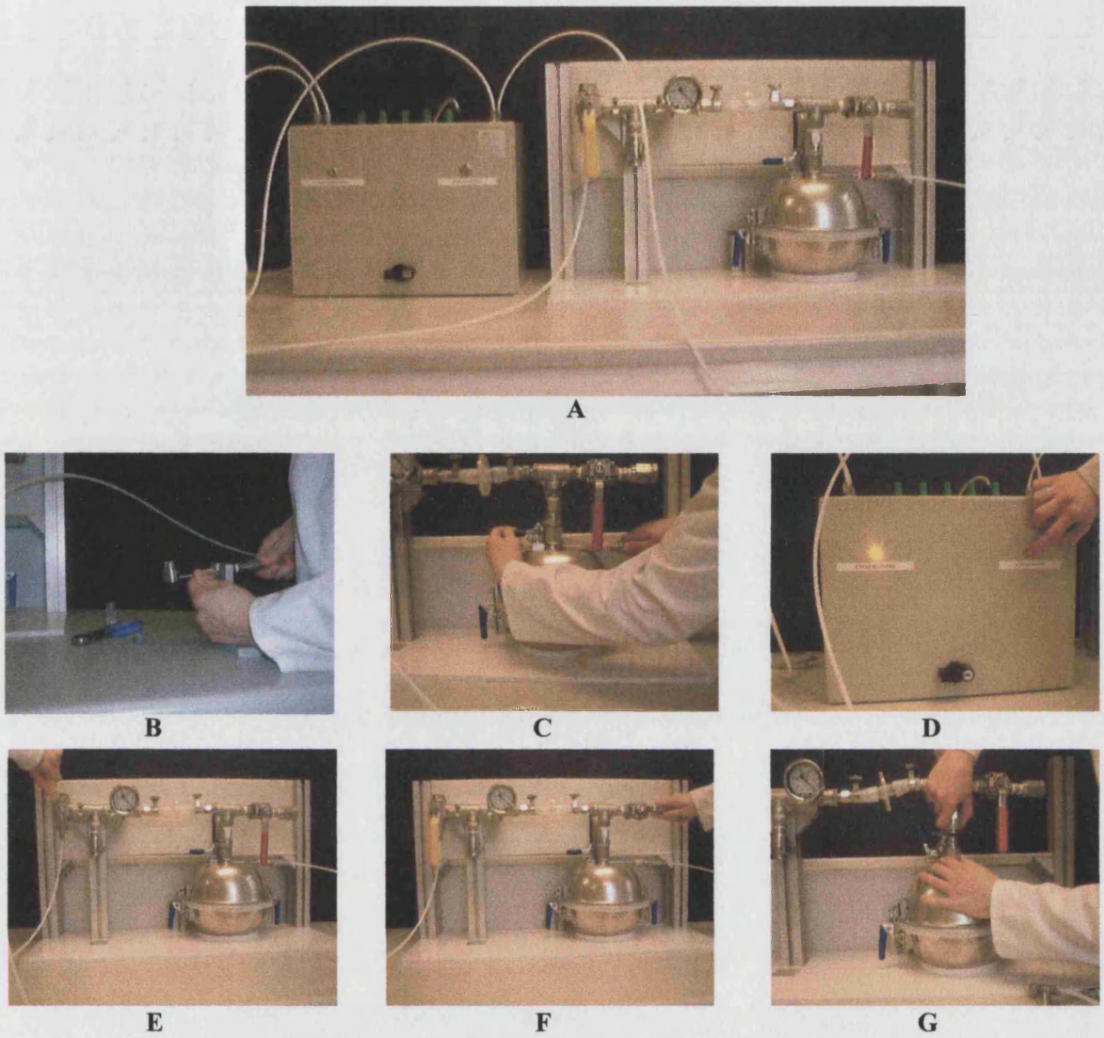

Figure 67: Various photographs of the SAPL delivery system.

a) The Main System b) Connection of the Mesh Holder to the air supply C) Loading of the Mesh Holder on to the Spacer D) Operation of the Control Unit E) Venting of the Spacer to Atmosphere F) Opening of the Air Inlet Valve G) Disconnection of the Spacer

5.3.3 Testing Criteria and Deposition Profiles

The delivery system described on page 184 was connected to an MSLI to evaluate the aerosol from the 100mg vials of MS. The samples were loaded and fired as described on page 181, and analysed using HPLC as outlined on page 98. The mass of MS in each stage was

glassware and diluting appropriately so that each test solution fell within the concentration range of the standard curve.

Pressure drop experiments across the device and sonic flow measurements were carried out using the set up procedures described earlier (see section 1.6 Aerosol Testing and Characterisation page 63). The pressure drop across the device was measured using a differential pressure transducer and was found to be 1.8kPa. Since the EP 1999 supplement recommended 4kPa pressure drop could not be achieved, all testing was carried out at 100 L min^{-1}. Sonic flow measurements were carried out using an absolute pressure transducer.

In order to evaluate the device and establish operating conditions, the following test criteria were employed:

a) Test flow rate: 100 L min^{-1}, shot time: 2.40secs
b) Volume of air drawn through the spacer was chosen to be 3, 4, 8, and 12L intended to mimic equivalent patient inhalations.
c) The settling time of the aerosolised cloud, before sampling into the MSLI, was chosen to be 20 and / or 30 seconds.
d) The effect of repeated inhalations from the same vial was determined by leaving the MSLI in place and allowing a ten second gap between each firing.
e) Dose uniformity experiments from the device were carried out using the set up described in section 1.7.1.

Results

Two vials of MS were used for each of the conditions specified on page 184, and the reported masses below are the sum totals. Table 70 below, shows the summary results of the tests described. Please refer to Appendix 6: Detailed tables for the HPLC analysis of MS- MSLI Results, page 261

Volume of Air Drawn Through Spacer	Equivalent patient Inhalations	Settling Time (secs)	Shot Time (sec)	Mass of MS loaded (mg)	Mass of MS delivered into spacer	Mass of MS delivered (% of loaded)
3L	One	30	1.80	136.1	119.8mg	88.0%
4L	One	30	2.40	179.1	150.3mg	83.9%
8L	Two	30	2x2.40	169.2	132.5mg	78.3%
12L	Three	30	3x2.40	162.0	133.1mg	82.2%
3L	One	20	1.80	129.7	107.9mg	83.2%
4L	One	20	2.40	113.5	94.0mg	82.8%
8L	Two	20	2x2.40	152.0	124.9mg	82.2%

Table 70: Summary of mass of MS loaded and delivered into the SAPL inhalation system.

Results represent the accumulative masses of two 100mg vials.

Table 71, page 186 below, shows the summary results for the emitted dose and fine particle fraction data obtained by MSLI analysis of the tests described on page184. Please refer to Appendix 13: MS Testing and Stability Study Raw HPLC Data, page 270.

Volume of Air Drawn Through Spacer	Equivalent patient Inhalations	Settling Time (secs)	ED (mg)	ED as a % of MS fired	FPD (mg)	FPD as a % of total amount	FPF (%)
3L	One	30	59.4	49.6	25.0	20.9	42.1
4L	One	30	55.3	36.8	46.7	31.0	84.3
8L	Two	30	60.6	45.7	45.5	34.3	75.1
12L	Three	30	62.4	46.9	49.9	37.5	80.0
3L	One	20	42.7	55.4	34.2	23.7	69.4
4L	One	20	55.4	51.3	46.1	42.7	83.2
8L	Two	20	51.1	54.3	41.5	44.2	81.2

Table 71: Summary of emitted dose and fine particle fraction data obtained on the SAPL inhalation system by MSLI analysis

Table 72, below, shows the summary results of the tests described above. Please refer to Appendix 13: MS Testing and Stability Study Raw HPLC Data, page 270

Volume of Air Drawn Through Spacer	Settling Time (sec)	Mass of MS Loaded (mg)	Mass of MS Delivered (mg)	Mass of MS Collected in DUSA (mg)	Mass Collected as a % of Delivered
4L	30	89.3	77.7	32.7	42
4L	30	87.1	75.8	33.9	45
4L	30	83.8	73.7	31.7	43
4L	30	83.8	64.7	35.2	54
4L	30	93.8	80.6	31.9	40
4L	30	88.0	70.5	28.3	40
4L	30	84.2	67.6	27.0	40
4L	30	88.3	74.3	27.8	37
4L	30	86.5	69.5	28.0	40
		Mean 87.2 SD 3.21	72.7 5.07	30.7 3.00	42.0 4.98

Table 72: Dose uniformity results of MS delivered at 100Lmin^{-1} into the SAPL inhalation system from individual 100mg vials.

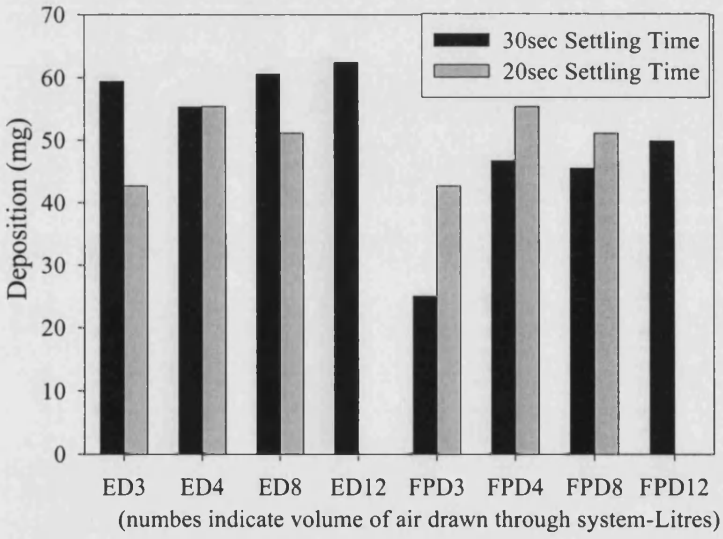

In-Vitro Aerosol Characterisation of MS

Figure 68: Emitted dose and fine particle dose of MS at 100Lmin^{-1} with varying volume of air drawn through the SAPL inhalation system at 20 and 30second aerosol settling time.

Discussion

Results seem to show that ED is independent of flow rate; this is evident when comparing the ED at 8L with that at 12L. FPD also seems to be independent of the number of inhalations, that is to say that 4L of air through the system seems to give comparable FPD results as that at 12L. FPD values at 20 second settling rate seem to be comparably higher than those at 30 seconds. This is not unexpected since more powder should settle and deposit on the spacer at the longer settling time. However, for clinical trial purposes, the 30second settling rate was chosen because of the number of operations that need to be carried out between firing of the vial and the patient inhalation is more easily managed. The inhalation system is intended to be high-dose unit for pulmonary delivery of SAPL, thus its rather large size and cumbersome control levers. The system utilises compressed air and comprises of an elobrate network of pipes and valves in order to produce the necessary deaggregating power needed to delivery SAPL. With regards to the actual dose delivered (~100mg), it is by far the greatest amount of powder administered to date from any DPI. Standard high-dose formulations, such as inhaled corticosteroids for chronic obstructive pulmonary disease only utilise about 1mg of drug per day as shown in the studies carried out by Culpitt *et al* (1999). The effect of high-dose fluticasone propionate and budesonide on lung function and asthma exacerbations in patients with severe asthma was investigated by Heinig *et al* (1999). This study utilised the Diskhaler® and Turbuhaler® to deliver 2mg of material to the lungs.

5.3.4 Stability Studies of MS

Samples of micronised MS previously filled by Penn Pharmaceuticals (Tredegar, Gwent, UK) as described on page 182 were stored in incubators at 25°C and 40%RH. Some samples were removed at various time intervals (see Table 77, page190 for details) and deposition studies using the MSLI were carried out to ascertain the effects of storage on aerosolisation.

Table 73, Table 74, Table 75, and Table 76 show the summary data obtained by MSLI analysis. Please refer to Appendix 13: MS Testing and Stability Study Raw HPLC Data, page 270 for the full results

	Tht	Stg1	Stg2	Stg3	Stg4	Stg5
PG Conc. (µg/ml)	8.92	7.74	5.09	9.98	15.0	14.6
DPPC Conc. (µg/ml)	21.5	13.7	37.5	34.5	40.8	41.8
Dilution Factor	100	100	100	400	500	100
PG Deposited (mg)	0.89	0.77	0.51	3.99	7.51	1.46
DPPC Deposited (mg)	2.15	1.37	3.75	13.8	20.4	4.14
MS Deposited (mg)	3.04	2.15	4.26	17.8	27.9	5.60

Table 73: Summary stability study (time point: 1 week) table of MSLI deposition data for MS (2x100mg vials) at 100Lmin^{-1}.

	Tht	Stg1	Stg2	Stg3	Stg4	Stg5
PG Conc. (µg/ml)	11.9	11.5	11.4	16.1	20.8	22.2
DPPC Conc. (µg/ml)	24.6	24.3	22.1	29.9	37.4	40.3
Dilution Factor	100	100	100	400	500	100
PG Deposited (mg)	1.18	1.14	1.13	6.40	10.4	2.22
DPPC Deposited (mg)	2.5	2.4	2.2	12.0	18.7	4.03
MS Deposited (mg)	3.65	3.57	3.35	18.4	29.1	6.25

Table 74: Summary stability study (time point: 2 week) table of MSLI deposition data for MS (2x100mg vials) at 100Lmin^{-1}.

	Tht	Stg1	Stg2	Stg3	Stg4	Stg5
PG Conc. (µg/ml)	13.4	9.45	19.1	30.1	18.0	11.5
DPPC Conc. (µg/ml)	31.3	22.0	44.7	70.2	42.1	26.7
Dilution Factor	50	50	50	100	200	50
PG Deposited (mg)	0.7	0.5	1.0	3.0	3.6	0.6
DPPC Deposited (mg)	1.6	1.1	2.2	7.0	8.4	1.34
MS Deposited (mg)	2.2	1.6	3.2	10.0	12.0	1.9

Table 75: Summary stability study (time point: 1 month) table of MSLI deposition data for MS (1x100mg vials) at 100Lmin^{-1}.

	Tht	Stg1	Stg2	Stg3	Stg4	Stg5
PG Conc. (µg/ml)	13.4	9.45	19.1	37.2	24.7	11.5
DPPC Conc. (µg/ml)	32.9	23.9	48.4	91.8	58.9	28.3
Dilution Factor	50	50	50	100	200	50
PG Deposited (mg)	0.67	0.47	0.96	3.70	4.92	0.60
DPPC Deposited (mg)	1.64	1.20	2.42	9.18	11.8	1.41
MS Deposited (mg)	2.31	1.67	3.37	12.9	16.7	1.99

Table 76: Summary stability study (time point: 3 months) table of MSLI deposition data for MS (1x100mg vials) at 100Lmin^{-1}.

Table 77, below, shows the summary results for the emitted dose and fine particle fraction data obtained by MSLI analysis.

Stability Time Point (wks)	Volume of Air Drawn Through Spacer	No. of Vials Fired	Equivalent patient Inhalations	Pause Between Inhalation (sec)	Settling Time (sec)	Shot Time (sec)	ED (mg)	FPD (mg)	FPF (%)
1Wk	8L	Two	Two	10	20	2x2.	60.7	51.3	84.5
2Wks	8L	Two	Two	10	20	2x2.	57.2	47.4	82.9
4Wks	4L	One	One	None	30	2.4	39.0	31.6	81.1
12Wks	4L	One	One	None	30	2.4	24.5	17.4	70.9

Table 77: Summary table of emitted dose, fine particle dose, and fine particle fraction data obtained for stability samples of MS by MSLI analysis (100 Lmin^{-1}) at various time points.

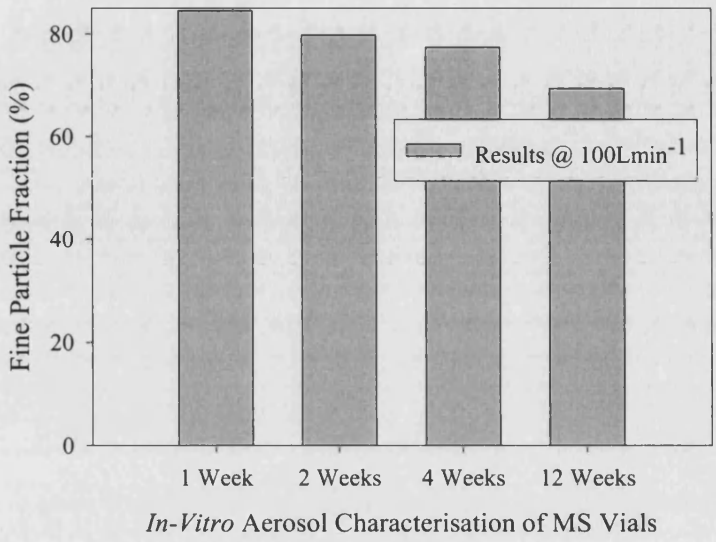

Figure 69: Graph showing the change in fine particle fraction of MS stability samples, stored at 25°C and 40%RH over a period of twelve weeks.

Results were obtained using the MSLI at 100Lmin^{-1} with varying volume of air drawn through the SAPL inhalation system at 20 and 30 seconds aerosol settling time.

5.3.4.1 Moisture Uptake of SAPL

The various SAPL powders were analysed in order to attain their moisture content using Karl-Fischer (KF) Analysis. In addition, the relative humidity (RH) conditions, see Table 78, page 192, were prepared in desiccators and samples of each powder were placed into the desiccators and their moisture uptake was monitored over a period of four weeks. The saturated salt solutions, shown below in Table 78, were prepared by adding an excess of the solute into distilled water.

Saturated Salt Solution	Moisture Range at 25°C
Potassium Hydroxide	4-10%
Calcium Chloride ($CaCl_2.6H_2O$)	31-35%
Ammonium Nitrate	62-67%

Table 78: Table showing the saturated salt solutions and corresponding moisture ranges at room temperature.

Method

The KF method for moisture determination has been previously described on page 116.

Results

	FDS, Pre Micronisation	FDS , Post Micronisation	LFDS, Pre Micronisation	LFDS, Post Micronisation
% Moisture Content	3.40 (±0.11)	5.20 (±0.14)	3.25 (±0.04)	1.43 (±0.05)
% Moisture After Treatment With P_2O_5	2.80 (±0.16)	3.90 (±0.09)	2.04 (±0.19)	1.21 (±0.24)

Table 79 : Table showing the moisture content for various SAPL powders stored under various conditions, n=5.

Table 79 shows the effect of micronisation on the moisture contents of various SAPL powders. It can be seen that after treament phosphorous pentoxide, the moisture content is reduced. P_2O_5 absorbs water to produce phosphoric acid and physically changes from a white powder to a waxy material. Table 80 and Table 81, page 194, shows the moisture uptake of SAPL over a period of 4 weeks. During the time in which the moisture measurements were made, the temperature and relative humidity of the laboratory were measured. The temperature variation was 20-33°C whereas the RH variation was 41-68%.

Time Point (Hrs / Days)	Sample ID	Storage Condition	% Moisture Content Average (n=5)
Zero	FDS	As Received	3.62 (±0.0680)
24hrs/1Day	FDS	KOH	4.62 (±0.320)
24hrs/1Day	FDS	$CaCl_2$	6.55 (±0.182)
24hrs/1Day	FDS	NH_4NO_3	7.26 (±0.377)
48hrs/2Days	FDS	KOH	6.14 (±0.203)
48hrs/2Days	FDS	$CaCl_2$	6.73 (±0.372)
48hrs/2Days	FDS	NH_4NO_3	7.76 (±0.425)
72hrs/3Days	FDS	KOH	6.18 (±0.430)
72hrs/3Days	FDS	$CaCl_2$	6.82 (±0.449)
72hrs/3Days	FDS	NH_4NO_3	8.45 (±3.29)
1 Week	FDS	KOH	6.42 (±0.371)
1 Week	FDS	$CaCl_2$	8.47 (±0.406)
1 Week	FDS	NH_4NO_3	11.22 (±0.782)
2 Weeks	FDS	KOH	7.66 (±0.405)
2 Weeks	FDS	$CaCl_2$	10.3 (±0.403)
2 Weeks	FDS	NH_4NO_3	14.1 (±0.384)
4 Weeks	FDS	KOH	7.63 (±0.261)
4 Weeks	FDS	$CaCl_2$	12.4 (±0.401)
4 Weeks	FDS	NH_4NO_3	16.1 (±0.651)

Table 80: Table showing the moisture uptake of FDS (n=3).

The moisture content values obtained for FDS were plotted against time, and are shown below.

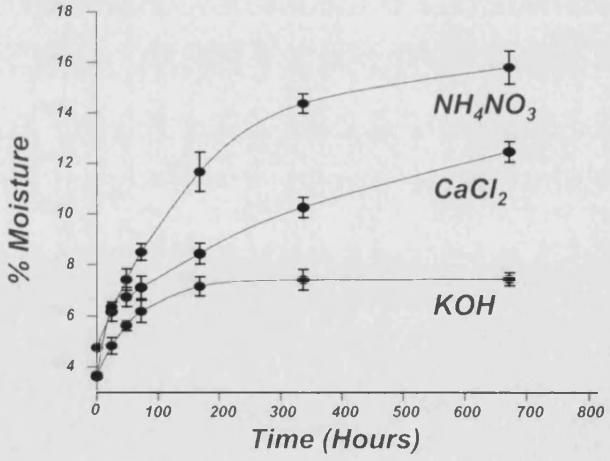

Figure 70: Moisture-uptake versus time for FDS under various storage conditions.

Time Point (Hrs /Days)	Sample ID	Storage Condition	% Moisture Content Average (n=5)
Zero	LFDS	As Received	5.87 (±0.392)
24hrs/1Day	LFDS	KOH	6.05 (±0.416)
24hrs/1Day	LFDS	$CaCl_2$	9.03 (±0.598)
24hrs/1Day	LFDS	NH_4NO_3	14.2 (±0.745)
48hrs/2Days	LFDS	KOH	6.79 (±0.526)
48hrs/2Days	LFDS	$CaCl_2$	10.8 (±0.315)
48hrs/2Days	LFDS	NH_4NO_3	18.7 (±0.793)
72hrs/3Days	LFDS	KOH	7.37 (±0.365)
72hrs/3Days	LFDS	$CaCl_2$	12.9 (±0.382)
72hrs/3Days	LFDS	NH_4NO_3	20.0 (±0.702)
1 Week	LFDS	KOH	7.81 (±0.483)
1 Week	LFDS	$CaCl_2$	13.3 (±0.360)
1 Week	LFDS	NH_4NO_3	20.5 (±0.853)
2 Weeks	LFDS	KOH	8.31 (±0.488)
2 Weeks	LFDS	$CaCl_2$	13.1 (±0.500)
2 Weeks	LFDS	NH_4NO_3	23.1 (±0.815)
4 weeks	LFDS	KOH	8.40 (±0.266)
4 weeks	LFDS	$CaCl_2$	16.1 (±0.906)
4 weeks	LFDS	NH_4NO_3	23.4 (±0.461)

Table 81: Table showing the moisture uptake of LFDS, n=3.

The moisture content values obtained for LFDS were plotted against time, and are shown below.

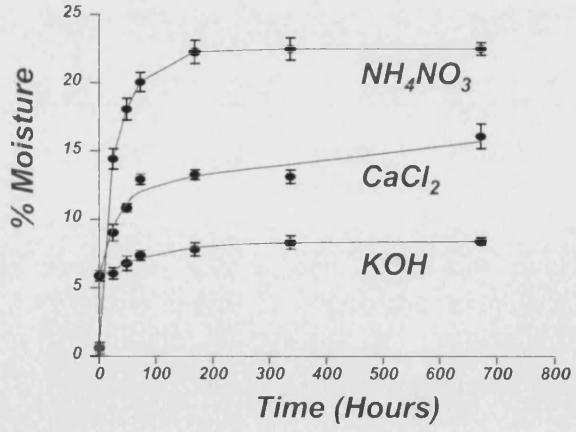

Figure 71: Moisture-uptake versus time for LFDS under various storage conditions.

5.3.4.2 Effect of Moisture Uptake on the Ability of SAPL to Reduce the Surface Tension of Water

Surface tension (ST) of a liquid is often defined as the force acting at right angles to any line of unit length on the liquid surface (Shaw 1996). It can also be defined as the work required to increase the area of a surface isothermally and reversibly by unit amount. There is no fundamental difference between the terms surface and interface, so far as to say that a boundary between two surfaces (one being gaseous) is called a surface, whilst the boundary between two non-gaseous phases is an interface. At the interface between two liquids there is again an imbalance of intermolecular forces but of a lesser magnitude. Interfacial tensions usually lie between the individual surface tensions of the liquids in question.

ST experiments on FDS and LFDS were carried out to ascertain the effect of moisture on the ability of the material to reduce the ST of water. These were not direct measurements of ST, but rather the change in ST of water when specific amount of surfactant was added to it. Prior to the experiments, materials were stored under varying relative humidity conditions for a period of four weeks, as described in the previous section. The conditions were: saturated potassium hydroxide solution: 4-10% RH, saturated calcium chloride solution 31-35% RH, and saturated ammonium nitrate solution 62-67% RH. The moisture content of the samples were as follows:

a) FDS: 7.63% (KOH), 12.4% ($CaCl_2$), and 16.1% (NH_4NO_3).

b) LFDS: 8.40% (KOH), 16.1% ($CaCl_2$), and 23.4% (NH_4NO_3).

The ability of these materials to reduce the ST of water were compared against:

(a) A fresh sample FDS: Obtained from a sterilised, 100mg crimped vial, as described in the section entitled Artificially Derived Surfactants.

(b) A fresh sample of LFDS: Obtained by the method described in the section entitled Fluorescent labelling of FDS.

Equipment

10L capacity water tank
Heating unit (Grant Instruments, Cambridge, UK) with thermostat control
Ultra-pure (tripled distilled) water (Millipore Ltd.,)
Tensiometer (constructed in-house) with a MIMA 9000 control unit (Coventry, UK)
An electronic balance, mounted onto the tensiometer in an inverted manner, with a small hook protruding from its lowest point to which a small filter paper (1 x 3cm, Whatman No 1) was attached to record the 'pull' from the surface of the water.
A small metal basket and 1, 10, 50 and 100mg aluminium weights.
Wide-bottomed glass flasks, cleaned using chromic acid, rinsed with tap water, distilled water, and finally with ultra-pure water.

5.4.3.3 Experiment to Prove the Linear Response of the Tensiometer

The wide-bottomed glass flasks were immersed into the water tank (heated to ~37°C) and filled with ultra-pure water and allowed to equilibrate. The small basket was attached to the hook protruding from the balance, and the reading (mN/m) was adjusted to zero. The aluminium weights (1, 10, 50 and 100mg) were placed in turn into the basket and the reading on the balance was recorded. The results obtained are shown below: -

Aluminium Calibration Wt (mg)	Reading on Tensiometer (mN/m)
1	0.6
10	5.4
50	25.7
100	52.1

Table 82: Table showing the aluminium calibration weights and corresponding tensiometer reading.

The readings above were used to construct the graph below.

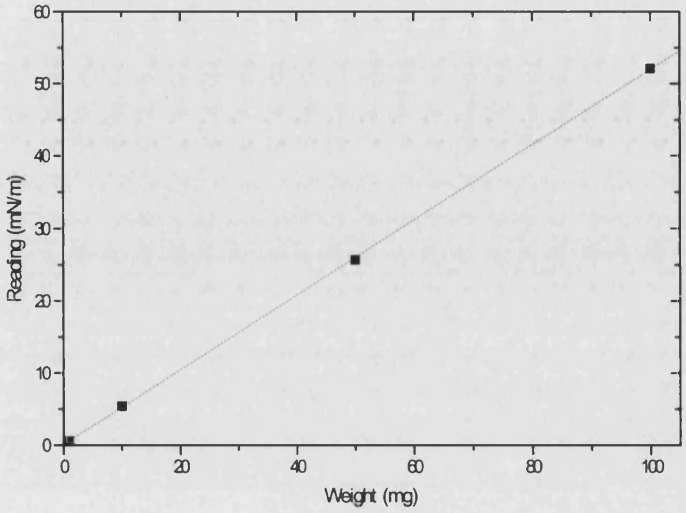

Figure 72: Graph showing the relationship between tensiometer reading and the aluminium calibration weights.

Slope	S.D (Slope)	Intercept	S.D. (Intercept)	Correlation Coefficient
0.519	0.00337	0.06038	0.18889	0.99996

Table 83: Table summarising the linear regression data obtained form the calibration plot of tensiometer reading versus aluminium calibration weights.

Method

The wide-bottomed glass flasks were immersed into the water tank (heated to ~37°C) and filled with ultra-pure water and allowed to equilibrate. The filter paper at the end of the hook was lowered so that it just broke the surface of the water in the flask. The filter paper was allowed to wet completely and the reading on the balance display was adjusted to zero. About 5mg of test material was introduced to the surface using a micro-spatula. The change in ST was recorded every minute over a period of 25minutes. The drift on the instrument was measured for a period of 25minutes, without any addition of surfactant and the value obtained was subtracted from subsequent readings.

Results

All the materials tested were seen to spread instantly over the surface of the water as soon as it was introduced. There was a sudden decrease in ST both with LFDS and FDS and equilibrium was reached after approximately 60seconds. The results obtained are shown graphically below

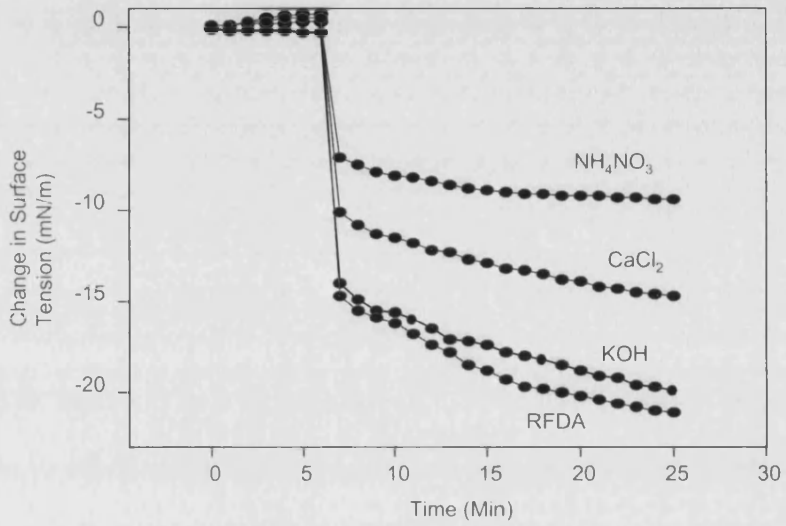

Figure 73: Graph showing the change in surface tension versus time for fresh FDS and FDS stored under at various humidity conditions.

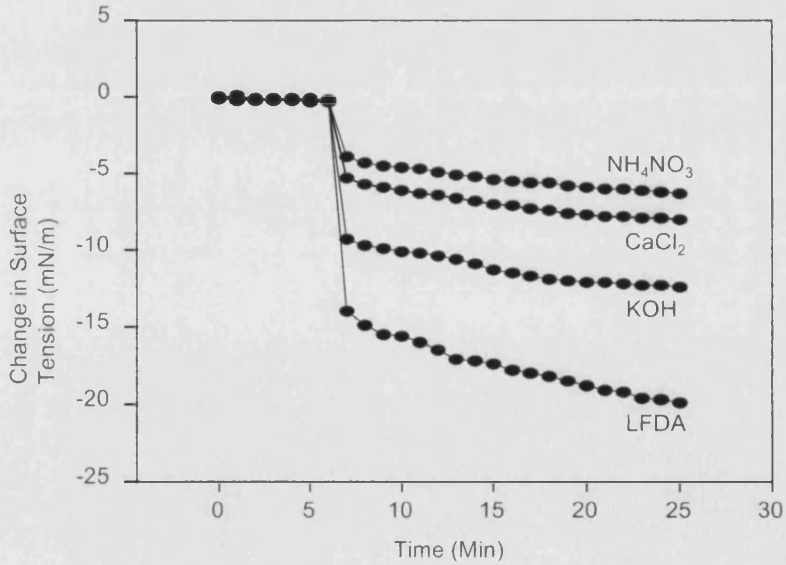

Figure 74: Graph showing the change in surface tension versus time for fresh LFDS and LFDS stored at various humidity conditions

5.3.5 General Discussion

A novel inhalation system, intended for use in the clinic, for the delivery of MS has been presented. The system has been tested to some extent and the scheduled programme is set to continue beyond the scope of this report. Findings have shown that the device performs significantly better than the Miat Monohaler and capsule systems outlined on page 170. To be more specific, the FPF is increased from 11.3% (for the capsule-based system) to between 70-85% for the present system. The FPD for the present system is between 45-50mg for two accumulative shots of 100mg of MS.

From the results, the following conclusions can also be drawn:

a) The total volume of air drawn through the delivery system as a result of multiple inhalations has a small effect on the mass of MS, but no significant effect on the FPD.

b) The volume of initial inhalation does significantly affect the FPD, with higher FPDs achieved for 4L inhalations than for 3L inhalations.

c) Settling time (i.e. the time between aerosolisation into the spacer and actual inhalation) does not have a significant effect on the FPD.

d) Mass of MS loaded directly affects the FPD, thus, higher masses leads to higher FPD but NOT necessarily higher FPF. This point is well illustrated in the stability study results, where the difference in FPF between 100mg and 200mg of delivered drug is marginal.

DUSA results for ten consecutive shots of MS into the inhalation system yielded values 28.0-35.2mg being collected in the collection vessel. The target dose for patients in the clinical trials is ~100mg (range 85-100mg) of SAPL in the peripheral and deep lungs. This corresponds to four vials of SAPL being administered to the patient over the course of the study. This figure of 100mg total dose is not an arbitrary one and is based on the dose of SAPL currently used for the treatment of nRDS where a 100mg of the material is nebulised to the infant over a period of 48-72hrs. Taking into consideration the relative larger size of the adult human lung and the fact that a powder formulation is used as opposed a nebulised liquid, then it seems a sensible to go with a 100mg total dose. The problem in deciding this final

dose was that there was no previous guideline or reference, either from literature or from the any governing body. Kurashima (1991) who carried out the first exogenous surfactant pilot study used a dose of 10mg/ml of Exosurf®, but had no idea of the volume to administer. Thus, the most sensible policy seemed to be to base our final dose on the existing SAPL product currently on the market.

Stability study programme is on-going and further time points at 6 months and 1 year are needed, both for use in the clinic and ultimately in deciding a shelf life for the final product. Although there appears to be a decrease of ~10% in FPF over the 3 month period, further data is required before comments can be made on the effect of the storage conditions on the fine particle properties of the powder.

Moisture determination experiments show that both labelled and raw SAPL are hygroscopic and pick up mositure progressively. However, in both cases the moisture content seems to reach a peak value after about two to four weeks. Upon closer inspection of the tables and graphs, it can be seen that labelled SAPL is slightly more hygroscopic than the raw material. The labelled SAPL seems to reach a peak moisture content of 23% compared with 16% for the raw material, the difference may be due to the labelling procedure (see page 121). Although SAPL is hygroscopic, the process is rate dependant and the material may be handled without too much due concern as long as it is not exposed to the environment for long periods. Surface tension experiments show that tension-lowering properties of FDS and LFDS are diminished with increasing moisture content of the sample. Furthermore, LFDS appears to be less effective in reducing ST than FDS, probably a side effect of the labelling process.

Chapter 6

Deposition Studies of Radiolabelled SAPL

6.0 Deposition Studies of Radiolabelled SAPL

Chemically radiolabelled PG (labelled with Tritium, ^{3}H) and DPPC (labelled with ^{14}C), two constituents of SAPL (3:7% v/v ratio) were provided by Amersham, International, Somerset, UK. These were used by Hills and Chen (1998) in *ex-vivo* experiments using bronchial epithelium (derived from porcine lungs) to prove the hypotheses that :

a) Exogenous surfactant can directly bind various tissue surfaces where the adsorption of endigenous surfactant had been demonstrated.
b) PG has a physiological role in promoting DPPC adsorption.

Porcine bronchial epithelium was chosen for its relevance to asthma and implication to RDS at the alveolar level. Refer to section 1.3 Surfactant Therapy, page 32

Using the materials from the same radiolabelled batch, the following set of experiments were intended to demonstrated that:

a) The two constituents could be mixed in solution, at the same ratio as in SAPL, and nebulised into an MSLI.
b) An *in-vitro* deposition of the materials could be quantified.
c) Deposition profiles of the chemically labelled SAPL could be used to validate the fluorescent labelling process employed in the detection of FDS, see page121.

6.1 Construction of the Calibration Curve

^{14}C and ^{3}H reference standards (Amersham International, UK) were used to produce two six-point calibration curves. To each of the six standards, varying quantities of the quenching agent CCl_4 and a small amount of scintillant was added. The quantity of the quenching agent varied from zero to 100µl in the six standards, hence a ratio of quenching agent to scintillant was established for each standard. The scintillant, Optipha 'Safe' (Wallac Scintillation Products, Milton Keynes, UK), was a multi-purpose cocktail of ethyl substituted benzenes, and its function was to convert the kinetic energy of nuclear particles into light photons. Samples were placed into plastic, screw top vials and placed into a β-Counter (Rack Beta Scintillation Counter, LKB Wallac Ltd, Finland) and their activity determined as disintergrations per minute (DPM). Since ^{14}C counting window overlapped with the ^{3}H window, it was necessary to establish the degree of overlap and the counting efficiency of the β-Counter. Therefore, three different types of measurements were made by the β-Counter:

a) ^{14}C alone in the Carbon window.

b) ^{3}H alone in the hydrogen window

c) ^{14}C in the ^{3}H window.

The counting efficiency of the β-counter was determined by measuring each standard set using the above combinations to produce six sets of efficiency graphs.

Since ^{14}C is a β-emitter, the ε_{max}= 0.16MeV, but in practice ^{14}C decays in the following way:

$^{14}C \longrightarrow 14N + \beta^{\ominus} + N$ (Neutrino). Therefore, the energy is not due to the β-ion alone. Since $\beta^{\ominus}$ has an energy of <0.10MeV, the counting window was set to 0.16Mev. A summary of the counting experiments are outlined below.

Results

Table 84, page203 shows a summary of the results obtained for the ^{3}H reference standard during the counting experiments.

Std No.	Ratio (Scint / Quench.)	Win No.	Counts per min	Counting Efficiency	Win No.	Counts Per Min	Counting Efficiency
1	0.447	1	2198	5.58%	2	157	0.40%
2	0.611	1	3729	9.51%	2	285	0.73%
3	0.733	1	5573	14.21%	2	402	1.02%
4	0.952	1	8417	21.46%	2	512	1.31%
5	1.207	1	11510	29.34%	2	809	2.06%
6	1.363	1	13566	34.59%	2	1170	2.98%

Table 84: Table showing ratio of scintillant to quenching agent, Counts per minute, and counting efficiency for the ^{3}H in window 1 (left) and window 2 (right) for the Rack Beta Scintillation Counter, LKB Wallac Ltd, Finland.

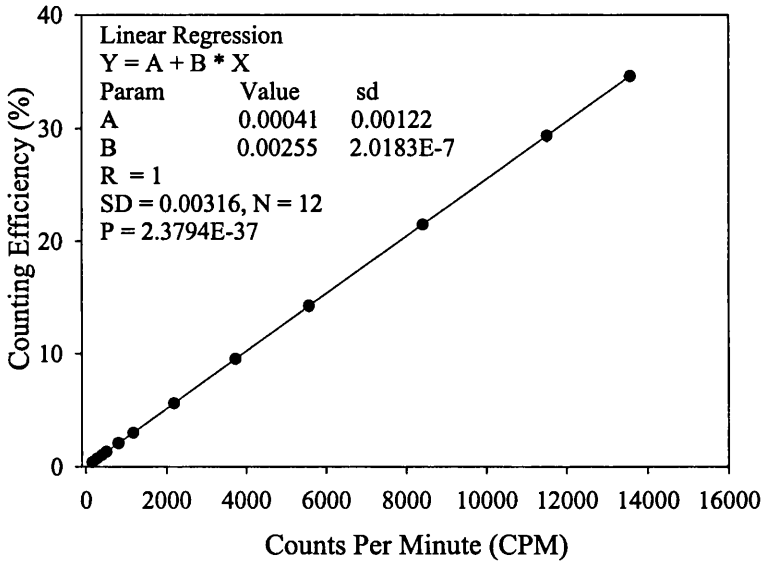

Figure 75: Graph Showing Counts per minute Vs Counting Efficiency for the ^{3}H reference standard.

Table 85, page 204, shows a summary of the results obtained for the ^{14}C reference standard during the counting experiments.

Std No.	Ratio (Scint / Quench.)	Win No.	Counts per min	Counting Efficiency	Win No.	Counts Per Min	Counting Efficiency
1	0.482	1	9596	55.28(%)	2	4295	24.74(%)
2	0.641	1	8803	50.71(%)	2	6333	36.48(%)
3	0.789	1	7566	43.58(%)	2	8670	49.94(%)
4	1.046	1	5628	32.42(%)	2	10907	62.83(%)
5	1.252	1	4553	26.23(%)	2	12138	69.92(%)
6	1.497	1	3616	20.83(%)	2	12985	74.80(%)

Table 85: Table showing ratio of scintillant to quenching, Count per minute, and counting efficiency for ^{14}C in window 1 (left) and window 2 (right) for the Rack Beta Scintillation Counter, LKB Wallac Ltd, Finland.

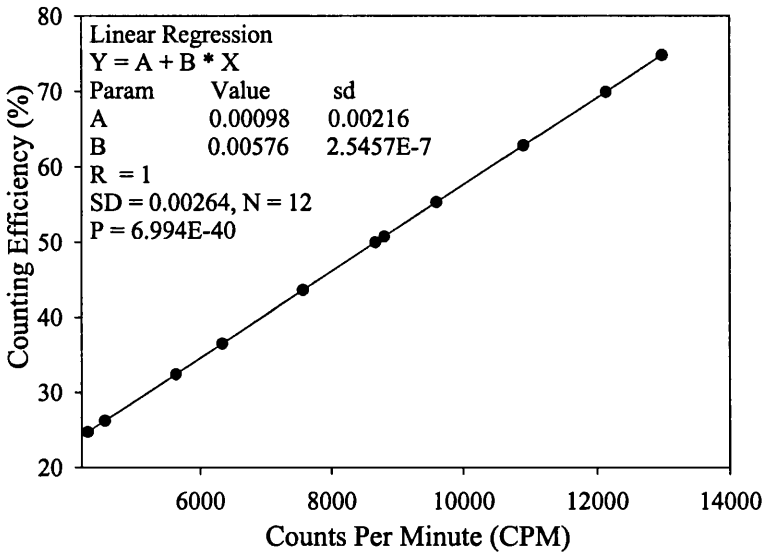

Figure 76: Graph Showing Counts per minute Vs Counting Efficiency for ^{14}C reference standard.

Statistics

The t-test at p=0.005 revealed no significant differences between the slopes of the two standard sets (t=0.000608, p=0.500).

Having obtained the calibration graphs for both isotopes and shown that the count range is linear, the β-Counter was reprogrammed with the counting efficiencies and was ready to read unknown samples. The sample readings were displayed in DPM since CPM to DPM conversion requires count efficiency ratings.

6.2 MSLI Analysis of Radiolabelled SAPL

Practical details of constructing a calibration curve for radio-detection of SAPL and the reasons for doing the experiment have been discussed in the previous two sections. This section outlines the results of the MSLI analysis of SAPL.

Materials & Equipment

L-3-Phosphatidy-DL-glycerol-2-[9,10(n)-^{3}H]Stearoyl-1-palmitoyl (PG) in Toluene : Ethanol (1:1, v/v)- Source (Amersham International, UK).
Total Activity= 5 mCi, Sample volume= 5ml, Specific Activity= 6.14 TBq/ml or 166 Ci/mmol, Radioactive concentration= 37 MBq/ml or 1mCi/ml.
L-3-Phosphatidylcholine, 1,2-di[1-^{14}C]Palmitoyl (DPPC) in Toluene : Ethanol (1:1, v/v)-)-Source (Amersham International, UK).
Total Activity= 10μCi, Sample Volume= 0.5ml, Specific Activity= 4.22 Gbq/mmol, or 5.72 MBq/mg.
Absolute ethanol (HPLC grade, Fisons, UK).
Compressor, Nebupump™ (Carri-Med Ltd, Dorking, UK), maximum output: 6.4L min^{-1}.
Nebuliser: Cirrus™ , maximum output: 3.8L min^{-1}.
Pump: Gast 1023, Rotor Vein, Oil-less, (Bucks., UK).
Rack Beta Scintillation Counter (LKB Wallac Ltd, Finland).
5-Stage Liquid Impinger, Stage 5 filter: Type A/E glass fibre, 76mm diameter (Gelman Sciences, Mich., USA).
Digital timing unit, Mass flow meter (Hastings Mass Flow Meter, HFM 201, Teledyne Brown Engineering, Hastings Instruments, VA, USA).

50µl and 1ml Gilson pipettes with disposable tips.

Dilutions

PG: 5000µci / 5ml original activity, therefore, 1000µci in 1ml. A 1ml of the PG stock was taken and pipetted into a 200ml volumetric with absolute ethanol to give a solution with a final activity of 5µci/ml. No further dilutions were necessary.

DPPC: 10µci total activity per 0.5ml. A 50µl aliquot was taken pipetted into 10ml volumetric (1:400 dilution) to give a solution with a final activity of 1.25 µci/10ml (0.125µci/ml). No further dilutions were necessary.

Method

20ml of absolute ethanol was pipetted into each of the four stages of the MSLI and each stage stoppered. 2.1ml of radiolabelled DPPC and 0.9ml of radiolabelled PG were pipetted into the nebuliser chamber. Flow rate through the MSLI was set at 60L min^{-1} using the mass flow meter. The nebuliser was connected to the MSLI via an adaptor, as shown below. The compressor was connected to the bottom of the nebuliser via vacuum tubing. The timing unit was adjusted so that the by-pass switch was activated, which allowed the pump to work continuously. The pump was switched on and the compressor was activated and the solution was nebulised. It took 8 minutes for the chamber empty to dryness. Stage 5 of the MSLI was disconnected from stages 1 to 4 and the MSLI swirled gently to collect droplets that had impacted on the sides and then turned up side down to was the ceiling of the apparatus. Stoppers from the four stages were removed and each stage was emptied into 50ml volumetric. Each stage was further washed with absolute ethanol to recover as much of the nebulised material as possible and the solutions were made up to volume using absolute ethanol. The metal throat and silicone adaptor were washed into a 50ml volumetric flask and made up to volume with absolute ethanol. The glass fibre filter from stage 5 was placed into a glass crystallising basin and washed with 20ml of absolute ethanol. The solution was poured into a 50ml volumetric and made up to volume with further absolute ethanol. The residual

liquid left in the nebuliser was washed into a 50ml volumetric flask and made up to volume using absolute ethanol. A 1ml aliquot from each of the seven 50ml samples were taken and placed into separate, white, plastic, screw-top scintillation tubes. To each 1ml aliquot, 6ml of scintillant was added. The tubes were placed into the scintillation counter and counted for five minutes or 10,000 counts.

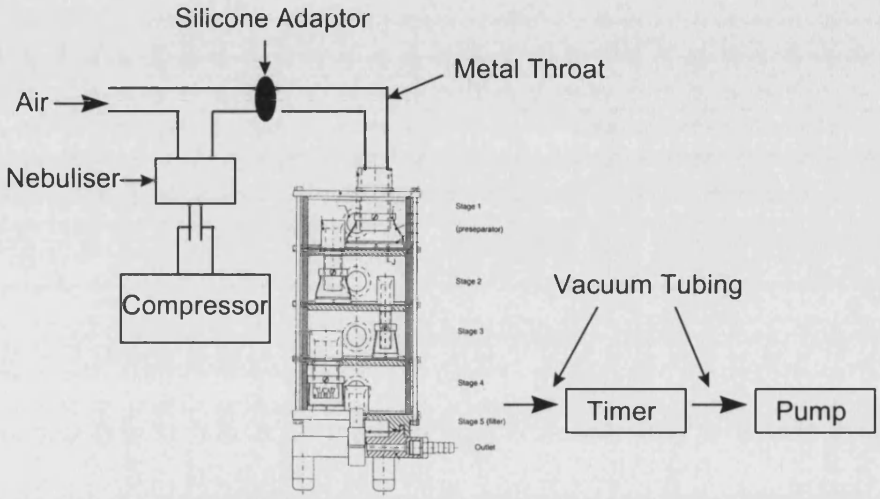

Figure 77: Schematic diagram showing the apparatus used in the deposition studies of radiolabelled SAPL.

Results

A total of five separate runs (n=5) were carried out with an additional dry-run using only absolute ethanol and scintillant as the final solution. The tables below show the distribution of PG and DPPC, respectively, within the various stages of the MSLI.

^{3}H (PG)							
Parameter	Cut-off Neb	Diameter T+A	13.0 Stg1	6.8 Stg2	3.1 Stg3	1.7 Stg4	0.0 Stg5
CPM		802 ±135	1340. ±111	1242 ±52	1832 ±128	3081 ±141	8938 ±373
Apparent DPM	43311 ±4673	1072 ±487	1792 ±402	1660 ±189	2450 ±461	4119 ±511	11950 ±1347
Corrected DPM	2165541 ±233654	53610 ±24339	89589 ±20076	83005 ±9447	122477 ±23045	205966 ±25559	597477 ±67326
% Recovery	65.3	1.6	2.7	2.5	3.7	6.2	18.0

Table 86: Distribution of radiolabelled PG within an MSLI at 60L min^{-1} flow rate, aerosolised from a Cirrus™ nebuliser using the Nebupump™ compressor operating at 6.4L min^{-1}.

Standard deviation values are also indicated, n=5

14C (DPPC)							
Parameter	Cut-off Neb	Diameter T+A	13.0 Stg1	6.8 Stg2	3.1 Stg3	1.7 Stg4	0.0 Stg5
CPM	3886 (±181)	136 (±15.2)	73.5 (±5.8)	74.3 (±11.8)	61.5 (±6.9)	163 (±26.8)	769 (±15.5)
Apparent DPM	11230 (±241)	394 (±55.1)	212 (±21.0)	215 (±42.5)	178 (±25.1)	470 (±96.8)	2222 (±56.1)
Corrected DPM	561488 (±12035)	19711 (±2755)	10621 (±1048)	10730 (±2125)	8887 (±1256)	23483 (±4841)	111091 (±2805)
% Recovery	75.3	2.6	1.4	1.4	1.2	3.1	14.9

Table 87: Distribution of radiolabelled DPPC within an MSLI at 60L min^{-1} flow rate, aerosolised from a Cirrus™ nebuliser using the Nebupump™ compressor operating at 6.4L min^{-1}.

The results from the previous two tables are summarised in Table 88, page 209.

Stage	^{3}H (PG) Deposition (%)	^{14}C (DPPC) Deposition (%)
Nebuliser	62.9	52.0
Throat + Adaptor	1.55	4.95
Stage 1	2.60	2.65
Stage 2	2.38	2.70
Stage 3	3.58	2.25
Stage 4	5.95	5.93
Stage 5	17.4	28.0
Total % Recovery	96.4	98.5
FPF(%)	26.9	36.2

Table 88: % Deposition of radiolabelled DPPC and PG within an MSLI at 60L min^{-1} flow rate, aerosolised from a Cirrus™ nebuliser using a Nebupump™ compressor operating at 6.4L min^{-1}.

The data in Table 88 can be represented graphically to produce Figure 78 below.

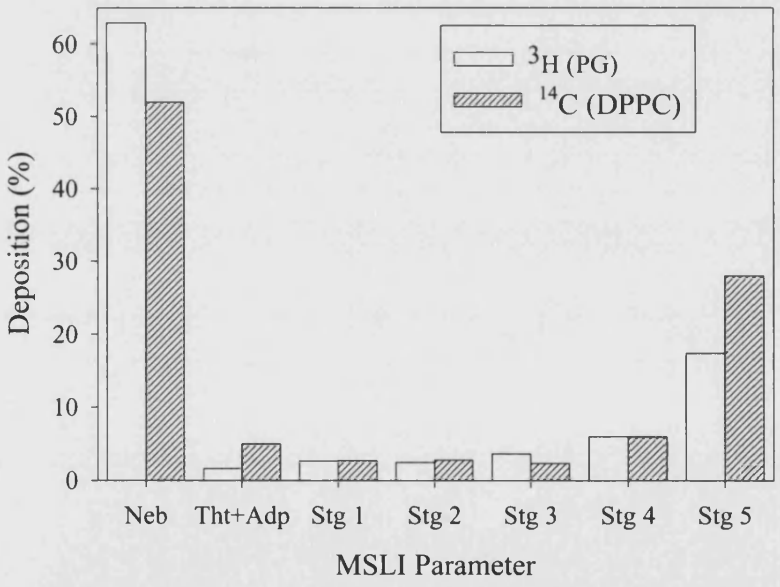

Figure 78: Deposition profiles of ^{3}H (PG) and ^{14}C (DPPC) in an MSLI at 60Lmin^{-1} flow rate, aerosolised from a Cirrus™ nebuliser using a Nebupump™ compressor operating at 6.4Lmin^{-1}.

Chapter 7

Dry Powder Fluidisation of MLFDS

6.3 General Discussion

The results from the Cirrus^{TM} nebuliser show that over 50% of the 3ml volume of radiolabelled material are not aerosolised and remain as residual (dead volume) material within the apparatus. For PG (labelled with tritium), only 37.1% of the material actually leaves the nebuliser whereas 48% of DPPC (labelled with Carbon-14) is expelled. The distribution of the two materials within the MSLI is comparable in stages 1,2, 3, and 4. However, distribution differences within the throat and stage 5 may be accountable to the fact that ^{14}C counting is only 35% efficient at best whereas ^{3}H counting is over 70% efficient. Fine particle fraction (FPF) expressed as a percentage is 26.9 and 36.2 for PG and DPPC respectively. Gilliard *et al* first carried out radiolabelling the phospholipids of lung surfactant in 1991. The procedure is now routinely used in the biochemistry field for pathway elucidation and adsorption studies (Perochon *et al* 1997).

7.0 Dry Powder Fluidisation of MLFDS

In this section a novel apparatus for delivering dry powder aerosols is described. The construction of the dry powder aerosol generator is and its subsequent coupling to a TSI to deliver MLFDS is discussed. No fludisation experiments were carried out on MS, as there were insufficient quantities of the drug available. The average particle size of MLFDS used during the deposition studies was 4.12μm, as determined by LALLS (see materials and general characterisations). The fluorimetric technique used to quantify the material has been previously described (see page 108).

7.1 Construction of a Novel Dry Powder Aerosol Generator (DPAG)

The design of the fluidisation chamber (see Figure 79, page 211) was based on that of Lord (1993).

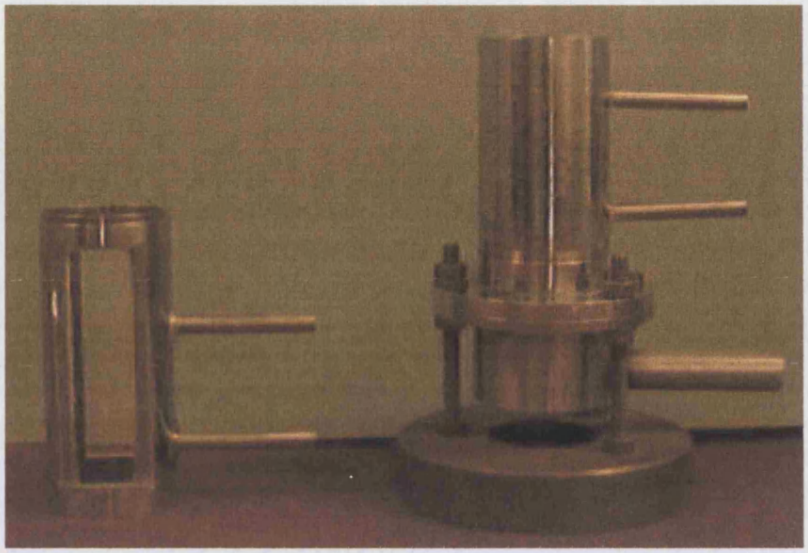

Figure 79: A Photograph of the dry powder aerosol generator (DPAG).

Initially, the chamber was constructed out of perspex (to enable visualisation of the powder bed) and later, stainless steel. The main body of the chamber consisted of a single unit (10cm x 4.2cm (OD) x 3.9cm (ID) tube, constructed from solid rods of perspex or stainless, bored and milled to the dimensions stated. On each side of the tube, a rectangular (10cm x 2.9cm) window, made of optically pure and homogenous glass (type: BK7, thickness 4mm, flatness $\lambda/4$, parallelity 15seconds of Arc) was glued on. Sintered glass discs (40mm (diameter) x 2.95mm (thickness)) with varying porosities of 0 to 5 (Aimer products, Enfield, UK), stainless steel discs, and brass were all used as the air distributors. A filter paper (Whatman No1, Maidstone, UK) was placed on top of the sintered glass disc during fluidisation to stop powder penetrating and blocking the distributor pores. To make the system more efficient (in terms of being less prone to air leakage), rubber o-rings were placed on top and bottom of the sintered glass / brass. The flanges on both the top and bottom half of the fluidisation apparatus, were fitted with screws to allow the operator to vary the tightness of the fit between the fluidisation chamber and the plenum and to ensure that air did not leak though the side walls of the distributor. The plenum of the apparatus was constructed of stainless steel and allowed air (supplied from a compressor pump, model 5KH10GGR28AS, General Electric, USA) to pass into the column. The flow rate was controlled by a needle valve placed on the tubing between the pump and the plenum inlet. The flow rate was monitored using a flow meter (type RS3,

'Meterate' flow tube GPE Ltd., Herts., UK), placed between the pump and the plenum. The whole apparatus was mounted on threaded metal studs (7cm) and supported by bolts and washers, allowing the height of the apparatus to be adjusted. To give the apparatus robustness, the metal threads were drilled into a metal base support (10cm (diameter) x 2.2 cm height x 1kg weight). A small spirit level was used to ensure that chamber was horizontal, prior to experiment commencement. The DPAG was connected to a TSI, as shown in Figure 80, this set-up was used in the deposition studies. Please refer to Appendix 10: Dimensions of the DPAG, page 263.

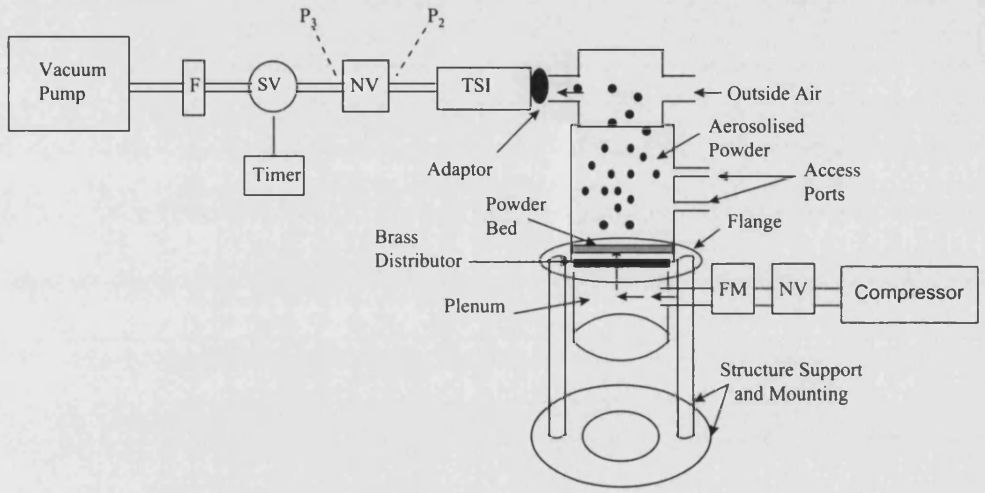

Figure 80: Diagram showing the DPAG-TSI experimental set-up.

SV: solenoid valve. NV: needle valve, F: pump protection filter, FM: flow meter

7.1.1 Experiments to Ascertain the Best Air-Distributing Material in the DPAG

A number of different materials were used as potential air-distributors within the DPAG. These included sintered glass and sintered brass. In order to determine which material performed best, pressure drop measurements were carried out using the set-up shown below in Figure 81 page 213.

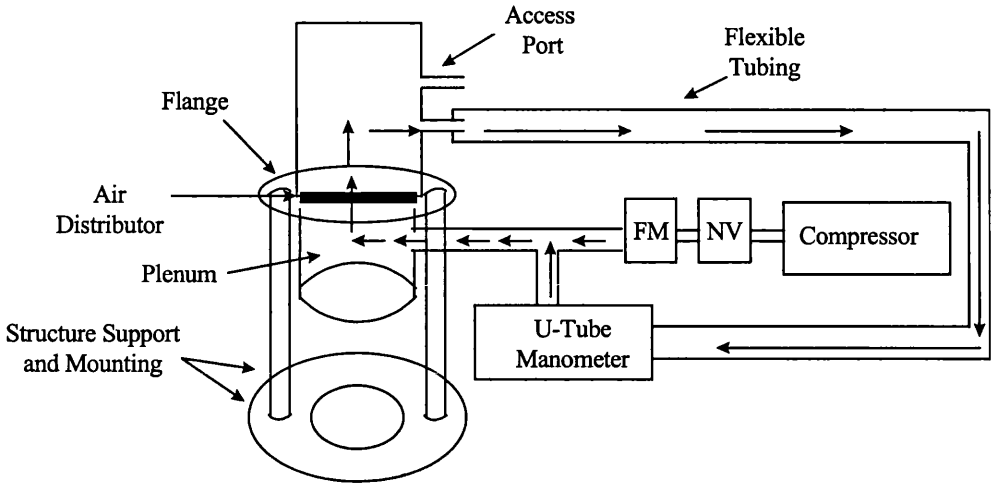

Figure 81: Diagram showing the set-up used for the pressure drop experiments to ascertain the best air-distributor in the DPAG.

Method

The experimental apparatus were set up as shown in Figure 81. The various different distributors were placed in the DPAG. The height of the water u-tube manometer was adjusted to zero. The compressor was switched on and the flow rate was adjusted using the needle valve. The corresponding pressure drop was measured on the u-tube manometer.

Results

Table 89 page 214, summarises the results obtained. Please refer to Appendix 11: Detailed Pressure Drop Tables Using the DPAG, page 264.

Distributor Type	Diameter (mm)	Thickness (mm)	Stated Pore Size (μm)	Measured Pore Size (μm)	Measured Flow Rate range ($Lmin^{-1}$)	Pressure Drop Range (cm/H_2O)	Press Drop Range (kPa)
Sintered Glass(P0)	39.	4.5	250	150-280	0-20.8	0.310-3.26	0.0304-0.320
Sintered Glass(P1)	39	5.0	160	50-200	0-20.8	0.460-5.05	0.0455-0.495
Sintered Glass(P2)	39	3.0	100	30-120	0-20.8	0.667-5.41	0.0654-0.530
Sintered Glass(P3)	39	5.0	40	10-45	0-3.3	13.6-95.3	0.703-9.35
Sintered Glass(P4)	39	5.0	<16	5-20	0-6.3	11.3-98.4	1.11-9.65
Sintered Brass	39	6.0	N/A	20-40	0-14	2.21-51.6	0.217-5.06

Table 89: Summary table showing the dimensions and performance of the various air-distributors used in the characterisation of the DPAG.

SEM photomicrographs in Figure 82 and Figure 83 show the images obtained for the sintered material.

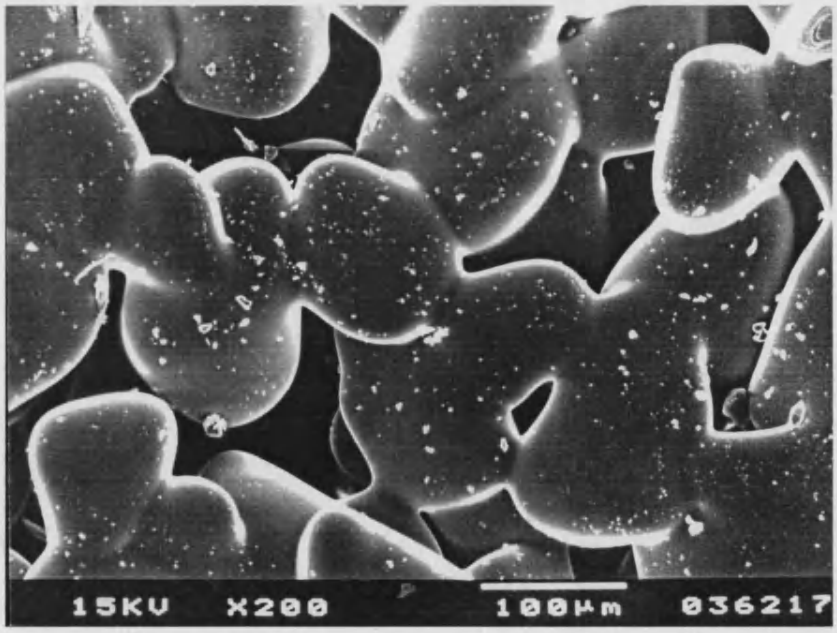

Figure 82: SEM photomicrograph of sintered glass at x200 magnification.

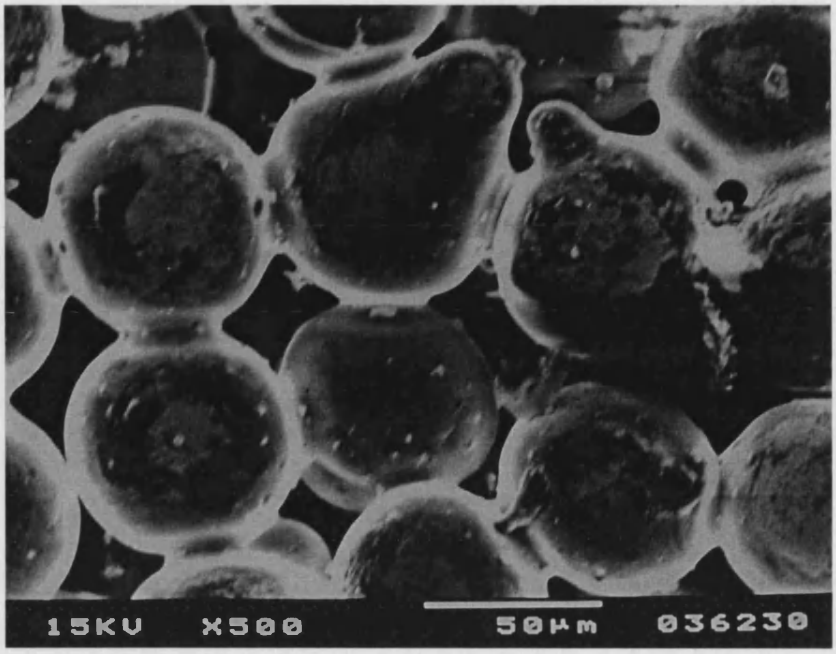

Figure 83: SEM photomicrograph of sintered brass at x500 magnification.

7.1.2 Discussion

Results for sintered glass show that, as porosity decreases there is greater resistance to the flow of air through the distributor resulting in increased pressure drops. However, the sintered brass used in the experiments does not exhibit the same resistance to the flow of air as its glass counterpart (i.e. porosity three). This discrepancy may be explained partially by studying the SEM images of the two materials. Sintered glass SEM images show dense, irregular pores compared with the more ordered pore structure of the sintered brass. It is possible that this irregular structure of the sintered glass accounts for the differences in performance, because the air has to negotiate a more complex route through the material. For this reason and also for its robustness, the brass was chosen as the distributor and used throughout the DPAG/TSI experiments. From additional experiments, it was determined that the sintered brass used in combination with a flow rate of $10Lmin^{-1}$ from the compressor fluidised the powder well. Thus, this flow rate was kept constant in all DPAG/TSI deposition studies.

7.2 TSI (Apparatus A) Deposition Profiles of MLFDS using the Dry Powder Aerosol Generator

A known amount of powder ~5g for the raw drug, and ~10g for the binary / ternary blends were placed into the chamber of the DPAG and the apparatus was coupled to a TSI as shown above. The *in-vitro* aerosol investigations were performed at 60.0 and 96.4 $Lmin^{-1}$ flow rate through the DPAG, whilst a compressor (Nebupump™ , Carri-Med Ltd, Dorking, UK) was operating at $10Lmin^{-1}$.

Flow Rate	Stage 1 Jet Diameter	Cut-off Diameter	Shot time
$60.1Lmin^{-1}$	14.2mm	6.55µm	4.0secs
$96.4Lmin^{-1}$	16.4mm	6.51µm	2.5secs

Table 90: Table showing the conditions used in the TSI (Apparatus A) DPAG deposition study of MLFDS.

Method

The DPAG was coupled to the TSI (see Figure 80, page212) containing 7ml and 30ml of HPLC grade methanol in stages 1 and 2 respectively, via an adaptor. The timing device was adjusted to run continuously. The aerosolised cloud from the DPAG was drawn into the air-stream created by the vacuum pump and MLFDS was delivered into the TSI. The system was turned off after five minutes or when no further sample appeared to be exiting the DPAG. The remaining sample in the powder bed and that adhered to the sides of DPAG and its removable head-chamber was weighed and the amount entering the TSI was quantified.

Once delivery of the powder was complete, stages 1 and throat (plus adaptor) of the TSI were washed into 100ml volumetric with methanol and diluted so as their intensity reading from the fluorimeter fell within the standard range. Stage 2 was washed into a 100ml volumetric and adjusted to volume with methanol, and diluted accordingly. The inside of the DPAG was washed into a 100ml volumetric and adjusted to volume with the methanol, and diluted accordingly. The relative intensity of the standards (see 2.2.5.2 Fluorimetric Detection of LFDS, page 108 for preparation) and the samples were measured on the Hitachi F2000 fluorimeter, Hitachi Ltd., Japan.

7.2.1 Drug Only

Results

The summary Table 91, page 217 shows the results obtained for MLFDS at 60.0, and 96.4Lmin^{-1}, compressor flow rate: 10Lmin^{-1}.

Parameter	FR	DPAG	Stage 1	Stage 2
Amount of powder by weight (g)	60.1	3.47(±0.223)	1.49(±0.196)	
	96.4	2.92(±0.271)	2.05(±0.178)	
Measured Intensity (%)	60.1	25.1(±0.138)	20.4(±0.143)	10.6(±0.106)
	96.4	21.3(±0.113)	25.9(±0.155)	22.5(±0.120)
Corr. Intensity (%)	60.1	23.9(±0.138)	19.2(±0.143)	9.4(±0.106)
	96.4	20.1(±0.113)	24.7(±0.155)	21.3(±0.120)
Conc. (µg/ml)	60.1	0.347(±0.074)	0.279(±0.048)	0.133(±0.003)
	96.4	0.292(±0.057)	0.360(±0.062)	0.309(±0.049)
Dilution Factor	60.1			
	96.4	10000	5000	800
Amount Deposited (g)	60.1	3.47(±0.267)	1.39(±0.115)	0.106(±0.004)
	96.4	2.92(±0.205)	1.80(±0.143)	0.247(±0.011)
(%) Deposited	60.1	69.9(±2.09)	28.0(±2.14)	2.1(±0.35)
	96.4	58.7(±2.38)	36.3(±2.44)	5.0(±0.85)

Table 91: Summary table of TSI deposition data for MLFDS using DPAG at 60.1, and 96.4Lmin^{-1} (compressor flow rate: 10Lmin^{-1}).

Values in brackets indicate standard deviation, n=10.

Table 92, below, was constructed from the results obtained above in Table 91.

Parameter	Value Obtained or calculated @ 60.1Lmin^{-1}	Value Obtained or calculated @ 96.4Lmin^{-1}
Mean Total Recovery	99.5%(±2.04)	99.4%(±1.32)
Mean Emitted Dose	1.46g(±0.168)	1.99g(±0.182)
Mean Emitted Dose	30.1%(±1.44)	41.2%(±1.67)
Mean FPD	0.103g(±0.015)	0.240g(±0.026)
Mean FPF	7.10%(±0.549)	12.1(±0.713)

Table 92: Summary table of various parameters calculated from TSI deposition data for MLFDS using the DPAG (compressor flow rate: 10Lmin^{-1}) at 60.0, and 96.4 Lmin^{-1}.

Values in brackets indicate standard deviation, n=10.

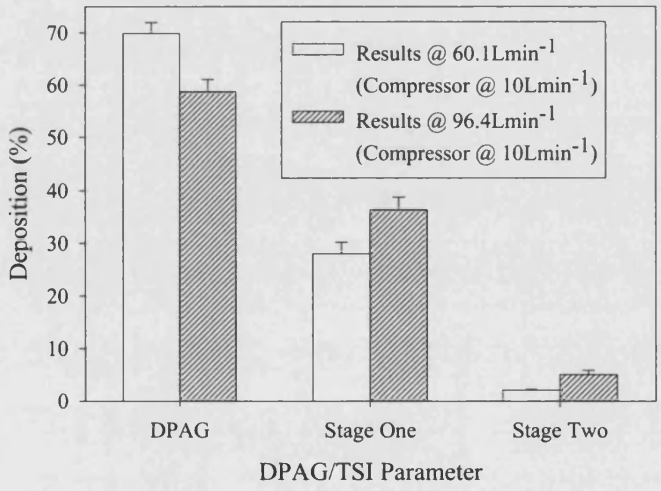

Figure 84: Distribution of MLFDS within Apparatus A at different flow rates in experiments using the DPAG.

Bars represent the mean + SD of 10 determinations.

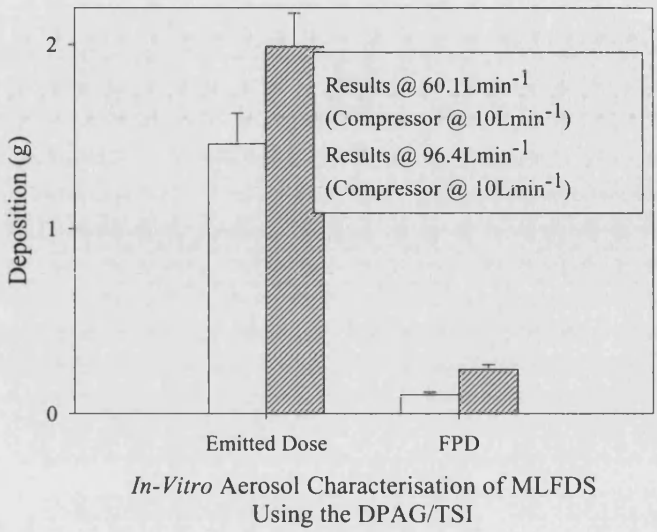

Figure 85: Emitted dose and fine particle dose of MLFDS at different flow rates in experiments using the DPAG.

Bars represent the mean + SD of 10 determinations.

Statistics

One way analysis of variance on the ED of MLFDS at 60.1, 96.4 with 10Lmin^{-1} compressor flow rate revealed significant differences ($F=44.2$, $p= <0.001$). Significant differences ($F=210$, $p= <0.001$) were also observed for the FPD values.

7.2.2 Binary Blends

Three different blends of MLFDS and lactose (see below), were prepared as described in chapter four using the rotary bladed blender (Kenwood Mini Chopper, CH100, Kenwood Ltd., Hants., UK) employing the mixing techniques outlined earlier (see page 118). The blends were tested for content uniformity and the optimum mixing time for each blend was determined, as previously outlined on page 139.

Blend ID	Blend Size	MLFDS (% w/w)	Lactose (% w/w)	Lactose Type
A	10g	10	90	Coarse (63-90μm) Fraction
B	10g	10	90	Fine (Microtose) (<10μm)
C	10g	5	95	Coarse (63-90μm) Fraction

Table 93: Table showing the details of the various binary blends of MLFDS with coarse and fine lactose used in DPAG deposition studies.

Content uniformity Experiments and SEM Images

Please refer to page 139, Figure 46, Figure 47, and Figure 48, page 142for the details and results of the content uniformity experiments and SEM photomicrographs of MLFDS binary blends.

Deposition Study Method

The *in-vitro* aerosol conditions and method employed were the same as those outlined om page 216. Flow rates of 60.1 ($ECD_{50\%}$ 6.55μm, stage 1 jet 14.2mm) and 96.4$Lmin^{-1}$ ($ECD_{50\%}$ 6.51μm, stage 1 jet 16.4mm) were used, compressor flow rate: 10$Lmin^{-1}$. Amount of powder placed into the DPAG chamber was ~10g. In a 10g load into the DPAG, blend A and B contain 1g of drug by weight, whereas blend C contains a total of 0.5g of MLFDS. Excess lactose particles aerosolised into the TSI were filtered before serial dilution of test solutions.

Results

Parameter	FR	Blend ID	DPAG	Stage 1	Stage 2
Amount of powder by weight (g)	60.1	A	7.39(±0.538)	2.57(±0.152)	
		B	6.92(±0.424)	3.18(±0.166)	
		C	7.37(±0.496)	2.29(±0.104)	
Measured Intensity (%)	60.1	A	31.2(±0.176)	30.7(±0.183)	19.4(±0.126)
		B	22.8(±0.153)	28.5(±0.179)	21.1(±0.148)
		C	29.8(±0.147)	25.7(±0.135)	14.1(±0.105)
Corr. Intensity (%)	60.1	A	25.5(±0.176)	25.0(±0.183)	15.6(±0.126)
		B	22.2(±0.153)	27.9(±0.179)	20.5(±0.148)
		C	28.4(±0.147)	24.3(±0.135)	12.7(±0.105)
Conc. (µg/ml)	60.1	A	0.493(±0.074)	0.484(±0.086)	0.302(±0.025)
		B	0.461(±0.051)	0.580(±0.062)	0.424(±0.018)
		C	0.566(±0.055)	0.435(±0.055)	0.234(±0.011)
Dilution Factor	60.1	A B C	1500	500	50
Amount Deposited (g)	60.1	A	0.739(±0.062)	0.242(±0.011)	0.0151(±0.003)
		B	0.672(±0.068)	0.282(±0.013)	0.0206(±0.005)
		C	0.737(±0.053)	0.211(±0.009)	0.011(±0.001)
(%) Deposited	60.1	A	74.2(±3.02)	24.3(±1.81)	1.52(±0.096)
		B	69.0(±3.15)	28.9(±1.96)	2.11(±0.105)
		C	76.8(±3.47)	22.1(±2.06)	1.18(±0.073)

Table 94: Summary table of TSI/DPAG deposition data for MLFDS binary blends A, B, and C at 60.1Lmin^{-1} (compressor flow rate: 10Lmin^{-1}), n=10.

Parameter	FR	Blend ID	DPAG	Stage 1	Stage 2
Amount of powder by weight (g)	96.4	A	7.02(±0.427)	2.96(±0.148)	
		B	6.63(±0.343)	3.23(±0.157)	
		C	6.97(±0.416)	2.72(±0.155)	
Measured Intensity (%)	96.4	A	30.0(±0.142)	34.9(±0.136)	29.0(±0.174)
		B	22.5(±0.141)	29.9(±0.147)	27.7(±0.163)
		C	28.2(±0.128)	30.8(±0.120)	22.0(±0.179)
Corr. Intensity (%)	96.4	A	24.4(±0.142)	28.6(±0.136)	23.6(±0.174)
		B	21.9(±0.141)	29.3(±0.147)	27.3(±0.163)
		C	26.8(±0.128)	29.4(±0.120)	20.5(±0.179)
Conc. (µg/ml)	96.4	A	0.473(±0.032)	0.552(±0.038)	0.457(±0.018)
		B	0.455(±0.030)	0.609(±0.024)	0.563(±0.023)
		C	0.478(±0.022)	0.523(±0.024)	0.369(±0.014)
Dilution Factor	96.4	A B C	1500	500	50
Amount Deposited (g)	96.4	A	0.709(±0.0456)	0.276(±0.143)	0.0228(±0.003)
		B	0.663(±0.0394)	0.296(±0.129)	0.0274(±0.003)
		C	0.697(±0.310)	0.254(±0.120)	0.0180(±0.001)
(%) Deposited	96.4	A	70.3(±4.16)	27.4(±1.86)	2.27(±0.134)
		B	67.2(±3.77)	30.0(±1.71)	2.78(±0.148)
		C	71.9(±3.96)	26.2(±2.01)	1.85(±0.100)

Table 95: Summary table of TSI/DPAG deposition data for MLFDS binary blends A, B, and C at 96.4Lmin^{-1} (compressor flow rate: 10Lmin^{-1}), n=10.

Parameter	Blend A		Blend B		Blend C	
	At 60.1	At 96.4	At 60.1	At 96.4	At 60.1	At 96.4
Mean Total Recovery(%)	99.7 (±2.52)	99.6 (±2.09)	99.2 (±3.07)	100.3 (±3.29)	100.2 (±3.19)	99.4 (±3.84)
Mean Emitted Dose(mg)	250 (±17.9)	291 (±26.0)	303 (±26.4)	323 (±28.5)	98.7 (±7.66)	100.6 (±10.3)
Mean Emitted Dose(%)	15.6 (±2.06)	17.9 (±2.14)	15.7 (±2.62)	16.6 (±2.88)	11.7 (±1.73)	14.1 (±1.16)
Mean FPD(mg)	14.7 (±1.88)	22.2 (±2.01)	20.6 (±.1.94)	27.4 (±2.05)	11.4 (±1.06)	18.0 (±1.75)
Mean FPF (%)	5.88 (±0.426)	7.64 (±.551)	6.81 (±0.557)	8.47 (±0.361)	5.11 (±0.412)	6.60 (±0.314)

Table 96: Summary table of various parameters calculated from TSI/DPAG deposition data for MLFDS binary blends A, B, and C at 60.1 and 96.4 Lmin^{-1} (compressor flow rate: 10Lmin^{-1}).

Values in brackets indicate standard deviation, n=10.

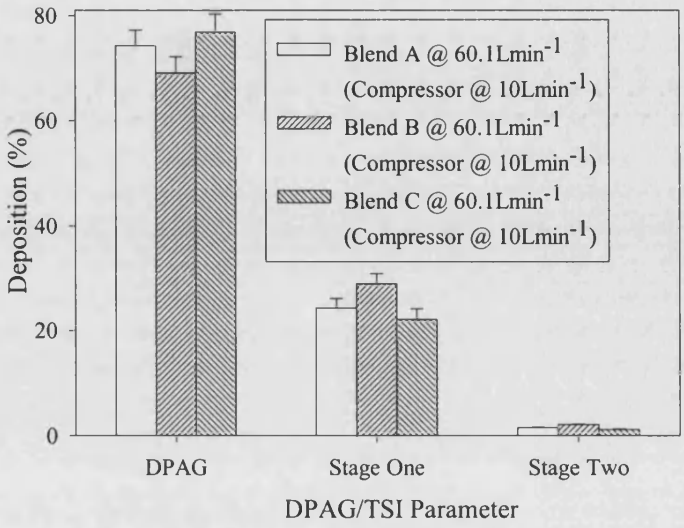

Figure 86: Distribution of MLFDS binary blends A, B and C within Apparatus A at 60.1Lmin^{-1} (compressor flow rate: 10Lmin^{-1}) in experiments using the DPAG.

Bars represent the mean + SD of 10 determinations.

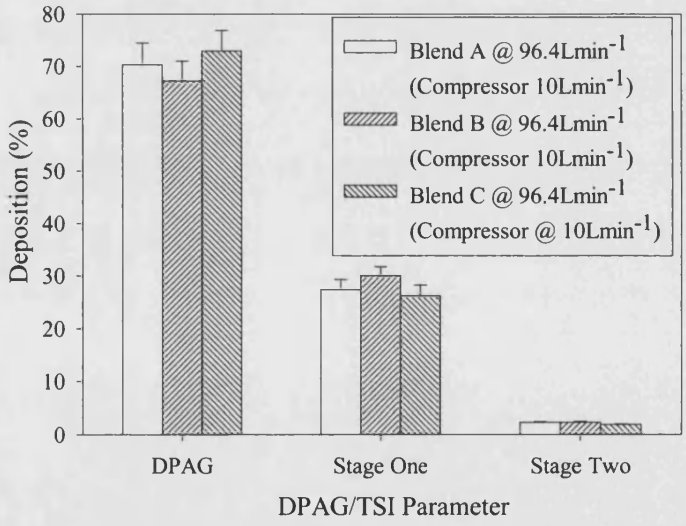

Figure 87: Distribution of MLFDS binary blends A, B and C within Apparatus A at 96.4Lmin^{-1} (compressor flow rate: 10Lmin^{-1}) in experiments using the DPAG.

Bars represent the mean + SD of 10 determinations.

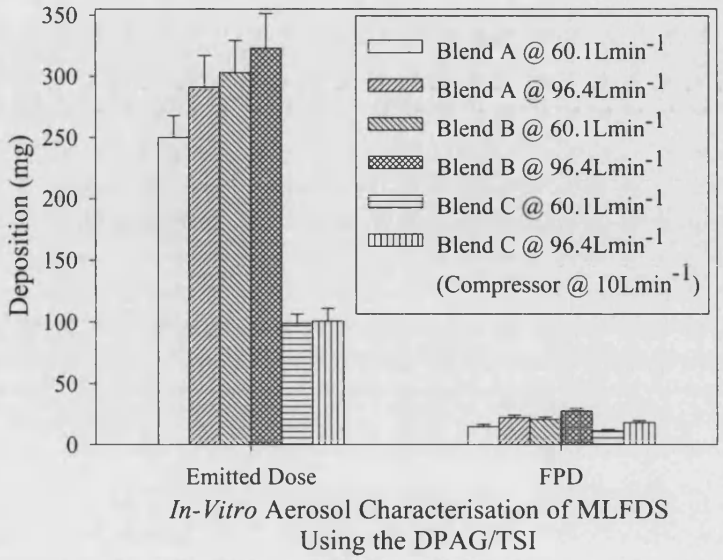

Figure 88: Emitted dose and fine particle dose of MLFDS binary blends A, B and C at 60 and 96.4Lmin^{-1} (compressor flow rate: 10Lmin^{-1}) in experiments using the DPAG.

Bars represent the mean + SD of 10 determinations.

Statistics

One way analysis of variance on the ED of MLFDS binary blends A, B, and C at 60.1Lmin^{-1} (with 10Lmin^{-1} compressor flow rate) showed significant differences (F=299, p=<0.001). Fisher's pairwise comparisons revealed that the ED of all three blends were all statistically significantly different and did not overlap in anyway. Similar findings were obtained for the ED values of the three blends at 96.4Lmin^{-1} (F=254, p=<0.001). Statistics on the FPD of the three blends at 60 and 96.4Lmin^{-1} also produced widely disagreeing results (F=91.7, p=<0.001), (F=58.3, p=<0.001) respectively.

7.3 General Discussion

Table 97 and Table 98, below, show the summary results obtained in the DPAG/TSI experiments.

Parameter	Summary DPAG/TSI Results at 60.1 and 96.4Lmin^{-1} / 10Lmin^{-1} Compressor							
	Drug-Only		Blend A		Blend B		Blend C	
	60.1	96.4	60.1	96.4	60.1	96.4	60.1	96.4
ED(mg)	1460 ±168	1990 ±182	250 ±17.9	291 ±26.0	303 ±26.4	323 ±28.5	98.7 ±7.66	100.6 ±10.3
FPD(mg)	103 ±15.0	240 ±26.0	14.7 ±1.88	22.2 ±2.01	20.6 ±1.94	27.4 ±2.05	11.4 ±1.06	18.0 ±1.73
FPF(%)	7.10 ±0.549	12.1 ±0.713	5.88 ±0.420	7.64 ±0.551	6.81 ±0.557	8.47 ±0.361	5.11 ±0.412	6.60 ±0.314

Table 97: Summary DPAG/TSI results obtained for MLFDS and its various blends at 60.1 and 96.4Lmin^{-1} (compressor flow rate: 10Lmin^{-1}), n=10.

From the above table and the data presented within this chapter, it can be seen that the drug only formulation appears to be performing the best. But, if the final FPD values were divided by ten, so as to make them directly comparable with blends A and B, and by twenty in the case of blend C, then a different pattern emerges (see below). Similarly, values for blend C have been multiplied by two to make them comparable with the other formulations.

Parameter	Summary DPAG/TSI Results at 60.1 and 96.4Lmin^{-1} / 10Lmin^{-1} Compressor							
	Drug-Only		Blend A		Blend B		Blend C	
	60.1	96.4	60.1	96.4	60.1	96.4	60.1	96.4
FPD(mg)	10.3 ±1.50	24.0 ±2.60	14.7 ±1.88	22.2 ±2.01	20.6 ±1.94	27.4 ±2.05	22.8 ±2.12	36.0 ±3.46

Table 98: Modified, summary DPAG/TSI results obtained for MLFDS and its various blends at 60.1 and 96.4Lmin^{-1} (compressor flow rate: 10Lmin^{-1}).

The modified results show that blend C actually performs best. If the results are analysed closely, then they are not so suprising. Blend C, contains the largest amount of lactose (w/w)

and the least amount of drug. Since lactose fluidises well in comparison to the raw drug, the implications are:

a) The DPAG does not effectively cause the separation of the drug particles from each other or the carrier particles. This is probably because the fluidising action is not turbulent enough and does not cause sufficient shear forces for physical separation.
b) The drug particles or aggregates of drug-drug and drug-carrier cannot negotiate the bend at the top of the fluidisation chamber (leading into the TSI) and impact on the ceiling of the DPAG, instead of following the airstream.
c) If the aggregates mentioned above do negotiate the bend, then they are not deaggregating sufficiently and deposit in stage 1, thus, low FPD values.

The DPAG is a concept device and a similar set-up to the DPAG/TSI system could not be found in cited literature. However, since the DPAG is essentially a fluidised bed, comparisons can be made to other such systems. Theory of fluidisation (Geldart 1973,1984, and Geldart *et al* 1986), factors affecting it (Baerns 1966, Vissier 1989), entrainment of particles from fluidised beds (Akiyama *et al* 1989) can be found elsewhere. Geldart (1973) proposed a system of classification of powders as A, B, C, and D-powders, on the basis of their varying modes of expansion when fluidised. Although the classification was based purely on empirical observations, it is still used today to describe powder behaviour. Geldart (1973) concluded that pharmaceutical powders (<20μm in diameter) are difficult to fluidised due to their cohesive nature and fall into group C in the classification system. This will explain why low FPD values were obtained for the studies carried out in this section.

The DPAG/TSI system is not sufficiently well developed or engineered to deliver MLFDS effectively. The reason for this is that on the outset of the project, the goals were to develop a dry powder fluidisation system, but as the objectives of the project changed, effort was directed to other areas. Further work is necessary to fully evaluate and develop the DPAG.

Chapter 8

A Novel Delivery Device for Glue Ear

8.0 A Novel Delivery Device for Glue Ear

A prototype glue ear delivery device (GEDD) for aerosolising a fixed amount of FDS from a vial is shown below (Figure 89, page 227). The device was designed and constructed at Bath University. The device consists of perspex housing which holds a vial of FDS (mounted onto a metal bracket), a plastic actuation chamber used to house a standard MDI canister, and a standard 20ml canister (100µl valve) filled with approximately 12-14ml of HFA134a. HFA 134a was preferred over HFA 227 because its vapour pressure is higher at 20°C (i.e. 5.70bar c.f. 3.90Bar, see appendix 1, page 250). The outlet from the chamber is connected to the vial of FDS via a small plastic (OD 2.23mm, ID <0.5mm) tube, plastic tubing (OD 2.58mm, ID 2.08mm) and by a 17-gauge needle was used to pierce the rubber septum on the vial. The inlet 17-gauge needle is used to channel the HFA aerosol into the vial once the canister is depressed, and is located approximately 20mm from the powder bed. A similar 17-gauge outlet needle provides an escape route for the aerosolised powder, which is directed into the ear insertion tube by more plastic tubing (OD 1.30mm, ID 0.68mm). A fine cloud of FDS is expelled from the metal ear insertion tube.

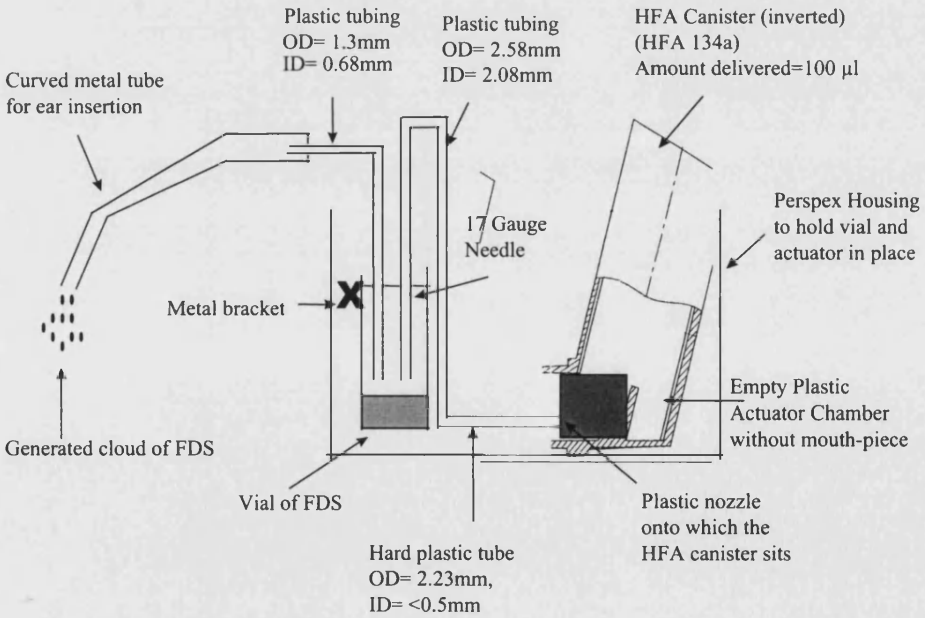

Figure 89: Glue ear delivery device (GEDD) for FDS

8.1 Testing and Evaluation of the Device

In order to evaluate the efficiency of delivery of FDS powder from the device the following experiments were devised:

a) Variation in delivery of HFA 134a from a pressurised canister fitted with 100µl valve.

b) The number of actuations needed to empty a vial containing 100mg of FDS powder, amount of powder aerosolised per actuation, and the particle size of the aerosol cloud produced.

c) Amount of residual FDS powder left in the vial, unaerosolised.

d) The calculation of the equivalent amount of air dispensed per actuation of HFA 134a from the canister.

Method & Results

Each of the above test criteria were carried out in turn, the method and subsequent result(s) obtained are given below.

a) 50 consecutive shots of HFA 134a were fired to waste from a pressurised canister containing 12-14ml of solution. Table 99 shows a summary of the variation in delivery.

Shot No	Wt of Canister Before Actuation (g)	Wt of Canister After Actuation (g)	Amount of HFA 134a Aerosolised (mg)
1	18.8038	18.6788	125.0
5	18.3025	18.1751	127.4
10	17.6643	17.5374	126.9
15	17.0343	16.9106	123.7
20	16.4090	16.2824	126.6
25	15.7819	15.6540	127.9
30	15.1464	15.0204	126.0
35	14.5208	14.396	124.8
40	13.8921	13.7678	124.3
45	13.2666	13.1389	127.7
50	12.6408	12.5168	124.0
		Average	125.7
		SD	1.59
		RSD (%)	1.27

Table 99: Table showing the variation in the amount of HFA 134a delivered from a standard 20ml pressurised canister fitted with a 100µl valve.

The results in Table 99 show an average of 125mg of HFA 134a delivered per shot. A relative standard deviation of <2% is acceptable.

b) A vial of freeze-dried SAPL containing 100mg of powder was loaded into the test apparatus as shown above. The weight of the vial was recorded before and after firing to determine the amount aerosolised. Particle size of the aerosol cloud produced, per shot, was assessed using the Malvern Master Sizer X. The insertion tube, shown above in the test apparatus was held at a fixed distance (~10mm) from the laser beam. The aerosol cloud produced caused ~20% obscuration of the beam, and the instrument was configured to analyse the cloud for a fixed period (i.e. 3 seconds). The 300mm lens (size range 0.2-180μm) was used during the measurements. The experiment was carried out in triplicate, and a summary of the results obtained is shown below.

Shot No	Wt of Vial Before Actuation (g)	Wt of Vial After Actuation (g)	Amount of FDS Delivered (mg)	Particle Size (μm) D(0.1)	D(0.5)	D(0.9)
1	14.6708 ±0.0536	14.6710 ±0.0536	-0.27	6.30 ±0.173	28.9 ±0.404	153 ±0.751
2	14.6711 ±0.0533	14.6759 ±0.0533	-4.77	5.25 ±0.254	22.9 ±0.231	106 ±9.76
3	14.6759 ±0.0530	14.6704 ±0.0530	5.47	5.03 ±0.023	20.4 ±0.346	136 ±1.39
4	14.6704 ±0.0528	14.6612 ±0.0528	9.23	3.75 ±0.0980	16.1 ±0.231	135 ±6.52
5	14.6612 ±0.0525	14.6527 ±0.0525	8.53	4.12 ±0.433	17.3 ±0.924	134 ±5.43
6	14.6527 ±0.0520	14.6463 ±0.0520	6.37	3.75 ±0.006	15.6 ±0.346	158 ±2.83
7	14.6463 ±0.0514	14.6417 ±0.0514	4.60	4.09 ±0.127	16.2 ±0.520	150 ±5.48
8	14.6417 ±0.0513	14.6358 ±0.0513	5.90	3.85 ±0.040	16.1 ±0.173	152 ±3.93
9	14.6358 ±0.0509	14.6326 ±0.0509	3.20	4.17 ±0.300	16.2 ±1.96	154 ±1.50
10	14.6326 ±0.0498	14.6309 ±0.0498	1.67	3.85 ±0.242	15.8 ±1.62	140 ±2.40
11	14.6309 ±0.0498	14.6290 ±0.0498	1.90	4.17 ±0.358	16.5 ±1.44	157 ±14.0
12	14.6290 ±0.0498	14.6277 ±0.0498	1.37	4.75 ±0.123	22.0 ±10.0	159 ±5.89
		Total	43.2			

Table 100: Table showing the variation in the amount of FDS delivered from a vial and the corresponding particle size of the aerosolised cloud.

c) After twelve consecutive shots, each vial was emptied and its contents weighed to determine the residual amount of FDS left. The results are shown below.

Number of Actuations Needed to Empty a vial	Total Amount of FDS Delivered (mg)	Residual Material Left in the Vial (mg)
12	39.5	31.0
12	45.2	24.7
12	48.0	23.4

Table 101: Summary table evaluating the GEDD for delivery of FDS.

d) Calculation of the equivalent amount of air dispensed per actuation of HFA 134a from the canister:-

Density of HFA 134a @ 20°C= 1226 $kgm^{-3} \equiv 1.226\ gcm^{-3}$

Valve size: $100\mu l \equiv 0.1cm^{-3}$ $\therefore$ 0.1226g or 122.6g of HFA 134a delivered per shot

Molecular Wt.:102.03 g/mol $\therefore$ $\frac{0.1226}{102.03}$ = Moles per shot = 1.202×10^{-3} mol

Under Standard Conditions, 1 mol of gas occupies $0.02241383m^3$ volume.

$\therefore$ Per shot: $(1.202 \times 10^{-3}) * 0.02241383 = \sim 2.7 \times 10^{-5} m^3 \equiv 27cm^3$

To confirm the above calculation experimentally, ten consecutive shots of HFA were fired into a water bath into an inverted measuring cylinder to record the volume of water displaced. The average volume of water displaced was found to be $\sim 31cm^3$.

8.3 General Discussion

GEDD was tested as stated above and the following information was attained:

a) The mass of HFA 134a delivered from a 100µl valve, pressurised canister was found to 125.7mg, with a variation of 1.27%. This equated to $\sim 27cm^3$ of equivalent air used to aerosolise the powder each time the canister was depressed.

b) On average, it took 12 shots to effectively empty a vial of FDS. It took two shots per vial before the system was primed, and although powder was aerosolised in the first two shots, there was a net weight gain in the system as a result of HFA introduction. Total, measurable amount of FDS delivered per vial was ~45mg with a ~25mg of powder left as residual material.

c) The average particle size of the aerosolised FDS is ~18µm, which is comparable to the findings revealed by TOFABS analysis (see materials and general characterisations).

The prototype GEDD needs to be developed further and refined before it is suitable for any type of clinical trial experiments on humans. However, the experiments in this section have

Chapter 9

A Novel Delivery Device for Post-Surgical Adhesion

shown that HFA is not a suitable propellant for this application as it appears to be absorbed by the SAPL. In addition, propellant-based systems may not be the best option for use in the middle ear, for obvious reasons. Published literature searches did not yield any applications of HFA propellants as a means of aerosolising powder.

9.0 A Novel Delivery Device for Post-Surgical Adhesions

The basic system described in chapter nine was used. The only modifications made were:

a) The size of the inlet and outlet needles was increased from 17 to 16-gauge.

b) The size of the tubing from the outlet need was increased.

c) The propellant used to aerosolise the powder was changed from HFA 134a to compressed medical grade carbon dioxide in order to aerosolise more powder per actuation.

d) The valves on the canister were changed from 100µl to a continuous type (Bespak BK0018005, King's Lynn, UK). This valve comprised of a standard core valve assembly with black nitrile elastomers and a standard force spring.

e) The canisters were also changed (see section 10.2).

The system with the modifications is shown below:

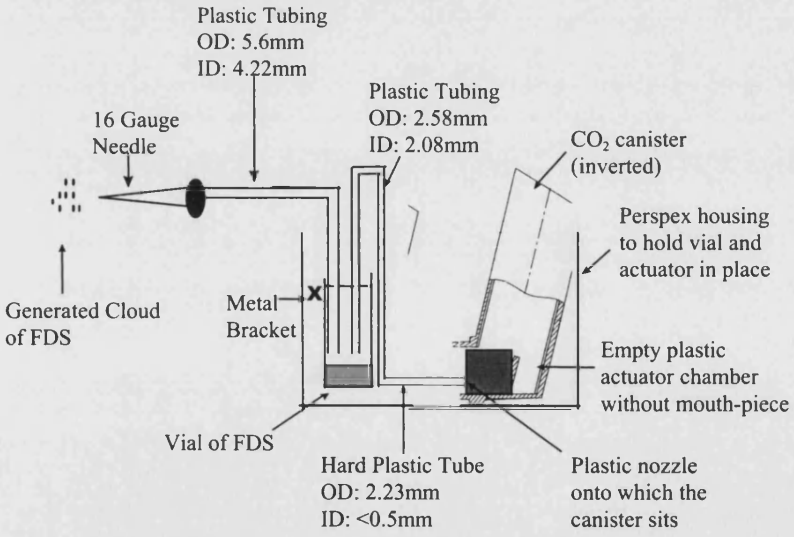

Figure 90: Schematic of the adhesion delivery system (ADS).

9.1 Clinical Requirements of the device

The primary concern was sterility of the product upon delivery, since it will be applied directly onto the site of action (i.e. abdominal cavity), thus, the use of medical grade CO_2. The final device may also need to be sterilised (perhaps with ethlyene oxide) but for animal studies this may not be applicable. The outlet tube needs to have an external, diameter of 5mm and needs to be between 30-33cm long. The amount of powder displaced per actuation was determined gravimetrically. The internal diameter of the tubing that enters the abdomen of patients undergoing laparascopic surgery will accommodate a 5mm (external diameter) catheter, but a 10mm (external diameter) catheter will be too big for the majority of ports.

9.2 Determination of the Leakage Rate from the Canisters

Presspart Manufacturing Ltd., Blackburn, UK, supplied the C128 canisters used in the study. These were standard 19ml pMDI canisters but possessed a strengthened inner wall to accommodate high-pressure gasses. The cans were first crimped with the BK0018005 valves and filled with compressed CO_2 at pressures of 10, 12, and 14 Bar, using the laboratory filling plant, Pamasol 2016 apparatus (DH Industries, UK). The crimping specifications for the canisters were the same as those employed for the standard Bespak BK357 valves (i.e. Height 6.7mm, Diameter 17.6mm). The canisters were stored in an oven at 25°C and 40%RH. At each time point (see below) five canisters were removed from the storage condition and its pressure recorded using the Pamosol pressure gauge (Haenni, Switzerland). The leakage rate of the cans are displayed below:

Time Point (Days / Wk)	Filled Canister Pressure Range	Measured Canister Pressure (Bar)	Filled Canister Pressure Range	Measured Canister Pressure (Bar)	Filled Canister Pressure Range	Measured Canister Pressure (Bar)
1 Day	9.8-10.3	9.92 (±0.217)	11.6-12.0	11.8 (±0.547)	13.6-14.1	13.7 (±0.707)
3 Days		9.52 (±0.179)		11.6 (±0.0837)		13.5 (±0.100)
1Week		9.06 (±0.152)		11.2 (±0.148)		13.2 (±0.130)
2Weeks		8.54 (±0.114)		10.9 (±0.130)		12.9 (±0.0894)
4Weeks		8.20 (±0.122)		10.5 (±0.207)		12.4 (±0.179)
12Weeks		7.06 (±0.109)		9.12 (±0.186)		11.2 (±0.346)

Table 102: Table showing the leakage rate of CO_2 from the strengthened C128 canisters. .

Over a period of three moths there is a loss of approximately 3Bar pressure form the canisters. This is represented graphically in Figure 91, page 234.

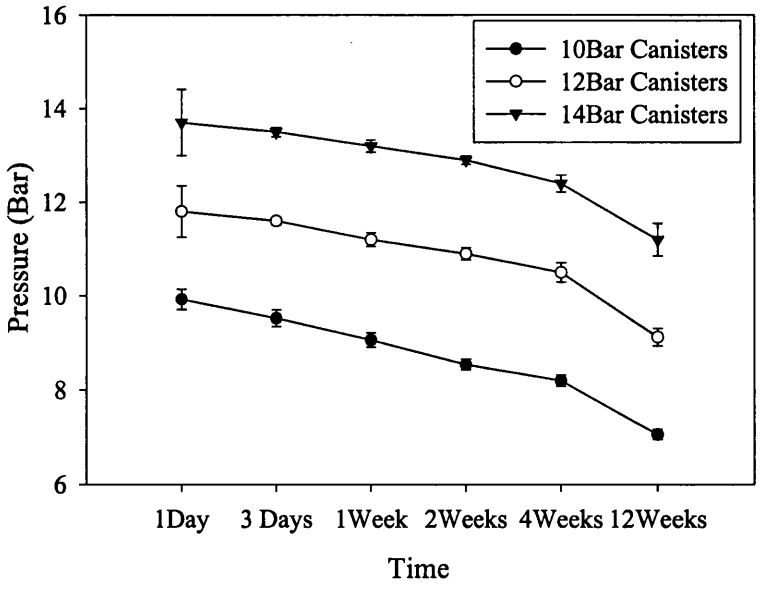

Figure 91: Graph showing the leakage rate of CO_2 from the C128 canisters over a period three months.

9.3 Determination of the amount of FDS Aerosolised using the ADS

The canister was placed into the empty plastic actuation chamber, ensuring the valve of the canister fitted into the nozzle embedded at the bottom of the actuation chamber. The canister was twisted during insertion to ensure a secure fit. The FDS vial was shaken and tapped vigorously before use to ensure the powder plug was fully dispersed. The vial was inserted upright into the metal bracket which was mounted onto the perspex housing. The circular covering from the top of the vial was removed, the rubber septum remained intact along with the rest of the crimp. The rubber septum was pierced with the 16-gauge needle (connected to the actuator chamber). The septum was pierced again with the needle connected to the outlet tubing. The outlet tubing was held and directed whilst the thumb was placed on top of the metal canister. The canister was depressed and held for about two seconds to accurately deliver the content of carbon dioxide. Before removing the empty vial of FDS, the needles were disconnected from the septum. When removing the empty canister, care was taken not to damage the embedded nozzle at the bottom of the actuator.

The FDS vials were weighed between successive shots to determine the amount aerosolised. Table 103, page 236 shows the summary results obtained.

Canister Pressure (Bar)	Vial No	Amount Expelled after 1st Shot (mg)	Amount Expelled After 2nd Shot (mg)	Amount Expelled After 3rd Shot (mg)	Total Amount Aerosolised (mg)
10	1	49.6	11.3	5.9	66.8
10	2	44.2	22.5	8.9	75.6
10	3	12.3	11.6	35.9	59.8
10	4	21.5	31.6	14.7	67.8
10	5	51.9	22.7	6.2	80.8
				Average	70.2(±8.17)
12	1	36.0	21.7	20.4	78.1
12	2	52.4	18.1	4.9	75.4
12	3	53.5	18.2	7.3	79.0
12	4	39.8	24.8	9.7	74.3
12	5	50.0	19.9	7.7	77.6
				Average	76.9(±1.96)
14	1	36.7	31.9	9.3	77.9
14	2	49.7	18.5	7.1	75.3
14	3	40.0	27.3	8.5	75.8
14	4	46.4	17.4	7.7	71.5
14	5	38.0	27.9	6.4	72.3
				Average	74.6(±2.63)

Table 103: Table showing the aerosolisation data on vials of FDS using the ADS with C128 canisters and BK0018005 valves.

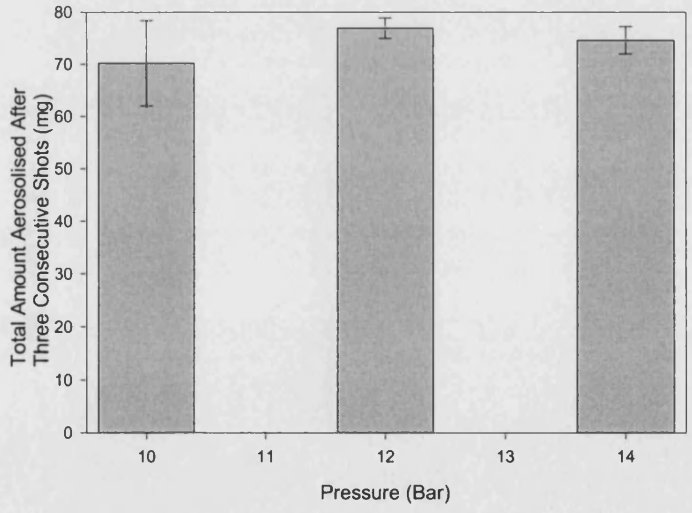

Figure 92: Graph showing the amount of drug aerosolised in three consecutive shots from a vial of FDS using the C128 canisters at 10, 12, and 14 Bars of compressed CO_2.

Figure 92, page 236 shows that 12 and 14Bar canisters aerosolise more powder from the FDS vials than the 10Bar canisters. There seems to be little or no difference between the 12 and 14Bar canister, with an average of ~75% (75mg) of the vial being emptied after three consecutive shots.

9.4 Further Development of the ADS

In order to improve the leakage rate from the canisters and to optimise the amount aerosolised from the vial, the crimping diameters (i.e. Height 6.98mm, Diameter 17.8mm) were fine-tuned and the C128 (19ml Volume) canister were changed to the C326 (28ml volume) canisters. In addition, four different types of valves were tested to ascertain which had lowest leakage rate.

Valve Number	Valve Details
BK0024956	This valve variant has standard black nitrile elastomers. It also possesses a modified core assembly with a larger sealing flange, to give a greater contact sealing area with the canister. It also has a high force spring to effect greater compression of core sealing flange on the outer seat.
BK0024958	This variant has a clean nitrile elastomers RB 190NT (carbon-black free), a modified core assembly with alarger sealing flange and a high force spring to effect greater compression of core sealing flange on the outer seat.
BK0024960	This variant has a clean nitrile elastomer RB 190NT (carbon-black free), a modified core assembly with a larger core sealing flange and a standard force spring.
BK0024971	This variant has a Trefsin© thermoplastic elastomer moulded outer seat and gasket with a clean nitrile elastomer RB 190NT inner seat. Like the others, above it also has a modified core assembly with a larger sealing flange and a high force spring.

Table 104: Table decribing the various valves used in the further development of the ADS.

Using the valves above, 50 canisters for each batch (total 200 canisters) were crimped and filled with medical grade CO_2 up to a pressure of 14Bar, as described previously, above. The filled canisters were split into equal groups and one half was placed into an oven at 25°C and 40%RH. At each time point (see below) five canisters were removed from the storage condition and its pressure recorded using the Pamosol pressure gauge (Haenni, Switzerland). The leakage rate of the cans is displayed below. The other half was irradiated (gamma radiation) by Isotron PLC, Swindon UK. The irradiation was carried out to prove two things. Firstly, the final product had to be sterile for clinical trial purposes, if the product were ever to go that far. Secondly, the effect of irradiation on the valve and the subsequent effect on leakage had to be ascertained. The samples were packed into steel boxes (in case of explosion) and exposed to a Cobalt (Co^{60}) source for 3-4 hours, receiving a dose of between 2.5-3.0MRad (25-30kGy) of radiation. This dose was sufficient to render the canister and its contents sterile, the samples were then placed in an oven at 25°C and 40%RH. The leakage test was carried out specific time points after the exposure by removing five canisters and testing them as before, the average results are shown below.

Valve Type	Time Point (Wk)	Filled Canister Pressure Range (Bar)	Subjected to Gamma Irradiation	Measured Canister Pressure
BK0024956	1 Week	13.7-14.5	No	14.1(±0.0831)
	1 Week		Yes	13.6±0.152
	4 Weeks		No	13.5±0.200
	4 Weeks		Yes	13.2±0.148
BK0024958	1 Week	14.1-14.8	No	13.8(±0.141)
	1 Week		Yes	13.2±0.228
	4 Weeks		No	13.4±0.122
	4 Weeks		Yes	12.9±0.167
BK0024960	1 Week	14.5-15.0	No	14.5(±0.265)
	1 Week		Yes	13.8±0.311
	4 Weeks		No	14.0±0.332
	4 Weeks		Yes	13.4±0.207
BK0024971	1 Week	14.0-14.5	No	13.5(±0.0894)
	1 Week		Yes	12.4±0.270
	4 Weeks		No	12.7±0.0550
	4 Weeks		Yes	11.9±0.179

Table 105: Table showing the leakage rate of CO_2 from the C326 (28ml volume) canister using four different batches of valves either subjected to gamma irradiation or not.

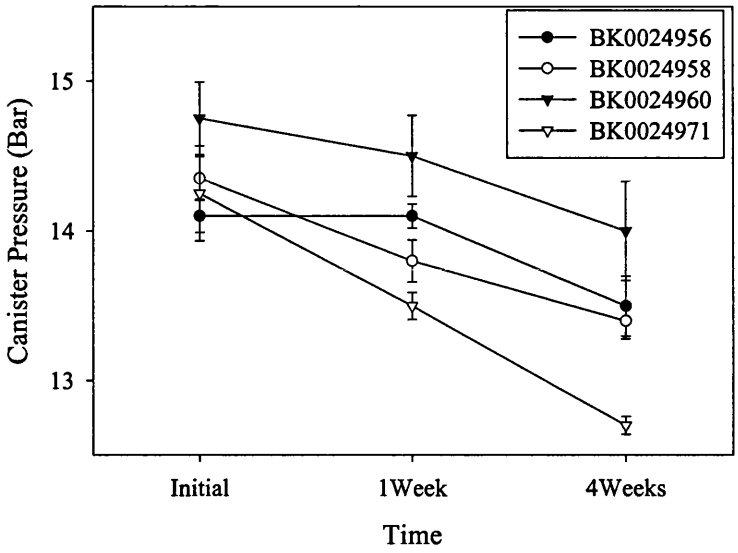

Figure 93: Graph showing the leakage rate of CO_2 from non-irradiated C326 canisters over four weeks.

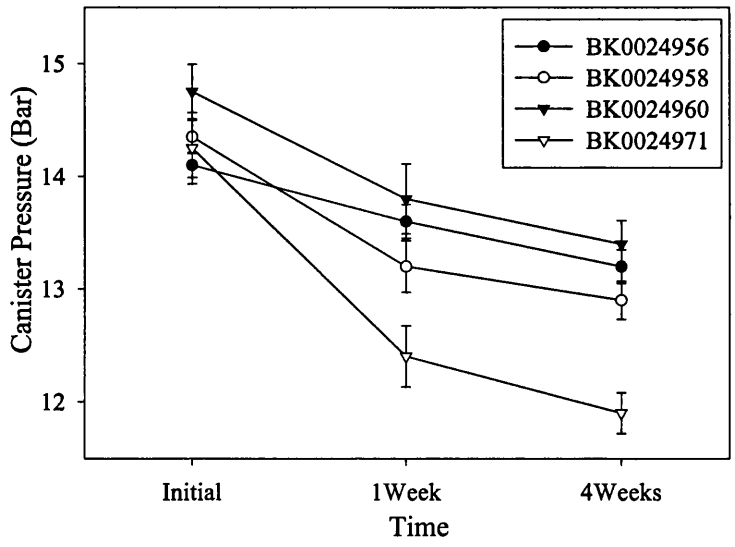

Figure 94: Graph showing the leakage rate of CO_2 from irradiated C326 canisters over four weeks.

C326 canisters coupled with surplus BK0018005 valves were filled and used immediately to generate aerosolisation data using the new canister. The results obtained are tabulated below.

Canister Pressure Range (Bar)	Vial No	Amount Expelled after 1st Shot (mg)	Amount Expelled After 2nd Shot (mg)	Amount Expelled After 3rd Shot (mg)	Total Amount Aerosolised (mg)
13.6-13.8	1	57.7	25.5	Zero	80.2
	2	63.3	20.8	5.7	89.8
	3	57.8	23.0	6.8	87.6
	4	34.6	38.5	10.0	83.1
	5	79.9	10.3	2.5	92.8
	6	69.3	18.1	3.8	91.1
	7	38.1	31.1	18.5	87.7
	8	60.2	25.7	8.0	94.0
	9	50.8	27.7	12.0	90.5
	10	43.9	29.0	5.1	78.0
				Average SD RSD(%)	87.5 5.38 6.15

Table 106: Table showing the aerosolisation data on vials of FDS using the ADS with C326 canisters and BK0018005 valves.

The results in Table 106 show that>85% of FDS vials are emptied after three consecutive shots using the C326 canisters.

The new prototype ADS currently being developed in association with Bespak PLC is shown below

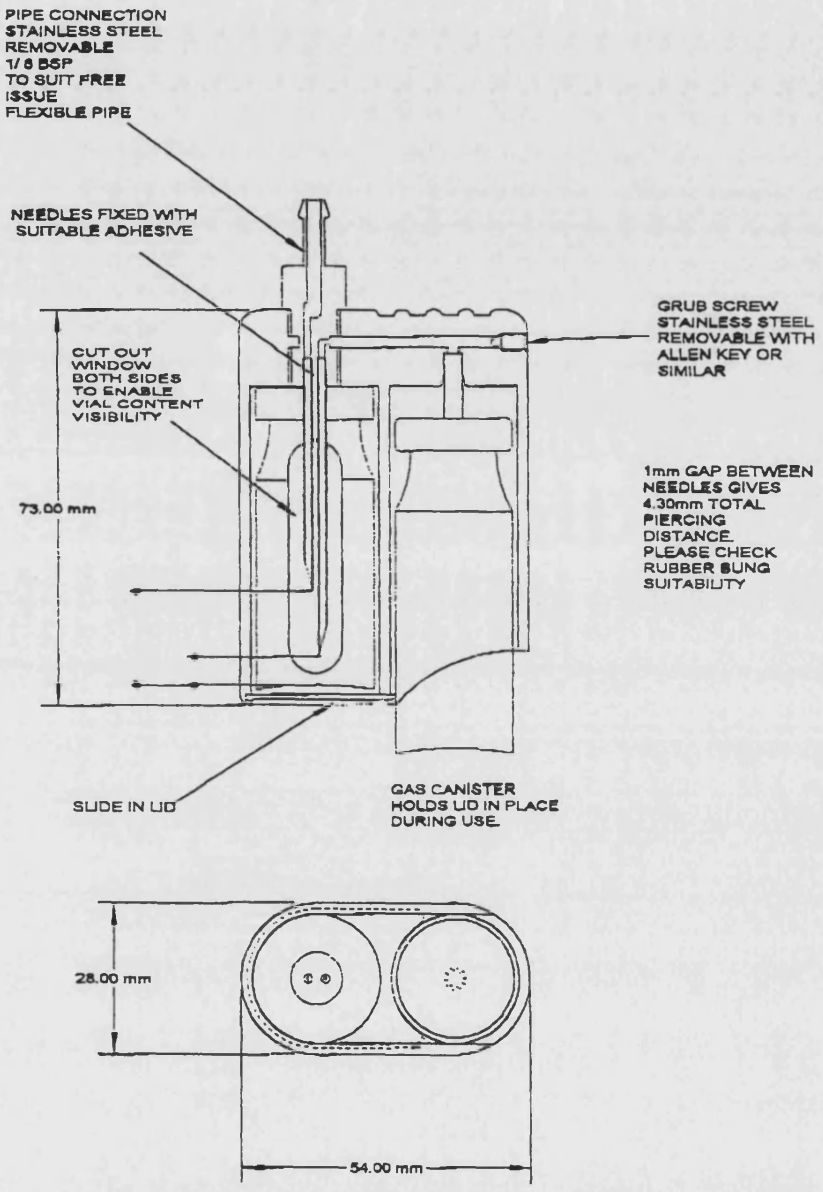

Figure 95: A schematic representation of the modified ADS.

9.5 General Discussion

From the results generated, the following conclusions were drawn:

The leakage rate of the CO_2 from the C128 (19ml volume) canisters has been determined. Approximately 2.5 Bar of pressure is lost over a period of three months. This leakage rate is unacceptable, and thus the need to develop the new prototype ADS coupled with C326 (28ml volume) canister. The leakage rate of non-irradiated C326 canisters, coupled with the four different valve variants, was between 0.5 and 1.5Bar over a period of four weeks. Of the four different valve variants, BK0024960 seems to perform the best, only losing 0.5Bar of pressure over four weeks. Next best is BK0024956, followed by BK0024958 and finally BK0024971, losing 1.5Bar of pressure over the same period. Irradiated canisters showed only marginally higher leakage rates and the effect of irradiation on the integrity of the canister seems to be minimal. The order of performance was unaffected by irradiation process

It takes three consecutive shots to effectively empty a 100mg vial of FDS. For the original C128 canisters, approximately 75% (75mg) of the vial is emptied, with about 25mg of powder remaining in the vial as residual material. The results for the C326 show that>85% of FDS vials are emptied after three consecutive shots. The increase in the amount aerosolised is probably due to the higher CO_2 volume throughput through the vial.

Implications of the findings to any future commercially or clinically viable system is that, multiple pressurised canisters (at the very least two canisters) will be necessary to deliver the FDS effectively. With this in mind, the new prototype shown earlier was designed with the ease of canister and vial replacement at the forefront of its development.

The ADS is not an inhaler and cannot be compared directly against devices on the market for inhalation. However, there are at least three devices currently in development that utilise compressed air as a means of dispersing the powder that they deliver. These include Airboost™, Biohaler™, and the Prohaler™ (Nichols 1997), see Table 2, page 58 for additional detail. Jet nebulisers also use a source of compressed air to deliver drug material, be it in a solution form, see page 61 for additional information. Nichols (1997) stated that inhalers utilising compressed air or similar type propellants might be more prominent in the future.

Chapter 10

Overall General Discussion and Conclusions

10.0 Overall General Discussion and Conclusions

This research programme was initially undertaken to improve the method of delivery of SAPL in neonatal RDS. Design, construction and testing of a DPAG for use in neonates was initiated, with the aim of producing a powder system which could nebulise a certain dose of SAPL over a period time. However, the course of the study was altered when literature published by a number of authors (Enhorning *et al* 1996, Hills *et al* 1996a, 1996b, Liu *et al* 1995, 1996) implied that SAPL had possible applications in respiratory diseases such as asthma, and ARDS. Other citations (Hills *et al* 1982, Grahame *et al* 1985, Rozga *et al* 1990, Kappas *et al* 1992, Anderson 1996, and Heu *et al* 1997) linking the possible, additional uses of SAPL in non-respiratory conditions such as intraperitoneal post-surgical adhesions and otitis media (Nemechek *et al* 1997) with effusion (glue ear) also served to change the goals of the programme. Thus, research was aimed at developing the SAPL product (ALEC^{TM} also called pumactant) produced by Britannia Pharmaceuticals Ltd., and licensed in the UK for neonatal RDS. Specifically, the main effort was diverted to produce a delivery system for principal use in asthma and to test the hypotheses that SAPL had a therapeutic effect against the disease, by getting the drug to phase I clinical trials. Smaller, but no less important, effort was directed towards investigating SAPL use in postsurgical adhesions and glue ear.

Various forms of SAPL, ranging from unmicronised freeze-dried labelled material to micronised non freeze-dried material have been studied and characterised. The way in which the material is manufactured seems to dictate its morphological properties. Freeze-drying produces amorphous particles, existing as aggregates of no definitive size. The amorphous nature of the particles is an artefact of the lyophilisation process in which the water is extracted from the system in a non-discriminative way (Craig *et al* 1999). Lyophilisation also tends to produce particles with smoother surfaces than counter-parts, which are produced via other routes. When subjected to labelling and micronisation, particles are no longer amorphous as shown by various photomicrographs. The route of manufacture that does not utilise freeze-drying produces large, irregularly shaped particles, which are reduced in size upon micronisation.

The route of manufacture does not affect true density and melting point properties of the various forms of SAPL. However, bulk densities of the materials do differ, FDS (Hausner ratio (HR) 1.48, Carr's index (CI) 32.6%) has been classified as having poor flow which improves if the material undergoes the labelling procedure to become LFDS (HR 1.18, CI 15.2%). UMS and MS both show good flow (HR 1.17, 1.18 and CI 14.6, 15.3 respectively).

XRPD analysis of SAPL produced diffractograms with a characteristic main, broad peak at ~21.0 two theta degrees. The broadness of this peak may arise from very small crystallite size, or lattice distortion, or both. The broad peak coupled with the noisy baseline observed in the results is indicative of the amorphous nature of most organic material, which tends to be semi-crystalline in nature as first described by Alexander and Klug (1974).

Moisture content analysis of SAPL was carried out using a Karl-Fischer coulometer. Results revealed that the various forms had an indigenous water content of between three to five percent. Moisture uptake experiments over a period of four weeks showed SAPL to be fairly hygroscopic. The level of hygroscopicity seemed to reach a maximum between two to four weeks for the various forms. Closer inspection of the results revealed that LFDS (23%) is slightly more hygroscopic than FDS (16%). Although SAPL picks up surrounding water readily, the process is rate dependant and careful handling and shielding from the environment severely limits the water content of the material. The hygroscopic nature of phospholipids is well documented and can be found in a recent review by Nakaya and Li (1999).

The analytical techniques used to separate and quantify SAPL involved the use of HPLC instrumentation coupled to an evaporative light scattering (mass) detector as well as fluorimetry. HPLC analysis of phospholipids coupled to a mass detector is routinely carried in industry for screening puroposes (Mancini *et al* 1997) and has been shown to be a reliable method of detection. The mass detection technique in this study showed that there was a binomial relationship between standard concentration and peak area. Statistical analysis of the linearity and repeatability experiments showed that the precision of the assay was acceptable. Fluorimetric analysis revealed that standard concentration versus sample intensity was linear. Statistical analysis showed the method to be robust and reproducible. Fluorimetric detection of LFDS was necessary because on the outset of the research programme a light scattering detector was not available; therefore, an alternative route of detection was necessary. Before deciding on fluorimetry, other routes of detection were investigated namely, UV, atomic

absorption (AA), and refractive index (RI) analysis. However, these proved unsuccessful since FDS does not have a chromophore for UV detection. Indirect AA quantification of FDS by measuring the calcium and sodium content levels also proved unsuccessful. The reasons for this were two-fold. Firstly, there were batch-to-batch variations in the levels of the salts. Secondly, and more importantly, FDS was poorly soluble in aqueous solutions. RI analysis of standards revealed that the technique was not significantly sensitive to detect small quantities of the drug. A full range scan of a relatively concentrated solution of FDS, using a fluorescence spectrophotometer, showed the drug to be very slightly fluorescent, too small to be quantifiable in any deposition studies. Thus, in order to quantify FDS and its various blends, a fluorescent probe (n-octadecyl dansylamide-1%w/w) was introduced to produce LFDS; similar experiments were carried out by (UbarretxenaBelandia *et al* 1999). The new, labelled material was identified by NMR analysis and characterised by the same physical tests used on FDS. In order to prove that the fluorescent probe was distributed uniformly throughout the drug, content uniformity experiments were undertaken and cross referenced with deposition experiments involving chemically labelled SAPL. Results showed that the probe was evenly distributed throughout a given sample of LFDS.

Micronisation of the various SAPL forms were initially carried out on a laboratory scale fluid energy mill, and later on industrial mills which were used to prepare the bath of MS used in the clinical trials for asthma. The reason for the change of strategy was three fold. Firstly, the efficiency of the milling in the lab-scale model was typically around 65%, with most of the sample being lost during transfer. Secondly, the industrial mills and their surroundings were better controlled and monitored. The milling was carried out under a stream of nitrogen and all air was eliminated from the system, so as not to expose the drug to moisture. Thirdly, standard bacterial swab tests were carried post micronisation to assess the level of hygiene, necessary for inhalation grade material.

In-vitro deposition studies of the various forms of SAPL were performed using traditional pharmaceutical testing apparatus and procedures. Blends of SAPL with coarse and fine lactose to produce binary and ternary mixtures were prepared using a high-shear blender. Geometric and ad-hoc blending techniques using a pestle and mortar were also employed but yielded poor content uniformity results. Also, the mechanical stress and grinding action produced by the hand blending raised questions about the stability of SAPL. Therefore, hand

blending was discontinued. Turbulent tumbling mixing also produced blends with poor content uniformity, probably due to low-shear. Thus, only the blends produced by the high-shear techniques were tested.

TSI analysis of MLFDS (drug only), binary, and ternary blends at 30, 60, and 96.4Lmin^{-1} using the Miat Monohaler and size three gelatine capsules produced varying results. The basic conclusions were that the drug-only formulation is the best in terms FPD and FPF, but its ED is flow rate dependant. At 30Lmin^{-1} the drug only formulation is not expelled well from the capsule and subsequent deaggregation is also poor, leading to lower FPF (7.1%). ED and FPF (16.4 and 20.2% at 60 and 96.4Lmin^{-1} respectively) improve with increasing flow rate. These blends compare favourably with ternary mixtures of standard salbutamol sulphate with coarse, intermidiate and fine lactose formulations, using the TSI at 60 and 90Lmin^{-1} via the Rotahaler™ and employing various mixing sequences, as carried out by Zeng *et al* (1999).

MSLI analysis of MLFDS and its various blends at 92Lmin^{-1} using the Miat Monohaler and size three gelatine capsules showed no appreciable differences in the FPF results obtained. However, the advantage of the drug-only formulation over the other blends was its ability to deliver a higher total ED and FPD. The FPF values obtained were on average about 2% higher than those achieved for the TSI analysis. One possible explanation for this increase could be that the airflow path through the MSLI is more conducive to deagglomeration of drug particles. Comparison of the data against *in-vitro* (MSLI at 60Lmin^{-1}) and *in-vivo* (scintigraphy) data obtained by Pitcairn *et al* (1997) on a novel asthma drug using a device similar to the Miat Monoler (i.e. Cyclohaler®), showed MLFDS deposition to be lower (~30% c.f. ~14%).

TSI analysis of MS (drug-only) at 30, 60, and 96.4Lmin^{-1} using the Miat Monohaler and size three gelatine capsules show that, as expected, ED, FPD and FPF are higher with increasing flow rate. No blends of MS were made or studied because it was decided that any SAPL formulation, which ultimately made it to clinical trials, using a size three capsule and Miat Monohaler, had to be delivered in greater quantities than had been possible in binary or ternary blends with lactose, previously studied for MLFDS. FPD and FPF values obtained for MS were compared with those for MLFDS. Results showed that FPD for MS was higher whereas its FPF was marginally lower. This means that MS is expelled from the capsule more efficiently but does not deaggregate as well as MLFDS. One possible reason for this is that

MS has a VMD of 2.39μm compared with 4.12μm for MLFDS. Therefore, smaller average size of MS would make the particles more cohesive and less susceptible to deaggregation.

MSLI analysis of MS at 92Lmin^{-1} using the Miat Monohaler and size three gelatine capsules produced the same trend in results as seen in TSI deposition profiles. Comparison of MS and MLFDS results also showed a higher FPD but a slightly lower FPF, due to the reasons outlined in the previous paragraph.

TSI and MSLI results for MS although good, only produced modest ED and FPD values in terms of weight. Thus, an alternative approach to delivering greater quantities of MS more efficiently was investigated. This led to the design, construction and testing of a novel asthma inhalation system. Before construction of the equipment, an asthma study protocol was designed and a dosing range of 85-100mg was chosen to be administered to the patient. Since there were no previous studies of SAPL, as a powder, being delivered to the lungs to use as a reference, the dosing range was based on the FDS currently on the market to treat RDS in neonates. Although in RDS the product is delivered as an intratracheal suspension, the total amount of material delivered was 100mg. Based on this information the inhalation system was constructed to effectively deliver 85-100mg of drug from single or multiple vials of MS filled under near sterile conditions. Deposition results on a 100mg vial of MS show ED values of >80%, FPF of ~25%. Although these are not great improvements over the Miat Monohaler and gelatine capsule delivery method, the mere fact that the initial load is five times as much make this route more attractive. The disadvantage of the inhalation system is that it is big, bulky, and tedious to use. However, since the initial objective was delivering a certain quantity of SAPL to the patient to test its therapeutic effect in asthma, the disadvantages of the system are of no immediate concern. Depending upon the results of the clinical trial, future work may be aimed at miniaturisation of the system or finding an alternative, equivalent system. Direct comparison of the results obtained for MS with other powder surfactant studies could not be made as such data does not exist. The only clinical data available are those from the studies carried out by Kurashima *et al* (1991) and Anzueto *et al* (1997). In both these studies, the surfactant was nebulised and improvements in the region of 11% for FVC and 25% for FEV_1 were reported.

The DPAG system, designed to carry out the initial objectives of the present study (to offer an alternative way of delivering SAPL in neonatal RDS) was designed and built over a period of

time. Modifications to the device were made with *in-vitro* testing in mind, such that it could be coupled to a TSI. Results of the testing on SAPL (drug-only) and binary blends showed low FPD and FPF values. This implied that the fluidisation method used was not turbulent enough to separate drug-drug or drug-carrier aggregates. In addition, the design of the top-half of the fluidisation chamber was not sufficiently optimised or engineered, causing aerosolised particles to impact on the ceiling of the apparatus. Further development work needs to be done on the system before it can efficiently deliver SAPL.

A novel delivery device for glue ear (GEDD) was constructed, utilising the current FDS vials on the market as well as HFA 134a as a propellant. The propellant filled into 19ml volume canisters and dispensed in shots of 100µl. This system was only partially tested and then discontinued. The reasons for this were two-fold, firstly firing of pressurised systems into the inner ear raised safety issues. Secondly, the use of HFA 134a as a propellant to aerosolise a powder system was novel and would require regulatory approval. The basic design of the GEDD was taken and modified to produce the ADS to be used in post-surgical adhesions. This system utilised pressurised large-volume (28ml) canisters of carbon dioxide at 10, 12, and 14Bar to aerosolise the FDS via a continuous valve. Various valve and gasket combinations on canisters were evaluated and tested for leakage rates before and after irradiation using a Cobalt-60 source. The canisters were irradiated because the system intended for phase I clinical trials had to be sterile, it therefore seemed more rational to fill the canister then irradiate, rather than fill in a sterile environment. The systems was refined with the final version expelling >85% of FDS from the 100mg vials. The ADS is not an inhaler and only a few inhalers utilising compressed air (Airboost™, Biohaler™, and the Prohaler™) as a means of dispersing the powder they deliver actually exist.

No definitive conclusions as to the success of the drug in asthma trials, or the efficiency of the inhalation system to deliver the required dose to the patient can be made, since the trial date is late 1999. However, one can conclude that the drug has a good chance of being delivered at the correct dose to the desired site of action. This statement can be partly justified by the *in-vitro* results obtained during this study, i.e. 25-30% FPF equating to 28-35mg of powder capable of being delivered to the lungs of asthmatics.

It may also be said that, trends seen in both the published literature and in patent applications point to the conclusion that surfactant therapy in respiratory disease treatment is on an upward

spiral. Whether or not SAPL has a sufficient therapeutic effect against asthma remains to be seen, but even if the improvements are minimal several interpretations can be obtained: -

a) The drug would be the first powdered surfactant to undergo trials for asthma.
b) A benchmark dosage of surfactant for asthma will be set.
c) The drug may have applications as a co-drug with another class of asthma drug; either in a solution based HFA form or incorporated into an existing formulation.

Appendices

Appendix 1: Summary of the Physical Properties of Hydro Fluoro Alkane (HFA) 134a and 227

HFA 134a= 1,1,1,2- Tetrafluoroethane (CF_3CH_2F)

Trade Name= Dymel®

Boiling point= -26.22°C at 1 bar, purity= 99.98%

Vapour pressure @ 20°C= 5.70 bar Vapour pressure @ 25°C= 6.63 bar

Molecular mass= 102.03 g/mol Density @ 20°C= 1226 kg/m^3

Physical form= Colourless gas

source of data= 1) Technical information booklet, DuPont Inc. (2) Physical property data sheet, ICI Klea, Cheshire, UK

2) HFA 227= 1,1,1,2,3,3,3- Heptafluoropropane (CF_3CHFCF_3)

Trade Name= Solkane® 227 Phams,

Produced by, Solvay Fluor und Derivative (SFD) GmbH, Hannover, Germany

International Name= Apaflurane

Molecular mass= 170.03 g/mol Physical Form= Coulourless gas

Boiling Point= -16.5°C at 1bar Vapour Pressure @ 20°C= 3.902bar

Density= 1.415 kg/l @ 20°C

Source of data= (1) Physical properties data booklet, Hoechst Chemicals, Frankfurt, Germany (2)SFD, Hannover, Germany.

Appendix 2: Detailed Particle Size Analysis Tables of SAPL Powders by Laser Light Diffraction (Malvern Analysis)

Sample ID	Dispersant or Solvent	Suspending Agent (w/v)	Sonic Bath Temp.(°C)	Sonication Time (secs /min)	Particle (μm) D(0.1)	Size (μm) D(0.5)	(μm) D(0.9)
FDS	Cyclohexane	0.1%Lecithin	25-30	0	14.8	54.8	120.8
FDS	Cyclohexane	0.1%Lecithin	25-30	15secs	4.85	36.9	92.8
FDS	Cyclohexane	0.1%Lecithin	25-30	30secs	3.95	22.1	57.6
FDS	Cyclohexane	0.1%Lecithin	25-30	1minute	3.72	19.6	42.9
FDS	Cyclohexane	0.1%Lecithin	25-30	2minutes	3.09	18.6	39.9
FDS	Acetone	None	25-30	0	34.4	135.8	172.9
FDS	Acetone	None	25-30	15secs	24.6	53.9	124.8
FDS	Acetone	None	25-30	30secs	10.3	38.3	101.0
FDS	Acetone	None	25-30	1minute	8.51	36.9	72.0
FDS	Acetone	None	25-30	2minutes	7.27	33.7	66.9
FDS	Air	None	n/a	n/a	25.9	83.3	164.7

Table 107: Particle size analysis results for FDS. For measurements using the small volume stirred cell n=5, for measurements using the dry powder feeder n=10.

Sample ID	Dispersant or Solvent	Suspending Agent (w/v)	Sonic Bath Temp.(°C)	Sonication Time (secs /min)	Particle (μm) D(0.1)	Size (μm) D(0.5)	(μm) D(0.9)
UMLF	Cyclohexane	0.1%Lecithin	25-30	0	6.58	49.4	151.1
UMLF	Cyclohexane	0.1%Lecithin	25-30	1minute	1.66	12.9	69.2
UMLF	Cyclohexane	0.1%Lecithin	25-30	2minutes	1.51	12.4	64.9
UMLF	Acetone	None	25-30	0	14.2	125.2	172.4
UMLF	Acetone	None	25-30	1minute	7.88	111.4	170.2
UMLF	Acetone	None	25-30	2minutes	4.28	53.1	164.6
UMLF	Air	None	n/a	n/a	21.2	64.9	140.2

Table 108: Particle size analysis results for UMLFDS. For measurements using the small volume stirred cell n=5, for measurements using the dry powder feeder n=10.

Sample ID	Dispersant or Solvent	Suspending Agent (w/v)	Sonic Bath Temp.(°C)	Sonication Time (secs /min)	Particle D(0.1)	Size D(0.5)	(μm) D(0.9)
MLFD	Cyclohexane	0.1%Lecithin	25-30	0	4.71	32.9	151.3
MLFD	Cyclohexane	0.1%Lecithin	25-30	15secs	3.48	22.0	87.8
MLFD	Cyclohexane	0.1%Lecithin	25-30	30secs	1.81	5.30	14.9
MLFD	Cyclohexane	0.1%Lecithin	25-30	1minute	1.69	4.19	8.90
MLFD	Cyclohexane	0.1%Lecithin	25-30	2minutes	1.61	4.12	8.51
MLFD	Acetone	None	25-30	0	29.2	135.3	174.0
MLFD	Acetone	None	25-30	15secs	21.8	98.6	166.0
MLFD	Acetone	None	25-30	30secs	13.2	56.9	154.3
MLFD	Acetone	None	25-30	1minute	3.43	21.5	134.2
MLFD	Acetone	None	25-30	2minutes	2.26	19.3	62.4
MLFD	Air	None	n/a	n/a	17.8	99.2	168.4

Table 109: Particle size analysis results for MLFDS. For measurements using the small volume stirred cell n=5, for measurements using the dry powder feeder n=10.

Sample ID	Dispersant or Solvent	Suspending Agent (w/v)	Sonic Bath Temp.(°C)	Sonication Time (secs /min)	Particle D(0.1)	Size D(0.5)	(μm) D(0.9)
UMS	Cyclohexane	0.1%Lecithin	25-30	0	12.7	83.1	165.3
UMS	Cyclohexane	0.1%Lecithin	25-30	15secs	9.85	51.4	92.0
UMS	Cyclohexane	0.1%Lecithin	25-30	30secs	7.27	36.9	61.3
UMS	Cyclohexane	0.1%Lecithin	25-30	1minute	3.25	14.1	31.3
UMS	Cyclohexane	0.1%Lecithin	25-30	2minutes	2.61	13.4	28.2
UMS	Acetone	None	25-30	0	11.2	58.8	86.2
UMS	Acetone	None	25-30	15secs	9.48	47.6	82.3
UMS	Acetone	None	25-30	30secs	9.06	42.8	79.9
UMS	Acetone	None	25-30	1minute	8.78	38.2	76.5
UMS	Acetone	None	25-30	2minutes	8.64	31.6	68.9
UMS	Air	None	n/a	n/a	14.3	78.7	160.9

Table 110: Particle size analysis results for UMS. For measurements using the small volume stirred cell n=5, for measurements using the dry powder feeder n=10.

Sample ID	Dispersant or Solvent	Suspending Agent (w/v)	Sonic Bath Temp.(°C)	Sonication Time (secs /min)	Particle Size (μm) D(0.1)	D(0.5)	D(0.9)
MS	Cyclohexane	0.1%Lecithin	25-30	0	1.70	4.68	27.8
MS	Cyclohexane	0.1%Lecithin	25-30	15secs	1.44	3.60	8.54
MS	Cyclohexane	0.1%Lecithin	25-30	30secs	1.41	3.05	8.38
MS	Cyclohexane	0.1%Lecithin	25-30	1minute	1.32	2.51	7.97
MS	Cyclohexane	0.1%Lecithin	25-30	2minutes	1.28	2.39	7.62
MS	Acetone	None	25-30	2minutes	4.83	12.7	24.6
MS	Air	None	n/a	n/a	10.4	61.9	147.8

Table 111: Particle size analysis results for MS. For measurements using the small volume stirred cell n=5, for measurements using the dry powder feeder n=10.

Appendix 3: Content Uniformity Experiments for Binary Blends of MLFDS

Blend ID	Time Point	Sample Wt (g)	Intensity (%)	Corrected Intensity (%)	Conc. (μg/ml)	Corrected Conc. (μg/ml)	Expected Conc. (μg/ml)
A	5	19.5	25.87	25.45	0.392	0.403	0.4
A	5	19.8	22.61	22.19	0.342	0.346	0.4
A	5	20.1	21.65	21.23	0.327	0.326	0.4
A	5	20.4	22.09	21.67	0.334	0.328	0.4
A	5	20.4	28.66	28.24	0.436	0.427	0.4
A	5	20.8	22.61	22.19	0.342	0.329	0.4
A	5	21.2	22.84	22.42	0.346	0.326	0.4
A	5	19.7	29.15	28.73	0.443	0.450	0.4
A	5	19.9	26.30	25.88	0.399	0.401	0.4
A	5	20.2	24.12	23.70	0.365	0.362	0.4
						Average 0.370 SD 0.0468 RSD(%) 12.7	
A	10	20.4	25.74	25.32	0.390	0.383	0.4
A	10	20.9	25.60	25.18	0.388	0.372	0.4
A	10	21.4	29.94	29.52	0.455	0.426	0.4
A	10	19.6	25.90	25.48	0.393	0.401	0.4
A	10	20.9	26.25	25.83	0.398	0.381	0.4
A	10	19.2	23.88	23.46	0.362	0.377	0.4
A	10	21.7	29.65	29.23	0.451	0.416	0.4
A	10	19.9	29.61	29.19	0.450	0.453	0.4
A	10	20.5	26.84	26.42	0.407	0.398	0.4
A	10	20.1	23.98	23.56	0.363	0.361	0.4
						Average 0.397 SD 0.0279 RSD(%) 7.0	
A	15	22.4	29.69	29.27	0.451	0.403	0.4
A	15	20.7	28.21	27.79	0.429	0.414	0.4
A	15	20.6	25.99	25.57	0.394	0.383	0.4
A	15	21.0	27.84	27.42	0.423	0.403	0.4
A	15	21.1	27.68	27.26	0.420	0.399	0.4
A	15	21.7	29.32	28.90	0.446	0.411	0.4
A	15	22.6	26.12	25.70	0.396	0.351	0.4
A	15	20.7	26.94	26.52	0.409	0.395	0.4
A	15	20.2	25.77	25.35	0.391	0.387	0.4
A	15	20.4	26.45	26.03	0.401	0.394	0.4
						Average 0.394 SD 0.0180 RSD(%) 4.6	

Table 112: Content uniformity table for MLFDS binary blend A (10% MLFDS:90% coarse lactose).

Blend ID	Time Point	Sample Wt (g)	Intensity (%)	Corrected Intensity (%)	Conc. (µg/ml)	Corrected Conc. (µg/ml)	Expected Conc. (µg/ml)
B	5	19.7	25.79	24.32	0.436	0.442	0.4
B	5	20.1	24.62	23.15	0.415	0.413	0.4
B	5	21.9	24.38	22.91	0.411	0.375	0.4
B	5	19.5	24.34	22.87	0.410	0.421	0.4
B	5	20.6	25.81	24.34	0.436	0.423	0.4
B	5	21.2	24.57	23.10	0.414	0.391	0.4
B	5	20.7	24.65	23.18	0.416	0.402	0.4
B	5	19.9	23.42	21.95	0.395	0.397	0.4
B	5	20.0	21.95	20.48	0.369	0.369	0.4
B	5	22.3	24.84	23.37	0.419	0.376	0.4
						Average 0.401 SD 0.0239 RSD(%) 6.0	
B	10	20.9	25.46	23.99	0.430	0.411	0.4
B	10	20.4	26.28	24.81	0.444	0.435	0.4
B	10	19.8	23.87	22.40	0.402	0.406	0.4
B	10	19.6	21.80	20.33	0.366	0.374	0.4
B	10	20.3	21.81	20.34	0.367	0.361	0.4
B	10	21.5	25.65	24.18	0.433	0.403	0.4
B	10	20.3	23.82	22.35	0.401	0.396	0.4
B	10	22.5	27.79	26.32	0.470	0.418	0.4
B	10	20.6	23.84	22.37	0.402	0.390	0.4
B	10	20.9	25.01	23.54	0.422	0.404	0.4
						Average 0.400 SD 0.0212 RSD(%) 5.3	
B	15	22.2	25.57	24.10	0.432	0.389	0.4
B	15	20.4	24.07	22.60	0.406	0.398	0.4
B	15	19.8	25.42	23.95	0.429	0.433	0.4
B	15	21.3	25.55	24.08	0.431	0.405	0.4
B	15	21.5	24.58	23.11	0.415	0.386	0.4
B	15	20.3	23.83	22.36	0.402	0.396	0.4
B	15	21.4	26.97	25.50	0.456	0.426	0.4
B	15	20.6	25.41	23.94	0.429	0.416	0.4
B	15	19.9	24.87	23.40	0.420	0.422	0.4
B	15	20.4	24.09	22.62	0.406	0.398	0.4
						Average 0.407 SD 0.0165 RSD(%) 4.1	

Table 113: Content uniformity table for MLFDS binary blend B (10% MLFDS:90% fine lactose).

Blend ID	Time Point	Sample Wt (g)	Intensity (%)	Corrected Intensity (%)	Conc. (µg/ml)	Corrected Conc. (µg/ml)	Expected Conc. (µg/ml)
C	5	20.4	17.91	17.49	0.269	0.264	0.2
C	5	20.6	15.84	15.42	0.237	0.231	0.2
C	5	19.9	16.43	16.01	0.247	0.248	0.2
C	5	19.6	12.85	12.43	0.191	0.195	0.2
C	5	20.8	16.03	15.61	0.240	0.231	0.2
C	5	20.5	11.05	10.63	0.163	0.159	0.2
C	5	19.7	11.98	11.56	0.178	0.181	0.2
C	5	19.7	12.09	11.67	0.180	0.182	0.2
C	5	20.6	14.23	13.81	0.213	0.206	0.2
C	5	20.3	15.00	14.58	0.224	0.221	0.2
						Average 0.212 SD 0.0329 RSD(%) 15.5	
C	10	19.2	14.87	14.45	0.222	0.232	0.2
C	10	19.8	12.51	12.09	0.186	0.188	0.2
C	10	19.5	12.84	12.42	0.191	0.196	0.2
C	10	20.1	15.23	14.81	0.228	0.227	0.2
C	10	20.4	15.04	14.62	0.225	0.221	0.2
C	10	19.8	13.85	13.43	0.207	0.209	0.2
C	10	20.6	14.69	14.27	0.220	0.213	0.2
C	10	21.1	15.07	14.65	0.226	0.214	0.2
C	10	20.3	14.16	13.74	0.212	0.208	0.2
C	10	19.5	15.47	15.05	0.232	0.238	0.2
						Average 0.215 SD 0.0155 RSD(%) 7.2	
C	15	22.5	16.51	16.09	0.248	0.220	0.2
C	15	20.6	13.90	13.48	0.208	0.201	0.2
C	15	22.8	15.98	15.56	0.240	0.210	0.2
C	15	21.2	14.94	14.52	0.224	0.211	0.2
C	15	19.8	13.04	12.62	0.194	0.196	0.2
C	15	20.6	13.55	13.13	0.202	0.196	0.2
C	15	21.1	15.89	15.47	0.238	0.226	0.2
C	15	20.8	14.40	13.98	0.215	0.207	0.2
C	15	20.4	14.00	13.58	0.209	0.205	0.2
C	15	20.1	13.98	13.56	0.209	0.208	0.2
						Average 0.208 SD 0.0095 RSD(%) 4.6	

Table 114: Content uniformity table for MLFDS binary blend C (5% MLFDS:95% coarse lactose).

Appendix 4: Content Uniformity Experiments for Ternary Blends of MLFDS

Time Point	Sample Wt (g)	Intensity (%)	Corrected Intensity (%)	Conc. (µg/ml)	Corrected Conc. (µg/ml)	Expected Conc. (µg/ml)
5	39.6	23.21	22.382	0.430	0.434	0.4
5	40.4	23.29	22.462	0.431	0.427	0.4
5	40.5	22.74	21.912	0.421	0.416	0.4
5	40.5	20.96	20.132	0.387	0.382	0.4
5	40.2	20.52	19.692	0.378	0.376	0.4
5	39.8	21.03	20.202	0.388	0.390	0.4
5	39.6	20.45	19.622	0.377	0.381	0.4
5	40.2	22.89	22.062	0.424	0.422	0.4
5	40.8	20.77	19.942	0.383	0.376	0.4
5	40.5	20.23	19.402	0.373	0.368	0.4
				Average 0.397 SD 0.0247 RSD(%) 6.2		
10	39.8	21.15	20.322	0.390	0.392	0.4
10	39.6	21.39	20.562	0.395	0.399	0.4
10	40.6	21.84	21.012	0.404	0.398	0.4
10	40.8	20.79	19.962	0.383	0.376	0.4
10	40.4	22.76	21.932	0.421	0.417	0.4
10	40.5	22.77	21.942	0.421	0.416	0.4
10	41.3	24.65	23.822	0.457	0.443	0.4
10	41.0	23.56	22.732	0.437	0.426	0.4
10	41.1	22.85	22.022	0.423	0.412	0.4
10	40.9	21.09	20.262	0.389	0.381	0.4
				Average 0.406 SD 0.0208 RSD(%) 5.1		
20	40.5	21.54	20.712	0.398	0.393	0.4
20	41.0	20.96	20.132	0.387	0.377	0.4
20	41.5	23.47	22.642	0.435	0.419	0.4
20	41.0	21.73	20.902	0.401	0.392	0.4
20	40.6	22.70	21.872	0.420	0.414	0.4
20	40.2	24.26	23.432	0.450	0.448	0.4
20	40.5	22.55	21.722	0.417	0.412	0.4
20	40.9	22.16	21.332	0.410	0.401	0.4
20	40.7	21.94	21.112	0.406	0.399	0.4
20	41.2	21.86	21.032	0.404	0.392	0.4
				Average 0.405 SD 0.0196 RSD(%) 4.9		

Table 115: Content uniformity table for a ternary blend of MLFDS, coarse lactose, and fine lactose (5:90:5% w/w).

Appendix 5: Detailed tables for the HPLC analysis of MS-TSI Results

Parameter	FR	Capsule	Device	Stage 1	Stage 2
Mean PG Area	30.0	37332 (±1872)	32200 (±3158)	94217 (±2041)	14027 (±1898)
Mean DPPC Area	30.0	111006 (±17237)	96542 (±4039)	256822 (±50730)	64229 (±3347)
PG as a % of Total Area	30.0	25.4 (±2.60)	25.0 (±1.28)	27.3 (±7.71)	17.9 (±1.18)
Mean PG Corr. Factor	30.0	1.19 (±0.130)	1.20 (±0.063)	1.17 (±0.396)	1.68 (±0.107)
DPPC as a % of Total Area	30.0	74.6 (±2.60)	75.0 (±1.28)	72.7 (±7.71)	82.1 (±1.18)
Mean DPPC Corr. Factor	30.0	0.939 (±0.032)	0.933 (±0.016)	0.970 (±0.097)	0.852 (±0.012)
Mean Corr. PG Area	30.0	44502 (±5394)	38623 (±6080)	105312 (±9207)	23477 (±1573)
Mean Corr. DPPC Area	30.0	103837 (±12586)	90120 (±4853)	245727 (±21483)	54779 (±3671)
PG Conc. (µg/ml)	30.0	2.37 (±0.015)	2.20 (±0.060)	3.70 (±0.163)	1.68 (±0.062)
DPPC Conc. (µg/ml)	30.0	7.95 (±0.483)	7.41 (±0.200)	12.2 (±0.531)	5.76 (±0.193)
Dilution Factor	30.0	100	100	1000	200
Amount of PG Deposited (mg)	30.0	0.237 (±0.015)	0.220 (±0.006)	3.70 (±0.163)	0.336 (±0.012)
Amount of DPPC Deposited (mg)	30.0	0.795 (±0.048)	0.741 (±0.020)	12.2 (±0.531)	1.15 (±0.039)
Normalised MS Deposition (mg)	30.0	1.04 (±0.049)	0.964 (±0.038)	16.0 (±0.381)	1.49 (±0.021)
% MS Deposited	30.0	5.31 (±1.48)	4.95 (±1.02)	82.1 (±3.76)	7.7 (±1.74)

Table 116: Summary table of TSI deposition data for MS at 30.0Lmin^{-1}.

Values in brackets indicate standard deviation, n=10.

Parameter	FR	Capsule	Device	Stage 1	Stage 2
Mean PG Area	60.0	20408 (±912)	15500 (±1183)	64730 (±1012)	23977 (±1649)
Mean DPPC Area	60.0	80256 (±2148)	54507 (±545)	328735 (±3501)	118227 (±2349)
PG as a % of Total Area	60.0	20.3 (±0.39)	22.1 (±1.32)	16.5 (±0.130)	16.8 (±0.69)
Mean PG Corr. Factor	60.0	1.48 (±0.028)	1.36 (±0.084)	1.82 (±0.014)	1.78 (±0.073)
DPPC as a % of Total Area	60.0	79.7 (±0.039)	77.9 (±1.32)	83.5 (±0.130)	83.2 (±0.690)
Mean DPPC Corr. Factor	60.0	0.878 (±0.004)	0.899 (±0.015)	0.838 (±0.001)	0.842 (±0.007)
Mean Corr. PG Area	60.0	30199 (±899)	21002 (±412)	118040 (±1310)	42661 (±1195)
Mean Corr. DPPC Area	60.0	70465 (±2098)	49006 (±960)	275426 (±3057)	99543 (±2789)
PG Conc. (µg/ml)	60.0	1.93 (±0.031)	1.58 (±0.017)	3.93 (±0.022)	2.32 (±0.034)
DPPC Conc. (µg/ml)	60.0	6.55 (±0.098)	5.45 (±0.054)	13.0 (±0.072)	7.79 (±0.109)
Dilution Factor	60.0	100	100	1000	200
Amount of PG Deposited (mg)	60.0	0.193 (±0.003)	0.158 (±0.002)	3.93 (±0.022)	0.464 (±0.007)
Amount of DPPC Deposited (mg)	60.0	0.655 (±0.010)	0.545 (±0.005)	13.0 (±0.072)	1.56 (±0.022)
Normalised MS Deposition (mg)	60.0	0.833 (±0.025)	0.691 (±0.015)	16.6 (±0.275)	1.99 (±0.038)
% MS Deposited	60.0	4.14 (±1.05)	3.43 (±0.916)	82.6 (±3.40)	9.9 (±1.19)

Table 117: Summary table of TSI deposition data for MS at 60.0Lmin^{-1}.

Values in brackets indicate standard deviation, n=10.

Parameter	FR	Capsule	Device	Stage 1	Stage 2
Mean PG Area	96.4	17182 (±2154)	12659 (±882)	61656 (±1259)	28325 (±1267)
Mean DPPC Area	96.4	71962 (±3412)	44301 (±3112)	295080 (±10015)	125896 (±8933)
PG as a % of Total Area	96.4	19.2 (±1.22)	22.2 (±0.201)	17.3 (±0.203)	18.4 (±0.486)
Mean PG Correction Factor	96.4	1.56 (±0.099)	1.35 (±0.012)	1.74 (±0.020)	1.63 (±0.043)
DPPC as a % of Total Area	96.4	80.8 (±0.099)	77.8 (±0.012)	82.7 (±0.020)	81.6 (±0.043)
Mean DPPC Correction Factor	96.4	0.867 (±0.013)	0.900 (±0.002)	0.846 (±0.002)	0.858 (±0.005)
Mean Corrected PG Area	96.4	26743 (±1669)	17088 (±1196)	107021 (±3379)	46266 (±3040)
Mean Corrected DPPC Area	96.4	62401 (±3894)	39872 (±2790)	249715 (±7883)	107955 (±7094)
PG Conc. (µg/ml)	96.4	1.81 (±0.062)	1.41 (±0.057)	3.73 (±0.060)	2.42 (±0.083)
DPPC Conc. (µg/ml)	96.4	6.16 (±0.194)	4.91 (±0.174)	12.4 (±0.195)	8.11 (±0.266)
Dilution Factor	96.4	100	100	1000	200
Amount of PG Deposited (mg)	96.4	0.181 (±0.006)	0.141 (±0.006)	3.73 (±0.060)	0.484 (±0.017)
Amount of DPPC Deposited (mg)	96.4	0.616 (±0.019)	0.491 (±0.017)	12.4 (±0.195)	1.62 (±0.053)
Normalised MS Deposition (mg)	96.4	0.783 (±0.028)	0.621 (±0.025)	15.8 (±0.181)	2.07 (±0.063)
% MS Deposited	96.4	4.06 (±0.994)	3.22 (±0.867)	82.0 (±3.11)	10.7 (±1.67)

Table 118: Summary table of TSI deposition data for MS at 96.4Lmin^{-1}.

Values in brackets indicate standard deviation, n=10.

Appendix 6: Detailed tables for the HPLC analysis of MS- MSLI Results

	Cap	Dev	Adp + Tht	Stg1	Stg2	Stg3	Stg4	Stg5
PG Area	34721 ±4584	32011 ±1728	98426 ±1133	97343 ±2630	90791 ±210	67205 ±2832	48829 ±1400	12928 ±403
DPPC Area	101598 ±1938	91392 ±1110	374757 ±14394	444612 ±10441	412955 ±6003	300356 ±12390	217494 ±1078	53757 ±356
PG as a % of Total Area	25.4 ±1.27	25.9 ±0.451	20.8 ±0.062	18.0 ±0.231	18.0 ±0.093	18.3 ±0.505	18.3 ±0.409	19.4 ±0.334
PG Corr. Factor	1.19 ±0.109	1.16 ±0.059	1.44 ±0.031	1.67 ±0.005	1.66 ±0.022	1.64 ±0.008	1.64 ±0.045)	1.55 ±0.032
DPPC as a % of total Area	74.6 ±1.27	74.1 ±0.451	79.2 ±0.062	82.0 ±0.231	82.0 ±0.093	81.7 ±0.505	81.7 ±0.409	80.6 ±0.334
DPPC Corr. Factor	0.939 ±0.027	0.945 ±0.016	0.884 ±0.005	0.853 ±0.001	0.854 ±0.002	0.857 ±0.002	0.857 ±0.001	0.868 ±0.004
Corr. PG Area	40896 ±186	37021 ±4658	141955 ±3920	162586 ±1767	151124 ±4559	110268 ±108	79897 ±220	20006 ±359
Corr. DPPC Area	95424 ±4565	86382 ±433	331228 ±10864	379368 ±9147	352622 ±4123	257293 ±10637	186426 ±252	46680 ±512
PG Conc. (µg/ml)	9.72 ±0.248	9.22 ±0.025	18.5 ±0.310	19.8 ±0.241	19.1 ±0.113	16.2 ±0.345	13.8 ±0.010	6.59 ±0.041
DPPC Conc.	20.1 ±0.486	19.1 ±0.048	37.5 ±0.619	40.1 ±0.483	38.7 ±0.226	33.0 ±0.688	28.1 ±0.019	14.0 ±0.078
Dilution	100	100	200	1000	200	100	100	100
PG (mg) Deposited	0.972 ±0.025	0.922 ±0.002	3.70 ±0.062	19.8 ±0.241	3.81 ±0.023	1.62 ±0.034	1.38 ±0.001	0.659 ±0.004
DPPC Deposited	2.01 ±0.049	1.91 ±0.005	7.49 ±0.124	40.1 ±0.483	7.73 ±0.045	3.30 ±0.069	2.81 ±0.002	1.40 ±0.008
Normalised MS Deposition	2.96 ±0.045	2.81 ±0.021	11.1 ±0.080	59.5 ±0.689	11.5 ±0.110	4.9 ±0.124	4.16 ±0.043	2.04 ±0.026
% MS Deposited	2.99 ±0.365	2.84 ±0.403	11.2 ±1.38	60.1 ±4.96	11.6 ±1.57	4.94 ±0.546	4.20 ±0.310	2.07 ±0.137

Table 119: Summary table of MSLI deposition data for MS at 92.0Lmin^{-1}.

Values in brackets indicate standard deviation, n=15.

Appendix 7: Structure and Physicochemical Properties of Dansyl Chloride

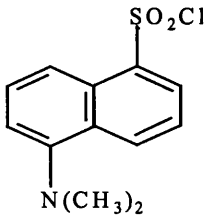

Figure 96: Dansyl Chloride (5-[Dimethylamino]Napthalene-1-Sulfonyl Chloride).

Formulae = $C_{12}H_{12}ClNO_2S$, RMM= 269.7, Purity ≈ 95%

Appendix 8: Structure and Physicochemical Properties of Octadecylamine

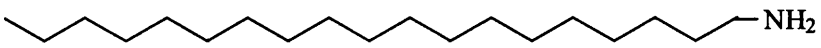

Figure 97 Octadecylamine (Stearylamine)

Formulae = $C_{18}H_{37}NH_2$, RMM= 269.5, Purity ≈ 98%

Appendix 9: Structure and Physicochemical Properties of n-Octadecyl Dansylamide

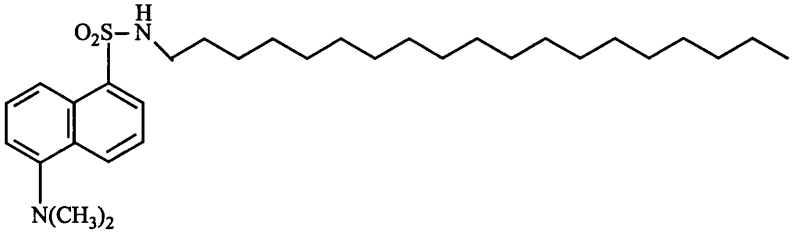

Figure 98 n-Octadecyl Dansylamide 1-(Dimethylamino)-5-Napthalene Sulfonyl Octadecylamine.

Formulae = $C_{28}H_{48}N_2SO_2$, RMM= 476, M.P= 69-72°C, λ_{ex}=345nm, λ_{em} = 482nm

Appendix 10: Dimensions of the DPAG

All the figures stated below are in mm.

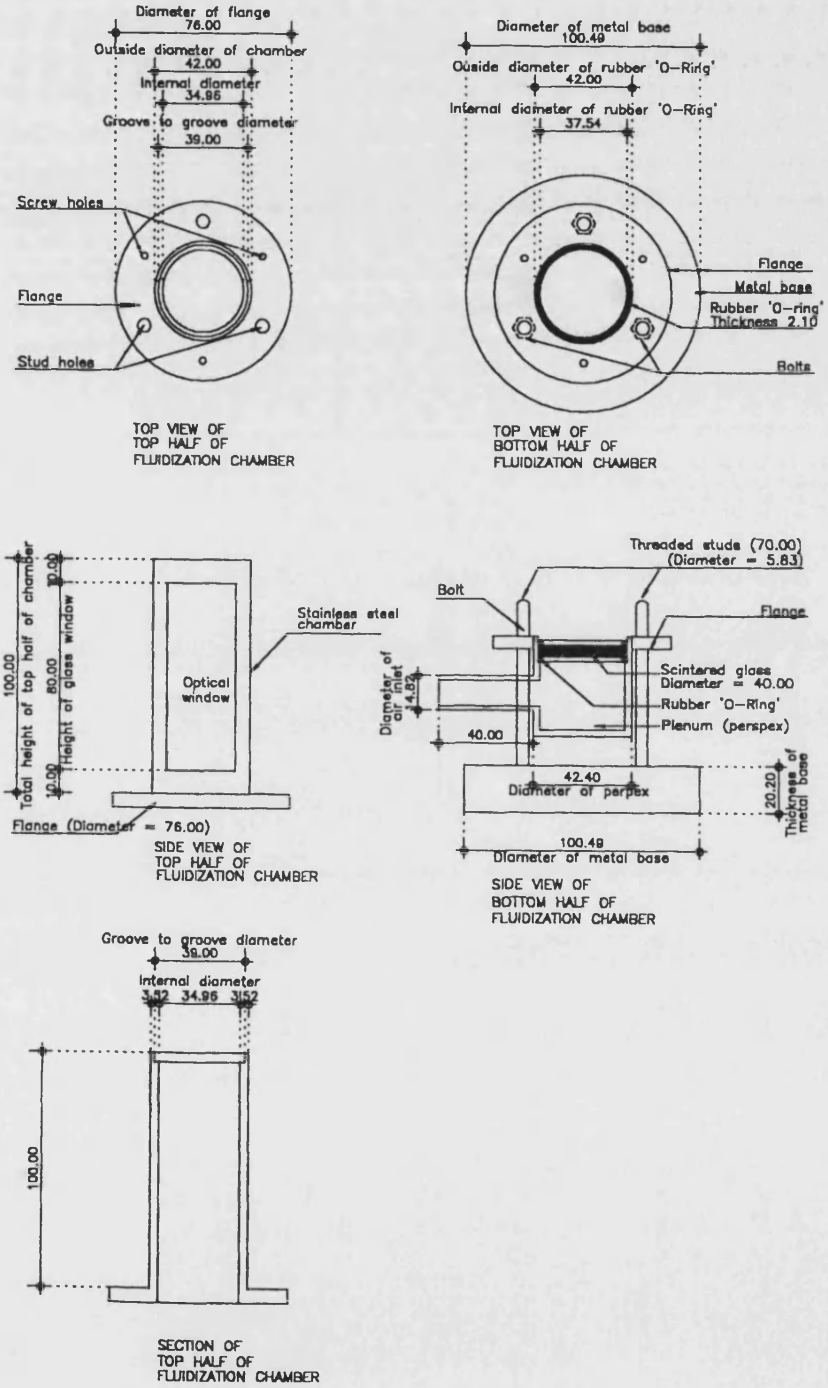

Figure 99: Detailed Dimensions of the DPAG

Appendix 11: Detailed Pressure Drop Tables Using the DPAG

DPAG Distributor Type: Sintered Glass (Porosity: 0)		
Flow Rate ($Lmin^{-1}$)	Pressure Drop (cm/H_2O)	Press Drop Range (kPa)
2.60	0.31	0.0304
4.80	0.44	0.0432
7.00	0.67	0.0661
9.60	1.01	0.0988
11.80	1.35	0.132
14.40	1.84	0.181
17.00	2.31	0.226
19.60	3.08	0.302
20.85	3.26	0.320

Table 120: Flow rate versus pressure drop for sintered glass (porosity zero).

DPAG Distributor Type: Sintered Glass (Porosity: 1)		
Flow Rate ($Lmin^{-1}$)	Pressure Drop (cm/H_2O)	Press Drop Range (kPa)
2.60	0.46	0.045453
4.80	0.95	0.092868
7.00	1.41	0.137994
9.60	2.01	0.197508
11.80	2.56	0.250809
14.40	3.15	0.309015
17.00	4.00	0.392400
19.60	4.57	0.447990
20.85	5.05	0.495405

Table 121: Flow rate versus pressure drop for sintered glass (porosity one).

DPAG Distributor Type: Sintered Glass (Porosity: 2)		
Flow Rate ($Lmin^{-1}$)	Pressure Drop (cm/H_2O)	Press Drop Range (kPa)
2.60	0.46	0.045453
4.80	0.95	0.092868
7.00	1.41	0.137994
9.60	2.01	0.197508
11.80	2.56	0.250809
14.40	3.15	0.309015
17.00	4.00	0.392400
19.60	4.57	0.447990
20.85	5.05	0.495405

Table 122: Flow rate versus pressure drop for sintered glass (porosity two).

DPAG Distributor Type: Sintered Glass (Porosity: 3)		
Flow Rate ($Lmin^{-1}$)	Pressure Drop (cm/H_2O)	Press Drop Range (kPa)
0.30	7.17	0.703377
0.80	13.59	1.333506
1.20	25.10	2.462637
1.65	38.54	3.780447
2.00	54.85	5.380458
2.55	71.38	7.002705
3.00	87.32	8.565765
3.20	93.65	9.187065
3.30	95.34	9.352854

Table 123: Flow rate versus pressure drop for sintered glass (porosity three).

DPAG Distributor Type: Sintered Glass (Porosity: 4)		
Flow Rate ($Lmin^{-1}$)	Pressure Drop (cm/H_2O)	Press Drop Range (kPa)
0.80	11.31	1.109184
1.65	25.62	2.512995
2.55	40.17	3.940350
3.45	54.27	5.323887
4.45	68.15	6.685515
4.90	75.66	7.421919
5.35	83.08	8.150475
5.80	90.30	8.858757
6.30	98.39	9.652059

Table 124: Flow rate versus pressure drop for sintered glass (porosity four).

DPAG Distributor Type: Sintered Brass (Porosity: N/A)		
Flow Rate ($Lmin^{-1}$)	Pressure Drop (cm/H_2O)	Press Drop Range (kPa)
0.80	2.21	0.216801
2.55	8.74	0.857067
3.45	11.87	1.164774
6.30	22.01	2.159508
7.25	25.56	2.507763
8.30	28.85	2.829858
11.30	40.00	3.924000
12.25	43.77	4.293510
14.00	51.62	5.063922

Table 125: Flow rate versus pressure drop for sintered brass (porosity N/A).

Appendix 12: Particle Size Distribution Curves for SAPL and Lactose.

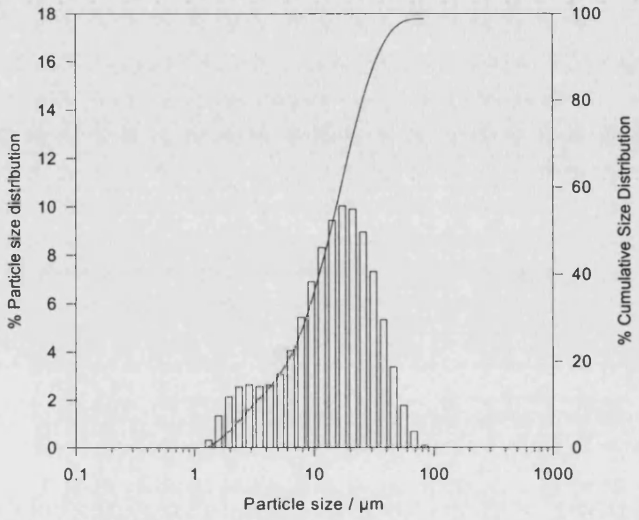

Figure 100: Particle Size Distribution of FDS.

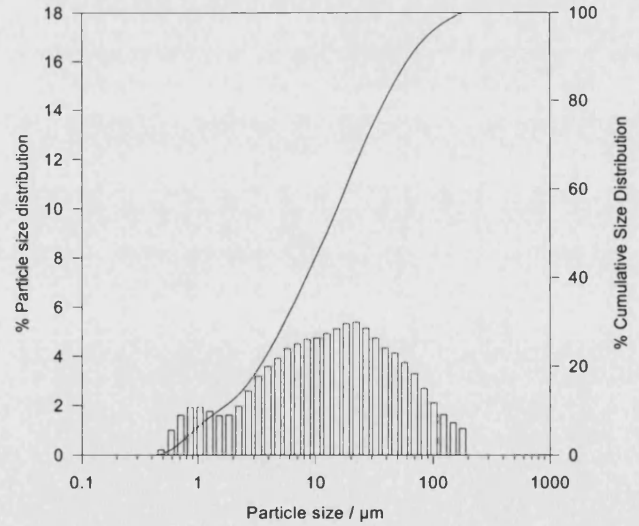

Figure 101: Particle Size Distribution of UMLFDS.

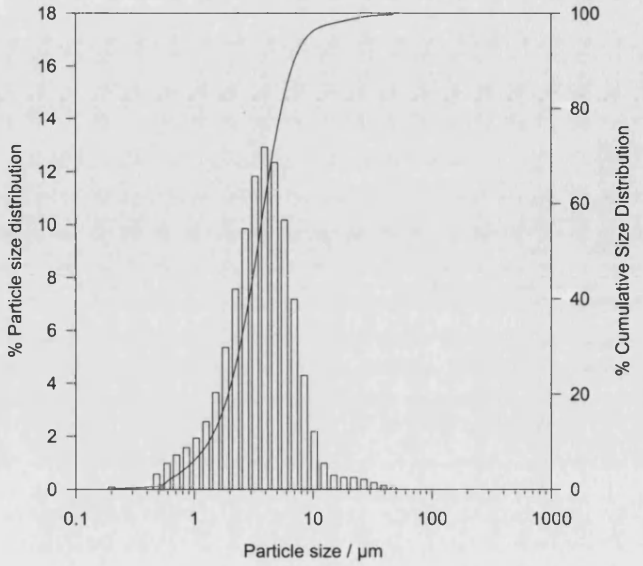

Figure 102: Particle Size Distribution of MLFDS.

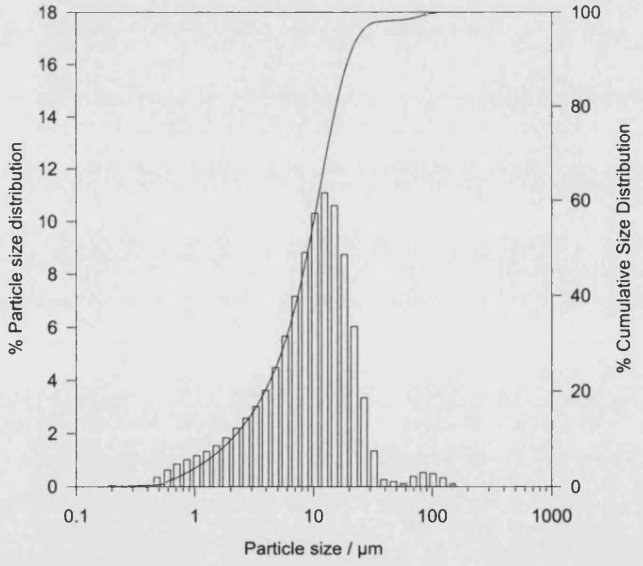

Figure 103: Particle Size Distribution of UMS.

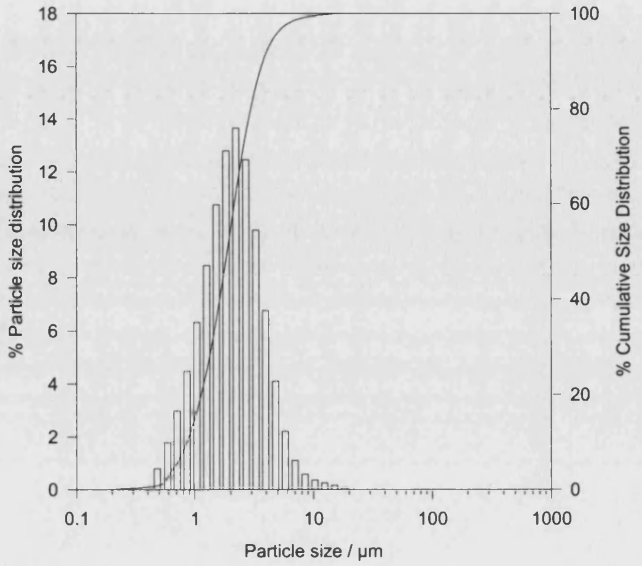

Figure 104: Particle Size Distribution of MS.

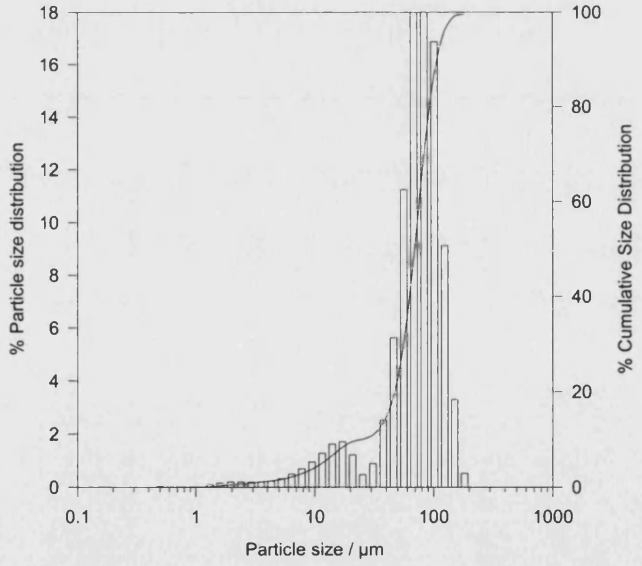

Figure 105: Particle Size Distribution of Coarse (Lactochem) Lactose (63-90µm fraction).

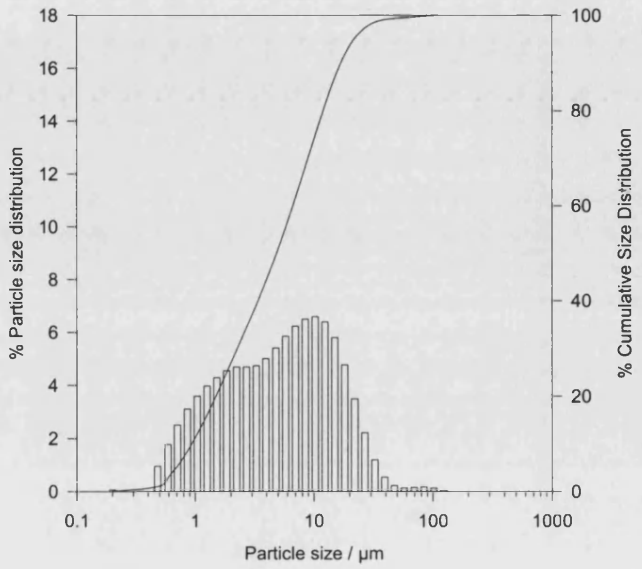

Figure 106: Particle Size Distribution of Fine (Sorbolac 400(Microtose/Pharmatose)) Lactose.

Appendix 13: MS Testing and Stability Study Raw HPLC Data

Deposition studies of ALEC, using the PA device-HPLC results

2x 100mg vials were fired into the MSLI at 100 l/min (2.0KPa pressure drop), 2 inhalations per vial.
30 seconds settling time
Sample dilutions: Adp to stg5 were washed into100ml volumetrics, then diluted as follows: adp+tht, stg1, stg2, stg3= 1:4, stg4= 1:5 diln, stg5= No diln
Chromatographic conditions: Duplicate injections at 8min per injection, PG Retention= 2.7min, DPPC+ 3.7min
Column= LiCN (10µm) 250x 4.6mm (Hichrom Ltd, UK), Column Temp= Ambient, Mobile Phase= HPLC grade Methanol
Flow rate= 1.0ml/min, Detector= PL-ELS 1000 (Polymer Labs, UK), N2 inlet pressure= 53psi, Evaporator temp= 80°C
Nebuliser Temp=80°C, Gas Flow= 0.7 SLM, Exhaust temp= 50°C
HPLC software: Borwin Chromatography Software V1.22 (JMBS developments, Grenoble, France)
HPLC Hardware: Jasco Systems Ltd, Detector software= PL-ELS 1000 V1.1

Concentration = A + B*sqrt(C+D*area)			
PG factors		DPPC factors	
A	-24.28	A	-9.1
B	0.0025	B	0.0013
C	96554501	C	61621500
D	3941	D	7621

Inj No	Sample ID	PG Area	DPPC Area	Mean PG Area	Mean DPPC Area	PG peak Area as a % of total	CF	Corrected PG as a % of total	DPPC as a% of total	Corrected Mean PG Area
1	Std1	11600	33348	11594	32620	25.8	1.16	30.0	70.0	13264
2		11588	31891			26.7	1.13	31.0	69.0	13698
3	Std 2	25608	95800	27152	95800	21.1	1.42	30.0	70.0	36885
4		28696	95799			23.0	1.30	32.8	67.2	40308
5	Std 3	46325	185251	47144	192887	20.0	1.50	30.0	70.0	72009
6		47962	200523			19.3	1.55	28.9	71.1	69480
7	Std 4	55991	245990	55793	251526	18.5	1.62	30.0	70.0	92195
8		55594	257061			17.8	1.69	28.8	71.2	88416
9	Std 5	67914	317787	66693	310413	17.6	1.70	30.0	70.0	113132
10		65472	303039			17.8	1.69	30.3	69.7	114151
11	Std 6	90141	469174	91945	469988	16.1	1.86	30.0	70.0	168580
12		93749	470801			16.6	1.81	30.9	69.1	173702
13	Tht+Adp	17868	67061	20253	64420	21.0	1.43	30.0	70.0	25402
14		22638	61778			26.8	1.12	38.2	61.8	32379
15	Stage 1	11638	30101	10514	32353	27.9	1.08	30.0	70.0	12860
16		9390	34604			21.3	1.41	23.0	77.0	9844
17	Stage 2	36911	161270	38198	160350	18.6	1.61	30.0	70.0	59564
18		39484	159429			19.8	1.51	32.0	68.0	63482
19	Stage 3	34292	137306	34758	139396	20.0	1.50	30.0	70.0	52246
20		35224	141486			19.9	1.51	29.9	70.1	52114
21	Stage 4	44054	184689	43982	185440	19.3	1.56	30.0	70.0	68826
22		43909	186190			19.1	1.57	29.7	70.3	68195
23	Stage 5	45851	189307	45967	189778	19.5	1.54	30.0	70.0	70723
24		46082	190248			19.5	1.54	30.0	70.0	70727

Sample ID	PG Conc from graph (µg/ml)	Dilution Factor	PG Deposited (mg)	DPPC Conc From Graph (µg/ml)	Dilution Factor	DPPC Deposited (mg)	Total Amount of ALEC (mg)
Throat	8.92	100	0.89	21.5	100	2.15	3.04
Stage 1	7.74	100	0.77	13.7	100	1.37	2.15
Stage 2	5.09	100	0.51	37.5	100	3.75	4.26
Stage 3	9.98	400	3.99	34.5	400	13.8	17.8
Stage 4	15.02	500	7.51	40.8	500	20.4	27.9
Stage 5	14.61	100	1.46	41.4	100	4.14	5.60
						Total	**60.7**

Fine particle fraction (mg) **51.3**
As a % of total amount fired **26.7**
As a % of total amount delivered= **84.5**

Deposition studies of ALEC, using the PA device-HPLC results

2x 100mg vials were fired into the MSLI at 100 l/min (2.0KPa pressure drop)
20 seconds settling time
Sample dilutions: Adp to stg4 were washed into100ml volumetrics, stg 5 to 50ml, then diluted as follows: adp+tht, stg1, stg2, all undiluted 3+4+5= 1:2 diln
Chromatographic conditions: Duplicate injections at 8min per injection, PG Retention= 2.7min, DPPC+ 3.7min
Column= LiCN (10µm) 250x 4.6mm (Hichrom Ltd, UK), Column Temp= Ambient, Mobile Phase= HPLC grade Methanol
Flow rate= 1.0ml/min, Detector= PL-ELS 1000 (Polymer Labs, UK), N2 inlet pressure= 53psi, Evaporator temp= 80°C
Nebuliser Temp=80°C, Gas Flow= 0.7 SLM, Exhaust temp= 50°C
HPLC software: Borwin Chromatography Software V1.22 (JMBS developments, Grenoble, France)
HPLC Hardware: Jasco Systems Ltd, Detector software= PL-ELS 1000 V1.1

Concentration = A + B*sqrt(C+D*area)			
PG factors		DPPC factors	
A	-20.07797271	A	-15.88912134
B	0.00278474	B	0.00041841
C	46267228	C	1443756895
D	3591	D	119500

Inj No	Sample ID	PG Area	DPPC Area	Mean PG Area	Mean DPPC Area	PG peak Area as a % of total	CF	Corrected PG as a % of total	DPPC as a% of total	Corrected Mean PG Area
1	Std1	13983	28119	11897	28579	33.2	0.90	30.0	70.0	12143
2		9810	29039			25.3	1.19	22.8	77.2	9232
3	Std 2	23632	81890	22956	83180	22.4	1.34	30.0	70.0	31841
4		22279	84469			20.9	1.44	28.0	72.0	29673
5	Std 3	40648	149337	40674	150297	21.4	1.40	30.0	70.0	57291
6		40700	151256			21.2	1.41	29.7	70.3	56775
7	Std 4	47695	185399	46923	190569	20.5	1.47	30.0	70.0	71247
8		46150	195738			19.1	1.57	28.0	72.0	66433
9	Std 5	56072	235131	57012	227124	19.3	1.56	30.0	70.0	85241
10		57951	219117			20.9	1.43	32.6	67.4	92591
11	Std 6	74747	354604	77118	343658	17.4	1.72	30.0	70.0	126233
12		79488	332711			19.3	1.56	33.2	66.8	139825
13	Tht+Adp	15901	65180	15500	66416	19.6	1.53	30.0	70.0	24575
14		15099	67652			18.2	1.64	27.9	72.1	22864
15	Stage 1	20822	62538	18811	57002	25.0	1.20	30.0	70.0	22744
16		16799	51465			24.6	1.22	29.6	70.4	22407
17	Stage 2	27827	125156	28573	123431	18.2	1.65	30.0	70.0	45601
18		29318	121706			19.4	1.55	32.0	68.0	48668
19	Stage 3	24519	155469	29077	150849	13.6	2.20	30.0	70.0	53978
20		33634	146228			18.7	1.60	41.2	58.8	74096
21	Stage 4	19983	81635	20797	80955	19.7	1.53	30.0	70.0	30525
22		21610	80274			21.2	1.41	32.4	67.6	32924
23	Stage 5	23948	114720	25823	112109	17.3	1.74	30.0	70.0	41379
24		27698	109497			20.2	1.49	35.1	64.9	48373

Sample ID (µg/ml)	PG Conc from graph	Dilution Factor (mg)	PG Deposited (µg/ml)	DPPC Conc From Graph	Dilution Factor (mg)	DPPC Deposited	% DPPC	Total Amount of ALEC (mg)
Throat	11.85	100	1.18	24.6	100	2.46	67.5	3.65
Stage 1	11.45	100	1.14	24.3	100	2.43	68.0	3.57
Stage 2	11.35	100	1.13	22.1	100	2.21	66.1	3.35
Stage 3	16.06	400	6.4	29.9	400	12.0	65.1	18.4
Stage 4	20.80	500	10.4	37.4	500	18.7	64.2	29.1
Stage 5	22.21	100	2.22	40.3	100	4.03	64.4	6.25
							Total	**64.3**

Fine particle fraction (mg) **53.7**
As a % of total amount fired **28.0**
As a % of total amount delivered= **83.6**

Deposition studies of ALEC, using the PA device, Penn filled vials-HPLC results

1x 100mg vials fired into the MSLI at 100 l/min (2.0KPa pressure drop). Single 4 litre inhalation.
30 seconds settle
Sample dilutions: Adp and stages 1, 2 and 5 were washed into 50ml volumetrics. Stgs 3 and 4 into 100ml volumetrics
Chromatographic conditions: Duplicate injections at 8min per injection, PG Retention= 2.7min, DPPC+ 3.7min
Column= LiCN (10µm) 250x 4.6mm (Hichrom Ltd, UK), Column Temp= Ambient, Mobile Phase= HPLC grade Methanol
Flow rate= 1.0ml/min, Detector= PL-ELS 1000 (Polymer Labs, UK), N2 inlet pressure= 53psi, Evaporator temp= 80°C
Nebuliser Temp=50°C, Gas Flow= 1.0 SLM, Exhaust temp= 50°C
HPLC software: Borwin Chromatography Software V1.22 (JMBS developments, Grenoble, France)
HPLC Hardware: Jasco Systems Ltd, Detector software= PL-ELS 1000 V1.1
Stgs 3 and 4 results using 2nd dose standards

Inj. No	Sample ID	PG Area	DPPC Area	Mean PG Area	Mean DPPC Area	PG peak area as a of total	Corr. Factor	DPPC peak area as a % of total	Corr. Factor	Corrected PG as a % of total	DPPC as a % of total	Corrected Mean PG
1	Std1	4555	8301	5210	7867	39.8	0.75	60.2	1.2	30	70	3923
2		5864	7432									
3	Std 2	7622	25240	7932	25531	23.7	1.27	76.3	0.9	30	70	10039
4		8241	25822									
5	Std 3	12526	55934	12311	54610	18.4	1.63	81.6	0.9	30	70	20076
6		12096	53286									
7	Std 4	17519	76464	18910	75802	20.0	1.50	80.0	0.9	30	70	28414
8		20301	75140									
9	Std 5	21285	99950	20465	99567	17.0	1.76	83.0	0.8	30	70	36009
10		19644	99183									
11	Tht+Adp	9163	30729	9342	30450	23.5	1.28	76.5	0.9	30	70	11937
12		9520	30170									
13	Stage 1	4300	17461	4702	17847	20.9	1.44	79.1	0.9	30	70	6765
14		5103	18233									
15	Stage 2	14280	64128	14150	63225	18.3	1.64	81.7	0.9	30	70	23212
16		14019	62322									
17	Stage 3	63782	227659	63320	228663	21.7	1.38	78.3	0.9	30	70	87595
18		62857	229667									
19	Stage 4	34318	94773	34805	93391	27.1	1.10	72.9	1.0	30	70	38459
20		35292	92008									
21	Stage 5	5339	24500	6995	23445	23.0	1.31	77.0	0.9	30	70	9132
22		8650	22389									

Concentration = A + B*sqrt(C+D*area)			
PG factors		DPPC factors	
A	1.6537545	A	3.8581856
B	0.0029797	B	0.0034758
C	-4506157	C	-18026538
D	1678	D	2877

Sample ID	Upper cut-off (µm)	Effective cut-off (µm) (µm)	PG Conc from graph (µg/ml)	Dilution Factor	PG Deposited (mg)	DPPC Conc From Graph (µg/ml)	Dilution Factor	DPPC Deposited (mg)	% DPPC	Total Amount of ALEC (mg)
Throat	n/a	n/a	13.4	50	0.67	32.9	50	1.64	71.0	2.31
Stage 1	n/a	10.07	9.45	50	0.47	23.9	50	1.20	71.7	1.67
Stage 2	10.07	5.27	19.1	50	0.96	48.4	50	2.42	71.6	3.37
Stage 3	5.27	2.40	37.2	100	3.7	91.8	100	9.18	71.1	12.9
Stage 4	2.40	1.32	24.7	200	4.9	58.9	200	11.8	70.4	16.7
Stage 5	1.32	0.00	11.5	50	0.6	28.3	50	1.41	71.2	1.99

Mass fired into device (mg)	**77.0**
Emitted dose (mg)	**39.0**
Emitted dose (% of fired)	**50.6**
Fine particle dose (mg)	**31.6**
FPD as a % of total amount fired	**41.1**
Fine particle fraction (%)	**81.1**

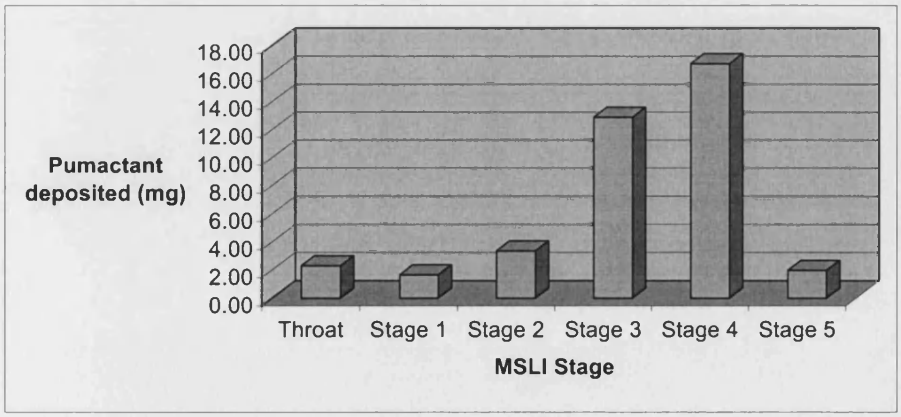

Deposition studies of ALEC, using the PA device, Penn filled vials-HPLC results

1x 100mg vials fired into the MSLI at 100 l/min (2.0KPa pressure drop). Single 4 litre inhalation.
30 seconds settle
Sample dilutions: Adp and stages 1, 2 and 5 were washed into 50ml volumetrics. Stgs 3 and 4 into 100ml volumetrics
Chromatographic conditions: Duplicate injections at 8min per injection, PG Retention= 2.7min, DPPC+ 3.7min
Column= LiCN (10µm) 250x 4.6mm (Hichrom Ltd, UK), Column Temp= Ambient, Mobile Phase= HPLC grade Methanol
Flow rate= 1.0ml/min, Detector= PL-ELS 1000 (Polymer Labs, UK), N2 inlet pressure= 53psi, Evaporator temp= 80°C
Nebuliser Temp=50°C, Gas Flow= 1.0 SLM, Exhaust temp= 50°C
HPLC software: Borwin Chromatography Software V1.22 (JMBS developments, Grenoble, France)
HPLC Hardware: Jasco Systems Ltd, Detector software= PL-ELS 1000 V1.1
Stgs 3 and 4 results using 2nd dose standards

Inj No	Sample ID	PG Area	DPPC Area	Mean PG Area	Mean DPPC Area	PG peak Area as a % of total	Correction Factor	DPPC peak area as a % of total	Correction Factor	Corrected PG as a % of total	DPPC as as a % of total	Corrected Mean PG Area	Corrected Mean DPPC Area
1	Std1	2868	6692	3255	6480	33.4	0.90	66.6	1.1	30	70	2920	6814
2		3641	6268										
3	Std 2	7861	26050	8714	24870	25.9	1.16	74.1	0.9	30	70	10075	23508
4		9566	23690										
5	Std 3	18125	71893	18434	69722	20.9	1.43	79.1	0.9	30	70	26447	61709
6		18743	67551										
7	Std 4	28078	111392	27969	108188	20.5	1.46	79.5	0.9	30	70	40847	95310
8		27860	104983										
9	Std 5	32720	141561	30881	145269	17.5	1.71	82.5	0.8	30	70	52845	123305
10		29041	148977										
11	Std 6	50967	259783	51803	248848	17.2	1.74	82.8	0.8	30	70	90195	210455
12		52638	237912										
13	Std 7	73329	380294	70163	373622	15.8	1.90	84.2	0.8	30	70	133135	310649
14		66997	366949										
15	Tht+Adp	11037	35946	11475	35641	24.4	1.23	75.6	0.9	30	70	14135	32981
16		11912	35336										
17	Stage 1	6731	17215	7236	16750	30.2	0.99	69.8	1.0	30	70	7196	16790
18		7741	16284										
19	Stage 2	22879	85742	20626	84384	19.6	1.53	80.4	0.9	30	70	31503	73506
20		18372	83025										
21	Stage 3	36601	146911	34278	148268	18.8	1.60	81.2	0.9	30	70	54764	127782
22		31955	149624										
23	Stage 4	17030	68503	16200	68072	19.2	1.56	80.8	0.9	30	70	25281	58990
24		15369	67640										
25	Stage 5	5539	9459	5291	10613	33.3	0.90	66.7	1.0	30	70	4771	11133
26		5043	11767										

Concentration = A + B*sqrt(C+D*area)			
PG factors		DPPC factors	
A	1.6537545	A	3.85818561
B	0.0029797	B	0.003475843
C	-4506157	C	-18026538
D	1678	D	2877

Sample ID	Upper cut-off (µm)	effective cut-off (µm)	PG Conc from graph (µg/ml)	Dilution Factor	PG Deposited (mg)	DPPC Conc From Graph (µg/ml)	Dilution Factor	DPPC Deposited (mg)	% DPPC	Total Amount of ALEC (mg)
Throat	n/a	n/a	14.71	50	0.7	35.8	50	1.8	70.9	2.5
Stage 1	n/a	10.07	9.85	50	0.5	22.9	50	1.1	70.0	1.6
Stage 2	10.07	5.27	22.37	50	1.1	56.0	50	2.8	71.4	3.9
Stage 3	5.27	2.40	29.51	100	3.0	74.1	100	7.4	71.5	10.4
Stage 4	2.40	1.32	20.00	100	2.0	50.2	100	5.0	71.5	7.0
Stage 5	1.32	0.00	7.23	50	0.4	16.2	50	0.81	69.1	1.2

Mass fired into device (mg)	**71.8**
Emitted dose (mg)	**26.6**
Emitted dose (% of fired)	**37.1**
Fine particle dose (mg)	**18.6**
FPD as a % of total amount fired	**25.8**
Fine particle fraction (%)	**69.7**

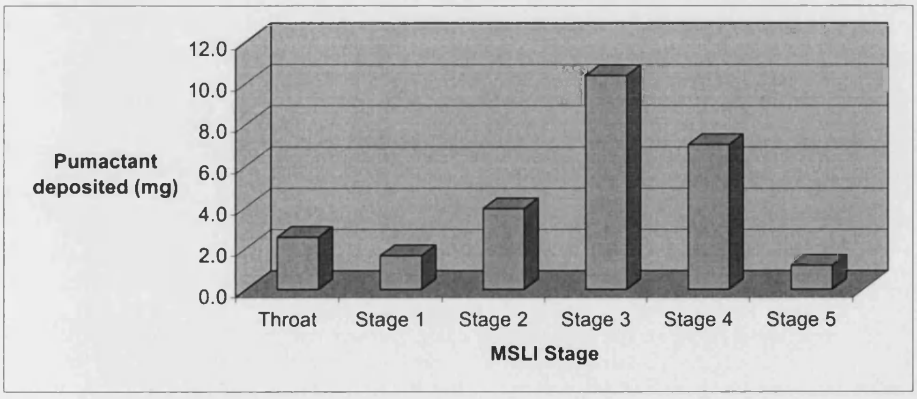

Appendix 14: Additional Information on SAPL

General Info about SAPL

(a) Transition temperature of SAPL is 34°C and higher. This is the temperature at which the surfactant spreads instantaneously over given surface to form the monolayer. More specifically, the transition temperature of DPPC is 40°C, and of PG is 31°C. When these components are mixed in the ratio of 7:3, the transition temperature becomes 34°C.

(b) Molecular formula and molecular weight of PG are dependent on the composition of its acyl substituents, which in turn is dependent on the source of purified lecithin used as raw material in the synthesis of PG. R_1 and R_2 are 5 fatty acids, C16:0, C18:0, C18:1, C18:2 and C20:4, in the approximate proportions 40, 10, 30, 20 and 3% respectively.

(c) DPPC has a single chiral centre at the 2-position in the glycerol backbone. PG has two chiral centres, one at the 2-position of the glycerol head group and the other at C2 in the glycerol backbone.

(d) Since there are several different acyl chain groups as well as two chiral centres, PG is theoretically a mixture of a considerable number of optical isomers.

(e) Nycomed-Amersham, UK manufactures SAPL. Synthesis of DPPC involves five steps, whereas PG is manufactured via two steps. The two components are mixed in a 7:3 ratio, dissolved in chloroform, filtered and freeze-dried.

Appendix 15: Structures of Lipids

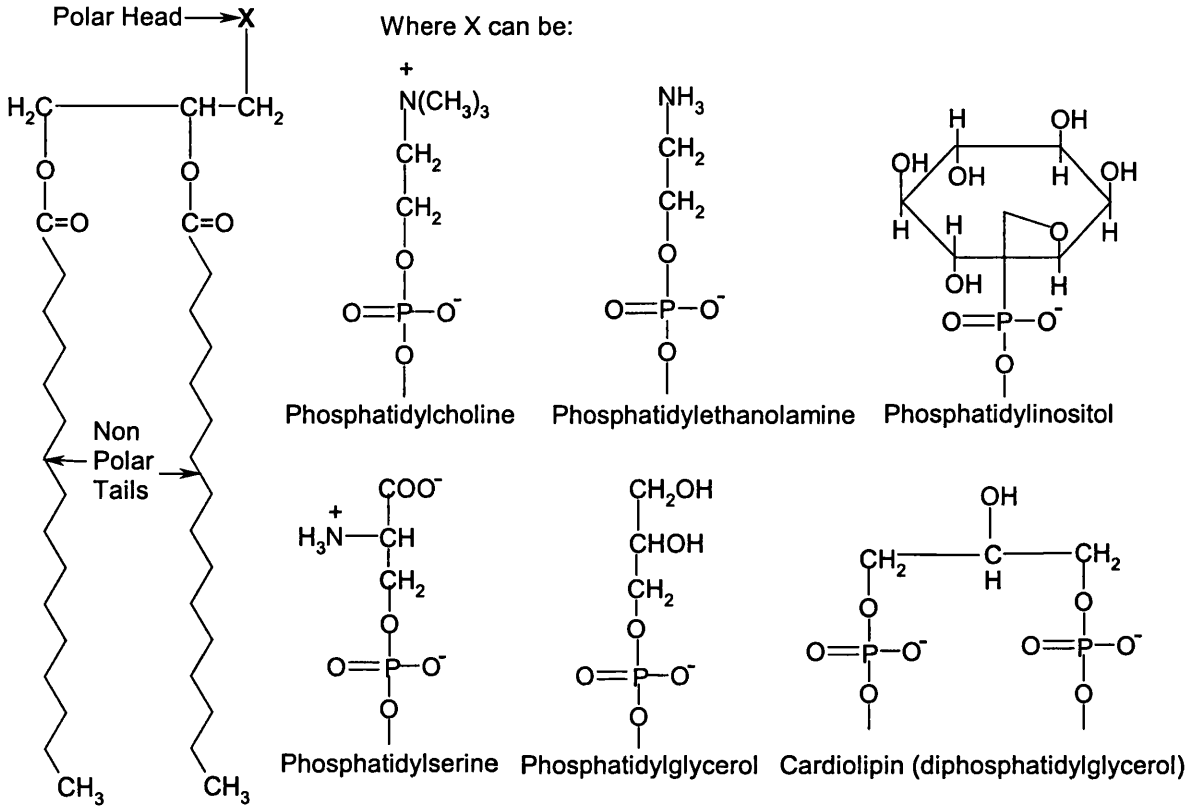

Figure 107: The General Structure of Phospholipids and the Various Head Groups.

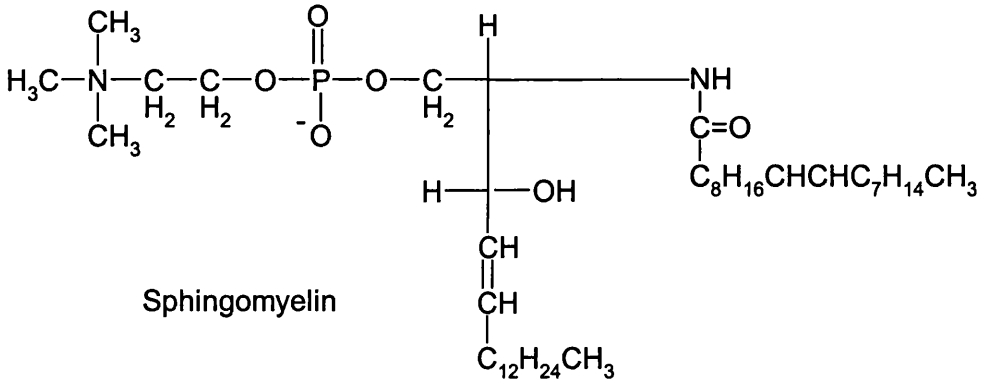

Figure 108: The Structure of Sphingomyelin.

References

Adkins J., and Brogden R. (1998). Zafirlukast: A Review of its Pharmacology and Therapeutic Potential in the Management of Asthma. *Drugs*, **55(1)**, 121-144.

Amirav I., Goren A., and Pawlowski N.A. (1994). What do Paediatricians in Training know about the Correct use of Inhalers and Spacer Devices ? J. *Allergy Clin. Immunol*, **94**, 669-674.

Anderson G. (1998). Review of Dry Powder Inhaler Technology. Management Forum, 2-Day International Conference, London.

Annapragada A., and Adjei A. (1996). An analysis of the Fraunhofer diffraction method for particle size distribution analysis and its application to aerosolised sprays. *Int. J. Pharm.*, **127**, 219-227.

Anzueto A., Jubran A., Ohar J.A., Piquetter C.A., Rennard S.I., Colice G., Pattishall E.N., Barrett J., Engle M., Perret K.A., and Rubin B.K. (1997). Effect of aerosolised surfactant in patients with stable chronic bronchitis. *JAMA*, **278 (17)**, 1426-1431.

Anzueto A., Baughman R., Guntupali K., and DeMaria E (1994). An International, Randomised, Placebo-Controlled Trial Evaluating the Safety and Efficacy of Aerosolised Surfactant in Patients with Sepsis-Induced ARDS. *Am. J. Respir. Crit. Care Med.*, **149(Suppl. PT2 of 2)**, A567

Ashbaugh D.G., Bigelow D.B, Pett, T.L, and Lane B.E. (1967). Acute respiratory Distress Syndrome in Adults. *Lancet*, **2**, 319-323.

Asking L., Olsson B. (1997). Calibration at Different Flow Rates of a Multi-Stage Liquid Impinger. *Aerosol Sci & Technol.*, **27**, 39-49.

Avery M.E., and Mead J. (1959). Surface properties in Relation to Atelectasis and Hyaline Membrane Disease. *Am. J. Dis. Child.*, **97**,517-523.

Babic I., Roy S., *et al* (1996). Changes in Microbial populations on Fresh Cut Spinach. *Int. J. Food Microbiol.*, **31**, 107-119.

Baerns M. (1966) Effect of Interparticulate Adhesive Forces on Fluidisation of Fine Particles. *I&EC Fund.*, **5(4)**, 508-516.

Bailey A. (1984). Electrostatic Phenomena During Powder Handling. *Powder Technol.*, **37**, 71.

Balachandran W., Ahmad C.N., and Barton S.A. (1991). Deposition of Electrically Charged Drug Aerosols in the Lungs. *Inst. Phys. Conf. Ser.*, **No 118**, Section 1.

Balachandran W. (1987). Electrostatic Effects in the Adhesion of Particles to Solid Surfaces. In: Briscoe B.J., and Adams M.J., (Eds). Tribology, Interparticulate Technology. Adam Hilger, Bristol and Philadelphia, pp 135-153.

Balaraman V., Meister J., Ku T., and Sood S. (1998). Lavage Administration of Dilute Surfactants After Acute Lung Injury in Neonatal Piglets. *Am. J. Respir. Crit. Care Med.*, **158(1)**, 12-17.

Bangham A.D. (1998). Artificial Lung Expanding Compound (ALEC). In: Lasic D. and Papahadjopoulos D. (Eds). Medical Applications of Liposomes, Elsevier, Amsterdam, pp 455-472

Bangham A.D. (1987). Lung Surfactant: How it Does and Does Not Work. *Lung*, **165**, 17-25.

Bangham A. and Horne R. (1964). Negative Staining of Phospholipids and their Structural Modification by Surface Active Agents as Observed in the Electron Microscope. *J. Mol.Biol.*, **8**, 660-668.

Bangham A., and Dawson R. (1959). The Relationship Between the Activity of Lecithinase and the Electrophoretic Charge of the Substrate. *Biochem. J.*, **72**, 486-492.

Barnes P.J., and Thompson N.C. (1992). Other Therapies Used in Asthma. In: Barnes P.J., Rodger I.W., and Thompson N.C., (Eds). Asthma, Blackwell publishing, UK., 659-666.

Barnes P.J., Rodger I.W., and Thompson N.C, (1989). Asthma: Basic Mechanisms and Clinical Management. Academic press, London.

Barrow R.E., and Hills B.A. (1979). A Critical Assessment of the Wilhelmy Method in Studying Lung surfactants. *J. Physiol.*, **295**, 217-227.

Batenburg J. (1995). Biosynthesis, Secretion, and Recycling of Surfactant Components. In: Robertson B., and Taeusch H., (Eds). Surfactant Therapy for Lung Disease, Marcel-Dekker, USA, pp 47-64.

Beck D.E. (1997). The Role of Seprafilm^{TM} Bioresorbable Membrane in Adhesion Prevention. *Eur. J. Surg.*, **577(Suppl)**, 49-55.

Beckett A., and Read N. (1986). Low Temperature Scanning Electron Microscopy. In: Aldrich H.C., and Todd W.J. (Eds). Ultrastrucrural Techniques for Micro-organisms. Plenum, NY, USA, pp 45-86.

Bell J., and Treneman B. (1994). Design and engineering of dry powder inhalers. *Respir. Drug. Del. IV*, 93-98.

Bell J.H., Brown K., and Glasby J. (1973). Variation in Delivery of Isoprenaline from various Pressurized Inhalers. *J. Pharm. Phamsc.*, **25 Suppl.**, 32P-36P.

Bersten A., Davidson K., Nicholas T., and Doyle I. (1998). Respiratory Mechanics and Surfactant in the Acute Respiratory Distress Syndrome. *Clin. Exper. Pharmacol. Physiol.*, **25(11)**, 955-963.

Bergbreaker D.E. (1990). Effect of solvent polarity in functionalised polyctisine- solution interfaces. *Am. Chem. Soc., Macromolecules*, **23 (3)**, 764-769.

Bernard G., Artigas A., Brigham K., Carlet J., Falke K., and Hudson L. (1994). The American-European Consensus Conference on ARDS. *Am. J Respir. Crit. Care Med.*, **149**, 818-824.

Bernstein J.A., and Bernstein I.L. (1993). Cromolyn and Nedocromil. *Immunol. Allergy Clin. NA.*, **13(4)**, 891-902.

Birken E., and Silen M (1973). Surface Tension Lowering Substance of the Eustachian Tube in Non-Suppurative Otitis Media: An Experiment with Dogs. *Laryng.*, **83**, 255-258.

Bolton S. (1996). Pharmaceutical Statistics: Practical and Clinical Applications, 3rd Edition, Marcel Dekker Inc., N.Y.

Borgstrom L., Asking L., Beckman O., Bondesson E., Kallen A., and Olsson B. (1996). Dose variation, within and between individuals, with different inhalation systems. *Respir. Drug Del V*, 19-24.

Bowman, W.C., and Rand, M.J., (1980). Textbook of Pharmacology. Blackwell Scientific Publications, London.

Brain J.D., and Blanchard J.D. (1993). Particle Size Analysis of Therapeutic Aerosols. In: Moren F., Dolovich M.B., Newhouse M.T., and Newman S.P., (Eds). Aerosols in Medicine: Principles, Diagnosis and Therapy. Elsevier, Amsterdam, pp 117-124.

Brain J., Valberg P., and Sneddon S. (1985). Mechanisms of Aerosol Deposition and Clearance. In: Moren F., Dolovich M.B., and Newhouse M.T., (Eds). Aerosols in Medicine: Principles, Diagnosis and Therapy. Elsevier, Amsterdam, pp 123-130.

Braun M., Oschmann R., and Schmidt P. (1996). Influence of Excipients and Storage Humidity on the Deposition of Disodium Cromoglycate in the Twin Stage Impinger. *Int. J. Pharm.*, **135**, 53-62.

British National Formulary (BNF), No 35, (1998). The Pharmaceutical Press, London, pp 122-136.

Byron P.R., (1994). Drug Delivery via the Respiratory tract. *J. Aerosol Med.*, **7** (1), 49-75.

Byron P.R., (1990). Pathophysiological and Disease Constraints on Aerosol delivery, In: Byron P.R. (Ed), Respiratory Drug Delivery. Boca Raton, FL., CRC press.

Calmanovici G. Boccio J., Lysionek A., Salgueiro M., Hager A., DePaoli T., Calcagno M., Nicolini J., Tarlati M., Caro R., and Zubillaga M. (1999). Tc-99m-ENS: A new Radiopharmaceutical for Aerosol Lung Scintigraphy. Comparison Between Different Freeze-Dried Formulations. *J. Nuc. Med.*, **40(6)**, 1080-1083.

Carson J. (1988). Overcoming Particle Segregation in the Pharmaceutical and Cosmetics Industries. *Drug Dev. and Ind. Pharm.*, **14(18)**, 2749-2758.

Carstensen J. (1993). Pharmaceutical Principles of Solid Dosage Forms. Technomic Publishing, Basel, pp 47-52.

Chan H. (ed) (1987). Autoxidation of Unsaturated Lipids. Academic Press, London, UK.

Chapman, K. (1994). The Best Method of Drug Delivery in Adults. International Respiratory Forum, Current Perspectives in Inhaled Drug Therapy, Royal Society of Medicine, London, 20-26.

Cheng Y., Plenderleith M., and Hills B.A., (1998). Influence of Surfactant on the Activity of Slowly Adapting Stretch Receptors in the Lung. *Respir. Physiol.*, **112(2)**, 135-143.

Cheng Y., Barr E., and Yeh H. (1989). A Venturi Disperser as a Dry Powder Generator for Inhalation Studies. *Inhal. Toxicol.*, **1**, 365-371.

Chowhan Z. (1995). Segregation of Particulate Solids. *Pharm. Technol.*, May, 56-70.

Chung K.F. (1986). Role of Inflammation in the Hyperactivity of the Airways in Asthma. *Thorax*, **41**, 657-662.

Clark A.R. (1995a). Medical Aerosol Inhalers: Past, Present, and Future. *Aerosol Sci. Technol.*, **23**, 374-391.

Clark A.R. (1995b). The use of laser diffraction for the evaluation of the aerosol clouds generated by medical nebulisers. *Int. J. Pharm.*, **115**, 69-78.

Clark A.R., and Hollingworth A.M. (1993). The Relationship Between Powder Inhaler Resistance and Peak Inspiratory Conditions in Healthy Volunteers-Implications for *In-Vitro* Testing. *J. Aerosol Med.*, **6(2)**, 99-110.

Clay M., and Clarke S.W. (1987). Effect of nebulised aerosol size on lung deposition in patients with mild asthma. *Thorax*, **42**, 190-194.

Clements J.A. (1962). Surface Phenomena in Relation to Pulmonary Function. *Physiologist*, **5**, 11-28.

Colacicco G. (1985). Arguments Against and Alternatives for an Extracellular Surfactant Layer in the Alveoli of Mammalian Lung. *J. Theor. Biol.*, **114**, 641.

Colbeck I. (1998). Introduction to Aerosol Science. In: Colbeck I. (Ed). Physical and Chemical Properties of Aerosols. Blackie Academic & Professional, London. pp1-30.

Conway J., Fleming J., and Holgate S.T (1997). Three-Dimensional Imaging of Inhaled Aerosols. *Eur. Respir. Rev.*, **44** (7), 180-183.

Craig D., Royall P., Kett V., and Hopton M. (1999). The Relevance of the Amorphous State to Pharmaceutical Dosage Forms: Glassy drugs and Freeze Dried Systems. *Int. J. Pharm.*, **179(2)**, 179-207.

Crompton G.K. (1991). DPIs: Advantages and Limitations. *J. Aero. Med.*, **3(4)**, 151-155.

Crompton G.K. (1982). Problems Patients Have Using Pressurised Aerosol Inhalers. *Eur. J. Respir. Dis.*, **63 (suppl 119)**, 1-4.

Culpitt S., Maziak W., Loukidis S., Nightingale J., Matthews J., and Barnes P. (1999). Effect of High-dose Inhaled Steroid on Cells, Cytokines, and Proteases in Induced Sputum in COPD. *Am. J. Resp. Crit. Care Med.*, **160(5)**, 1635-1639.

Current Perspectives in Inhaled Drug Therapy.(1994). Proceedings of a symposium held on Nov. (1994) at the Royal Society of Medicine, London.

Dalby R., and Tiano S. (1996). Medical Devices for the delivery of Therapeutic Aerosols to the Lungs. In: Hickey A.J. (Ed). Inhalation Aerosols: Physical and Biological Basis for Therapy. Marcel-Dekker Inc., New York, pp 441-467.

Davis S., Hardy J., Newman S., and Widing I. (1991). Gamma Scintigraphy in the Evaluation of Pharmaceutical Dosage Forms. *Eur. J. Nuclear Med.*, **19**, 971-986.

Diffraction Training: Windows Diffraction Training Manual (1993). Malvern Instruments Ltd., Malvern, UK.

Dobbie J.W. (1996). Surfactant Protein A and Lamellar Bodies: A Homologous Secretory Function of Peritoneum, Synovium, and Lung. *Perit. Dial. Int.*, **16(6)**, 574-481.

Dolovich J., Zinmemsn B., and Hargreaves F. (1983). Allergy in Asthma, In: Clark T.S.H, and Godfrey S., (Eds). Asthma. Chapman and Hall, London, pp 132-157.

Dunbar C., Hickey A., and Holzner P. (1998). Dispersion and Characterisation of Pharmaceutical Dry Powder Aerosols. *KONA, Powder and Particle*, **No. 16**, 7-41.

Duncan J., Ning A., and Crompton G.K. (1990). Clinical Assessment of a New Multi-Dose Non-Pressurised Multi-Dose Inhaler. *Drug Invest.*, **2**, 136-137.

Durand D., Clyman R., and Heymann M. (1985). Effects of a Protein-Free Synthetic Surfactant on Survival and Pulmonary Function in Preterm Lambs. *J. Paediatr.*, **107**, 775-780.

Edwards D., Ben-Jebria A., and Langer R. (1998a). Recent Advances in Pulmonary Drug Delivery Using Large, Porous Inhaled Particles. An Invited Review, *J. Appl. Physiol.*, **84(2)**, 15-22.

Edwards D., Chen D., Wang J., and Ben-Jebria A (1998b). Controlled- Release Inhalation Aerosols. *Respir. Drug Del. VI*, 5-Day International Conference, South Carolina, USA, pp 9-14.

Edwards D., Hanes J., and Caponetti G. (1997). Large Porous Particles for Pulmonary Drug Delivery. *Science*, **276**, 1868-1871.

Egberts J., de Winter P., and Sedin G (1993). Comparison of Prophylaxis and Rescue treatment wih Curosurf in Neonates Less Than 30 Weeks' Gestation. A Randomised Trial. *Paediatrics*, **92**, 768-774.

Elliot C., Morris A., and Cengiz M. (1981). Pulmonary Function and Exercise Gas Exchange in Survivors of Adult Respiratory Distress Syndrome. *Am. Rev. Respir. Dis.*, **123**, 492-495.

Ellis H., Morgan B.J., Thompson J., Parker M., Wilson M., and Menzies D. (1999). Adhesion-Related Hospital Readmission after Abdominal and Pelvic Surgery: A Retrospective Cohort Study. *The Lancet*, **353**, 1476-1480.

Enhorning G., Yarussi A., Rao P., and Vargas (1996). Increased Airway Resistance Due to Surfactant Dysfunction can be Alleviated With Aerosol Surfactant. *Can. J. Physiol.*, **74**, 687-691.

Enhorning G., Duffy L., and Welliver R. (1995). Pulmonary Surfactant Maintains Airway Patency of Conducting Airways in the Rat. *Am. J. Respir. Crit. Care Med.*, **151**, 554-556.

Enhorning G. (1989). Asthma, a Condition of Surfactant Deficiency. In Ekleund L., Jonson B., Malm L. (Eds). Surfactant and the Respiratory Tract. Elsevier Science Publications, Amsterdam, pp 273-281.

Ergan F.A., Notter R.H., and Shapiro D.R. (1985). Double-Blind Clinical Trial of Calf-Lung Surfactant Extract for the Prevention of Hyaline Membrane Disease in Extremely Premature Infants. *Paediatrics*, **76**, 585-592.

European Pharmacopoeia Supplement (1999). Preparations for Inhalations, 984-989.

Flament M-P., Leterme P., and Gayot A.. (1995). Factors Influencing Nebulising Efficieny. *Drug Dev. & Ind. Pharm.*, **21** (20), 2263-2285.

Fornadley J., and Burns J. (1994). The Effect of Surfactant on Eustachian Tube Function in a Gerbil Model of Otitis Media with Effusion. *Otolaryngol. Head & Neck Surg.*, **110(1)**, 110-114.

Fraisse A., Paut O., and Camboulives J. (1998). Recent Developments in Paediatric Acute Respiratory Distress Syndrome Therapy. *Arch. De Pediatrie*, **5(10)**, 1107-1121.

Frew A.J., and Holgate S.T. (1993). Clinical Pharmacology of Asthma: Implications for treatment. *Drugs*, **46**, 847-862.

Fuhrer C. (1996). Interparticulate attraction mechanisms. In: Alderborn G., and Niystrom, C. (Eds). Pharmaceutical Powder Compaction Technology. Marcel-Dekker Inc., New York.

Fujiwara T., Chida S., and Mirka T. (1980). Artificial Surfactant Therapy in Hyaline Membrane Disease. *Lancet*, **i**, 55-59.

Galdston M., and Shah D. (1967). Surface Properties and Hysteresis of Dipalmitoyllecithin in Relation to the Alveolar Lining Layer. *Biochem. Biophys. Acta,* **137**, 255.

Ganderton D. (1996). International Harmonisation: The Revision of the "Inhalanda" Monograph of the European Pharmacopoeia. *Pharmeuropa*, **8**, 245-258.

Ganong W.F., (1989). Review of Medical Physiology, 14th edition, Aplleton & Lange, Prentice-Hall Int. (UK) Ltd, London, pp 547-562.

Gatti R., Andrisamo V., Dipietra A., and Cavrini V. (1995). Analysis of Aliphatic Dicarboxylic-Acids in Pharmaceuticals and Cosmetics by HPLC with Fluoresecence detection. *J. Pharm. Biomed. Anal.*, **13(4-5)**, 589-595.

Geldart D. (1986). Characteristics of Fluidized Systems, Chapter 1, in: Gedldart D. (Ed) Gas Fluidisation Technology. John Wiley & Sons Ltd, England, pp 1-153.

Geldart D., Harnby N., and Wong A.C. (1984). Fluidisation of Cohesive Powders. *Powder Technol.*, **37**, 25-37.

Geldart, D. (1973). Types of Gas Fluidisation. *Powder Technol.*, **7**, 285-292.

Gerrity T.R (1994). Aerosol Deposition Using New Radioaerosol Imaging Techniques. *Respir. Drug Del. IV*, 179-186.

Gilliard N., Pappert D., Merritt T., and Spragg R. (1991). Radiolabeling of the Hydrophobic Components of Lung Surfactant with 3-(Trifluoromethyl)-3-(M-[125I]Iodophenyl)Diazirine. *Anal. Biochem.*, **193(2)**, 310-315.

Gonda I. (1990). Aerosols for Delivery of Therapeutic and Diagnostic Agents to the Respiratory Tract. *Crit. Rev. Ther. Drug. Carr. Sys.*, **6** (4), 273-313.

Gortner L., Bartmann P., Pohlandt F., *et al* (1992). Early Treatment of Respiratory Distress syndrome with Bovine Surfactant in Very Preterm Infants: A Multi-Centre Controlled Clinical Trial. *Pediatr. Pulmonol.*, **14**, 4-9.

Grahame G., Torchia M., *et al* (1985). Surface-Active Material In Peritoneal Effluent of CAPD Patients. *Perit. Dial. Bull.*, **April-June**, 109-111.

Greaves I., Hildebrandt J., and Hoppin F. (1986). Micromechanics of the Lung. In: Bethesda M.D. (Ed). Handbook of Physiology. The Respiratory System. Mechanics of Breathing. *Am. Physiol. Soc.* Section 3, Vol. III, Part 1, Chapter 14, pp 217-232.

Gregory T., Gadek J., Weiland J., Hyers T., Crim C., Hudson L., *et al* (1994). Survanta Supplementation in Patients in Patients with Acute Respiratory Distress Syndrome. *Am. J. Respir. Crit. Care Med.*, **149(Suppl PT2 of 2)**, A567.

Griese M., and Westerburg B. (1998). Surfactant Function in Neonates with Respiratory Distress Syndrome. *Respiration,* **65**, 136-142.

Gross N.J. (1988). Ipratropium Bromide. *N. Eng. J. Med.*, **319**, 486-494.

Grossman J., (1994). The Evaluation of Inhaler Technology. *J. Asthma*, **31** (1), 55-64.

Gunstone F., Harwood J., and Padley F. (1994). Autoxidation and Photo-Oxygenation. In: Gunstone F., Harwood J., and Padley F. (Eds). The Lipid Handbook, 2nd ed., Chapman & Hall, UK., pp 566-593.

Guyton A., Moffat D., and Adair T. (1984). Role of Alveolar Surface Tension in Transepithelial Movement of Fluid. In: Robertson B., van Golde L., and Batenburg J. (Eds.) (1984). Pulmonary Surfactant. Elsevier Science Publishers, The Netherlands, pp 171-186.

Haller C.J. (1994). A Scanning and Transmission Electron Microscopic Study of the Development of the Surface Structures of Neuroepithelial Bodies in the Mouse Lung. *Micron*, **25**, 527-538.

Hallman M., Merritt T.A, and Mannino F. (1985). Exogenous Human Surfactant for Treatment of Severe RDS: A Randomised Clinical Trial. *J. Paediatr.*, **106**, 963-969.

Hallworth G.W., and Westmoreland D.G. (1987). The Twin Stage Impinger: A Simple Device for Assessing the Delivery of Drugs from Metered Dose Pressurised Aerosol Inhalers. *J. Pharm. Pharmacol.*, **34**, 966-972.

Hardy J., Newman S., and Knoch M. (1993). Lung Deposition from Four Nebulisers. *Respir. Med.*, **87**, 461-465.

Hawgood S. (1992). The hydrophilic Surfactant Protein SP-A: Molecular Biology, Structure and Function. In: Robertson B, Van Golde L., and Batenburg J., (Eds). Pulmonary Surfactant: From molecular Biology to Clinical Practice. Amsterdam: Elsevier, pp 33-54.

Hawgood S., and Clements J.A (1990). Pulmonary Surfactant and its Apoproteins. *J. Clin. Invest.*, **86**, 1-6.

Heinig J., Boulet L., Croonenborghs L.,and Mollers M. (1999). The Effect of High-Dose Fluticasone Propionate and Budesonide on Lung Function and Asthma Exacerbations in Patients with Severe Asthma. *Respir. Med.*, **93(9)**, 613-620.

Hellmann J. (1995). Surfactant replacement therapy in neonatal respiratory distress syndrome. *Paed. Anaesthesia*, **5**, 81-88.

Herbert S., Bouchet B., Riaublanc A., Dufour E., and Gallant DJ (1999). Multiple fluorescence labelling of proteins, lipids and whey in dairy products using confocal microscopy. *LAIT*, **79(6)**, 567-575.

Herridge M., Slutsky A., and Colditz G. (1998). Has High Frequency Ventilation Been Inappropriately Discarded in ARDS ? *Crit. Care Med.*, **26(12)**, 2073-2077.

Hersey J.A. (1975). Ordered Mixing: A New Concept in Powder Mixing Practice. *Powder Technol.*, **11**, 41-44.

Hickey A., and Concessio N. (1997). Descriptors of Irregular Particle Morphology and Powder Properties. *Adv. Drug Del. Revs.*, **26**, 29-40.

Hickey A., Fults K., and Pillai R. (1992). Use of Particle Morphology to Influence the Delivery of Drugs from Dry powder Aerosols. *J. Biopharm. Sci.*, **3(1/2)**, 107-113.

Hills B.A. (1999). An Alternative View of the Role(s) of Surfactant Alveolar Model. *J. Appl. Physiol.*, **87(5)**, 1-17.

Hills B.A., and Masters I.B. (1998). "Dewatering" the Lungs. *Arch. Dis. Child Fetal Neonatal Ed.*, **80**, F78.

Hills B.A., Burke J.R., and Thomas K. (1998a). Surfactant Barrier Lining Peritoneal Mesothelium: Lubricant and Release Agent. *Perit. Dial. Int.*, **18(2)**, 157-165.

Hills Y.C., Chen Y., and Hills B.A. (1998). Quantification of the Adsorption of DPPC to Bronchial and Peritoneal Epithelium and its Promotion by PG. Paediatric Respiratory Research Centre, Mater Children's Hospital, Brisbane, Australia. Unpublished data.

Hills B.A., and Masters I.B. (1998). "Dewatering" of the Lungs at Birth. *Arch. Dis. Child Fetal Neonatal Ed.*, 79, F221-F222.

Hills B.A. (1997). How Does Surfactant Really Work ? *J. Paediat. Child Health*, **33(6)**, 471-475.

Hills B.A. (1996a). Asthma: Is There an Airway Receptor Barrier? *Thorax*, **51** (8), 773-776.

Hills B.A. (1996b). A Mechanism for Masking Receptors with Particular Applications to Asthma. *Med. Hypoth.*, **46**, 33-41.

Hills B.A. (1996c). Lubrication of Visceral Movement and Gastric Motility by Peritoneal Surfactant. *J. Gastroenterol. Hepatol.*, **11**, 797-803.

Hills B.A. (1995). Does adsorbed Surfactant Normally Mask Airway Receptors ? *Proc. Ann. Sci. Mtg TSANZ*, Hobart, Tasmania, 47

Hills B.A. (1992a). A hydrophobic Oligolamellar Lining to the Surfaces in Various Tissue: A Possible Ubiquitous Barrier. *Med. Sci. Res.*, **20**, 543-550.

Hills B.A. (1992b). Graphite-Like Lubrication of Mesothelium by Oligolamellar Pleural Surfactant. *J. Appl. Physiol.*, **73(3)**, 1034-1039.

Hills B.A (1991). Physiological Mechanisms for the Action of Pulmonary Surfactant. In: Bourbon J. (Ed). Pulmonary Surfactant: Biochemical, Functional, Regulatory, and Clinical Concepts. Boca Raton, Florida: CRC press, pp 185-223.

Hills B.A. (1990). A Physical Identity for the Gastric Mucosal Barrier. *Med J. Aust.*, **153**, 76-81.

Hills B.A. (1988). The Biology of surfactant. Cambridge University Press.

Hills B.A. (1984). Analysis of Eustachian Surfactant and its Function as a Release Agent. *Arch. Otolaryngol.*, **110**, 3-9.

Hills B.A., Butler B.D., and Lichtenberger L. (1983). Gastric Mucosal Barrier: the Hydrophobic Lining to the Lumen of the Stomach. *Am. J. Physiol. GI & Liver Physiol.*, **6**, G561-568.

Hills B.A. (1982). Water Repellency Induced by Pulmonary Surfactants. *J. Physiol.*, **325**, 175-186.

Hills B.A., Butler B.D., Barrow R.E. (1982). Boundary Lubrication Imparted by Pleural Surfactants and their Identification. *J. Appl. Physiol.*, **53**, 463-469.

Hindle M., and Byron P. (1996). Impaction and Impingement Techniques for Powder Inhalers- Comparisons, Problems and Validation. *Respir Drug Del. V*, 263-272.

Hindle M., and Bryon P.R. (1995). Size Distribution Control of Raw Materials for Dry Powder Inhalers Using the Aerosizer® with the Aero-Disperser™. *Pharm. Technol.*, **June**, 64-73.

Hindle M., Rajkumari N., and Byron P. (1994). Dose Emissions from Market Inhalers: Influence of Flow Volume and Environment. In: Byron P., Dalby R., and Farr S. (Eds), Respiratory Drug Delivery IV.

Hinds W.C. (1999). Aerosol Technology: , Behaviour and Measurement of Airborne Particles (2nd Edition). Wiley Interscience, New York.

Hinds W.C. (1982). Aerosol Technology: Properties, Behaviour and Measurement of Airborne Particles. Wiley Interscience, New York.

Hodge L., Peat J., Salome C., and Haby M. (1995). Oily Fish Consumption Reduces the Risk of Childhood Asthma. *Proc. Ann. Sci.*, Mtg. ANZ Thoracic Society, No. 38, Hobart, Tasmania.

Hodge L., Peat J., and Salome C. (1994). Increased Consumption of Polyunsaturated Oils may be a Cause of Increased Prevalence of Childhood Asthma. *Aust. NZ. J. Med.*, **24**, 727-728.

Hohlfeld J., Fabel H., and Hamm H. (1997). The Role of Pulmonary Surfactant in Obstructive Airways Disease. *Eur. Respir. J.*, **10**, 482-491.

Holgate S.T. (1998). The Bronchial Epithelium as a Key Regulator of Airway Inflammation and Remodelling in Asthma. Unpublished data.

Horsley, M. (1988). Nebuliser Therapy. *Pharm. J.*, **Jan 2**, 22-24.

Hoymann H., Hecht M., Emmendorffer A., *et al* (1998). Effect of Budesonide on Airway Hyperactivity and Inflammatory Response in Rat Model of Allergic Asthma. *Naunyn-Schmiedeberga Arch. Pharmacol.*, **358(4S3)**, 53.

Hue C., Rubio B., *et al* (1997). Expression of Hydrophilic Surfactant Proteins by Mesentery Cells in Rat and Man. *Biochem. J.*, **328(1)**, 251-256.

Ishisaka D.Y. (1996). Exogenous Surfactant Use in Neonates. *Ann. Pharmocother.*, **30**, 389-398.

Jackson W.F. (1995). Inhalers in Asthma, the New Perspective, Clinical Vision Ltd, Oxfordshire, 4-5.

Jashani R.N., Byron P.R, and Dalby R.N. (1995). Testing of Dry Powder Aerosol Formulations in Different Environmental Conditions. *Int. J. Pharm.*, **113**, 123-130.

Jager-Waldau R., Mehring H., and Wiggins J. (1994). Feasibility of a Low Dosage Dynamic Powder Disperser for Drug Delivery to the Lungs. *J. Aerosol Med.*, **7**, 205-208.

Johanson K. (1996). Predicting Segregation of Bimodal Particle Mixtures Using the Flow Properties of Bulk Solids. *Pharm. Technol. Eur.*, **1(8)**, 38-44.

Johnson K.A. (1997). Preparation of Peptide and Protein Powders for Inhalation. *Adv. Drug Del Rev.*, **26**, 3-15.

Jones K.D. (1990). Markers for Impending ARDS. *Respiratory Med*, **84**, 89-91.

Juhn S., and Huff J. (1976). Biochemical Chjaracteristics of Middle Ear Effusions. *Ann. Otol., Rhinol. Laryngol.*, **Suppl. 25, 85,** 103-109.

Kakuta Y., Sasaki H., and Takishima T. (1991). Effect of Artificial Surfactant on Ciliary Beat Frequency in Guinea Pig Trachea. *Respir. Physiol.*, **83**, 313-321.

Kaliner M.A. (1990). Inhaled Corticosteroids for Chronic Asthma. *Am. Fam. Physician*, **42(6)**, 1609-1616.

Kappas A., Barsoum G., *et al* (1992). Prevention of Peritoneal Adhesions in Rats with Verapamil Hydrocortisone Sodium Succinate and Phosphatidylcholine. *Eur. J. Surg.*, **158**, 33-35.

Karra V., and Fuerstenau D. (1977). The Effect of Humidity on the Trace Mixing Kinetics in Fine Powders. *Powder Technol.*, **16**, 97-105.

Kassem N., and Ganderton D. (1990). The Influence of Carrier Surface on the Characteristics of Inspirable Powder Aerosols. *J. Pharm. Pharmacol.*, **42(Suppl)**, 11p.

Katzenstein A.L. (1982). Diffuse Alveolar Damage, In: James, L., Bennington, M., (Eds), Surgical Pathology of Non-Neoplastic Lung Disease, Saunders, Philadelphia, pp 9-42.

Kay A.B. (1991). Asthma and Inflammation. *J. Allergy Clin. Immunol.*, **87**, 892-910.

Kaye B.H. (1999). Characterisation of Powders and Aerosols. Wiley-VCH Verlag GmbH, Weinheim, Germany.

Keeder W.H., and MacKey G.S. (1950). Nebulised Cortisone in Bacterial Pneumonia. *Dis. Chest*, **18**, 528-534.

Kennedy M., Phelps D., and Ingenito E. (1997). Mechanisms of Surfactant Dysfunction in Early Acute Lung Injury. *Expt. Lung Res.*, **23**, 171-189.

Klug H., and Alexander L. (1974). X-Ray Diffraction Procedures- for Crystalline and Amorphous Material. Wiley Interscience, UK.

Knoch M., and Wunderlich E. (1994). *In-Vitro* Assessment of a New Efficient Nebuliser System for Continuous Operation. *Respir. Drug Del. IV*, 265-271.

Kohler D., Fleischer W., and Mathys H. (1988). A New Method for Easy Labelling of β_2-Agonists in the MDI with 99m-TC. *Respiration*, **53**, 65.

Kondoh Y., and Takano S. (1987). Analysis of Acylglycerols by HPLC with Postcolumn Derivatization, 4 Simultaneous Analysis of Mono-Acylglycerol, Di-Acylglycerol and Triacylglycerol. *J. Chromatog.*, **393 (3)**, 427-432.

Konty M.J., and Mulski C.A. (1989). Gelatine Capsules: Brittleness as a Function of Relative Humidity at Room Temperature. *Int. J. Pharm.*, **54**, 79-85.

Kraut T.H., Drtina P., Knoch M., and Frohn, A. (1990). Size Distribution of a Medical Respirator- Comparison of Two Light-Scattering Measurement Techniques. *J. Aerosol Sci.*, **21 (suppl 1)**, s543-s546.

Kulvanich P., and Stewart P. (1988). Influence of Relative Humidity on the adhesive Properties of a Model Interactive system. *J. Pharm. Pharmacol.*, **40**, 453-458.

Kurashima K., Fujimura M., Matsuda, and Kobayashi T. (1997). Surface Activity of Sputum from Acute Asthmatic Patients. *Am J Respir Crit Care Med.*, **155**, 1254-1259.

Kurashima K., Ogawa H., Ohka T., Fujimura M., Matsuda T., and Kobayashi T. (1991). A Pilot Study of Surfactant Inhalation for the Treatment of Asthmatic Attack. *Jpn. J. Allergol.*, **40** (2), 160-163.

Kumar P.J., and Clark M.K. (1990). Clinical Medicine, 2nd edition, Bailliere Tindall, London., 627-704.

Kwong M., Egan E, Notter R., and Shapiro D (1985). Double-Blind Clinical trial of Calf Lung Surfactant Extract for the Prevention of Hyaline Membrane Disease in Extremely Premature Infants. *Paediatrics*, **76**, 585-592.

Lacey P. (1954). Developments in the Theory of Particle Mixing. *J. Appl. Chem.*, **4**, 257-268.

Lachmann B., and van Daal G.J. (1992). ARDS: Animal Models in: Pulmonary Surfactant; From Molecular Biology to Clinical Practice, Robertson, B. (Ed): Elsevier Science Publications, Holland, pp 635-636.

Lachmann B. (1989). Animal Models and Clinical Pilot Studies of Surfactant Replacement in Adult Respiratory Distress Syndrome. *Eur. Respir. J.*, **3(Suppl)**, 98s-103s.

Lai F., and Hersey J. (1979). A Cautionary Note on the Use of Ordered Powder Mixes in Pharmaceutical Dosage Forms. *J. Pharm. Pharmacol.*, **31**, 800.

Lalor C., and Hickey A. (1998). Pharmaceutical Aerosol for Delivery of Drugs to the Lungs. In: Colbeck I. (Ed). Physical and Chemical Properties of Aerosols. Blackie Academic & Professional, London, pp 391-421.

Lasic D. (1993). Liposomes- From Physics to Applications. Elsevier Science B.V., Amsterdam, the Netherlands.

Lee J., Turner J.S., Morgan C.J., Keogh B.I, and Ewans T.W. (1994). ARDS: Has There been a Change in Outcome of Predictive Measure? *Thorax*, **49**, 597-597.

Lehninger A.L. (1976). Biochemistry, 2nd Ed., New York, Worth.

Lemons L., Blackmon L., Kanto W., and MacDonald H. (1999). Surfactant Replacement Therapy for Respiratory Distress Syndrome. *Paediatrics*, **103(3)**, 684-685.

Lemarchand P., Chinet T., and Collignon M. (1992). Bronchial clearance of DTPA is Increased in Acute Asthma but not in Chronic Asthma. *Am. Rev. Respir. Dis.*, **145**, 147-152.

Lewis J.F., and Veldhuizen R.A.W. (1995). Factors Influencing Efficacy of Exogenous Surfactant in Acute Lung Injury. *Biol. Neonate*, **67 (Suppl 1)**, 48-60.

Lewis R., Fleming J., Balachandran W., and Tattersfield A. (1981). Particle size distribution and deposition from a jet nebuliser: Influence of humidity and temperature. *Clin. Sci.*, **62**, 5p-11p.

Lichtenberger L., Richards J., and Hills B.A. (1985). Effects of Prostaglandin (PGE^2) on the Surface Hydrophobicity of Asprin-Treated Canine Gastric Mucosa. *Gastroenterology*, **88**, 308-314.

Liu M., Wang L., Holm B.A., and Enhorning G. (1997). Dysfunction of Guinea-Pig Pulmonary Surfactant and Type II Pneumocytes After Repetitive Challenge with Aerosolised Ovalbumin. *Clin. Expt. Allergy*, **27**, 802-807.

Liu M., Wang L., and Enhorning G. (1996). Pulmonary Surfactant Given Prophylactically Alleviates an Asthma Attack in Guinea-Pigs. *Clin. Expt. Allergy*, **26**, 270-275.

Liu M., Wang L., and Enhorning G. (1995). Surfactant Dysfunction Develops When the Immunised Guinea-Pig is Challenged with Ovalbumin Aerosol. *Clin. Expt. Allergy*, **25**, 1053-1060.

Liu M., Wang L., Li E., and Enhorning G. (1991). Pulmonary Surfactant Will Secure Free Airflow Through a Narrow Tube. *J. Appl. Physiol.*, **71**, 742-748.

Lodge JP, and Chan TL (1986). The Cascade Impactor, *Am. Ind. Hyg. Assoc.*, ISBN 0932627-24-2, 80.

Lord J., and Staniforth J. (1996). Particle Size Effects on Packing and Dispersion of Powders. *Respir. Drug Del. V*, International Conference, pp 75-84.

Lord J.D. (1993). Particle Interactions in Dry Powder Inhalations. PhD Thesis, University of Bath, School of Pharmacy and Pharmacology.

Lowell S., and Shields J. (1984). Powder Surface Area and Porosity. Chapman and Hall, N.Y., USA.

Lucas P., Anderson K., and Staniforth J. (1997). Protein Deposition from Dry Powder Inhaler: Fine Particle Lactose and Polyethylene Glycol as Performance Modifiers. *Drug Del. to the Lungs VIII*, 2-Day International Conference, London, pp 18-21.

Luce J.M. (1998). Acute Lung Injury and the Acute Respiratory Distress Syndrome. *Crit. Care Med.*, **26(2)**, 369-376.

Mancini F., Miniati E., and Montanari L. (1997). Performance of Some Evaporative Light Scattering Detectors (ELSD) in the Analysis of Triglycerides and Phospholipids. *Italian J. Food Sci.*, **9(4)**, 323-336.

Marks L., Nolher R. Oberdogster G., and McBride J. (1983). Ultrasonic and Jet Aerosolisation of Phospholipids and the Effect on Surface Activity. *Paediatr. Res.*, **17**, 742-747.

Maw R., and Wilks J. (1999). Early Surgery Compared with Watchful Waiting for Glue Ear and Effect on Language Development In Preschool Children: A randomised Trial. *Lancet*, **353**, 960-963.

May K.R. (1966). The Multi-Stage Liquid Impinger. *Bacteriological Reviews*, **30**, 559-570.

McCallion O., Taylor K., Bridges P., Thomas M., and Taylor A. (1996). Jet Nebulisers for Pulmonary Drug Delivery. *Int. J. Pharm.*, **130**, 1-11.

McFadden R.G., Borron P., Fraher L., Lewis J., and Possmayer F. (1994). Pulmonary Surfactant Protein-A Alter *In-Vitro* Human Lymphocyte Proliferation and Cytokine Production. *Am. J. Respir. Crit. Care Med.*, **149(4)**, A679.

McHugh L., Milberg J., and Whitcomb M. (1994). Recovery of Function in Survivors of the Acute Respiratory Distress Syndrome. *Am. J. Respir. Crit. Care Med.*, **150**, 90-94.

Meakin B.J. (1998). Fine Particle Dose Control of Solution Based pMDIs. *Management Forum*, 2-Day International Conference, London.

Medicines Control Agency-Department of Health (1998). EuroDirect: Note for Guidance on Dry Powder Inhalers. MCA EuroDirect Publication No: 158/96(QWP), 1-6.

Menzies D., and Ellis H. (1990). Intestinal Obstruction from Adhesions: How Big is the Problem ? *Ann. R. Coll. Surg. Engl.*, **72**, 60-63.

Messent M., and Griffiths M. (1992). Pharmacotherapytherapy in Lung Injury. *Thorax*, **47**, 651-656.

Miller N.C. (1990). The Effects of Water in Inhalation Suspension Aerosol Formulations. In: Byron, P.R., (Ed). *Respir. Drug Del.* Boca Raton: CRC Press, Appendix 250-257.

Milner A.D. (1993). How Does Exogenous Surfactant Work ? *Arch. Dis. Child.*, **68**, 253-254.

Montgomery A., Stager M., and Carrico C. (1985). Causes of Mortality in Patients with Adult Respiratory Distress Syndrome. *Am. Rev. Respir. Dis.*, **132**, 485-489.

Morley C.J, and Morley, R. (1990). Follow-up of Premature Babies Treated with SAPL. *Archives of Diseases in Childhood*, **65**, 667-669.

Morley C.J.(1988). Surfactant Therapy for Very Premature Babies. *Br. Med. Bull.*, **44**, 919-934.

Morley C.J. (1987). Surfactant Substitution in the Newborn by Application of Artificial Surfactant. *J. Paediatr. Med.*, **15**, 469-478.

Nakaya T, and Li Y. (1999). Phospholipid Polymers. *Prog. Polymer Sci*, **24(1)**, 143-181.

Nemechek A., Pahlavan N., and Cote D. (1997). Nebulised Surfactant for Experimentally Induced Otitis Media with Effusion. *Otolaryngol. Head & Neck Surg.*, **117(5)**, 475-479.

Newman S.P. (1996). Characteristics of Radiolabelled Versus Unlabelled Inhaler Formulations. *J. Aerosol Med.*, **9** (suppl 1), s37-s47.

Newman S.P. (1996a). Variability in Drug Delivery from Aerosol Inhalers *in-vitro* and *in-vivo*. *Respir. Drug. Del. V*, 11-18.

Newan S.P. (1995). A Comparison of Lung Deposition Patterns Between Different Asthma Inhalers. *J. Aerosol Med.*, **8 (suppl 3)**, s21-s27.

Newman, S.P. (1994). Measurement of Drug Delivery to the Lungs. International Respiratory Forum, Current Perspectives in Inhaled Drug Therapy, Royal Society of Medicine, London., 10-17.

Newman S.P., Hollingworth A.H, and Clark A.R. (1994a). Effect of Different Modes of Inhalation on Delivery from a DPI. *Int. J. Pharm.*, **102**, 127-132.

Newman S.P. (1993). Scintigraphic Assessment of Therapeutic Aerosols. *Crit. Rev.Ther. Drug Carrier Sys.*, **10 (1)**, 65-109.

Newman S.P. (1993a). Therapeutic Aerosol deposition in Man. In: Moren F., Dolovich M.B., Newhouse M.T., and Newman S.P., (Eds). Aerosols in Medicine: Principles, Diagnosis and Therapy. Elsevier, Amsterdam, pp 383-387.

Newman, S.P. (1991). Aerosol Generation and Delivery Systems. *Respir. Care*, **36**, 939-951.

Newman S.P, Moren F., Trofast E., Talaee N., and Clarke S. (1991). Terbutaline Sulphate Turbuhaler™: Effect of Inhaled Flow-Rate on Drug Deposition and Efficacy. *Int. J. Pharm*, **74**, 209-215.

Newman S.P., Moren F., Trofast E., and Clarke S. (1989). Deposition and Clinical Efficacy of Terbutaline Sulphate from Turbuhaler. *Eur. Resp. J.*, **2**, 247-256.

Nichols S. (1997). Dry Powder Inhalers- What New Idea? Management Forum, 2-day International Conference, London.

Niven R.W (1993). Aerodynamic Particle Size Testing Using a Time-of-Flight Aerosol Beam Spectrometer. *Pharm. Technol.*, **17 (1)**, 72-78.

Noack G., Beggren P., and Curstadt T. (1987). Severe Neonatal RDS Treated with Isolated Phospholipid Fractions of Natural Surfactant. *Acta Paediatr. Scan.*, **76**,687-705.

Nolan S., Burgess K., Hopper L., and Braude S. (1997). Acute Respiratory Distress Syndrome in a Community Hospital ICU. *Intensive Care Med.*, **23**, 530-538.

Norton N.S. (Editorial) (1990). Exogenous Surfactant Treatment for ARDS ? A historical Perspective, *Thorax*, **45**,825-830.

Nosaka J., Sakai T., and Yoshikawa K. (1990). Surfactant for Adults With Respiratory Failure. *Lancet*, **336**, 947-948.

Olsson B., Asking L., Johansson M. (1998a). Choosing a Cascade Impactor. In: Byron P., Dalby R., and Farr S. (Eds). *Respir. Drug Del. VI*, Interpharm Press, Buffalo Grove, IL., 133-138.

Olsson B. (1995). Aerodynamic Fine Particle Assessment of DPIs at Different Flow Rates using an Extended MSLI. Unpublished data.

Olsson B., and Asking L. (1994). A Model for the Effect of Inhalation Device Flow Resistance on the Peak Inspiratory Flow Rate and its Application in Pharmaceutical Testing. *J. Aerosol Med.*, **7** (2), 201-204.

Osada H.; Tanaka H.; Fujii T.; Tsunoda I.; Yoshida T.; and Satoh K. (1999). Clinical Evaluation of a Haemostatic and Anti-Adhesion Preparation used to Prevent Post-Surgical Adhesions. *J Int. Med. Res.*, **27(5)**, 247-52.

Parrott E.L. (1970). Pharmaceutical Technology: Fundamental Pharmaceutics. Burgess, Minn., U.S.A., pp 1-36.

Partridge M.R, and Sanders K.B., (1981). Site of Action of Ipratropium Bromide and Clinical and Physiological Determinations of Response in Patients with Asthma. *Thorax*, **36**, 530-533.

Patterson I.C., and Crompton G.K. (1976). Use of Pressurised Aerosols by Asthmatic Patients. *Br. Med. J.*, **1**, 76-77.

Pauwels R., Newman S., and Borgstrom L. (1997). Airway Deposition and Airway Effects of Anti-asthma Drugs Delivered From Metered-Dose Inhalers. *Eur. Respir. J.*, **10**, 2127-2138.

Pearlman H.B. (1967). Normal Tube Function. *Arch., Otolaryngol.*, **86**, 50-56.

Peart J. (1996). Electrostatic Charge Interactions in Pharmaceutical Dry Powder Aerosol. PhD Thesis, University of Bath, UK, pp 19-21.

Pedersen S., Hansen O.R., and Fugisang G. (1990). Influence of Inspiratory Flow Rate upon the Effect of a Turbuhaler™. *Arch. Dis. Child*, **65**, 308-310.

Pepe P.E., Reus D.H., and Hudson, L.D. (1990). Clinical Predictors of ARDS. *Am. J. Surg.*, **144**, 124-130.

Perochon E., Leray C., Cremel G., and Hubert P. (1997). Radiolabeling of the Lipids of Chinese Hamster Ovary Cells with the Probe [3-(trifluoromethyl)-3(m-[(125)]iodophenyl)diazirine]. *Anal. Biochem.*, **254(1)**, 109-118.

Phillips M.C., and Chapman S. (1968). Monolayer Characteristics of Saturated, 1-2-Diacyl Phosphatidylcholines (Lecithins) and Phosphatidylethanolamines at the Air-Water Interface. *Biochem. Biophys. Acta*, **163**, 301-313

Phunek P., Roche W., Turzikova J., Kurdmann J., and Warner J. (1997). Eosinophilic Inflammation in the Bronchial Mucosa of Children with Bronchial Asthma. *Eur. Respir. J.*, **19(Suppl 25)**, 160s (Abstract).

Pitcairn G., Lim J., Hollingworth A., and Newman S. (1997) Scintigraphic assessment of drug delivery from the ultrahaler dry powder inhaler. *J. Aerosol Med.-Dep. Clearance. & Effects in the Lung*, **10(4)**, 295-306.

Pitcairn G., Hooper G., *et al* (1997). A scintigraphic Study to Evaluate the Deposition Patterns of a Novel Anti-Asthma Drug Inhaled from the Cyclohaler Dry Powder Inhaler. *Adv. Drug Del. Rev.*, **26**, 59-67.

Pitcairn G., Hunt H., Dewberry H., Pavia D., and Newman S. (1994). A Comparison of *In-Vitro* Drug Delivery from 2 DPIs, the Aerohaler® and the Rotahaler®. *Stp Pharma Sci.*, **4(1)**, 33-37.

Plummer D.T (1987). An Introduction to Practical Biochemistry, 3rd Ed., McGraw-Hill International (UK) Ltd., pp 189-204.

Postle A.D. (1995). Editorial: Lung Surfactants and Asthma. *Clin. Exp. Allergy.*, 1030-10303.

Pride N.B. (1992). Physiology. In: Barnes P., Rodger I., and Thompson N. (Eds). Asthma. Oxford: Blackwell Publishing, pp 41-57.

Prime D., Atkins P.J., Slater A., and Sumby B. (1997). Review of Dry Powder Inhalers. *Adv. Drug Del Rev.*, **26**, 51-58.

Prior M., Prem H., and Rhodes M. (1990). Size Reduction. In: Rhodes M. (Ed). Principles of Powder Technology. John Wiley & Sons, UK, pp 227-296.

Purewal T.S. (1998). A Review of pMDI Technology: Some of the Developments Over the Last Decade. Management Forum, 2-Day International Conference, London.

Rajab A., and Snoj M. (1995). Exogenous Phospholipid Reduces Postoperative Peritoneal Adhesions in Rats. *Eur. J. Surg.*, **161**, 341-344.

Rajab A., and Ahren B. (1991). Phosphatidylcholine Prevents Postoperative Peritoneal Adhesions: An Experimental Study in the Rat. *J. Surg. Res.*, **50**, 212-215.

Raymondos K., Leuwer K., and Haslam M. (1999). Compositional, Structural, and Functional Alterations in Pulmonary Surfactant in Surgical Patients After the Early Onset of Systemic Inflammatory Response syndrome or Sepsis. *Crit. Care Med.*, **27(1)**, 82-89.

Reddington A., Simes P., Howart P., and Holgate S. (1998). Fibroblasts and Extracellular Matrix in Asthma. In: Inflammatory Mechanisms in Asthma. Holgate S., and Busse E., (Eds). Lung Biology in Health and Disease. Lenfant C., (Exec Ed), Vol 117, Marcel Dekker, NY, pp 443-467.

Repka M., Hudak M., Parsa C., and Tielsch J. (1992). Calf Lung Surfactant Extract Prophylaxix and Retinopathy of Prematurity. *Opthalmology*, **99**, 531-536.

Robertson B., van Golde L., and Batenburg J. (Eds.) (1984). Pulmonary Surfactant. Elsevier Science Publications, The Netherlands.

Robertson B. (1980). Surfactant Substitution, Experimental Models and Clinical Applications. *Lung*, **158**, 57-68.

Roper N. (1987). Pocket Medical Dictionary, 14th Edition, Churchill-Livingstone.

Rozga J., and Andersson R. (1990). Influence of Phosphatidylcholine on Intra-Abdominal Adhesion Formation and Peritoneal Macrophages. *Nephron*, **54**, 134-138.

Sacchetti M., and Van Oort M. (1996). Spray-Drying and Supercritical Fluid Particle Generation Techniques.. In: Hickey A.J. (Ed). Inhalation Aerosols: Physical and Biological Basis for Therapy. Marcel-Dekker Inc., New York, pp 337-384.

Sanders R.L. (1982). The Compisiton of Pulmonary surfactant. In: Farrel P.M. (Ed), Lung Development: Biological and Clinical Perspectives, Academic Press. Vol. 1, pp 193-210.

Sbabarti A., Ceresi E., and Accordini C. (1991). Surfactant-like Material on the Chemoreceptorial Surface of the Frog's Taste Organ: An Ultrastructural and Electron Spectroscopic Imaging Study. *J. Struct. Biol.*, **107**, 128-135.

Schurch S., Gehr P., Geiser M., *et al* (1990). Surfactant Displaces Particles Toward the Epithelium in Airways and Alveoli. *Respir. Physiol.*, **80**, 17-32.

Scott-Coombes D., Vipond M., and Thompson J. (1993). General Surgeons' Attitudes to the Treatment and Prevention of Abdominal Adhesions. *Ann. R. Coll. Surg. Engl.*, **75**, 123-128.

Sehgal S., Ewing C., Richards T., and Taeusch H. (1994). Modified Bovine Surfactant (Survanta®) Versus Protein Free Surfactant (Exosurf®) in the Treatment of Respiratory Distress Syndrome in Preterm Infants: A Pilot Study. *J. Natl. Med. Assoc.*, **86**, 46-52.

Shaw D.J. (1996). Introduction to Colloid and Surface Chemistry, Reed Educational and Professional Publishing Ltd., Oxford, UK, pp1-2.

Sheth K., and Lemanske F. (1995). The Early and Late Asthmatic Response to Allergen. In: Busse W., and Holgate, (Eds). Asthma and Rhinitis. Blackwell Science, Inc., USA. Chapter 72, pp 946-960.

Smith C.M., and Anderson S.D. (1990). Bronchial Hyperresponsiveness as assessed by Non-Isotonic Aerosols. *Progr. Resp. Res.*, **24**, 105-116.

Snoj M., and Rajab A. (1992). Effect of Phosphatidylcholine on Postoperative Adhesions After Small Bowel Anastomosis in the Rat. *Eur. J. Surg.*, **79**, 427-429.

Spragg R.G., Gillard N., Richman P., Smith R., Hite R., Pappert D., Robertson B., Curstedt T., and Strayer D. (1994). Acute Effects of a Single Dose of Porcine Surfactant on Patients with the Adult Respiratory Distress Syndrome. *Chest*, **105**, 195-202.

Spragg R.G., Gillard N., and Richman P. (1992). ARDS: Clinical Aspects Relevant to Surfactant Supplementation, In: Pulmonary Surfactant: From Molecular Biology to Clinical Practice, Robertson, B. (Ed), Elsevier Science Publications, Chapter 28, pp 685-699.

Srichana T., Martin G., and Marriott C. (1998). Dry Powder Inhalers: The Influence of Device Resistance and Powder Formulation on Drug and Lactose Deposition *In Vitro*. *Eur. J. Pharm. Sci.*, **7(1)**, 73-80.

Staniforth J.N. (1997). Advances in Powder Technology: Turning Dry Powder Inhalers into Efficient Drug Delivery Systems. Management Forum, 2-Day International Conference, London.

Staniforth J.N. (1987). Order out of Chaos. *J. Pharm. Pharmacol.*, **39**, 329-334.

Staniforth J.N. (1982). Advances in Powder Mixing and Segregation in Relation to Pharmaceutical Processing. *Int. J. Pharm. Tech. & Prod. Mfr.*, **3 (suppl)**, 1-12.

Stephenson P., and Thiel W. (1980). The Effect of Humidity on the Production of Ordered Mixtures. *Powder Technol.*, **25**, 115-119.

Stevens E., and Kochuyt A.M. (1984). A New Aerosol Formulation of Sodium Cromoglycate Compared with Conventional Powder in the Treatment of Asthma. *Allergy*, **39**, 179-182.

Stevenson D., Walther F., and Long W. (1992). Controlled Trial of a Single Dose of Synthetic Surfactant at Birth in Premature Infants Weighing 500 to 699 grams. The American Exosurf® Neonatal Study Group, *J. Paediatr.*, **120**, S3-S12.

Steventon R., and Wilson R. (1986). A Guide to Apparatus for Home-nebuliser Therapy. Allen & Hanbury Ltd, Middlesex, UK, pp 5-6.

Stewart P. (1986). Particle Interaction in Pharmaceutical Systems. Pharmacy International, June, pp 146-149.

Taylor K.M.G., and McCallion O.N.M (1997). Ultrasonic nebulisers for Pulmonary Drug Delivery. *Int. J. Pharm.*, **153**, 93-104.

Ten-Centre Study Group (1987). Ten-Centre Trial of SAPL in Very Premature Babies. *Br. Med. J.*, **294**, 991-996.

Thiel W., and Stephenson P. (1982). Assessing the Homogeneity of an Ordered Mixture. *Powder Technol.*, **31**, 45-50.

Timsina M.P., Martin G.P., Marriott C., Ganderton D., and Yianneskis M. (1994). Drug Delivery to the Respiratory Tract Using Dry Powder Inhalers. *Int. J. Pharm.*, **101**, 1-13.

Torday J., Smith B., Giroud C. (1975). The Rabbit Foetal Lung as a Glucocorticoid Target tissue. *Endocrinology*, **96**, 1462-1467.

Travers D. (1988). Mixing. In: Aulton M. (Ed). Pharmaceutics: The Science of Dosage Form Design. Churchill-Livingstone, London, pp 550-563.

Travers D. (1975). Some Observations on the Ordered Mixing of Micronised Sodium Bicarbonate with Sucrose Crystals. *Powder Technol.*, **12**, 189-190.

Travers D., and White R. (1971). The Mixing of Micronised Sodium Bicarbonate with Sucrose Crystals. *J. Pharm. Pharmacol.*, **23(Suppl)**, 260s-261s.

UbarretxenaBelandia I., Hozeman L., vanderBrinkvanderLaan E., Pap E., Egmond M., Verheij H., and Dekker N. (1999). Outer Membrane Phospholipase A is Dimeric in Phospholipid Bilayers: A Cross-Linking and Fluorescence Resonance Energy Transfer Study. *Biochem.*, **38(22)**, 7398-7405.

Ueda S., Kawamura K., and Ishii N. (1985). Ultrastructural Studies on Surface Lining Layer of the Lungs: Part IV. Resected Human Lungs. J. *Jap. Med. Soc. Biol. Interface*, **16**, 34-60.

Urschel H., and Paulson D. (1967). Gastroesophageal Reflux and Hiatus Hernia. *J. Thoracic Cardiovasc. Surg.*, **53**, 21-28.

Vanderzwan J., McCaig L., and Mehta S. (1998). Characterising Alterations in the Pulmonary Surfactant in a Rat Model of Pseudomonas Aeruginosa Pneumonia. *Eur. Respir. J.*, **12(6)**, 1388-1396.

Van Iwaarden J.F. (1992). Surfactant and the Pulmonary Defence System. In: Robertson B., van Golde L., Batenburg J. (Eds). Pulmonary Surfactant. From Molecular Biology to Clinical Practice. Elsevier Science Publications, Amsterdam, pp 215-227.

Van Oort M., and Downey B. (1996). Cascade Impaction of MDIs and DPIs: Induction Port, Inlet Cone, and Pre-separator Lid Designs Recommended for Inclusion In the General Test Chapter Aerosols <601>. *Pharmaco. Forum*, **22 (2)**, 2204-2209.

Vidgren M., Arppe J., Vidgren P., Hyvarinen L., Vainio P., Silvasti M., and Tukianen H. (1994). Pulmonary Deposition and Clinical Response of ^{99m}TC-labelled Salbutamol from a Novel Multiple Dose Powder Inhaler. *Pharm. Res.*, **11(9)**, 1320-1324.

Vidgren P., Vidgren M., and Paronen P. (1989). Physical Stability and Inhalation Behaviour of Mechanically Micronised and Spray Dried Sodium Cromoglycate in Diffrerent Humidities. *Acta Phamsceutica Fennica*, **98**, 71-78.

Vidgren M., Karkkainen A., Karjalainen P., Paranonen P., and Nuutinen J. (1988). Effect of powder inhaler design on drug deposition in the respiratory tract. *Int. J. Pharm.*, **42**, 211-216.

Vissier J. (1989). An Invited Review of Van der Waals and other Cohesive Forces Affecting Powder Fluidization. *Powder Technol.*, **58**, 1-10.

Voorhorst R., Spieksma F., and Varekamp H. (1967). The House Dust Mite and the Allergens it Produces. Identity with the Mouse Dust Allergen. *J. Allergy*, **39**, 325-339.

Wade A., (Ed) (1988). Pharmaceutical Handbook, 19th Edition., The Pharmaceutical Press, London, 623-624.

Wallin A., Sandstorm T., Rosenhall L., and Melander B. (1993). Time Course and Duration of Bronchodilation with Formoterol in Patients with Stable Asthma. *Thorax*, **48**, 611-614.

Wang J., Shieh C., and You P. (1998). Inhibitory Effect of Pulmonary Surfactant Proteins A and D on Allergen-Induced Lymphocyte Proliferation and Histamine Release in Children with Asthma. *Am. J. Respir. Crit. Care Med.*, **158(2)**, 510-518.

Ward M., MacFarlane J., and Davies D. (1985). A Place for Ipratropium Bromide in the Treatment of Severe Acute Asthma. *Br. J. Dis. Chest*, **79**, 374-377.

Watling S.M., and Yanos J. (1995). Acute Respiratory Distress Syndrome. *The Ann. Pharmacotherapy*, **29**, 1002-1009.

Webb P.A., and Orr C. (1997). Analytical Studies in Fine Particle Technology. Micromeritics Instruments Corporation, GA., USA.

Weibel E.R., Limacher W., and Bachofen H. (1982). Electronmicroscopy of Rapidly Frozen Lungs: Evaluation on the Basis of Standard Criteria. *J. Appl. Physiol.*, **53**, 516.

Weibel E.R. (1963). Morphometry of the Human Lung, Springer-Verlag, Berlin.

Weibel E.R. (1962). Architecture of the Human Lung., *Science*, **137,** 3530.

Welsh M.J. (1994). The Path of Discovery in Understanding the Biology of Cystic Fibrosis and Approaches to Therapy. *Am. J. Gastroenterol.*, **89 (8)**. S97-S105.

Wetterlin K. (1988). Turbuhaler™: A New Powder Inhaler for Administration of Drugs to the Airways. *Pharm. Res.*, **5**, 566-568.

Wiedemann H., Baughman R., Boisblanc B., Schuster D, Caldwell F., and Weg J. (1992). A Multi-Centered Trial in Human Sepsis Induced ARDS of an Aerosolised Synthetic Surfactant. *Am. Rev. Respir. Dis.*, **145**, A184.

Wilding I., Coupe A.J., and Davis S. (1991). The Role of Gamma Scintigraphy in Oral Drug Delivery. *Adv. Drug Del. Rev.*, **7**, 87-117.

Williams D.J., Williams A.C., and Kruchek, D.G. (1993). Problems in Assessing Contents of MDI's. *Br. Med. J.*, **307**, 771-772.

Williams J. (1969). The Properties of Non-Random Mixtures of Solid Particles. *Powder Technol.*, **3**, 189-194.

Woltmann G., Ward R., Wardlaw A., and Pavord I. (1997). Induced Sputum to Assess Airway Inflammation in Asthma. Validity and Repeatability of Sputum Differential Cell Counts. *Thorax*, **52(suppl 6),** A14.

Wong L.W., and Pilpel M. (1988). The Effect of the Shape of Fine Particles on the Formation of Ordered Mixtures. *J. Pharm. Pharmacol.*, **40**, 567-568.

Wood R.E., and Knowles M.R. (1994). Recent Advances in Aerosol Therapy. *J. Aerosol Med.*, **7 (1)**, 1-6.

Woodcock A.J. (1992). Management of Asthma in Adults. In: Barnes P., Rodger I., and Thompson N. (Eds). Asthma. Academic Press, UK, pp 679-699.

Yamanaka N., and Kobayashi K. (1991). Implication of Surfactant Apoprotein in Otitis Media with Effusion. *Ann. Otology Rhinol. & Laryngol.*, **100(10)**, 835-840.

Yarborough J., Mansfield L.E., and Ting S. (1985). Metered Dose Inhaler induced Bronchopspasm in Asthmatic Patients. *Ann. Allergy*, **55**, 25-27.

Yeung C. (1979). Fine Powder Mixing. M.Pharm. Thesis, Victorian College of Pharmacy, Melbourne, Australia.

York P., and Hanna M. (1997). Particles for Respiratory Drug Delivery Using Supercritical Fluid Technologies- Particles and Scale-Up by Design. Management Forum, 2-Day International Conference, London.

Zachariades N., Agouridakis P., and Parker J. (1993). The Adult Respiratory Distress Syndrome: A Review. *J. Oral Maxillofac. Surg.*, **51**, 402-407.

Zeng X., Martin G., Tee S., AbuGhoush A., and Marriott C. (1999). Effects of Particle Size and Adding Sequence of Fine Lactose on the Deposition of Salbutamol Sulphate from a Dry Powder Formulation. *Int. J. Pharm.*, **182(2)**, 133-144.